Journal of Analytical Methods in Chemistry

Advances in MS-Based Analytical Methods: Innovations and Future Trends

Lead Guest Editor: Federica Bianchi
Guest Editors: Leopold Ilag, Veronica Termopoli, and Lucia Mendez

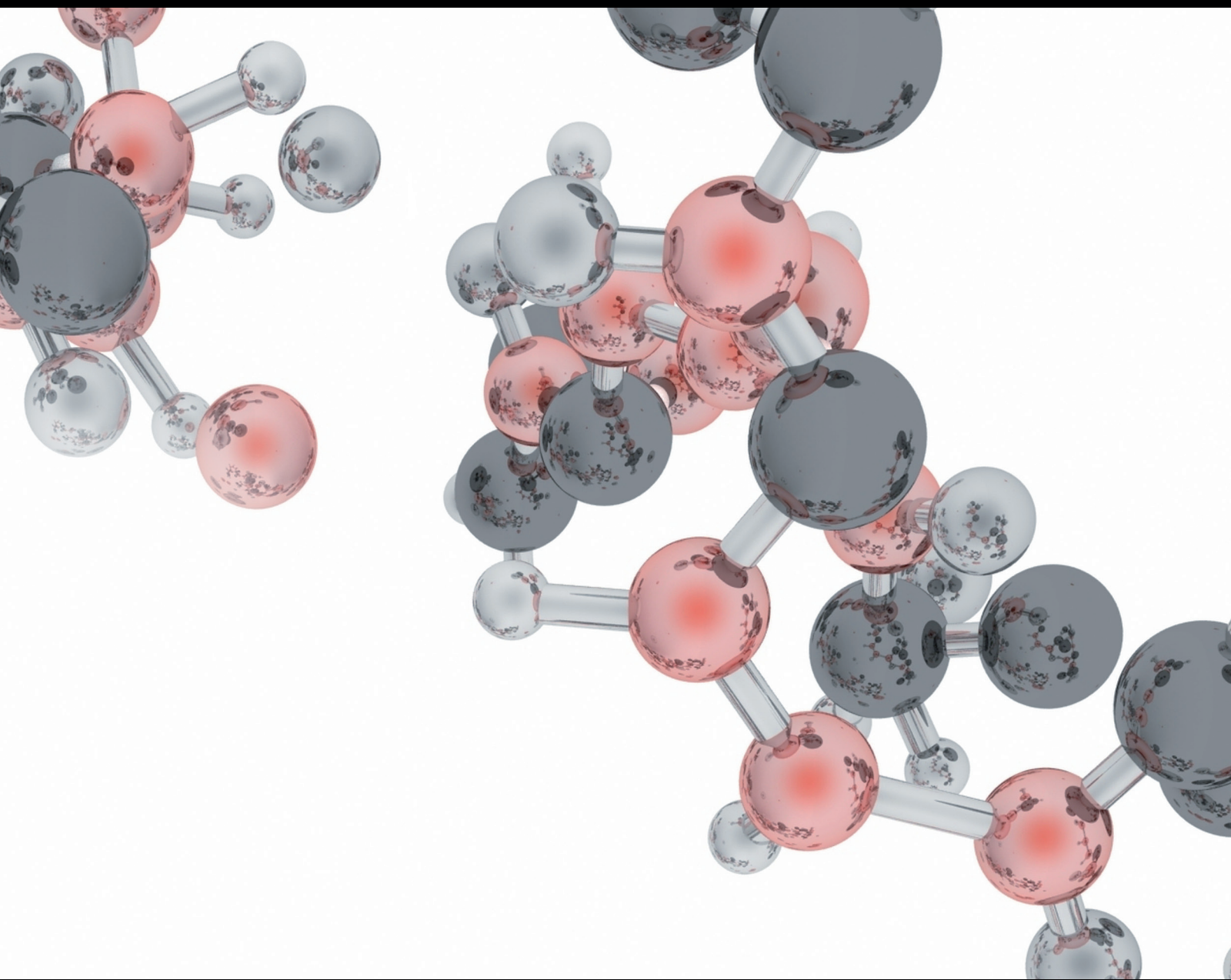

Advances in MS-Based Analytical Methods: Innovations and Future Trends

Journal of Analytical Methods in Chemistry

Advances in MS-Based Analytical Methods: Innovations and Future Trends

Lead Guest Editor: Federica Bianchi
Guest Editors: Leopold Ilag, Veronica Termopoli, and Lucia Mendez

Editorial Board

Contents

Hindawi
Journal of Analytical Methods in Chemistry
Volume 2018, Article ID 2084567, 2 pages
https://doi.org/10.1155/2018/2084567

Editorial

Advances in MS-Based Analytical Methods: Innovations and Future Trends

Federica Bianchi,[1] **Leopold Ilag**,[2] **Veronica Termopoli**,[3] **and Lucia Mendez**[4]

[1]*Department of Chemistry, Life Sciences and Environmental Sustainability, Parma University, Parco Area delle Scienze 17/A, 43124 Parma, Italy*
[2]*Department of Environmental Science and Analytical Chemistry, Stockholm University, 10691 Stockholm, Sweden*
[3]*Department of Pure and Applied Sciences, LC-MS Laboratory, Piazza Rinascimento 6, 61029 Urbino, Italy*
[4]*Instituto de Investigaciones Marinas, Spanish National Research Council (IIM-CSIC), Eduardo Cabello, 6, E-36208 Vigo, Spain*

Correspondence should be addressed to Federica Bianchi; federica.bianchi@unipr.it

Received 9 September 2018; Accepted 10 September 2018; Published 8 October 2018

Mass spectrometry (MS) is a widely used technique for food safety, environmental, pharmaceutical, biological, and forensic investigations where the simultaneous detection of targeted and nontargeted compounds is of pivotal importance. A plethora of analytical MS methods also coupled to different separation techniques such as gas- and liquid-chromatography and their multidimensional analogues or capillary electrophoresis have been developed and validated in order to analyze complex matrices. However, despite the rapid evolution from its beginning, the development of online and real-time analytical MS methodologies especially ambient ionization methods is strongly demanded to perform high-throughput analysis and to obtain highly informative spectra. In this context, novel materials and instrumental configurations are under study to enhance the performance of the different instruments, whereas powerful high-resolution mass spectrometers are required to univocally identify targeted compounds. Finally, libraries of compounds, including MS-based information such as accurate mass, isotopic patterns, and collision-induced fragmentation, are strongly demanded together with studies regarding the establishment of recognized analytical performance criteria to assess the occurrence of residues in the environment. Mass spectrometric imaging is another emerging powerful analytical technique that can be applied to perform analyses of multiple molecules in complex samples without labeling, thus providing a distinct advantage over preexisting methods for label-free and simultaneous detection of drugs and metabolites.

This special issue covers the broad area of MS-based analytical methods starting from the development of novel LC-MS and LC-MS/MS methods for the quantitation of compounds of environmental and pharmaceutical concern to the use of more advanced separation technologies coupled to mass spectrometry for the analysis of atmospheric samples. More precisely, F. Bianchi et al. have provided a discussion of some instrumental innovations and their applications in the field of mass spectrometry with particular attention to spray-based MS methods and LC-EI-based MS interfaces. New materials, prototypes, and instrumental configurations able to increase the performance of the developed methods are presented and discussed. Finally, an overview of the most recent MS-based methods in food analysis is given covering the state of the art from 2012 up to 2017. L. F. Angeles and D. S. Aga have described the role of the ion ratio in the reconnaissance of pharmaceutical compounds in aquatic environment using LC-MS. Establishing performance criteria for the global reconnaissance of pharmaceuticals is important since it minimizes the occurrence of false-positive and false-negative detection. Based on these assumptions, a performance criterion was disclosed by the authors and applied to several equal-to-real samples. For environmental assessment, in situ radiogenic isotope determinations with microscale resolution can represent a powerful tool especially for geological and life sciences: S. Di Salvo et al. have presented a detailed methodological description of the analytical procedure from sampling to elemental purification and Sr-isotope measurements. The

proposed method offers the potential to attain isotope data at the microscale on a wide range of solid materials with the use of minimally invasive sampling.

Mass spectrometry plays a pivotal role also in the forensic field: in this context, N. Mogollon and coworkers have reviewed the recent developments in MS for forensic analysis focusing their attention to the identification and quantification of drugs of abuse in biological fluids, tissues, and synthetic samples. Both the most common methodologies and the new methodologies used for screening and target forensic analyses are reviewed, thus including high-resolution MS as well as the use of ambient ionization ion sources for high throughput and real-time monitoring.

When very complex matrices have to be analyzed, multidimensional chromatography coupled to mass spectrometry can offer increased selectivity and separation power to solve different analytical problems: Y. G. Ahn et al. compared the performances of gas chromatography with quadrupole mass spectrometry and GC × GC-TOFMS for quantitative analysis of eighteen target polycyclic aromatic hydrocarbons in ambient aerosol. Although similar results were obtained in terms of both detection and quantitation limits, a larger number of analytes were identified by using the GC × GC-TOFMS method, thus suggesting that comprehensive two-dimensional gas-chromatography coupled to mass spectrometry such as GC × GC-TOFMS could be applicable to atmospheric and related sciences with simultaneous target and nontarget analyses in a single run.

Mass spectrometry can be considered the technology of the future for medicine: its capabilities in biomarker discovery, development, and validation suggest the implementation of MS instruments in clinical labs. Nowadays, MS-based lab detection methods are increasingly used in hospital labs as well as in legal medicine: in this context, R. Hösli and coworkers have compared the analytical performances of a GC-MS and a LC-MS/MS method, respectively, for the determination of phenytoin in different body compartments, i.e., blood, saliva, and human brain dialysate. The LC-MS/MS method proved to be more sensitive than the GC-MS procedure, being also less time-consuming and requiring small amount of sample. Finally, L. Huang et al. have reported the role of trichloroacetic acid in enhancing the MS signal of tobramycin. Using a simple dilution with trichloroacetic acid as pairing reagent, a sensitive LC-MS/MS method was developed and validated in a bacterial medium.

Conflicts of Interest

The editors declare that they have no conflicts of interest.

Federica Bianchi
Leopold Ilag
Veronica Termopoli
Lucia Mendez

Hindawi
Journal of Analytical Methods in Chemistry
Volume 2018, Article ID 4142527, 17 pages
https://doi.org/10.1155/2018/4142527

Review Article

New Advances in Toxicological Forensic Analysis Using Mass Spectrometry Techniques

Noroska Gabriela Salazar Mogollón,[1,2] **Cristian Daniel Quiroz-Moreno**,[1] **Paloma Santana Prata**,[2] **Jose Rafael de Almeida**,[1] **Amanda Sofía Cevallos**,[1] **Roldán Torres-Guiérrez**,[1] **and Fabio Augusto**[2]

[1]*Ikiam-Universidad Regional Amazónica, Km 7 Via Muyuna, Tena, Napo, Ecuador*
[2]*Institute of Chemistry, State University of Campinas, Cidade Universitária Zeferino Vaz, 13083-970 Campinas, SP, Brazil*

Correspondence should be addressed to Noroska Gabriela Salazar Mogollón; gaby867@gmail.com

Received 8 March 2018; Revised 30 May 2018; Accepted 12 July 2018; Published 29 August 2018

Academic Editor: Veronica Termopoli

This article reviews mass spectrometry methods in forensic toxicology for the identification and quantification of drugs of abuse in biological fluids, tissues, and synthetic samples, focusing on the methodologies most commonly used; it also discusses new methodologies in screening and target forensic analyses, as well as the evolution of instrumentation in mass spectrometry.

1. Introduction

The development of mass spectrometry methods has offered new possibilities for forensic toxicology analyses, where the identification and quantification of drugs of abuse are the most concerning issues in the forensic science [1]. The prevalence of drug addiction and abuse in the population worldwide is significantly high, resulting in one of the main causes of high criminal activities [2]. The excessive use of psychotropic substances, natural drugs, hallucinogens, and most recently "new psychoactive substances," which are designed from skeletons of some natural drugs previously known, are the main focus of the development of new analytical methodologies, where mass spectrometry has had a key role [3, 4]. When a toxicological analysis needs to identify and quantify metabolites from unknown drugs, a screening can be performed by coupling different chromatography techniques, such as liquid and gas chromatography to mass spectrometry. In cases where an increment in the signal/noise ratio (S/N) is necessary, and the structure of the compound is known (target analysis) [5, 6] an additional selectivity can be provided using tandem mass spectrometry (MS/MS) in ion products or selected reaction monitoring (SRM). This latter one is the most widely used because of its increase in the specificity, selectivity, and detectability; however, the analyses become too time-consuming when a previous chromatographic separation and sample preparation are required [6, 7].

Moreover, ionization mass spectrometry techniques such as direct analysis in real time (DART), desorption electrospray ionization (DESI), low-temperature plasma (LTP), desorption atmospheric-pressure photoionization (DAPPI), paper spray (PS), touch spray mass spectrometry (TS-MS), more recently in toxicological analysis laser diode thermal desorption (LDTD), and atmospheric solids analysis probe (ASAP) have gained popularity as they can be used with less or even without sample preparation [8–10]. Nevertheless, depending on the matrix sample, compounds with identical patterns of fragmentation cannot be identified; this is the reason why more development in mass spectrometry needs to be conducted in order to provide relevant information that can help solve a crime [11]. In this sense, this review presents the main current applications of mass spectrometry for the control of drugs of abuse and the discovery of synthetic drugs in biological and synthetic matrices; besides, methodological limitations as well as

innovative methodologies to enhance forensic toxicology analysis are discussed, examining the current literature in the past eight years.

2. Chromatography and Mass Spectrometry

2.1. Conventional MS Methods. The coupling of chromatography techniques with mass spectrometry has been widely used in drugs of abuse analysis, especially when the screening of the sample is needed, having separation techniques such as gas chromatography-mass spectrometry (GC-MS), liquid chromatography-mass spectrometry (LC-MS), liquid chromatography-mass spectrometry in tandem (LC-MS/MS) and, more recently, two-dimensional gas chromatography-MS (GC × GC-MS) as the most commonly used.

Normally, the analyses of nonobjective analytes, after the chromatographic separation, have the same steps to follow. First, a scan is performed by the mass spectrometer in order to identify or recognize some compounds of interest; then, it is necessary to perform a selected ion monitoring (SIM) [12, 13] in order to increase the sensitivity and selectivity of the analysis, in which only fragments of a specific group of molecules are monitored, resulting in an increased *S*/*N*. Consequently, this technique is the most widely used in quantitative analysis of compounds.

The focus in this section is on the most recent and innovative analyses that have been performed using mass spectrometry coupled to chromatographic techniques, including all the new methodologies developed in toxicological analyses. Table 1 provides a summary with their advantages and disadvantages, and Figure 1 shows these methodologies as well.

2.1.1. GC-MS. The advances in techniques using MS coupled to gas chromatography have not been very significant due to the type of analyte that can be analyzed using this chromatographic technique (low molecular weight, volatiles). Even though high molecular weight compounds can be derivatized and analyzed by GC, the sample treatment is not appealing for the forensic toxicological analysis of drugs of abuse where the quickness of analysis is fundamental. For this reason, most of the advances using GC-MS focus on the resolution and separation capacity during the analysis. However, toxicological analysis methods in various matrices are well established and widely used in the analysis of drugs, in order to confirm forensic toxicology from samples of blood, urine, saliva, and hair, among others, during specific screening analysis, demonstrating high selectivity, detectability, and robustness.

In this sense, in order to improve the detection and identification of compounds using GC-MS, negative and positive modes of analysis in MS have been integrated, taking advantage of the stability of the fragments after a positive or negative ionization. For instance, Wu et al. used GC-MS with electron impact ionization and negative chemical ionization (GC/NCI-MS) and the traditional GC-MS with electron ionization mass spectrometry (GC/EI-MS) to analyze opiates, amphetamines, and ketamines in human hair. These analyses were capable of providing more sensitivity at low concentration of pictogram (pg) using only 25 mg from the sample and improving the detection of compounds during the analysis owing to the electronegative moieties. The strategy also avoided wrong results and misinterpretations obtaining lower limits of detection, in comparison with the use of only traditional GC/EI-MS in mode SIM; therefore, NCI can serve as a complementary technique in order to improve the sensitivity during the analysis [14].

The use of a miniaturized analytical method is the aim during the development of new analytical methods, and the analysis of drugs of abuse by mass spectrometry is not the exception. Most recently, GC-MS methodologies have used cold EI to analysis of heroin and cocaine [15, 16]. Here, the GC has an interface known as a supersonic molecular beam (SMB) where the ionization vibration cold sample is in an axial fly-through ion source configuration (Figure 1(a)), providing mass spectra with enhanced molecular ions that are compatible with reference libraries, and the range of compounds are amenable to GC-MS compounds. Additionally, this configuration allowed the increment of the flow rate in GC-MS without declines in the sensitivity in the analysis in the EI source, since the fly-through ion source sensitivity is fully independent on the column flow rate; therefore, column flow rate increase is automatically offset by a corresponding reduction in the helium make-up gas flow rate, the supersonic nozzle backing pressure, and the SMB flow rate are stabilized. The authors considered this aspect during the determination of heroin and cocaine in paper money and composite drug powders using column flow programming as a tool to further reduce the time of analysis. With this method, the time of analysis decreased, allowing the use of a column flow from 1 mL/min to 32 mL/min and the use of relatively small column dimension (5 m 0.25 mm) [55].

However, if the analysis aims to identify target compounds, and if specific fragments of a molecule are known, it is possible to increase the *S/N* with the use of mass spectrometry in tandem (MS/MS). GC-MS/MS is commonly used in SRM and *product ion scan* modes with collision-induced dissociation (CID). On the one hand, an ion precursor is generated into the collision cell during SRM mode, and then one ion product is monitored—this monitoring is also called transitions—this mode is widely used in quantitative analysis because of its selectivity. On the other hand, *product ion scan* consists of scanning product ions once the molecules are fragmented in the collision cell, generating, as a result, high reliability results due to the specificity of the monitored transitions. This method is generally used for transition optimization and the creation of libraries in MS/MS. Thus, these analyses can obtain an unequivocal identification of the eluted analyte. For example, this method identified methamphetamines in blood and urine with a simple and quick LLE and derivatization, as well as managed to differentiate between them [56].

Versace et al. used GC-MS to perform a screening of unknown compounds without an excessive sample preparation in urine samples and GC-MS/MS with the purpose of increasing the specificity using SRM transitions, identifying

Table 1: Main modifications and modes of analysis applied in mass spectrometry in forensic toxicological analysis.

Ionization techniques in mass spectrometry coupled to separations techniques			
Type of MS analysis	Advantages	Disadvantages	References
Negative chemical ionization	(i) It provides more sensitivity at low concentration (pg) based on the stability of electronegative moieties. (ii) Avoids wrong interpretations of correct results reducing time consumption.	(i) Better results are provided when the technique is combined with EI-MS in order to obtain more structural information. (ii) This method requires an additional reagent for the ionization; methane is commonly used.	[14]
Cold electrospray ionization	(i) It can be considered as a miniaturized analytical method because of the interface that it uses and the supersonic molecular beams through analysis with short columns and high column flow rates. (ii) Can provide enhanced molecular ions to much larger and more polar compounds with GC, using the same library to EI-MS (NIST). (iii) The flow rate can be increased up to 100 mL/min, and its fly-through ion source sensitivity is fully independent from the column flow rate. (iv) In this method, the nozzle flow rate is constant; as a result, the cold EI fly-through ion source is unaffected by the column flow rate, unlike any other ion source. (v) The use of GC-MS with cold EI has no limitations for the column used.	(i) Additional instrumentation is required.	[15, 16]
Surface-activated chemical ionization	(i) The ionization of solutes occurs upon the polarization of neutral, solvent molecules, which makes it a highly sensitive method. (ii) The electrostatically charged surface increases the ESI ionization efficiency. (iii) When it is used with ESI, the efficiency of proton-transfer ionization reactions is enhanced by the polarization of neutral solvent molecules or by charged solute molecules induced by the proximity of the charged surface. (iv) The solvent and the analyte ions are better focused towards the analyzer. (v) The increase in signal intensity provides an increase in sensitivity, because there is a reduction in the chemical noise observed in the mass analyzer.	(i) SACI is used to maximize the sensitivity in the analysis of highly polar compounds, but data about less polar compounds have not been revealed until now.	[17]

Table 1: Continued.

Ionization techniques in mass spectrometry coupled to separations techniques			
Type of MS analysis	Advantages	Disadvantages	References
	New methods of analysis used in mass spectrometry		
Dynamic multiple reaction monitoring mode of analysis	(i) This method monitors the analytes only around the expected retention time, decreasing the number of concurrent MRM transitions, allowing both the cycle and the dwell time, which can be optimized in order to obtain higher sensitivity, accuracy, and reproducibility. (ii) dMRM allows the monitoring of more MRM transitions in a single run without compromising data quality. (iii) The dwell time is intelligently optimized by association with the delta retention time. Additionally, information about delta retention time and retention time are key to maximize the dwell time and increasing sensitivity. (iv) This method gives the possibility of applying simultaneous quantifications of multiple components.	(i) It is necessary to maintain the analyte analysis in the same polar mode since a switch of polarity within a single run would reduce the sensitivity and accuracy of quantification with the applied MS instrumentation. (ii) The retention time must be informed, optimized, and defined with reference standards using established chromatographic conditions if it is possible. If the retention time drifts, this might result in an incomplete peak definition and quantitation. (iii) It is necessary to optimize the MS conditions for the all transitions.	[17–20]
	Ambient ionization techniques in mass spectrometry		
Desorption electrospray ionization-mass spectrometry	(i) Direct analysis with high-velocity nebulizing gas. (ii) The selectivity and sensitivity of this technique can be increased by a pretreatment sample.	(i) During analysis of drugs in biological matrix with a high amount of salt, the suppression ionization effect is elevated. (ii) The ion source geometry affects the dynamic of the splashing mechanism resulting in changes in droplet size, charge, and analyte dissolution extent. (iii) A high velocity of nebulization can mechanically ablate delicate samples/powders.	[8, 21–23]
Desorption atmospheric-pressure photoionization	(i) Matrix with high salt content do not provide an elevated suppression of ionization.	(i) High suppression ionization can be found depending of the biological matrix. (ii) Sample preparation is commonly needed in order to avoid suppression of ionization.	[8, 21–25]
Direct analysis in real time	(i) It is commonly used in the analysis of drugs of low molecular weight; therefore, its sensitivity depends on analyte volatility. (ii) The geometrical configuration of the ion source is simple and robust for its operation. (iii) Pretreatment of sample can increase the selectivity of the analysis in complex biological samples.	(i) Compounds of high molecular weight may need derivatization. (ii) Its sensitivity depends of the temperature of the ionization region; therefore, the higher the temperature is the higher the risk of damage is. (iii) Its reproducibility depends on the position of the sample inside the ion source, which represents a big problem in the quantification of the analysis.	[4, 8, 11, 26–35]

Table 1: Continued.

Ionization techniques in mass spectrometry coupled to separations techniques			
Type of MS analysis	Advantages	Disadvantages	References
Low-temperature plasma	(i) It is possible to perform direct analysis without sample preparation. (ii) The instrumentation is simple, and its configuration provides low consumption of discharge gas and the possibility of using air as the discharge gas. (iii) High sensitivity and sensitivity can be obtained without pretreatment of the samples.	(i) This technique is exclusively used with small organic molecules with low to moderate polarity.	[8, 36]
Matrix-assisted laser desorption electrospray ionization	(i) It can be coupled to mass spectrometric imaging (MSI) in order to obtain the distribution spectra of the target. (ii) A mode of analysis called "dynamic pixel" can be used to obtain an imaging method that is faster to do a screening of the compounds. (iii) The analysis does not need sample preparation. This method is based on a direct analysis over the sample. (iv) The sensitivity of the analysis can be improved using a specific matrix. For example, umbelliferone matrix obtained better results in the analysis of methamphetamine in hair than the common matrices CHCA or DHB. (v) The technique has been tested along with MAMS, and it is possible to cause reproducibility of the signal with this technology.	(i) Quantitative analysis has not been carried out until this present date.	[8, 37–41]
Metal-assisted secondary ion mass spectrometry	(i) It can be coupled to mass spectrometric imaging (MSI) in order to obtain the distribution spectra of the target. (ii) The limits of detection are lower than those obtained with MALDESI and also compared with the ones with LC-MS/MS. (iii) It is not necessary to perform preparation of the sample.	(i) Quantitative analysis has not been carried out.	[8, 42, 43]
Paper spray	(i) This technique can analyze a wide range of molecules, from small to large biomolecules. (ii) The use of a pretreatment of the sample can enhance the sensitivity of the analysis.	(i) It has a high matrix effect on most of the drugs. (ii) The paper can extract impurities from the surface and cause the suppression of ionization.	[8, 44–51]
High-performance ion mobility spectrometry	(i) Methods of introduction of samples such as a chromatographic separation can be used to minimize the suppression of ionization.	(i) Direct analysis can result in suppression of ionization.	[50, 51]

Table 1: Continued.

Ionization techniques in mass spectrometry coupled to separations techniques			
Type of MS analysis	Advantages	Disadvantages	References
Differential mobility spectrometry-mass spectrometry separation	(i) Separation conditions of the target analysis can be selectively transmitted into a mass spectrometer. (ii) It can be considered as an ionization technique coupled to a separation method that has a small interface which gives results in few seconds.	(i) This technique is rarely being implemented in commercial devices, and it is not known yet whether it can be used to establish profiles of drug mixtures in complex biological samples.	[52]
Touch spray	(i) The substrate (medical swabs) used can serve as a sample collection tool; thus, ionization helps in the analysis of solid or liquid samples without pretreatment. (ii) The TS-MS can allow noninvasive and direct sampling of neat oral fluids.	(i) The drying step of this substrate represents the most time-consuming part of the analytical protocol.	[9]
Laser diode thermal desorption	(i) The method is completely automatic.	(i) It is not possible to perform a simple interchange between negative and positive modes of ionization. (ii) Effects of interferences in complex biological samples must be explored, and more sample preparation is necessary before the liquid samples are transferred towards the capillary surface.	[53]
Atmospheric solids probe analysis	(i) It is possible to perform analysis of solids and liquids easily. (ii) This design allows the possibility of positive/negative switch during the analysis.	(i) Effects of interferences in complex biological samples must be explored with more detail. (ii) This technique provides better sensitivity during the analysis of small-molecule drugs, decreasing the analysis of the high-molecule compounds.	[53, 54]

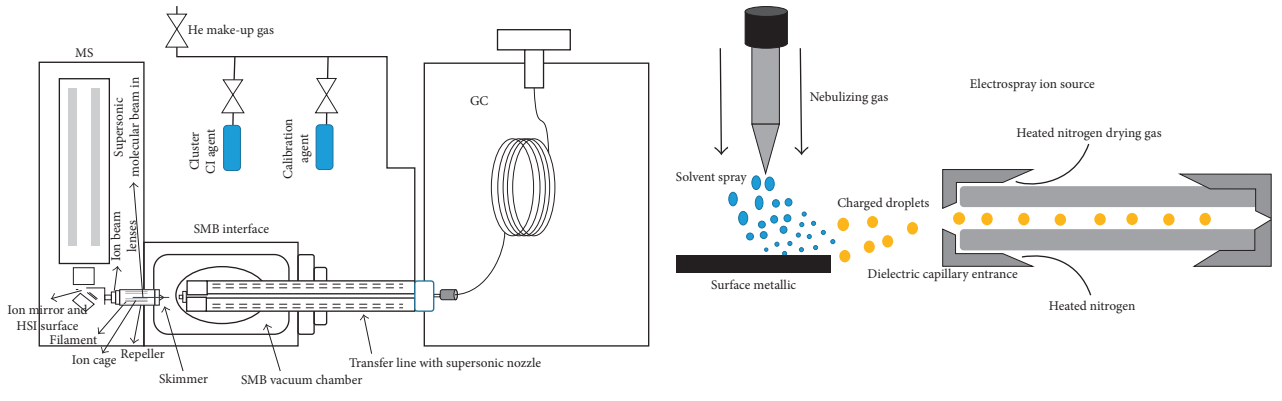

Figure 1: Main advances in mass spectrometry coupled to chromatographic technique in toxicological analysis are (a) gas chromatography interface-supersonic molecular beam with ionization vibration cold sample to mass spectrometry and (b) electrospray ionization and surface-activated chemical ionization to mass analyzed coupled with liquid chromatography.

54 drugs (i.e., 11-nor-9-carboxy-Δ^9-tetrahydrocannabinol, cocaine, hydrocodone, and flurazepam) [57], while Emidio et al. developed a new methodology to determine cannabinoids in hair using 10 mg of sample and headspace solid-phase microextraction (HS-SPME) and GC ion trap/tandem mass spectrometry. Here, CID was used to adjust the breakage of the cannabinoid fragment (ion precursor) and improve the detectability of the technique, demonstrating an excellent linearity range between 0.1 and 8.0 ng/mg with a limit of quantification (LOQ) of

0.007–0.031 ng/mg and 0.012–0.062 ng/mg, which are smaller than the cutoff value established by the Society for Toxicological and Forensic Chemistry (GTFCh) [58].

On the other hand, ethyl glucuronides (a biomarker of ethanol), commonly used in the detection of chronic and excessive alcohol consumption, were identified using MS/MS operating in NCI-MS and SRM mode, obtaining differences between teetotalers and moderate drinkers, according to the current cutoff (i.e., 7 pg/mg hair). In this case, the use of negative mode provided an enhanced sensitivity in low concentration samples which were combined with the specificity of the fragments in the SRM analysis.

Therefore, a better analytical selectivity and S/N were achieved along with long-term markers for the detection of chronic and excessive alcohol consumption [6].

In the same manner, GC-MS/MS has been used to differentiate among important isomers such as methoxyethylamphetamines and monomethoxydimethylamphetamines, as synthetic drugs without derivatization. Using CID and SRM, the specificity of the fragments obtained provided intensity differences in product ions among the isomers, enabling mass spectrometric differentiation of the isomers [59]. One the contrary, GC × GC as a previous treatment can be used in order to increase sensitivity, detection, separation, and resolution. In this sense, GC × GC-MS was used in the determination of cannabinoid-like drugs in 1 mL of postmortem blood, which present a challenge due to the matrix interferences in endogenous lipophilic compounds, proteins, drug degradation/formation, and production of artefacts. With this technique, a limit of detection of 0.25 ng/mL for 11-hydroxy-Δ^9-tetrahydrocannabinol was obtained [60].

The same methodology was applied in oral fluid samples, where it is common to have a small volume of samples, and the concentration of some drugs is usually lower, which can complicate the analysis [61]. The compounds were identified using GC × GC-MS with cold trapping and NCI-MS, obtaining a limit of detection of 0.5 ng/mL [61]. Additionally, GC × GC coupled with time-of-flight-MS (GC × GC-TOFMS) was used to analyze codeine, morphine, and amphetamines in sample extracts from hair suspected of containing various drug compounds. The analytical technique also identified metabolites such as cocaine, diazepam, and methaqualone, which are not included in the target analysis [62].

2.1.2. LC. The use LC as a versatile separation technique (volatile and nonvolatile analytes) has improved the detection and quantification of analytes such as amphetamines, benzodiazepines, hallucinogens, cannabinoids, opiates, cocaine, designer drugs, pharmaceutical products, or illicit drugs in several matrices.

Ultrahigh-performance liquid chromatography has been used along with tandem mass spectrometry (UHPLC-MS/MS) operating in SRM mode in order to establish an individual ion transition ratio to each analyte. Thus, each analyte is infused into the electrospray capillary, and the declustering potential was adjusted to maximize the intensity of the protonated molecular species $[M + H]^+$. The signals were optimized using a source block temperature of 500°C and an on-spray in the determination of Δ^9-tetrahydrocannabinol, cannabidiol, and cannabinol in 50 mg of 179 hair samples. This method allowed the identification of one new synthetic cannabinoid, obtaining an LOQ of around 0.07 pg/mg and 18 pg/mg in the analysis [63].

High-resolution (HR) MS has been used successfully along with LC in the drug of abuse analysis. The resolving power and the high mass accuracy obtained with HRMS were advantageous in the analysis of complex matrices and data acquisition in a targeted and nontargeted manner in order to decrease the number of interferences caused by biological matrix in the drugs analysis. In this case, the authors used UHPLC-HR-TOFMS to analyze cannabinoids and cathinones in 1 mL of urine. During the analysis, a broad-band collision-induced dissociation (bbCID) was used with the purpose of providing a confirmation-level screening featuring both high sensitivity and wide scope. The precursor ions were fragmented in the collision cell without preselection, and the analysis allowed the identification of 75 compounds with cannabinoids spectra database with cutoff concentration values of 0.2–60 ng/mL and cathinones 0.7–15 ng/mL, respectively [64, 65].

The methods of ionization are fundamental to ensure the correct ionization of the sample and, therefore, the identification of the compounds, especially in complex matrices. Wang et al. performed an analysis of cocaine and their metabolites under three types of ionization such as electrospray ionization (ESI), atmospheric-pressure chemical ionization (APCI), and atmospheric-pressure photoionization (APPI) in order to evaluate the chemical suppression during the analysis of 17 illicit drugs in 100 μL of oral fluids using UHPLC-MS/MS in mode SRM. The authors found that ESI presents the smallest ion suppression for all cocaine metabolites analyzed facing the APPI and APCI mode. However, the method developed obtained LOQs in ESI, APCI, and APPI in a range from 0.11 to 1.9 ng/mL, 0.02 to 2.2 ng/mL, and 0.02 to 2.1 ng/mL, respectively. The authors recommended further investigation to determine the causes of higher ion suppression in APCI and APPI on ESI in oral fluids, since ESI may suffer important matrix effects, as it is widely known. Nevertheless, they state that APCI and APPI probes evaporate inlet solutions and ionize analytes via gas-phase chemistry and, consequently, are less affected than ESI. For example, oral fluids may contain many salts and small molecules partitioned from plasma instead of macromolecules, which can lead to an increase in ion suppression in APCI and APPI. As a result, authors suggest the use of ESI in this type of analysis [66].

Liquid chromatography has also taken advantage the benefits of negative mode in mass spectrometry. In this case, LC coupled to (HR)-MS was used along with Orbitrap technology in the analysis of metabolites of drugs such as cocaine, ephedrine, and morphine in urine. The analyses were performed in full-scan mode with positive/negative switching, and subsequently making use of a selective screening through data dependent acquisition (DDA) mode, resulting in a fast analysis. Additionally, the risk of false-negative results caused by ion suppression or isomer overlapping could be reduced by

including metabolites and artefacts, as well as recording in the positive and negative modes [67].

Recently, new methods of analyses in MS/MS have been coupled with LC techniques. Dynamic multiple reaction monitoring (dMRM) has been used in toxicological analysis, and it is recognized by the use of a timetable based on the retention time for each analyte. Such technique monitors the analytes only around the expected retention time, and decreases the number of concurrent SRM transitions, also known as multiple reaction monitoring (MRM), allowing both the cycle time and the dwell time to be optimized to the highest sensitivity, accuracy, and reproducibility [18]. For example, a quantitative LC-MS/MS method has been developed for the simultaneous determination of 17 antipsychotic drugs in human postmortem brain tissue; these drugs are of forensic interest because they have been associated with sudden death cases.

In this method, the analysis was performed operating on dMRM mode, using ESI+. Calibration curves prepared in the spiked brain tissue were linear in the range 20–8000 ng/g ($R^2 > 0.993$) for all drugs, except olanzapine [19]. Besides, LC-MS/MS in dMRM mode was used by Shah et al. in order to identify around 200 drugs/metabolites, such as methamphetamine, amphetamines, ephedrine, and cocaine in hair samples [20]. This method proved an interesting alternative for fast analysis of drugs. All these analyses were performed in one chromatographic run (i.e., 8 min), showing a high sensitivity and accuracy [20].

With the purpose of identifying cannabinoids, such as Δ^9-tetrahydrocannabinol, Conti et al. coupled LC along with two ionization systems, electrospray ionization, and surface-activated chemical ionization (ESI-SACI-MS) to several types of mass analyzer (ion trap, triple quadrupole, and Orbitrap) to improve the detection of 11-nor-9-carboxy-tetrahydrocannabinol in biological samples (urine and hair) operating in SRM mode. This coupling consists in a metallic surface that keeps a fixed voltage and that is inserted into a commercial ESI source (Figure 1(b)). This electrostatically charged surface is able to improve the ESI ionization efficiency, and it increases the ion focusing efficiency towards the mass spectrometric analyzer. The authors show that the sensitivity provided was better with SACI-ESI than with the classical ESI approach alone [17, 68].

Furthermore, an ultrafast and sensitive microflow liquid chromatography-MS/(MFLC-MS/MS) was used to quantify hallucinogens such as LSD and their metabolites in 500 μL of plasma in order to miniaturize and accelerate the analysis of drugs of abuse using LC techniques; this coupling is known by its decrease in run numbers, a higher ionization yield, and reduced ion suppression/enhancement effects. Here, the MS ion trap operated in *product ion scan* and SRM mode in order to perform the quantification along with a dynamic fill-time trap; this method allowed sensitive detection and fast analysis, obtaining LOQs corresponding to 0.01 ng/mL for all analytes [69].

3. Current Analytical Approaches to Target Analyses

3.1. Mass Spectrometry. Mass spectrometry is the preferred technique when the aim is to perform a quick analysis directly on the sample. The main difference between chromatography-MS methods is the sample introduction. MS instrumentation is assembled by ion sources, mass analyzer, and detector [13]. However, the challenge in forensic analysis is the possibility of decreasing the time and cost of analysis per sample. A primary analytical focus in toxicology is determining the presence or absence of drug metabolites in biological samples. In this sense, the use of ambient ionization technique mass spectrometry has allowed the analysis of the entire sample without an excessive preparation of sample. These techniques make possible the concept of open-air surface analysis directly under ambient conditions, being particularly useful for surface analysis of solids, avoiding many, if not all, sample preparation steps typically required [8].

HRMS is widely employed in the coupling with ambient mass spectrometry currently because of its capability of measuring accurate masses and differentiating among compounds with identical nominal masses, providing a comprehensive full-scan MS and MS/MS for the search for any analyte without sample pretreatment. This provides accurate m/z values that can be used to generate chemical formulas with high mass accuracy (<5 ppm mass error) [70]. Therefore, HRMS can be theoretically applied in different configurations with interchangeable ionization sources and sophisticated data acquisition capabilities, making HRMS one of the preferred techniques for the analysis of new drugs [71].

Ambient ionization mass spectrometry can be divided depending on the desorption technique, which will be discussed in the next section about the most used procedures in the analysis of drugs of abuse. Table 1 and Figure 2 present the advantages and disadvantages of these techniques or procedures.

3.1.1. Ambient Ionization Technique Mass Spectrometry: Desorption by Solid-Liquid Extraction. In these techniques, the desorption occurs by solid-liquid extraction followed by ESI-like ion-production mechanisms; the ionization can be performed by DESI (Figure 2(a)) or DAPPI (Figure 2(b)) [8].

DESI-MS is used in forensics due to its ability for in situ analysis. However, direct analyses that involve DESI and DAPPI are less common in toxicological analysis due to the interferences which can be caused by the suppression of ionization product of the matrix effects in the samples; therefore, adding an additional step in the preparation of the sample is often required. For instance, matrix-suppression effects were studied within direct analysis of benzodiazepines and opioids from 1 mg/mL of urine with DESI-MS and DAPPI-MS [21]. The authors found that the urine matrix affects the ionization mechanism of the opioids in DAPPI-MS and favors the proton transfer over charge exchange reaction. However, the sensitivity of the drugs in the solvent matrix was at the same level in DESI-MS and DAPPI-MS with limits of detection of 0.05–6 μg/mL, along with a decrease in sensitivity for the urine matrix that was higher with DESI (typically 20–160-fold) than with DAPPI (typically 2–15-fold), indicating better matrix tolerance in DAPPI over

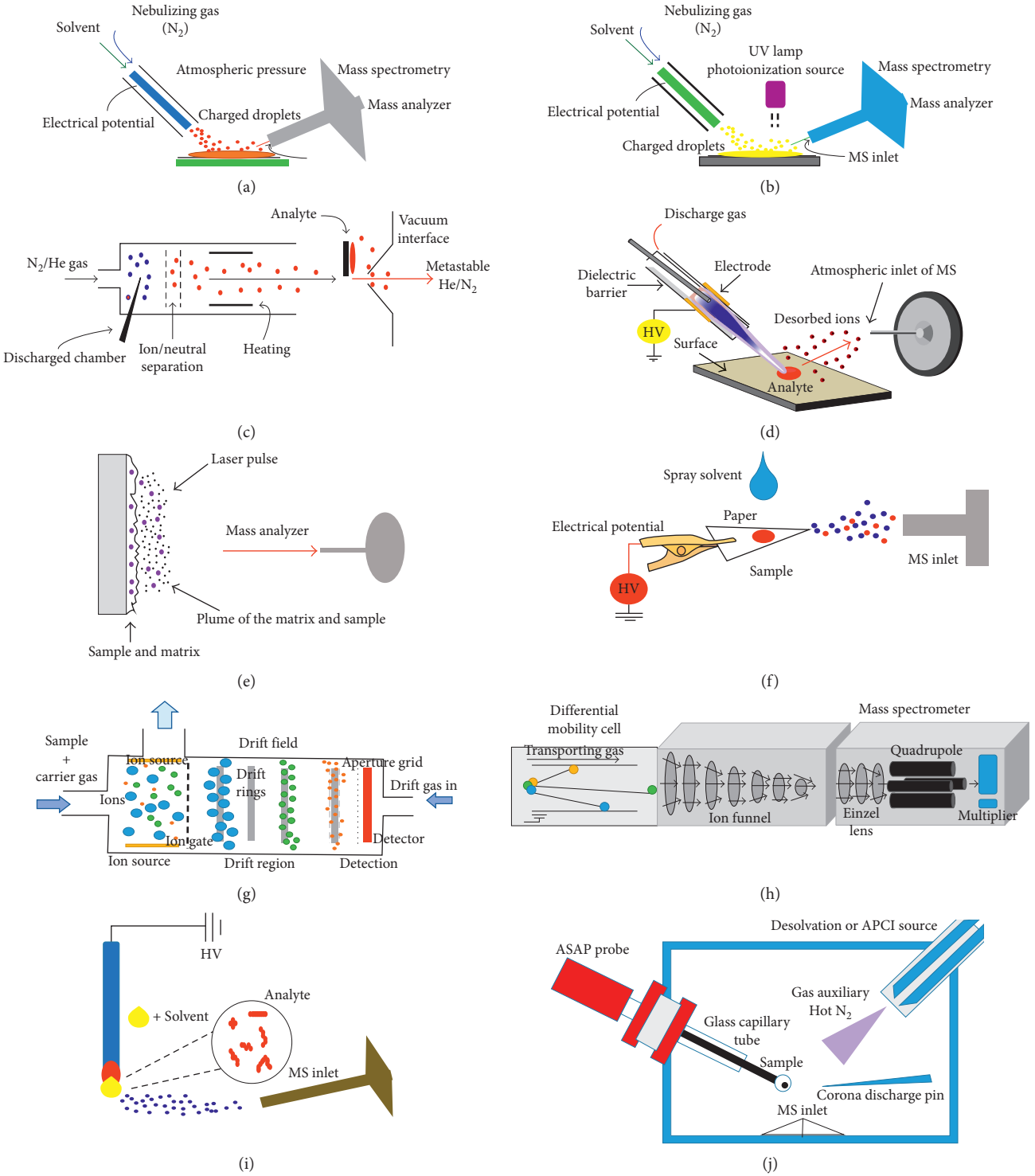

Figure 2: Continued.

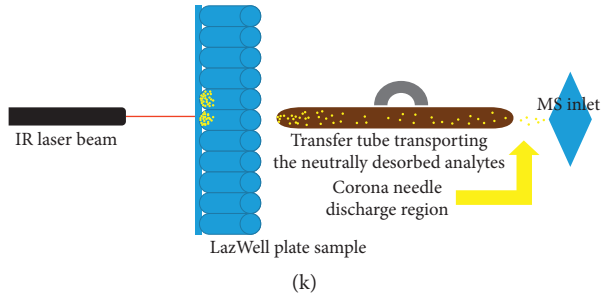

Figure 2: Main ambient ionization techniques used in toxicological forensic analysis. (a) DESI-MS, (b) DAPPI-MS, (c) DART-MS, (d) LTP-MS, (e) MALDI-MS, (f) PS-MS, (g) HPIMS, (h) IMS-MS, (i) TS, (j) ASAP-MS, and (k) LDTD-MS.

DESI. This illustrates that urine contains high concentrations of salts in DAPPI, and the salts in the urine samples are not efficiently evaporated from the sampling surface which do not significantly interfere with the ionization [21].

DESI-MS also allowed the analysis of common drugs in urine samples such as pethidine, diphenhydramine, nortriptyline, and methadone using pretreatment sample by liquid-phase microextraction (LPME). These selective extraction capabilities of three-phase LPME provided a significant reduction in the matrix effects observed in direct aqueous LPME extracts [22]. However, some drugs such as Δ^9-tetrahydrocannabinol and cannabidiol that have identical fragmentation spectra presented significant interference, resulting in the impossibility of an unequivocal identification of each other [22]. Additionally, DESI-MS/MS has been used coupled with solid-phase extraction (SPE) in order to analyze clenbuterol in urine specimens to detect doping; the authors mentioned that the suppression effects were minimized by SPE using DESI-MS/MS [23].

Moreover, DAPPI-MS has been used coupled with quadurople-ion trap MS and MS/MS mode to analyze directly herbal products such as *Catha edulis*, *Phycybe* mushoms, opium, designer drugs in tablets, confiscated drug samples of several forms as tablets, blotter paper, plant resin, and powder forms that contain meta-chlorophenylpiperazine, 3-fluoromethamphetamine, methylenedioxypyrovalerone, amphetamines, phenazepam, buprenorphine, and methylone. DAPPI-MS proved a specific analysis without sample preparation [24], showing that it is sufficient in most criminal cases where the main purpose is to do a qualitative screening [25].

3.1.2. Thermal or Chemical Sputtering Neutral Desorption. These techniques involve metastable and reactive ions, in which the species react with the analyte directly or indirectly through proton- and charge-transfer reactions [8]. In the analysis of drugs of abuse, DART (Figure 2(c)) and LTP (Figure 2(d)) can be used; the former is the most preferred in toxicology forensic analysis and uses a negatively biased point-to-plane atmospheric-pressure glow discharge at lower currents, physically separated from the ionization region by one or several electrodes. The metastable species are formed within the discharge supporting gas that typically is He or N_2, generating protonated water clusters. The main advantage of DART is the analysis of samples in solid, gas, and liquid states, handling polar and nonpolar analytes with masses below 1 kDa [26].

Compounds are identified by combining information about elemental compositions from exact masses and isotopic abundances with fragment-ion mass spectra obtained by collisional activation. In toxicological forensic analysis, DART has been widely used in the detection of small drugs, but its quantitation remains a big problem due to its minor reproducibility, which depends on the position of the sample inside the ion source, making the number of drugs that can be quantified very limited [27]. However, when it is necessary to obtain more details in the identification matrix based on the natural products, high temperatures of ionizing gas can be used during the analysis, benefitting the resolution of more complex spectra [28].

DART achieved the detection of γ-hydroxy butyrate without any sample preparation or other illicit synthetic cannabinoid products coupling mass spectrometry DART-MS with CID analysis. The use of fragments obtained by CID provided a sensitive and specific detection, increasing the limit of detection to identify individual components and showing the ions related to each synthetic cannabinoid, since the $[M+H]^+$ precursor ions were still present in the mass spectra [29]. Thus, an unambiguous differentiation of each species could be accomplished. $[M+H]^+$ precursor ions could also be used as a complement in the analysis of drugs through screening in order to identify new and unknown drugs.

DART-TOFMS detected alprazolam, which is one of the ingredients of the "Houston Cocktail," containing hydrocodone/acetaminophen, and achieved an analysis with high mass accuracy [30]. Habala et al. identified six synthetic cannabinoids in methanolic extracts from solid herbal material using a DART source coupled with a hybrid ion trap—LTQ ORBITRAP—mass analyzer, discovering that the leaves have a greater concentration than the stems of the plant material [11].

In the identification of new psychoactive substances (NPS), DART-MS has had an important role. Gwak and Almirall [4] performed a screening of 35 NPS in urine using DART coupled with hybrid TOFMS and ion mobility spectrometry (IMS), identifying synthetic cathinones with a single phenethylamine as the most common compounds. The analytes detected had an error within ±5 ppm, but isomeric compounds could not be differentiated. Similarly,

DART-TOFMS was used in order to detect synthetic cannabinoid in botanical matrices like *Coriandrum sativum*, *Ocimum basilicum*, and *Mentha spicata* [28]. In this research, intensive sample preparation was not required, just methanol dissolution, which is a method that allowed the identification of the synthetic cannabinoids such as AM-251 and JWH-015. Although botanical samples exhibit relatively complex mass spectral profiles, this did not prohibit the identification of the target compounds. Additionally, the DART-TOFMS analyses were conducted with different ionizing gas (helium) temperatures in order to determine the optimum desorption temperature, and it was observed that higher temperatures had the additional benefit of yielding more complex spectra that could permit a more detailed identification of the plant matrix based on the natural products [28].

Grange and Sovocool [31] developed a methodology for the extraction and clean-up of drugs in smoke deposited on household surfaces so as to determine the exposure of the patients to drugs of abuse using DART-TOFMS. A field sample carrier and an auto sampler were used to minimize the time per analysis. The sampling was performed just with cotton swab wipes with isopropanol, finding a quantification of each drug of around $0.025\,\mu g/100\,cm^2$. However, Δ^9-tetrahydrocannabinol and nicotine had m/z 315 and m/z 163 interferences, respectively. The authors found that this interference could be a sugar unit from the cellulose of the cotton-swabs. In spite of this interference, the method is highly recommended for the analysis of residues in clandestine drug laboratories [31].

Moreover, phenethylamine, a synthetic drug known by its effects similar to LSD and its sublingual consumption via blotter paper, was analyzed directly in the sample by DART-TOFMS. This was studied in blotter paper street samples, and the results can be used in preliminary identifications, since this technique is extremely fast and advantageous for the quick screening of unknown street samples in crime laboratories [32]. Poklis et al. used DART coupled with HRMS in the analysis of legal purchases on the Internet under the name "Raving Dragon Novelty Bath Salts and Raving Dragon Voodoo Dust" and found out that they contain methylone and pentedrone, respectively, which can be identified as unsupervised drug market [33].

More recently, DART has been developed using SPME-fiber format for coupling nanogold surfaces with mass spectrometry in order to perform an effective drug capture in toxicological matrices like methamphetamine, diazepan, and alprozolam in human plasma. The authors used LC-MS/MS and DART-MS/MS, in this case, coupling antibodies to nanogold-coated wires. An antibody with cross reactivity to multiple drugs was used for simultaneous extraction of a mixture of drugs. The immunoaffinity nanogold is known by its possibility of eliminating chemical noise. The limits of detection achieved with DART-MS/MS were comparable to those observed with LC-MS/MS [34].

Different mass analyzers have been used to evaluate sensitivity and selectivity in the detection of Δ^9-tetrahydrocannabinol (THC) from intact hair samples using DART [35]. The mass analyzers evaluated were an Orbitrap, a quadrupole-Orbitrap, a triple quadrupole, and a quadrupole time-of-flight (QTOF). The authors found that only the quadrupole-Orbitrap in high-resolution mode achievement distinguished THC in hair samples from endogenous isobaric interferences [35]. Those are important data since when the resolution in the mass analyzers is low, the risk of obtaining false/positive is high.

Different from DART, LTP was developed for direct sampling ionization in chemical analysis using mass spectrometry. The plasma here is generated by dielectric barrier discharge (DBD) and a discharge of gas at low flow rate (<500 mL/min), and a high-voltage to sustain the plasma in an ambient environment [8]. This technique has proved a powerful tool in direct analyses, exclusively with small organic molecules with low to moderate polarity. For this reason, it is not commonly used in the analysis of illicit high molecular weight drugs as it limits the analysis of unknown drugs. However, LTP proved effective in the analysis of stomach fluid content of a diseased dog suspected to have died from ingestion of insecticide. Direct sampling ionization was applied in MS analysis and protonated Terbufos, and Terbufos sulfoxide were observed [72]. These two compounds are common in Terbufos-based insecticides, which were suspected to be the cause of the death of the dog.

Furthermore, the analysis of drugs of abuse in urine and 25 mg of hair extract samples were systematically investigated, where several drugs such as amphetamine, benzoylecgonine, caffeine, cannabidiol, cocaine, codeine, diazepam, ephedrine hydrochloride, heroin, ketamine, methadone, methamphetamine, morphine, and Δ^9-tetrahydrocannabinol were identified obtaining a limit of detection of around 10 ng/mL without any sample preparation [36].

3.1.3. Laser Desorption/Ablation. In these techniques, the analytes are desorbed or ablated from a surface by an IR or UV laser with or without a matrix (Figure 2(e)). The sample is subsequently merged with an electrospray droplet cloud or a plasma stream, depending on the ionization source used [8]. When the source excites an exogenous matrix that cocrystallizes and has energy absorbent capabilities, it can coat the sample surface to be analyzed. Then, a laser adds excess energy to the matrix-sample complex, where the matrix absorbs laser energy to pass it to the sample and, finally, to produce ions from analytes; this technique is called matrix-assisted laser desorption electrospray ionization (MALDESI) [73]. In contrast to MALDESI, metal-assisted secondary ion mass spectrometry (MetA-SIMS) procedure adds small amounts of metals onto sample surface to enhance mass spectra analysis [42]. These two methods may provide an image coupled with ionization mass spectrometric imaging (MSI), which is a powerful technique to obtain spatial information (distribution) of compound mass spectra.

Porta et al. used MALDESI coupled to MSI in order to monitor the distribution of cocaine and its metabolites in 12 mL of extracts of intact single hair samples from chronic users. The acquisitions were performed applying rastering mode in the SRM mode on a MALDI triple quadrupole

linear-fitted ion trap. The time of analysis of an intact single hair sample of 6 cm was of 6 min approximately. Cocaine and its metabolites were identified and quantified, and the results were obtained with a limit of detection of 5 ng/mL, becoming an excellent methodology to detect cocaine consumption [37]. In the same manner, matrix-assisted laser desorption/ionization-mass spectrometry imaging (MALDI-IMS) was used to rapidly screen longitudinally sectioned drug user hair samples for cocaine and its metabolites; using continuous raster imaging, the optimization of the spatial resolution and raster speed were performed on cocaine-contaminated intact hair samples. Besides, the MALDI-MS/MS images showed the distribution of the most abundant cocaine, using *product ion scan* as a mode of analyzing. With this method, it is possible to obtain mass spectra with the main fragment of the molecule target.

An SRM experiment was also performed using the "dynamic pixel" imaging method to screen for cocaine and a range of its metabolites, in order to differentiate between contaminated hairs and drug users. Therefore, these methods are important when the imaging information on drug distribution is necessary, for example, in human hair without extensive sample preparation, or when labelling techniques are required. However, it should be noted that it only provides qualitative data about administered drugs, through a pixelated representation [38]. MALDESI has also been coupled with HRMS during the identification of 74 drug samples which were detected using the ionic liquid matrix N,N diisopropylethylammonium α-cyanohydroxycinnamate. This method allowed the identification of new designer drugs, which come from the use of safrole as a precursor for the synthesis. Nevertheless, the result obtained presents weaker resolution and lower sensitivities, leading to lower peak intensities. The authors affirm that this limitation is a consequence of the matrix, since this can be related to the formation of adducts, but the matrix may be enhanced by adding specific cations and anions. Further investigations to improve ionization through matrix additives are still necessary in the field. Another limitation of this methodology is the impossibility to distinguish drug position isomers, such as methamphetamine and 4-methylamphetamine, as well as structural elucidation of unknown compounds. The authors recommend the combination between this methodology and bioinformatics software tools which provide untargeted compound searches, even if respective HRMS spectra are not included in a library just based on the precursor ion fingerprinting [39].

On the contrary, MALDI-MSI and MALDI-Fourier transform ion cyclotron resonance (FTICR-MS) have also been used for mapping and direct detection of methamphetamine in longitudinal sections of the single hair sample in positive mode, in which umbelliferone was used as a matrix. This matrix has the advantage of being hydrophobic and capable of assisting in the ionization of methamphetamine in hair. The authors observed that the detection and sensitivity provided by this matrix is higher than α-cyano-4-hydroxycinnamic acid (CHCA) or 2,5-dihydroxybenzoic acid (DHB). In addition, the distribution semi-quantitative of methamphetamine can be performed. This method enhances the detection and sensitivity of target drugs embedded in a hair matrix, achieving a detection level down to nanogram per milligram; for this reason, the authors compared the results with the obtained by LC-MS/MS, but in this case with less sample amount required [40].

More recently, Kernalléguen et al. [41] have made possible the semiquantification of cocaine and its metabolites (benzoylecgonine, cocaethylene, and ecgonine methyl ester) in hair, using microarrays for MS and MALDI-MS/MS. So far, it is well known that the inhomogeneous MALDI matrix crystallization and laser shot-to-shoot variability make the quantitation more difficult; therefore, the authors used a high-throughput MALDI method, along with an innovative high-density microarray for mass spectrometry (MAMS) technology. This technology consists of a sample preparation slide containing lanes of hydrophilic spots, and an automated slider which drags a sample droplet over several small spots, with the purpose of achieving homogeneous crystallization of the matrix-analyte mixture and, therefore, to a reproducible signal. In this manner, it was possible to establish a calendar of consumption in only 1 mg of hair with a great correlation, becoming an excellent methodology when urgent results are required [41].

However, metal MetA-SIMS was used to determine the differentiation between systemic exposure and external contamination that remains in the hair because of exposure to drugs after following the protocols of decontamination (hair wash) [43]. The authors reached a comparison of the results among MetA-SIMS, MALDESI-MS, and LC-MS/MS, showing that there is still cocaine detected after the washes of decontamination, using MetA-SIMS. MALDESI was in turn inefficient for forensic hair analysis since no cocaine was detected after decontaminating the samples. LC-MS/MS detected 5 ng/10 mg in the sample after the washing. Finally, the authors concluded that the washing protocols are not reliable, because external cocaine can migrate into the hair, and recommended a simple analysis of images which makes the evaluation of the differences among hair samples contaminated externally and the interpretation of the correct results easier [43].

3.1.4. Other Methods of Ionization. Paper spray (PS) technique was introduced in 2009 and has been used in the development of a wide range of quantitative and qualitative applications. Here, the sample is deposited in the paper with a sharp point, and ions are produced by voltage applied, while the substrate is held by a metal clip in the paper and placed in the front of the inlet of a mass spectrometer. Then, the front mass spectrometer performs the detection after the sample elution, which can be carried out in the same manner of paper chromatography, but with a direct sample injection to the mass spectrometer (Figure 2(f)). In this technique, a wide range of chemicals can be ionized by paper spray, from small molecules to large biomolecules [8].

Paper spray ionization coupled to high-resolution tandem mass spectrometry (PSI-HR-MS/MS) have also been used in order to validate a screening of drugs in urine such as codeine-6-glucuronide, diclofenac, among others, and to validate a comprehensive urine screening. Nevertheless, the procedure showed

high matrix effects for most drugs, but also acceptable limits of identification that have the potential of reducing workload. However, the authors recommend its implementation as a promising alternative to conventional procedures, but they warned that there is a risk of false positive/negative results caused by mixed spectra during the detection of low concentrations. Therefore, some problems should be solved before implementing it in routine analysis [44].

Thin-layer chromatography (TLC) has been also used as an introductory sampling method combined with PS-MS to analyze cocaine and its adulterants in 10 μL of sample. This analysis obtained promising results in which the limit of detection was reduced five thousand times (1.0 μg/mL), showing an $R^2 > 0.999$ that is another indicator of the reliability of this technique, and the possibility to be implemented in routine analyses [45]. In the same manner, simultaneous analyses of methamphetamines, cocaine, morphine, and Δ^9-tetrahydrocannabinol were performed in a single blood spot by PS-MS in only 2 minutes, with minimal sample preparation through the extraction of the compounds by solvents [46].

PS-MS has also been used in positive ionization mode to obtain chemical profiles of illicit drugs such as blotter papers containing extracts and leaves of natural cannabinoids and synthetic cannabinoids; here, 1 mg of blotter paper was used as the PS ionization source. For this reason, the authors recommend to be careful with the low sensitivity of this technique that was observed to possibly occur due to an ionic suppression process, caused by the matrix effect (extracted impurities from the surface of the blotter paper). The results provided a limit of detection of around 0.17 ppb [47].

PS-MS/MS has been used in targeted drug screening using an Orbitrap QMS, one in positive mode and the other in negative mode. In the positive ion mode, over 130 drugs and drug metabolites in postmortem samples were semiquantitatively determined, proving an adequate method in postmortem analysis. In the analysis in negative mode, an ion-screening method was also developed for a small panel of barbiturates and structural analogs. This method showed good qualitative agreement with LC–MS-MS; the true positive rate of paper spray MS/MS was 92%, and the true negative rate was over 98%. This result shows that this technique possesses the necessary potential for acidic drug detection and screening without sample preparation; however, the authors did not present a list of possible interferences during the analysis [48].

Most recently, PS-MS has been used modifying the paper through molecularly imprinted polymers (MIP) to create a specific site for cocaine analysis in 1 mL of the oral fluid. In this case, the PS was set by holding the membrane connected directly to the outlet probe of the ESI with a 0.5 mm wire using an alligator-type clip and applying a voltage of 4 V, obtaining an LOQ of 100 ng/mL, and becoming a promising method to analyze cocaine [49].

High-performance ion mobility spectrometry (HPIMS) has been used along with electrospray ionization to detect codeine and morphine in urine samples without extra sample pretreatment (Figure 2(g)). However, issues of charge suppression in the presence of drug mixtures interfering with matrix components were observed, so the authors recommended considering some previous steps before sample preparation. For instance, the authors introduced a sample into a drift tube via pulse Bradbury–Neilson ion gate and operated it in positive mode, and the ions passed to desolvation to be separated [50]. This method achieved a resolving power double than the currently accepted method without an excessive necessity of sample preparation [51].

Ion mobility-based separation methods can be combined with mass spectrometry (IMS-MS) in order to minimize chemical suppression caused by interference and the use of chromatography separations to targeted applications (Figure 2(h)). The interface has only a few centimeters in length and operates in seconds; besides, it can be adapted to any MS system using atmospheric-pressure ionization-targeted applications. In this analysis, a miniature differential ion mobility filter is used and placed in front of the entrance of the mass spectrometer, and a solution of 10 ng/mL of the sample was introduced using infusion introduction of ions created by electrospray ionization source coupled with ion trap MS/MS. This method allowed the characterization of samples in 30 seconds, reducing case backlogs in the targeted analysis of analytes of interest, showing the range of quantification of around 0.01–10 ng/uL of cocaine [52].

Recently, a new method has been developed coupling microfluidics with a miniature mass spectrometer in order to quantify cocaine in urine samples. This method is able to deliver droplets of solvents to dried urine samples, separating droplets of 80 μL of extracts, then performing splits from the hydrophilic dried urine zones and driving them to the destination electrode for analysis. The LOQ for cocaine was 40 ng/mL [74].

Another recent method of direct analysis is touch spray (TS). In this technique, the sample is transferred to a substrate with subsequent ionization; in this manner, the substrate can serve both as the means for the sample collection, ionization, and as straightforward handling analysis of either solid or liquid samples without pretreatment (Figure 2(i)). Using TS-MS coupled with MS/MS, drugs of abuse like Δ^9-tetrahydrocannabinol and buprenorphine were identified in spiked oral fluid using medical swabs directly, providing limits of detection of around 50 ng/mL, which are sought by international forensic and toxicological societies. This adaptation of medical swabs for TS-MS analysis allows noninvasive and direct sampling of neat oral fluids; however, the authors affirm that the drying step represents the most time-consuming part of the analytical protocol, but the potential of the technique is high in terms of specificity, selectivity, and sensitivity [9].

More recently, laser diode thermal desorption (LDTD) and atmospheric solids analysis probe (ASAP) have been coupled with HRMS using APCI ionization in order to generate high-quality data from multiple samples with none or minimal sample preparation, with the purpose of identifying synthetic cannabinoids/cathinones through full-MS and MS/MS experiments. In ASAP, a melting-point capillary tube is used to introduce the sample into a stream of heated nitrogen gas, which results in the sample being desorbed from

the capillary [53], and the desorbed sample is then ionized by a corona discharge needle. During ASAP-MS analysis, it was possible to examine solid and liquid samples transferred to the capillary surface (Figure 2(j)); whereas in the LDTD-MS analysis, the samples were extracted by a solvent. This method uses a specially designed 96-well plate with stainless alloy steel inserts, where the sample is thermally desorbed from the stainless steel by an infrared laser which forms neutral gas-phase molecules [54] (Figure 2(k)). These gas-phase molecules are carried into the mass spectrometer inlet by compressed air. Before they enter the mass spectrometer inlet, a corona discharge needle ionizes the neutral molecules.

This LDTD-APCI-MS method results in a completely automated analysis with low sampling times. The authors recommended the use of both methods of ambient ionization, which allow rapid experiments from a single sample introduction. However, when performing the optimization, they verified that the simplicity of ASAP design allows it to be easily switched between API techniques and possible positive/negative switching for a single sample introduction, which provides many possibilities of optimization during the analysis. More studies in this field are required, especially in possible interference of suppression of ionization [75].

4. Conclusions

Mass spectrometry is the most important technique used in toxicological forensic analysis. MS coupled with chromatography are the preferred techniques to identify new drugs or metabolites through screening analysis, providing excellent results in limit of detection, precision, accuracy, and sensitivity, although it may be a time-consuming process. Direct techniques with MS (with less sample preparation) are more likely to be used in target analysis or in routine qualitative analysis. However, sample complexity complicates the identification among compounds with similar fragmentation patterns, along with the problems caused by ionization chemical suppression. As a result, recent developments in MS are concerned with the necessity of creating new software in order to help improve simplicity and robustness in the identification of drugs. There is a growing necessity to develop more innovative methodologies to reduce time consumption in the analyses, enhance sensitivity, and finally move forward towards greener chemistry.

Conflicts of Interest

The authors declare that there are no conflicts of interest regarding the publication of this paper.

References

[1] C. Moore, L. Marinetti, C. Coulter, and K. Crompton, "Analysis of pain management drugs, specifically fentanyl, in hair: application to forensic specimens," *Forensic Science International*, vol. 176, no. 1, pp. 47–50, 2008.

[2] O. Beck, "Exhaled breath for drugs of abuse testing—evaluation in criminal justice settings," *Science and Justice*, vol. 54, no. 1, pp. 57–60, 2014.

[3] H. H. Lee, J. F. Lee, S. Y. Lin, and B. H. Chen, "Simultaneous identification of abused drugs, benzodiazepines, and new psychoactive substances in urine by liquid chromatography tandem mass spectrometry," *Kaohsiung Journal of Medical Sciences*, vol. 32, no. 3, pp. 118–127, 2016.

[4] S. Gwak and J. R. Almirall, "Rapid screening of 35 new psychoactive substances by ion mobility spectrometry (IMS) and direct analysis in real time (DART) coupled to quadrupole time-of-flight mass spectrometry (QTOF-MS)," *Drug Testing and Analysis*, vol. 7, no. 10, pp. 884–893, 2015.

[5] C. Poole, *Gas Chromatography*, Elsevier, New York, NY, USA, 1st edition, 2012.

[6] D. Cappelle, H. Neels, M. Yegles et al., "Gas chromatographic determination of ethyl glucuronide in hair: Comparison between tandem mass spectrometry and single quadrupole mass spectrometry," *Forensic Science International*, vol. 249, pp. 20–24, 2015.

[7] M. Chèze, A. Lenoan, M. Deveaux, and G. Pépin, "Determination of ibogaine and noribogaine in biological fluids and hair by LC-MS/MS after Tabernanthe iboga abuse. Iboga alkaloids distribution in a drowning death case," *Forensic Science International*, vol. 176, no. 1, pp. 58–66, 2008.

[8] M. Domin and R. Cody, *Ambient Ionization Mass Spectrometry*, Royal Society of Chemistry, Cambridge, UK, 2014.

[9] V. Pirro, A. K. Jarmusch, M. Vincenti, and R. G. Cooks, "Direct drug analysis from oral fluid using medical swab touch spray mass spectrometry," *Analytica Chimica Acta*, vol. 861, pp. 47–54, 2015.

[10] H. Wang, J. Liu, R. G. Cooks, and Z. Ouyang, "Paper spray for direct analysis of complex mixtures using mass spectrometry," *Angewandte Chemie*, vol. 122, no. 5, pp. 889–892, 2010.

[11] L. Habala, J. Valentová, I. Pechová, M. Fuknová, and F. Devínsky, "DART–LTQ ORBITRAP as an expedient tool for the identification of synthetic cannabinoids," *Legal Medicine*, vol. 20, pp. 27–31, 2016.

[12] M. Carson and S. Kerrigan, "Quantification of suvorexant in urine using gas chromatography/mass spectrometry," *Journal of Chromatography B*, vol. 1040, pp. 289–294, 2017.

[13] J. Greaves and J. Roboz, *Mass Spectrometry for the Novice*, CRC Press, Boca Raton, FL, USA, 2008.

[14] Y.-H. Wu, K. Lin, S.-C. Chen, and Y.-Z. Chang, "Integration of GC/EI-MS and GC/NCI-MS for simultaneous quantitative determination of opiates, amphetamines, MDMA, ketamine, and metabolites in human hair," *Journal of Chromatography B*, vol. 870, no. 2, pp. 192–202, 2008.

[15] A. Amirav, A. Gordin, M. Poliak, and A. B. Fialkov, "Gas chromatography-mass spectrometry with supersonic molecular beams," *Journal of Mass Spectrometry*, vol. 43, no. 2, pp. 141–163, 2008.

[16] T. Alon and A. Amirav, "How enhanced molecular ions in Cold EI improve compound identification by the NIST library," *Rapid Communications in Mass Spectrometry*, vol. 29, no. 23, pp. 2287–2292, 2015.

[17] M. Conti, V. Tazzari, M. Bertona, M. Brambilla, and P. Brambilla, "Surface-activated chemical ionization combined with electrospray ionization and mass spectrometry for the analysis of cannabinoids in biological samples. Part I: analysis of 11-nor-9-carboxytetrahydro-cannabinol," *Rapid Communications in Mass Spectrometry*, vol. 25, no. 11, pp. 1552–1558, 2011.

[18] J. Liang, W.-y. Wu, G.-x. Sun et al., "A dynamic multiple reaction monitoring method for the multiple components quantification of complex traditional Chinese medicine preparations: Niuhuang Shangqing pill as an example," *Journal of Chromatography A*, vol. 1294, pp. 58–69, 2013.

[19] M. C. Sampedro, N. Unceta, A. Gómez-Caballero et al., "Screening and quantification of antipsychotic drugs in human brain tissue by liquid chromatography-tandem mass spectrometry: application to postmortem diagnostics of forensic interest," *Forensic Science International*, vol. 219, no. 1–3, pp. 172–178, 2012.

[20] I. Shah, A. Petroczi, M. Uvacsek, M. Ránky, and D. P. Naughton, "Hair-based rapid analyses for multiple drugs in forensics and doping: application of dynamic multiple reaction monitoring with LC-MS/MS," *Chemistry Central Journal*, vol. 8, no. 1, p. 73, 2014.

[21] N. M. Suni, P. Lindfors, O. Laine et al., "Matrix effect in the analysis of drugs of abuse from urine with desorption atmospheric pressure photoionization-mass spectrometry (DAPPI-MS) and desorption electrospray ionization-mass spectrometry (DESI-MS)," *Analytica Chimica Acta*, vol. 699, no. 1, pp. 73–80, 2011.

[22] J. Thunig, L. Fløe, S. Pedersen-Bjergaard, S. H. Hansen, and C. Janfelt, "Liquid-phase microextraction and desorption electrospray ionization mass spectrometry for identification and quantification of basic drugs in human urine," *Rapid Communications in Mass Spectrometry*, vol. 26, no. 2, pp. 133–140, 2012.

[23] Z. Lin, S. Zhang, M. Zhao, C. Yang, D. Chen, and X. Zhang, "Rapid screening of clenbuterol in urine samples by desorption electrospray ionization tandem mass spectrometry," *Rapid Communications in Mass Spectrometry*, vol. 22, no. 12, pp. 1882–1888, 2008.

[24] T. J. Kauppila, A. Flink, M. Haapala et al., "Desorption atmospheric pressure photoionization–mass spectrometry in routine analysis of confiscated drugs," *Forensic Science International*, vol. 210, no. 1–3, pp. 206–212, 2011.

[25] T. J. Kauppila, V. Arvola, M. Haapala et al., "Direct analysis of illicit drugs by desorption atmospheric pressure photoionization," *Rapid Communications in Mass Spectrometry*, vol. 22, no. 7, pp. 979–985, 2008.

[26] R. B. Cody and J. A. Larame, "Versatile new ion source for the analysis of materials in open air under ambient conditions," *Analytical Chemistry*, vol. 77, no. 8, pp. 2297–2302, 2005.

[27] E. S. Chernetsova and G. E. Morlock, "Determination of drugs and drug-like compounds in different samples with direct analysis in real time mass spectrometry," *Mass Spectrometry Reviews*, vol. 35, no. 5, pp. 875–883, 2011.

[28] R. A. Musah, M. A. Domin, M. A. Walling, and J. R. E. Shepard, "Rapid identification of synthetic cannabinoids in herbal samples via direct analysis in real time mass spectrometry," *Rapid Communications in Mass Spectrometry*, vol. 26, no. 9, pp. 1109–1114, 2012.

[29] R. A. Musah, M. A. Domin, R. B. Cody, A. D. Lesiak, A. John Dane, and J. R. E. Shepard, "Direct analysis in real time mass spectrometry with collision-induced dissociation for structural analysis of synthetic cannabinoids," *Rapid Communications in Mass Spectrometry*, vol. 26, no. 19, pp. 2335–2342, 2012.

[30] W. C. Samms, Y. J. Jiang, M. D. Dixon, S. S. Houck, and A. Mozayani, "Analysis of alprazolam by DART-TOF mass spectrometry in counterfeit and routine drug identification cases," *Journal of Forensic Sciences*, vol. 56, no. 4, pp. 993–998, 2011.

[31] A. H. Grange and G. W. Sovocool, "Detection of illicit drugs on surfaces using direct analysis in real time (DART) time-of-flight mass spectrometry," *Rapid Communications in Mass Spectrometry*, vol. 25, no. 9, pp. 1271–1281, 2011.

[32] M. K. McGonigal, J. A. Wilhide, P. B. Smith, N. M. Elliott, and F. L. Dorman, "Analysis of synthetic phenethylamine street drugs using direct sample analysis coupled to accurate mass time of flight mass spectrometry," *Forensic Science International*, vol. 275, pp. 83–89, 2017.

[33] J. L. Poklis, C. E. Wolf, O. I. ElJordi, K. Liu, S. Zhang, and A. Poklis, "Analysis of the first- and second-generation raving dragon novelty bath salts containing methylone and pentedrone," *Journal of Forensic Sciences*, vol. 60, pp. S234–S240, 2015.

[34] K. M. Evans-Nguyen, T. L. Hargraves, and A. N. Quinto, "Immunoaffinity nanogold coupled with direct analysis in real time (DART) mass spectrometry for analytical toxicology," *Analytical Methods*, vol. 9, no. 34, pp. 4954–4957, 2017.

[35] W. F. Duvivier, T. A. van Beek, and M. W. F. Nielen, "Critical comparison of mass analyzers for forensic hair analysis by ambient ionization mass spectrometry," *Rapid Communications in Mass Spectrometry*, vol. 30, no. 21, pp. 2331–2340, 2016.

[36] A. U. Jackson, J. F. Garcia-Reyes, J. D. Harper et al., "Analysis of drugs of abuse in biofluids by low temperature plasma (LTP) ionization mass spectrometry," *Analyst*, vol. 135, no. 5, p. 927, 2010.

[37] T. Porta, C. Grivet, T. Kraemer, E. Varesio, and G. Hopfgartner, "Single hair cocaine consumption monitoring by mass spectrometric imaging," *Analytical Chemistry*, vol. 83, no. 11, pp. 4266–4272, 2011.

[38] B. Flinders, E. Beasley, R. M. Verlaan et al., "Optimization of sample preparation and instrumental parameters for the rapid analysis of drugs of abuse in hair samples by MALDI-MS/MS imaging," *Journal of The American Society for Mass Spectrometry*, vol. 28, no. 11, pp. 2462–2468, 2017.

[39] K. M. Ostermann, A. Luf, N. M. Lutsch et al., "MALDI orbitrap mass spectrometry for fast and simplified analysis of novel street and designer drugs," *Clinica Chimica Acta*, vol. 433, pp. 254–258, 2014.

[40] H. Wang and Y. Wang, "Matrix-assisted laser desorption/ionization mass spectrometric imaging for the rapid segmental analysis of methamphetamine in a single hair using umbelliferone as a matrix," *Analytica Chimica Acta*, vol. 975, pp. 42–51, 2017.

[41] A. Kernalléguen, R. Steinhoff, S. Bachler et al., "High-throughput monitoring of cocaine and its metabolites in hair using microarrays for mass spectrometry and matrix-assisted laser desorption/ionization-tandem mass spectrometry," *Analytical Chemistry*, vol. 90, no. 3, pp. 2302–2309, 2018.

[42] E. Cuypers et al., "Article a closer look into the consequences of decontamination procedures in forensic hair analysis using MetA-SIMS analysis," *Analytical Chemistry*, 2016.

[43] E. Cuypers, B. Flinders, C. M. Boone et al., "Consequences of decontamination procedures in forensic hair analysis using metal-assisted secondary ion mass spectrometry analysis," *Analytical Chemistry*, vol. 88, no. 6, pp. 3091–3097, 2016.

[44] J. A. Michely, M. R. Meyer, and H. H. Maurer, "Paper spray ionization coupled to high resolution tandem mass spectrometry for comprehensive urine drug testing in comparison to liquid chromatography-coupled techniques after urine precipitation or dried urine spot workup," *Analytical Chemistry*, vol. 89, no. 21, pp. 11779–11786, 2017.

[45] T. C. De Carvalho, F. Tosato, L. M. Souza et al., "Thin layer chromatography coupled to paper spray ionization mass spectrometry for cocaine and its adulterants analysis," *Forensic Science International*, vol. 262, pp. 56–65, 2016.

[46] R. D. Espy, S. F. Teunissen, N. E. Manicke et al., "Paper spray and extraction spray mass spectrometry for the direct and simultaneous quantification of eight drugs of abuse in whole blood," *Analytical Chemistry*, vol. 86, no. 15, pp. 7712–7718, 2014.

[47] E. Domingos, T. C. de Carvalho, I. Pereira et al., "Paper spray ionization mass spectrometry applied to forensic chemistry–drugs of abuse, inks and questioned documents," *Analytical Methods*, vol. 9, no. 30, pp. 4400–4409, 2017.

[48] J. McKenna, R. Jett, K. Shanks, and N. E. Manicke, "Toxicological drug screening using paper spray high-resolution tandem mass spectrometry (HR-MS/MS)," *Journal of Analytical Toxicology*, vol. 42, no. 5, pp. 300–310, 2018.

[49] L. S. Tavares, T. C. Carvalho, W. Romão, B. G. Vaz, and A. R. Chaves, "Paper spray tandem mass spectrometry based on molecularly imprinted polymer substrate for cocaine analysis in oral fluid," *Journal of The American Society for Mass Spectrometry*, vol. 29, no. 3, pp. 566–572, 2017.

[50] A. J. Midey, A. Patel, C. Moraff, C. A. Krueger, and C. Wu, "Improved detection of drugs of abuse using high-performance ion mobility spectrometry with electrospray ionization (ESI-HPIMS) for urine matrices," *Talanta*, vol. 116, pp. 77–83, 2013.

[51] T. Gabowitcz, D. Ridjosic, and S. Nacson, *Ion Mobility Spectrometer Having Improved Sample Receiving Device, US 2008/0101995 A1*, 2008.

[52] A. B. Hall, S. L. Coy, E. G. Nazarov, and P. Vouros, "Rapid separation and characterization of cocaine and cocaine cutting agents by differential mobility spectrometry-mass spectrometry," *Journal of Forensic Sciences*, vol. 57, no. 3, pp. 750–756, 2012.

[53] E. Jagerdeo, J. A. Clark, J. N. Leibowitz, and L. J. Reda, "Rapid analysis of forensic samples using an atmospheric solid analysis probe interfaced to a linear ion trap mass spectrometer," *Rapid Communications in Mass Spectrometry*, vol. 29, no. 2, pp. 205–212, 2015.

[54] J. Wu, C. S. Hughes, P. Picard et al., "High-throughput cytochrome P450 inhibition assays using laser diode thermal desorption-atmospheric pressure chemical ionization-tandem mass spectrometry," *Analytical Chemistry*, vol. 79, no. 12, pp. 4657–4665, 2007.

[55] A. Amirav, "Fast heroin and cocaine analysis by GC–MS with cold EI: the important role of flow programming," *Chromatographia*, vol. 80, no. 2, pp. 295–300, 2017.

[56] M. K. Woźniak, M. Wiergowski, J. Aszyk, P. Kubica, J. Namieśnik, and M. Biziuk, "Application of gas chromatography–tandem mass spectrometry for the determination of amphetamine-type stimulants in blood and urine," *Journal of Pharmaceutical and Biomedical Analysis*, vol. 148, pp. 58–64, 2018.

[57] F. Versace, F. Sporkert, P. Mangin, and C. Staub, "Rapid sample pre-treatment prior to GC–MS and GC–MS/MS urinary toxicological screening," *Talanta*, vol. 101, pp. 299–306, 2012.

[58] E. S. Emídio, V. de Menezes Prata, and H. S. Dórea, "Validation of an analytical method for analysis of cannabinoids in hair by headspace solid-phase microextraction and gas chromatography–ion trap tandem mass spectrometry," *Analytica Chimica Acta*, vol. 670, no. 1-2, pp. 63–71, 2010.

[59] K. Zaitsu, H. Miyagawa, Y. Sakamoto et al., "Mass spectrometric differentiation of the isomers of mono-methoxyethylamphetamines and mono-methoxydimethylamphetamines by GC–EI–MS–MS," *Forensic Toxicology*, vol. 31, no. 2, pp. 292–300, 2013.

[60] R. Andrews and S. Paterson, "A validated method for the analysis of cannabinoids in post-mortem blood using liquid–liquid extraction and two-dimensional gas chromatography–mass spectrometry," *Forensic Science International*, vol. 222, no. 1–3, pp. 111–117, 2012.

[61] G. Milman, A. J. Barnes, R. H. Lowe, and M. A. Huestis, "Simultaneous quantification of cannabinoids and metabolites in oral fluid by two-dimensional gas chromatography mass spectrometry," *Journal of Chromatography A*, vol. 1217, no. 9, pp. 1513–1521, 2010.

[62] B. Guthery, T. Bassindale, A. Bassindale, C. T. Pillinger, and G. H. Morgan, "Qualitative drug analysis of hair extracts by comprehensive two-dimensional gas chromatography/time-of-flight mass spectrometry," *Journal of Chromatography A*, vol. 1217, no. 26, pp. 4402–4410, 2010.

[63] A. Salomone, E. Gerace, F. D'Urso, D. Di Corcia, and M. Vincenti, "Simultaneous analysis of several synthetic cannabinoids, THC, CBD and CBN, in hair by ultra-high performance liquid chromatography tandem mass spectrometry. Method validation and application to real samples," *Journal of Mass Spectrometry*, vol. 47, no. 5, pp. 604–610, 2012.

[64] M. Sundström, A. Pelander, V. Angerer, M. Hutter, S. Kneisel, and I. Ojanperä, "A high-sensitivity ultra-high performance liquid chromatography/high- resolution time-of-flight mass spectrometry (UHPLC-HR-TOFMS) method for screening synthetic cannabinoids and other drugs of abuse in urine," *Analytical and Bioanalytical Chemistry*, vol. 405, no. 26, pp. 8463–8474, 2013.

[65] E. Partridge, S. Trobbiani, P. Stockham, T. Scott, and C. Kostakis, "A validated method for the screening of 320 forensically significant compounds in blood by LC/QTOF, with simultaneous quantification of selected compounds," *Journal of Analytical Toxicology*, vol. 42, no. 4, pp. 220–231, 2018.

[66] I.-T. Wang, Y.-T. Feng, and C.-Y. Chen, "Determination of 17 illicit drugs in oral fluid using isotope dilution ultra-high performance liquid chromatography/tandem mass spectrometry with three atmospheric pressure ionizations," *Journal of Chromatography B*, vol. 878, no. 30, pp. 3095–3105, 2010.

[67] A. G. Helfer, J. A. Michely, A. A. Weber, M. R. Meyer, and H. H. Maurer, "Orbitrap technology for comprehensive metabolite-based liquid chromatographic–high resolution-tandem mass spectrometric urine drug screening–exemplified for cardiovascular drugs," *Analytica Chimica Acta*, vol. 891, pp. 221–233, 2015.

[68] T. R. Fiorentin, F. B. D'Avila, E. Comiran et al., "Simultaneous determination of cocaine/crack and its metabolites in oral fluid, urine and plasma by liquid chromatography-mass spectrometry and its application in drug users," *Journal of Pharmacological and Toxicological Methods*, vol. 86, pp. 60–66, 2017.

[69] A. E. Steuer, M. Poetzsch, L. Stock et al., "Development and validation of an ultra-fast and sensitive microflow liquid chromatography-tandem mass spectrometry (MFLC-MS/MS) method for quantification of LSD and its metabolites in plasma and application to a controlled LSD administration study in huma," *Drug Testing and Analysis*, vol. 9, no. 5, pp. 788–797, 2017.

[70] F. Xian, C. L. Hendrickson, and A. G. Marshall, "High resolution mass spectrometry," *Analytical Chemistry*, vol. 84, no. 2, pp. 708–719, 2012.

[71] D. Pasin, A. Cawley, S. Bidny, and S. Fu, "Current applications of high-resolution mass spectrometry for the analysis of new

psychoactive substances: a critical review," *Analytical and Bioanalytical Chemistry*, vol. 409, no. 25, pp. 5821–5836, 2017.

[72] J. D. Harper, N. A. Charipar, C. C. Mulligan, X. Zhang, R. G. Cooks, and Z. Ouyang, "Low-temperature plasma probe for ambient desorption ionization," *Analytical Chemistry*, vol. 80, no. 23, pp. 9097–9104, 2008.

[73] J. M. Wiseman, B. Gologan, and R. G. Cooks, "Mass spectrometry sampling under ambient conditions with desorption electrospray ionization," *Science*, vol. 306, no. 5695, pp. 471–474, 2004.

[74] A. E. Kirby, N. M. Lafrenière, B. Seale, P. I. Hendricks, R. G. Cooks, and A. R. Wheeler, "Analysis on the go: quantitation of drugs of abuse in dried urine with digital microfluidics and miniature mass spectrometry," *Analytical Chemistry*, vol. 86, no. 12, pp. 6121–6129, 2014.

[75] E. Jagerdeo and A. Wriston, "Rapid analysis of forensic-related samples using two ambient ionization techniques coupled to high-resolution mass spectrometers," *Rapid Communications in Mass Spectrometry*, vol. 31, no. 9, pp. 782–790, 2017.

Hindawi
Journal of Analytical Methods in Chemistry
Volume 2018, Article ID 7019204, 9 pages
https://doi.org/10.1155/2018/7019204

Research Article

Establishing Analytical Performance Criteria for the Global Reconnaissance of Antibiotics and Other Pharmaceutical Residues in the Aquatic Environment Using Liquid Chromatography-Tandem Mass Spectrometry

Luisa F. Angeles and Diana S. Aga

Department of Chemistry, The State University of New York, Buffalo, NY 14260, USA

Correspondence should be addressed to Diana S. Aga; dianaaga@buffalo.edu

Received 10 March 2018; Accepted 26 April 2018; Published 4 June 2018

Academic Editor: Veronica Termopoli

The occurrence of antibiotics in the environment from discharges of wastewater treatment plants (WWTPs) and from the land application of antibiotic-laden manure from animal agriculture is a critical global issue because these residues have been associated with the increased emergence of antibiotic resistance in the environment. In addition, other classes of pharmaceuticals and personal care products (PPCPs) have been found in effluents of municipal WWTPs, many of which persist in the receiving environments. Analysis of antibiotics by liquid chromatography-tandem mass spectrometry (LC-MS/MS) in samples from different countries presents unique challenges that should be considered, from ion suppression due to matrix effects, to lack of available stable isotopically labeled standards for accurate quantification. Understanding the caveats of LC-MS/MS is important for assessing samples with varying matrix complexity. Ion ratios between quantifying and qualifying ions have been used for quality assurance purposes; however, there is limited information regarding the significance of setting criteria for acceptable variabilities in their values in the literature. Upon investigation of 30 pharmaceuticals in WWTP influent and effluent samples, and in receiving surface water samples downstream and upstream of the WWTP, it was found that ion ratios have higher variabilities at lower concentrations in highly complex matrices, and the extent of variability may be exacerbated by the physicochemical properties of the analytes. In setting the acceptable ion ratio criterion, the overall mean, which was obtained by taking the average of the ion ratios at all concentrations (1.56 to 100 ppb), was used. Then, for many of the target analytes included in this study, the tolerance range was set at 40% for WWTP influent samples and 30% for WWTP effluent, upstream, and downstream samples. A separate tolerance range of 80% was set for tetracyclines and quinolones, which showed higher variations in the ion ratios compared to the other analytes.

1. Introduction

In recent years, studies have reported the occurrence of pharmaceuticals and personal care products (PPCPs), including antibiotics and selective serotonin reuptake inhibitors (SSRIs), in the environment [1–6]. These drugs are being released through different routes, such as discharges from wastewater treatment plant (WWTP) effluents to surface water, where hospitals and private households contribute a large volume of antibiotics and other pharmaceuticals [2, 7–9]. The presence of PPCPs in effluents of WWTPs in different geographical regions has been documented, with concentrations reported as high as about 125 μg/L [10]. In Germany, the environmental concentration in municipal sewage that comes from the discharge of antibiotics from hospitals and households is predicted to be about 71 mg/L annually [9]. The presence of high levels of pharmaceuticals in the environment has a wide range of ecological effects; for instance, antibiotics may contribute to the development of antibiotic resistance in bacteria due to selective pressure, which is a threat to global health [9, 11, 12].

Analysis of PPCPs in environmental samples is typically performed using liquid chromatography-tandem mass spectrometry (LC-MS/MS) to quantify pharmaceutical concentrations based on triple quadrupole MS [3, 6, 13]. The high selectivity and sensitivity obtained using triple quadrupole MS is achieved when performing selected reaction monitoring (SRM), where a precursor ion is isolated from the first quadrupole and fragmented in the collision cell, followed by isolating selected product ions in the third quadrupole. However, despite this high selectivity, there is still a possibility that a compound other than the target analyte will produce a signal that has a similar m/z value to either the qualifying ion or the quantifying ion at the same retention time [14], resulting in a significant deviation in the expected ion ratio for the selected fragment ions being monitored by the two SRM transitions.

In order to confirm the presence of a compound, the chromatographic peak must have both the quantitative and qualitative ion transitions with retention times matching those of the standard analyte. In addition, the ion ratio of the two SRM transitions has been used as an additional confirmation criterion, as stated in some legal documents from different organizations such as the European Union (EU) and the US Food and Drug Administration (US FDA), which provide guidelines for the analysis of official samples [15–19]. Having this additional criterion is important since LC-MS/MS has now become the mandatory technique for the analysis of official samples that are used for establishing legal policies [15–19]. Monitoring the ion ratios will provide improved confidence in reporting analyte concentrations, avoiding false positives and false negatives, which have been reported in the literature [14].

Different legal guidelines are currently available from the United Nations (UN), the EU, and the United States of America (USA). The UN set the ion ratio tolerance to be ±20% [16] for the testing of illicit drugs in seized materials and biological specimens. The European Commission Decision (2002/657/EC) requires a tolerance of ±20% to ±50% for the ion ratio, depending on the ion intensities [17], for analytical methods that are used for the testing of official samples in control laboratories. The European Workplace Drug Testing Society sets it at ±20% [19]. The US Department of Agriculture requires a ±20% tolerance in the ratio of the ion transitions [18], while the US FDA sets an ion ratio tolerance of ±20% and ±30% if 2 and 3 diagnostic ions are being monitored, respectively [15]. The weakness of these guidelines, however, is that they are not based on experimental data and are arbitrarily assigned.

Recent studies [20, 21] have been published on performance criteria for the analyses of pesticides in fruits and vegetables and veterinary drugs in biological matrices. For pesticides, a tolerance range of ±20% was established for all compounds at all concentrations, except when one or both product ions have an S/N of 3–15, in which case, a range of ±45% was set. For veterinary drugs, a fixed tolerance range of ±50% for all the compounds at all concentrations was set after evaluation of the ion ratios in different matrices such as muscle, urine, milk, and liver [20, 21]. However, these tolerance values cannot be used for PPCPs because the variability of ion ratios differs per compound and the nature of the sample matrix. This variability is due to differences in the ionization behavior of analytes and the extent of matrix effects. It is not unexpected to observe different effects on the ion ratios of the analytes in wastewater and surface water matrices because the composition of the interferences in environmental samples is different relative to biological samples.

Establishing performance criteria is important because it minimizes the occurrence of false-positive and false-negative detections. In fact, a doubling of false-positive detections was reported without the application of the ion ratio criterion in the analysis of veterinary drugs in the muscle, urine, milk, and liver [14]. Most published and existing methods do not mention the use of any ion ratio criteria [3, 6, 13]. In the US Environmental Protection Agency (EPA) Method 1694 for the determination of PPCPs in environmental samples by LC-MS/MS, the presence of a compound in a sample extract is confirmed when the signal-to-noise ratio (S/N) of the fragment ion of the compound is greater than or equal to 2.5 and its retention time is within ±15 seconds of the calibration verification standard. If these criteria are not met, then an experienced analyst must confirm the presence or absence of a compound [22]. Additionally, in the EPA Method 542, which is for the analysis of PPCPs in drinking water, the acceptable retention time window for the compounds in a sample is within 3 standard deviations for a series of injections. Quality control for this method involves the confirmation of the presence of the quantifying ion of the internal standard and requires that it must be within ±50% of the average area measured in the initial calibration [23]. No criteria regarding the ion ratios have been mentioned in both EPA methods. The absence of quality control measures in published methods may be due to the lack of suitable guidelines in the literature. In order to determine an appropriate tolerance value for the ion ratios, variabilities resulting from the physicochemical nature of the analytes should be investigated at high and low concentrations. The variability in the signal intensities of the qualifier ions is expected to be more significant than that of the quantifier ions because of the relatively lower signals for the qualifier ions.

The aim of this study is to validate and provide guidelines on the use of ion ratios as a criterion for quality control in reporting concentrations of PPCPs in wastewater and surface water samples with varying complexity. To achieve this goal, the ion ratios of 30 PPCPs in different matrices were determined at different concentrations in order to determine a tolerance value that is sufficient to eliminate false positives and false negatives. The matrices studied were WWTP influent and effluent samples and surface water samples from upstream and downstream of the WWTP discharge point collected from the US, Sweden, Switzerland, Hong Kong, and the Philippines, allowing the set tolerance levels to be robust, given that the composition of water samples varies significantly in different parts of the world. The data obtained from these analyses were the basis for the construction of a more accurate and reliable ion ratio criterion which takes into account the differences in the properties of compounds at different concentrations.

2. Materials and Methods

Acetaminophen (ACT), acetylsulfamethoxazole (ASMX), azithromycin (AZI), caffeine (CAF), carbamazepine (CBZ), clarithromycin (CLA), enrofloxacin (ENRO), erythromycin (ERY), iopamidol (IOPA), norfloxacin (NOR), oxytetracycline (OTC), sarafloxacin (SARA), sulfachloropyridazine (SCP), sulfadiazine (SPD), sulfadimethoxine (SDM), sulfamerazine (SMR), sulfameter (SMT), sulfamethazine (SMZ), sulfamethizole (SMI), sulfamethoxazole (SMX), tetracycline (TC), and trimethoprim (TMP) were purchased from Sigma-Aldrich. Ciprofloxacin (CIP) and diclofenac (DIC) were obtained from Cambridge Isotope Laboratories, Inc. (Tewksbury, MA). Sulfathiazole was purchased from ICN Biomedicals, Inc. (Irvine, CA). Carbamazepine-d10 (d10-CBZ) was purchased from CDN Isotopes (Quebec, Canada). Chlortetracycline (CTC) was obtained from Acros Organics (VWR International, Westchester, PA). Paroxetine maleate (PRX) and venlafaxine (VEN) were obtained from Cerilliant (Sigma-Aldrich, St Louis, MO). The Barnstead NANOpure™ DIamond (Waltham, MA) purification system was used to obtain 18.2 MΩ water. LC-MS grade methanol and acetonitrile were obtained from EMD Millipore Corporation (Billerica, MA), and formic acid (88%) was purchased from Fisher Chemical (Pittsburgh, PA). Oasis™ HLB solid-phase extraction (SPE) cartridges were purchased from Waters (Milford, MA).

2.1. Sample Preparation. Wastewater and surface water samples (0.5 L) were collected in amber glass bottles which were pre-rinsed with 10% nitric acid. The samples were acidified to about pH 2.5 using 40% phosphoric acid and then passed through 0.45 μm glass microfiber filters to remove microorganisms and particulate matter. Then, 2 mL of Na_2EDTA (5% *w*/*v* in water) was added to each sample. The samples were then spiked with surrogate standards (50 μL of 1000 μg/L surrogate mix solution).

The samples were passed through Oasis HLB SPE cartridges (500 mg, 6 cc) for cleanup and concentration. The SPE cartridges were first conditioned with 6 mL acetonitrile, followed by 6 mL NANOpure water, before the water samples were loaded at a rate of approximately 3–5 mL/min. After loading, the cartridges were dried by keeping them on the SPE manifold with the vacuum on. Then, the SPE cartridges were wrapped in aluminum foil, stored in Ziploc® bags, and shipped with ice to the University at Buffalo for elution and LC-MS/MS analysis. Once received, the samples were eluted using 8 mL of acetonitrile and then dried under N_2 gas at 35°C. The samples were then spiked with 100 ppb of the internal standard, carbamazepine-d10, in order to account for possible differences in measurements in-between injections due to variations caused by the instrument.

2.2. LC-MS/MS Analysis. A Waters Cortecs™ $C18^+$ column (Milford, MA) with dimensions 2.1 × 150 mm and 2.7 μm particle size was used for the separation of the 30 PPCPs. Analysis was performed using an Agilent 1200 LC system (Palo Alto, CA) and a Thermo Scientific TSQ Quantum Ultra triple quadrupole MS (Waltham, MA) equipped with a heated electrospray ionization (HESI) probe, operated under positive ionization mode. Timed-SRM mode transition was performed, and the SRM transitions used for the compounds are shown in Table S1.

Table 1: Target pharmaceuticals used for establishing the ion ratio criterion.

Class	Compound
Antibiotics	
Macrolides	Anhydroerythromycin
	Azithromycin
	Clarithromycin
Quinolones	Ciprofloxacin
	Enrofloxacin
	Norfloxacin
	Sarafloxacin
Sulfonamides	Acetylsulfamethoxazole
	Sulfachloropyridazine
	Sulfadiazine
	Sulfadimethoxine
	Sulfamerazine
	Sulfamethazine
	Sulfamethizole
	Sulfamethoxazole
	Sulfamethoxydiazine
	Sulfathiazole
Tetracyclines	Chlortetracycline
	Oxytetracycline
	Tetracycline
Other PPCPs	
	Acetaminophen
	Caffeine
	Carbamazepine
	Diclofenac
	Iopamidol
	Trimethoprim
	Bupropion
	Paroxetine
	Sertraline
	Venlafaxine

The mobile phase used for the separation consisted of aqueous 0.3% formic acid (A), and 75% methanol and 25% acetonitrile (B). The gradient began with 90% A and 10% B for three minutes and is ramped up linearly to 100% B for 22 min; this condition was kept for 5 min before it was switched back to 90% A, where it was maintained for 14 min to allow for column equilibration. The flow rate was set at 0.2 mL/min, and the total run time was 45 min.

The spray setting used for the MS was as follows: spray voltage 3000 V, ion sweep gas pressure 0 arbitrary units, vaporizer temperature 350°C, sheath gas pressure 40 arbitrary units (N_2), auxiliary gas pressure 35 arbitrary units (N_2), capillary temperature 325°C, collision gas pressure 1.5 mTorr (Ar), cycle time 0.300 s, and Q1 peak width 0.70 FWHM.

2.3. Design of the Study

2.3.1. Assessment of Ion Ratio Behavior of PPCPs across Varying Concentrations. A total of 30 PPCPs were studied

for the development of an ion ratio criterion (Table 1). A mixture of all the native PPCP standards was prepared using the starting mobile phase of the LC-MS/MS method as the solvent. An initial solution of 100 ppb (μg/L) was made, and then it was serially diluted to obtain mixtures with concentrations of 50, 25, 12.5, 6.25, 3.13, and 1.56 ppb. These standards were analyzed by LC-MS/MS, with nine replicates for each concentration, to obtain the areas of both the quantifying and qualifying ions. The ion ratios were calculated by dividing the area of the quantifying ion by the area of the qualifying ion for each analyte. The average ion ratio and the deviations from the average value for the ion ratios were calculated at all concentrations for each compound.

2.3.2. Assessment of Ion Ratio Behavior of Pharmaceuticals in the Matrix. Samples from WWTP influents and effluents and from receiving surface waters upstream and downstream of the WWTPs were collected from selected sites in five countries: Central, Hong Kong; Manila, Philippines; Vastergotland, Sweden; Zurich, Switzerland; and Virginia, US. The samples from the Philippines were collected in December 2016, while the others were collected in June or July 2016. The exact names and locations of the WWTPs cannot be disclosed as part of the agreement with the WWTP operations. A total of 19 samples were each spiked with 1.56 ppb, 12.5 ppb, 25 ppb, and 100 ppb of the native standard mix and were analyzed by LC-MS/MS to determine the mean ion ratios and standard deviations from the mean for each compound. The variabilities of the ion ratios in the different sample matrices were then evaluated and compared with the values observed in the standards.

2.3.3. Optimization of the Ion Ratio Criterion. The proposed formula to be used in order to optimize the appropriate ion ratio tolerance that will give the least false negative is a mean ion ratio and a tolerance range that will account for variations in the sample matrix. This tolerance range should not be too wide so as to avoid having false positives. To determine the optimum tolerance level, different values were tested for all compounds; the same test was also used to determine whether a single tolerance range would be used for all the matrices or if different ones should be used for wastewater and for surface water. To check the appropriateness of the selected tolerance values, the number of false negatives will be determined using the water extracts spiked with known amounts of standards.

3. Results and Discussion

3.1. Ion Ratio Variability at Different Concentrations. A total of 30 PPCPs, which include 23 antibiotics, were studied for the development of an ion ratio criterion (Table 1). The classes of antibiotics that were included in this study were sulfonamides, macrolides, quinolones, and tetracyclines.

First, the ion ratio behavior of the compounds was studied at different concentrations by analyzing nine replicates of the standard solutions of 1.56, 3.13, 6.25, 12.5, 25.0, 50.0, and 100 ppb in the LC-MS/MS. The overall mean, which is the average ion ratio of all nine replicates at all concentrations, was obtained for each compound (Table S2). The relative percent deviation was then calculated by subtracting the overall mean from each of the data points and then dividing by the overall mean. These values were then plotted against the seven concentrations to see how the ion ratios at each concentration vary from the overall mean of each compound, as shown in Figure 1. The trend for all the compounds is that the variation is highest at the lowest concentration. The average relative standard deviation for all the compounds at 1.56 ppb was 18%, while that for compounds at 100 ppb was only 4%. These results indicate that the differences in the ion ratios at different concentrations should be taken into account because if only one tolerance limit is applied across all concentrations, it is likely that false-negative results will occur at low concentrations, especially at concentrations between 1.56 to 12.5 ppb.

The general trend in the ion ratios for 23 PPCPs is shown in Figure 1; a separate plot for tetracyclines and quinolones was prepared (Figure 2) because the variabilities in the ion

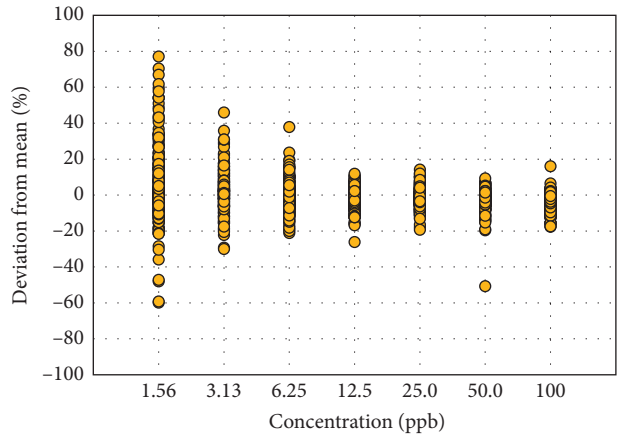

Figure 1: Deviation of ion ratios from the overall mean across different concentrations of 23 PPCPs without tetracyclines and quinolones.

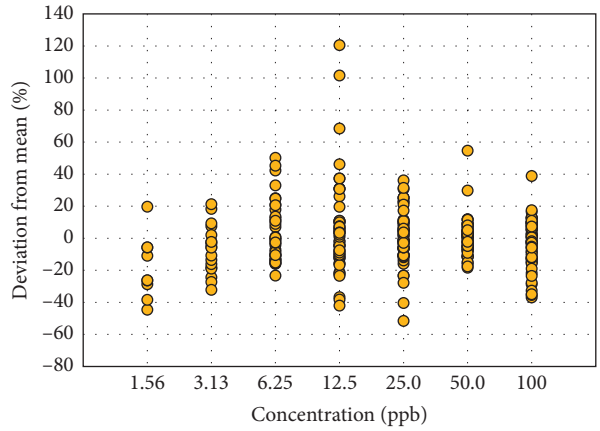

Figure 2: Deviation of ion ratios of tetracyclines and quinolones from the overall mean across different concentrations.

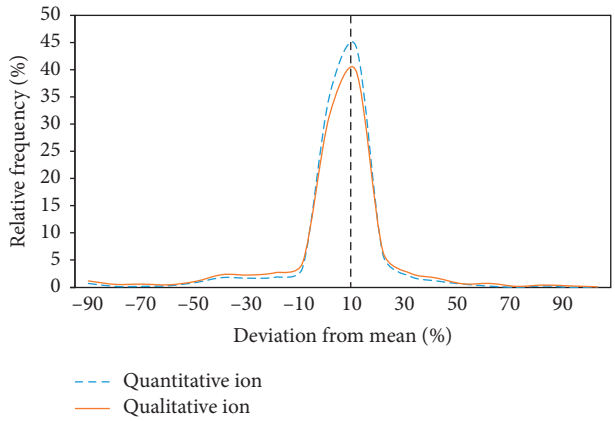

Figure 3: Distribution of the deviation of the quantitative and qualitative ion areas from the mean.

ratios were notably higher in these classes of antibiotics than the rest of the PPCPs. Data points at lower concentrations of some compounds were removed in cases where the qualitative ion was not detectable. For example, oxytetracycline was not detected below 25 ppb, chlortetracycline and tetracycline were not detected below 12.5 ppb, sarafloxacin and norfloxacin were not detected below 6.25 ppb, and enrofloxacin was not detected at 1.56 ppb. Therefore, a separate chart (Figure 2) was created for tetracyclines and quinolones since they do not follow the same behavior as the other pharmaceuticals. Based on these data, a separate ion ratio tolerance range is needed for tetracyclines and quinolones in order to capture the wide variations, without affecting the other compounds. It can be observed that the variations in Figure 2 are lower at 1.56 ppb compared to the higher concentrations, but this is because most of these compounds were no longer detected at 1.56 ppb, and these data points were removed in the chart. The deviation from the mean reaches up to 120% at 12.5 ppb for tetracyclines and up to 50% for quinolones at 6.25 ppb. At the highest concentration of 100 ppb, the deviations from the mean in both tetracyclines and quinolones are at 40%, while those for the other PPCPs are only 20%.

The areas of both the quantitative and qualitative ions were investigated separately in order to identify which of the two ions causes high variations. The deviations in the areas of these ions from the mean were calculated and compared with each other. Since the distribution of variation of both the qualitative and quantitative areas is similar, as seen in Figure 3, this means that both of them contribute equally to the variations, and the ion ratio deviations cannot be attributed to just the quantitative or qualitative ion alone.

3.2. Ion Ratio Variability in Wastewater and Surface Water Matrices. A total of 19 different samples were spiked with the pharmaceutical standards at 4 concentrations: 1.56, 12.5, 25.0, and 100 ppb, in order to determine how the differences in the nature of the matrices influence the ion ratios.

Figure 4 shows how the ion ratios change in the influent, effluent, upstream, and downstream water samples in comparison with the clean standard. It can be seen that the variations are higher in the wastewater as compared to those of the surface water samples, with relative standard deviation values of 13%, 11%, 10%, and 9%, for the influent, effluent, downstream, and upstream samples, respectively. This trend was expected since the upstream and downstream samples are less-complex matrices (lower organic matter content than wastewater). It can be seen in the lowest concentration studied (1.56 ppb) that the standards in the clean matrix varied more than the ones spiked in the samples, with relative standard deviations of 18% for the standards and 20%, 14%, 15%, and 12% for the influent, effluent, downstream, and upstream samples, respectively. This is due to the removal of 22 data points at 1.56 ppb because the qualitative ions were no longer detected in the samples.

3.3. Optimization of a Tolerance Range for the Ion Ratio Criterion. The formula for the ion ratio criterion that was used is a tolerance range from the mean of each standard compound in the clean matrix. This tolerance range should account for the deviations because of differences in concentrations and the matrix being analyzed. The goal in setting this range is to have the least number of false positives and false negatives. False negatives will occur when the ion ratio of analytes in spiked environmental samples does not meet the tolerance criteria such that the analyte in question will be considered "nondetect." On the contrary, one cannot set a tolerance range too wide that will likely result in a significant number of false positives. Therefore, a range that will still capture all the variations at the 95% confidence level in both matrices and at different concentrations is needed.

In order to provide an appropriate criterion, the overall mean, which is obtained by taking the average of the ion ratios at all concentrations (1.56 to 100 ppb), will be used. This way, the variations of the ion ratios from low to high concentrations will be taken into account. The tolerance range must then be optimized for the spiked matrices. Tolerance ranges from 10% to 50% were tested to see which one will give the least number of false negatives for each of the water matrices (Table 2). The overall false-negative rate is the weighted average of the percent false negatives for each matrix type.

Since the tetracyclines and quinolones were found to have greater variations than the rest of the PPCPs as seen in Figure 2, a test was performed to check if tetracyclines and quinolones should use a different tolerance level than what is used for the other classes of PPCPs. Table 3 shows the percentage of false negatives in the samples when the tetracyclines and quinolones were removed. If tetracyclines and quinolones were included, a tolerance range of 50% would give a false-negative result of ≤5%. If removed, a tolerance range of 30% would be enough to give the same value of ≤5% for false negatives.

It is important to have a separate tolerance range for tetracyclines and quinolones because as seen in Table 2, a tolerance range of 50% is needed in order to capture them at the 95% confidence level. This value, however, would be too high for the other PPCPs, where only 30% is required to

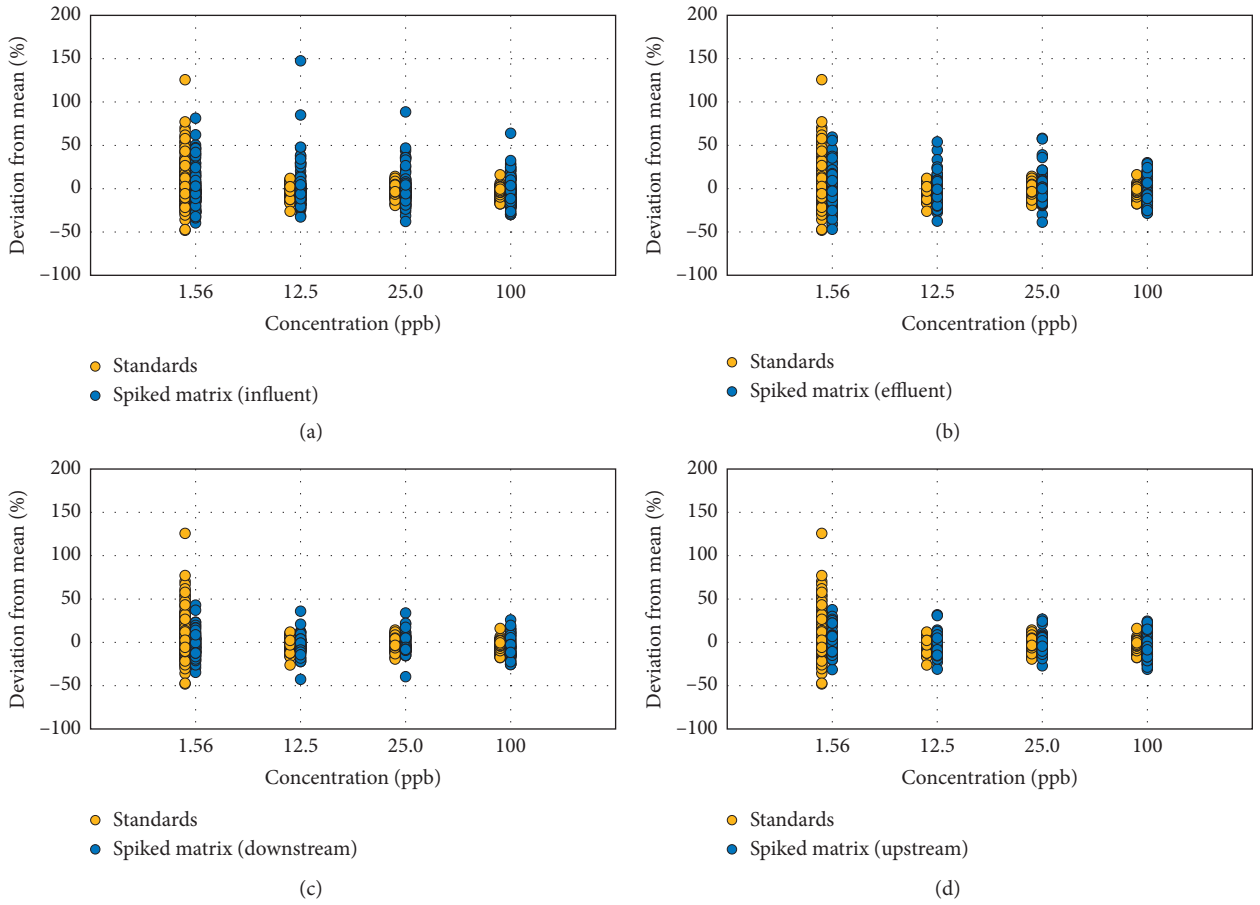

Figure 4: Comparison of ion ratios in spiked matrices and in clean standards. (a) WWTP influent samples; (b) WWTP effluent samples; (c) upstream surface water samples; (d) downstream surface water samples.

Table 2: Percent false negatives in spiked environmental matrices at different tolerance ranges for all 30 PPCPs.

Tolerance range	Matrix				Overall false negatives
	Influent	Effluent	Downstream	Upstream	
±10%	54%	49%	47%	42%	38%
±20%	26%	20%	16%	14%	16%
±30%	13%	9%	7%	6%	8%
±40%	8%	6%	4%	3%	6%
±50%	5%	4%	2%	2%	4%

Table 3: Percent false negatives in spiked environmental matrices at different tolerance ranges for 23 compounds without tetracyclines and quinolones.

Tolerance range	Matrix				Overall false negatives
	Influent	Effluent	Downstream	Upstream	
±10%	48%	42%	41%	35%	31%
±20%	20%	13%	10%	8%	10%
±30%	8%	4%	2%	2%	4%
±40%	4%	2%	0%	0%	2%
±50%	2%	1%	0%	0%	1%

have the same confidence level (Table 3). Therefore, a fixed tolerance range of 50% for all compounds could potentially result in high false negatives for tetracyclines and quinolones and high false positives for the other PPCPs. Also, at the 50% tolerance range, even if the overall false negatives were already below 5% for many PPCPs, as seen in Table 2, it was observed that the tetracyclines and quinolones still had very high values, with ciprofloxacin having 96% false negatives (Table 4).

For chlortetracycline, ciprofloxacin, enrofloxacin, norfloxacin, and tetracycline, the range needed to be from 70%

Table 4: Percent false negatives for tetracyclines and quinolones at the 50% tolerance range in spiked environmental matrices.

Compounds	Matrix				Overall false negatives
	Influent	Effluent	Downstream	Upstream	
Chlortetracycline	10%	0%	0%	0%	2%
Ciprofloxacin	96%	71%	33%	13%	61%
Enrofloxacin	5%	0%	0%	0%	1%
Norfloxacin	0%	4%	0%	0%	1%
Oxytetracycline	0%	30%	29%	22%	21%
Sarafloxacin	12%	16%	0%	20%	13%
Tetracycline	11%	0%	0%	0%	3%

Table 5: Percent false negatives for tetracyclines and quinolones in spiked environmental matrices at the 80% tolerance range.

Compounds	Matrix				Overall false negatives
	Influent	Effluent	Downstream	Upstream	
Chlortetracycline	10%	0%	0%	0%	2%
Ciprofloxacin	0%	0%	0%	0%	0%
Enrofloxacin	0%	0%	0%	0%	0%
Norfloxacin	0%	4%	0%	0%	1%
Oxytetracycline	0%	0%	29%	0%	6%
Sarafloxacin	6%	11%	0%	20%	10%
Tetracycline	0%	0%	0%	0%	0%

Table 6: Results of the application of the ion ratio criterion in real wastewater and surface water samples.

Matrix	Tolerance range	Total no. of detections	No. of detections outside the range
Influent	±40%	102	0
Effluent	±30%	90	2
Downstream	±30%	37	2
Upstream	±30%	39	1

A number of detections outside the range are data points that were considered positive detections but had ion ratios outside the set tolerance range.

to 85% in order to have a false-negative rate of ≤5%. Oxytetracycline and sarafloxacin, on the contrary, still have false negatives of up to 29% (downstream) and 20% (upstream), respectively, at a tolerance range of 80% (Table 5). However, setting a wider range may result in greater probability of false positives. Therefore, a tolerance range of 80% was set for the tetracyclines and quinolones, but it is recommended that other criteria such as retention time, peak areas, and the number of points per peak be investigated more carefully in the confirmation of these compounds.

Once the acceptable tolerance range for the mean ion ratio for each analyte was established based on spiked environmental samples, the ion ratio in each sample matrix was also assessed in order to adjust this range accordingly for the influent, effluent, upstream, and downstream samples. The tolerance range that would give ≤5% false negatives was recorded for each matrix type. These values were 40% for the influent samples and 30% for the effluent, upstream, and downstream samples (Table 3). It is expected that the compounds would have higher variations in more complex matrices such as the influent. Since the tolerance range for the influent differed by 10%, it is recommended to establish a different tolerance limit for influent samples to avoid a high false-negative rate in this matrix. If a fixed range of ±20% is used as the tolerance value (Table 2) for all types of matrices, the number of false negatives would be much higher, 26%, 20%, 16%, and 14%, for the influent, effluent, downstream, and upstream samples, respectively. Therefore, it is important to have a separate tolerance range for certain compounds in different environmental matrices.

3.4. Applying the Optimized Ion Ratio Criterion in Real Water Samples from around the World. The optimized ion ratio criterion for each of the target PPCPs was applied to real environmental samples that were not spiked with standards. These samples were wastewater influents and effluents and receiving surface waters which are located upstream and downstream of the respective WWTPs, collected from 5 different countries. For influent samples, an analyte is said to be positively detected in the sample if its ion ratio is within the mean ± 40% of the reference standard. For effluent, upstream, and downstream samples, analytes with the mean ion ratio within ±30% of the standards are considered positive detection. Note that the results in Table 6 do not include detections for tetracyclines and quinolones, for which a different tolerance range was set.

The compounds that were detected outside the range were acetylsulfamethoxazole in the effluent samples, azithromycin in the effluent and upstream samples, and clarithromycin in the downstream samples, with the details shown in Table 7.

Table 7: Compounds with ion ratios detected outside the set tolerance range of ±40% for WWTP influent samples and 30% for WWTP effluent, upstream, and downstream samples.

Matrix	Compound	Tolerance range	Calculated ion ratio
Effluent	Acetylsulfamethoxazole	0.88–1.64	1.74
	Azithromycin	1.89–3-5	1.86
Downstream	Clarithromycin	1.28–2.38	2.41
	Clarithromycin	1.28–2.38	2.42
Upstream	Azithromycin	1.89–3-5	1.74

The compounds with ion ratios that fell outside the set tolerance range were investigated individually to confirm if these were real detections or not by checking the presence of both the quantitative and qualitative ions and if the shift in retention time is not more than 0.5 min. It was found that all of them had both ions, and their retention times were within the acceptable range. Since their calculated ion ratios are still close to the limits of the range, these were still considered as positive detections. In cases like this where the calculated ion ratios are close to the limits of the range and retention times are within the acceptable shift, it is recommended that the qualitative ion be checked to make sure that its signal is at least 3 times that of the noise (Table 6).

A total number of 37 detections for ciprofloxacin, norfloxacin, and tetracycline were found for tetracyclines and quinolones in the samples. The ion ratios of all 37 peaks in all matrices were within the set tolerance range of 80%, and they passed other criteria for peak confirmation.

An example of a false-positive detection that was found through the use of the ion ratio is diclofenac. The quantitative and qualitative ion transitions of diclofenac are 296 → 214 and 296 → 250 and its retention time is at 27.5 min. Figure 5 shows a comparison of the two chromatograms, both of which have peaks at 27 min for both SRM transitions.

When the ion ratios were calculated, an influent sample (Figure 5) gave an ion ratio of 0.15, which falls outside the range for diclofenac in the influent which is from 1.57 to 3.67. Furthermore, it can be observed that, for WWTP A, the retention time of the qualitative ion, which is at 27.16 min, is slightly different from that of the quantitative one at 27.78 min, further proving that this is a false-positive detection since the retention times of both ions should be the same. Upon removal of 7 false-positive diclofenac peaks that did not match the ion ratio criterion and retention times for both the quantitative and qualitative ions, the total number of detections was reduced from 312 to 305.

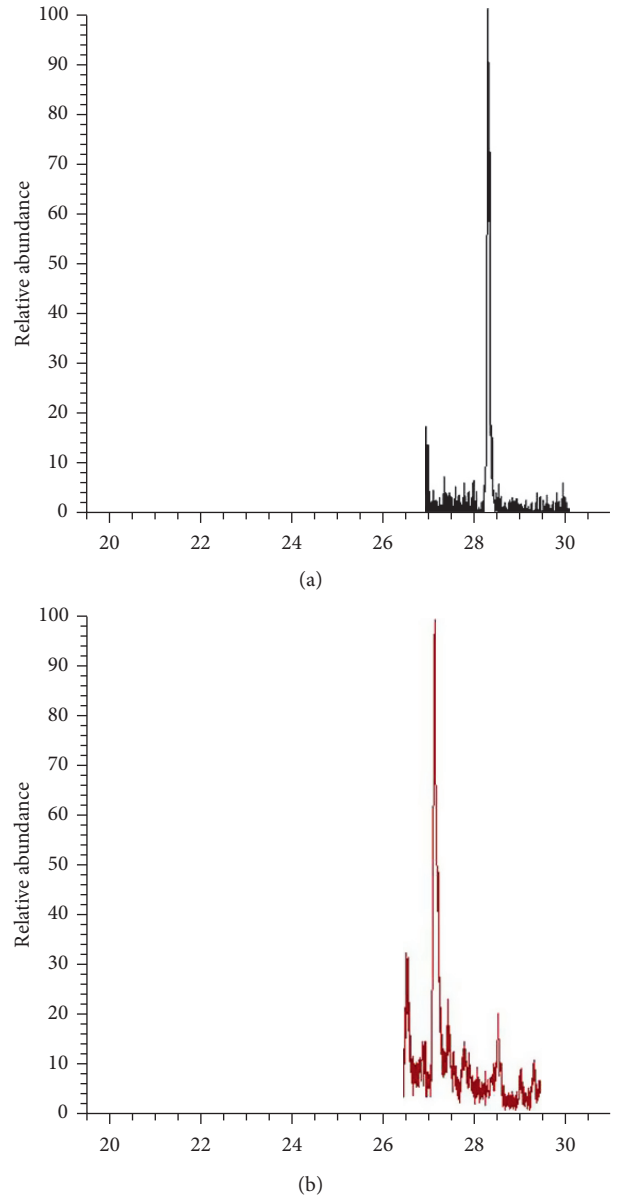

Figure 5: False-positive detection of diclofenac in wastewater. The calculated ion ratio, 0.15, falls outside the ion ratio tolerance range of 1.57 to 3.67. The chromatograms show (a) the peak for the quantitative ion with a transition of 296 → 214 and (b) the peak for the qualitative ion with a transition of 296 → 250.

4. Conclusions

An ion ratio criterion has been optimized for six classes of pharmaceuticals in wastewater and surface water using LC-MS/MS. For 23 PPCPs, values for mean ± tolerance for the ion ratios in the different types of environmental matrices were established based on the variabilities of the ion ratios in spiked samples. The variabilities of the ion ratios of the compounds were found to increase at lower concentrations from 4% at 100 ppb to 18% at 1.56 ppb. Therefore, the mean ion ratio that was used in the formula is the average of the ion ratios from 1.56, 3.13, 6.25, 12.5, 25, 50, and 100 ppb so that it can capture the variations at different concentrations. The ion ratios for tetracyclines and quinolones were found to have higher variations, which are twice that of the other PPCPs; therefore, these two classes of compounds were analyzed separately so as not to increase the possibility of false positives for the other compound classes. For tetracyclines and quinolones, the tolerance range was set to 80%, but it is recommended that other criteria such as retention time, peak areas, and the number of points per peak be investigated carefully before reporting their detections.

For the sulfonamides, macrolides, SSRIs, and other PPCPs, the ion ratios were studied in the different

environmental matrices. It was found that the variations also increase with the complexity of the matrix. The optimized tolerance range that would give <5% false negatives was 40% for the influent and 30% for the effluent, upstream, and downstream. This optimized ion ratio criterion was then applied to real wastewater and surface water samples that were not spiked with standards and resulted in the reduction of the total number of detections from 312 to 305, after false positives were eliminated.

Data Availability

All data underlying the findings of this study can be accessed in the supplementary information provided.

Conflicts of Interest

The authors declare that they have no conflicts of interest.

Acknowledgments

The authors would like to acknowledge support from the National Science Foundation (PIRE-HEARD, Award no. 1545756).

Supplementary Materials

Table S1: retention time and transitions of pharmaceuticals in the study. Table S2: average ion ratios of pharmaceuticals at different concentrations. (*Supplementary Materials*)

References

[1] P. Arnnok, R. R. Singh, R. Burakham, A. Pérez-Fuentetaja, and D. S. Aga, "Selective uptsake and bioaccumulation of antidepressants in fish from effluent-impacted Niagara River," *Environmental Science and Technology*, vol. 51, no. 18, pp. 10652–10662, 2017.

[2] K. Kummerer, "Antibiotics in the aquatic environment–a review–part I," *Chemosphere*, vol. 75, no. 4, pp. 417–434, 2009.

[3] I. Senta, I. Krizman-Matasic, S. Terzic, and M. Ahel, "Comprehensive determination of macrolide antibiotics, their synthesis intermediates and transformation products in wastewater effluents and ambient waters by liquid chromatography-tandem mass spectrometry," *Journal of Chromatography A*, vol. 1509, pp. 60–68, 2017.

[4] I. Senta, S. Terzić, and M. Ahel, "Simultaneous determination of sulfonamides, fluoroquinolones, macrolides and trimethoprim in wastewater and river water by LC-tandem-MS," *Chromatographia*, vol. 68, no. 9-10, pp. 747–758, 2008.

[5] L. J. Zhou, G. G. Ying, S. Liu et al., "Occurrence and fate of eleven classes of antibiotics in two typical wastewater treatment plants in South China," *Science of the Total Environment*, vol. 452-453, pp. 365–376, 2013.

[6] M. Pedrouzo, F. Borrull, R. M. Marce, and E. Pocurull, "Ultra-high-performance liquid chromatography-tandem mass spectrometry for determining the presence of eleven personal care products in surface and wastewaters," *Journal of Chromatography A*, vol. 1216, no. 42, pp. 6994–7000, 2009.

[7] E. Kristiansson, J. Fick, A. Janzon et al., "Pyrosequencing of antibiotic-contaminated river sediments reveals high levels of resistance and gene transfer elements," *PLoS one*, vol. 6, no. 2, article e17038, 2011.

[8] L. Rizzo, C. Manaia, C. Merlin et al., "Urban wastewater treatment plants as hotspots for antibiotic resistant bacteria and genes spread into the environment: a review," *Science of the Total Environment*, vol. 447, pp. 345–360, 2013.

[9] K. Kümmerer and A. Henninger, "Promoting resistance by the emission of antibiotics from hospitals and households into effluent," *Clinical Microbiology and Infection*, vol. 9, no. 12, pp. 1203–1214, 2003.

[10] N. H. Tran, M. Reinhard, and K. Y. H. Gin, "Occurrence and fate of emerging contaminants in municipal wastewater treatment plants from different geographical regions-a review," *Water Research*, vol. 133, pp. 182–207, 2018.

[11] WHO, *Antimicrobial Resistance*, WHO, Geneva, Switzerland, 2017, http://www.who.int/mediacentre/factsheets/fs194/en/.

[12] H. L. Schoenfuss, E. T. Furlong, P. J. Phillips et al., "Complex mixtures, complex responses: assessing pharmaceutical mixtures using field and laboratory approaches," *Environmental Toxicology and Chemistry*, vol. 35, no. 4, pp. 953–965, 2016.

[13] N. H. Tran, H. Chen, M. Reinhard, F. Mao, and K. Y. Gin, "Occurrence and removal of multiple classes of antibiotics and antimicrobial agents in biological wastewater treatment processes," *Water Research*, vol. 104, pp. 461–472, 2016.

[14] B. J. Berendsen, T. Meijer, H. G. Mol, L. van Ginkel, and M. W. Nielen, "A global inter-laboratory study to assess acquisition modes for multi-compound confirmatory analysis of veterinary drugs using liquid chromatography coupled to triple quadrupole, time of flight and orbitrap mass spectrometry," *Analytica Chimica Acta*, vol. 962, pp. 60–72, 2017.

[15] FDA, *Guidance for Industry 118 Confirmation of Identity of Animal Drug Residues*, Food and Drug Administration, Silver Spring, MD, USA, 2003.

[16] UNODC, *Guidance for the Validation of Analytical Methodology and Calibration of Equipment Used for Testing of Illicit Drugs in Seized Materials and Biological Specimens*, UNODC, New York, NY, USA, 2009.

[17] The European Communities, *Commission Decision 2002/657/EC Implementing Council Directive 96/23/EC Concerning the Performance of Analytical Methods and the Interpretation of Results*, The European Communities, 2002.

[18] USDA, *Data and Instrumentation Revision 5. Agricultural Marketing Service*, United States Department of Agriculture, Washington, DC, USA, 2017.

[19] EWDTS, *European Laboratory Guidelines for Legally Defensible Workplace Drug Testing (EWDTS)*, CRC Press, BocaRaton, FL, USA, 2002, http://www.eapinstitute.com/documents/EWDTS-Guidelines.pdf.

[20] H. G. Mol, P. Zomer, M. Garcia Lopez et al., "Identification in residue analysis based on liquid chromatography with tandem mass spectrometry: experimental evidence to update performance criteria," *Analytica Chimica Acta*, vol. 873, pp. 1–13, 2015.

[21] B. J. Berendsen, T. Meijer, R. Wegh et al., "A critical assessment of the performance criteria in confirmatory analysis for veterinary drug residue analysis using mass spectrometric detection in selected reaction monitoring mode," *Drug Testing and Analysis*, vol. 8, no. 5-6, pp. 477–490, 2016.

[22] USEPA, *Method 1694: Pharmaceuticals and Personal Care Products in Water, Soil, Sediment, and Biosolids by HPLC/MS/MS*, U.S Envorinmrntal Protection Agency, Washington, DC, USA, 2007.

[23] USEPA, *Method 542: Determination of Pharmaceuticals and Personal Care Products in Drinking Water by Solid Phase Extraction and Liquid Chromatography Electrospray Ionization–Tandem Mass Spectrometry (LC/ESI-MS/MS)*, U.S Envorinmrntal Protection Agency, Washington, DC, USA, 2016.

Hindawi
Journal of Analytical Methods in Chemistry
Volume 2018, Article ID 7965124, 8 pages
https://doi.org/10.1155/2018/7965124

Research Article

Determination of Tobramycin in M_9 Medium by LC-MS/MS: Signal Enhancement by Trichloroacetic Acid

Liusheng Huang,[1] **Janus Anders Juul Haagensen**,[2] **Davide Verotta**,[1] **Vincent Cheah**,[1] **Alfred M. Spormann**,[3] **Francesca Aweeka**,[1] **and Katherine Yang**[1]

[1]*Department of Clinical Pharmacy, School of Pharmacy, University of California San Francisco, San Francisco, CA, USA*
[2]*Novo Nordisk Foundation Center for Biosustainability, Technical University of Denmark, 2800 Kongens Lyngby, Denmark*
[3]*Department of Civil and Environmental Engineering, Stanford University, Palo Alto, CA, USA*

Correspondence should be addressed to Liusheng Huang; liusheng.huang@ucsf.edu and Katherine Yang; Katherine.Yang2@ucsf.edu

Received 8 December 2017; Accepted 6 February 2018; Published 26 April 2018

Academic Editor: Lucia Mendez

It is well known that ion-pairing reagents cause ion suppression in LC-MS/MS methods. Here, we report that trichloroacetic acid increases the MS signal of tobramycin. To support studies of an *in vitro* pharmacokinetic/pharmacodynamic simulator for bacterial biofilms, an LC-MS/MS method for determination of tobramycin in M_9 media was developed. Aliquots of 25 μL M_9 media samples were mixed with the internal standard (IS) tobramycin-d_5 (5 μg/mL, 25 μL) and 200 μL 2.5% trichloroacetic acid. The mixture (5 μL) was directly injected onto a PFP column (2.0 × 50 mm, 3 μm) eluted with water containing 20 mM ammonium formate and 0.14% trifluoroacetic acid and acetonitrile containing 0.1% trifluoroacetic acid in a gradient mode. ESI^+ and MRM with ion m/z 468 → 324 for tobramycin and m/z 473 → 327 for the IS were used for quantification. The calibration curve concentration range was 50–25000 ng/mL. Matrix effect from M_9 media was not significant when compared with injection solvents, but signal enhancement by trichloroacetic acid was significant (~3 fold). The method is simple, fast, and reliable. Using the method, the *in vitro* PK/PD model was tested with one bolus dose of tobramycin.

1. Introduction

Tobramycin (TBM) is an aminoglycoside antibiotic widely used for the treatment of multidrug-resistant Gram-negative bacterial infections by inhibiting protein synthesis and altering integrity of the bacterial cell membrane [1]. It is also named 3′-deoxykanamycin B, nebramycin 6, and chemically O-3-amino-3-deoxy-α-D-glucopyranosyl-(1-6)-O-[2,6-diamino-2,3,6-trideoxy-α-D-ribo-hexopyranisyl-(1-4)]-2-deoxy-D-streptamine (Figure 1). It is water soluble and stable at ambient temperature at a wide range of pH 1–11 [2].

To support pharmacokinetic (PK) and pharmacodynamic (PD) studies of TBM for biofilm-mediated infections using an *in vitro* model, an analytical method to quantitate TBM in M_9 medium is needed. Two considerable challenges in determination of TBM in biological matrices are (1) poor retention on commonly used reverse-phase HPLC columns due to its higher hydrophilicity and (2) lack of chromophores for detection. Numerous assays have been reported including HPLC coupled with UV [3], electrochemical [4, 5], or fluorescence detectors [6], and these assays lack sensitivity and usually require derivatization. LC-MS/MS assays have also been reported, but the sensitivity of these assays requires concentrations ≥100 ng/mL [7–9]. Trichloroacetic acid (TCA) has been used in sample preparation to remove proteins, especially for hydrophilic analytes, with the advantage of direct injection of resulting sample solution [10]. We found that TCA not only increased the retention time but also the MS signal of TBM. Built on this observation, we report a simple LC-MS/MS method to determine TBM in M_9 medium using TCA as the ion pair reagent in the injection sample instead of the mobile phase. In addition, this assay utilized a PFP column, which yielded a better retention factor for TBM ($k = 1.8$). The calibration range was 50–25000 ng/mL.

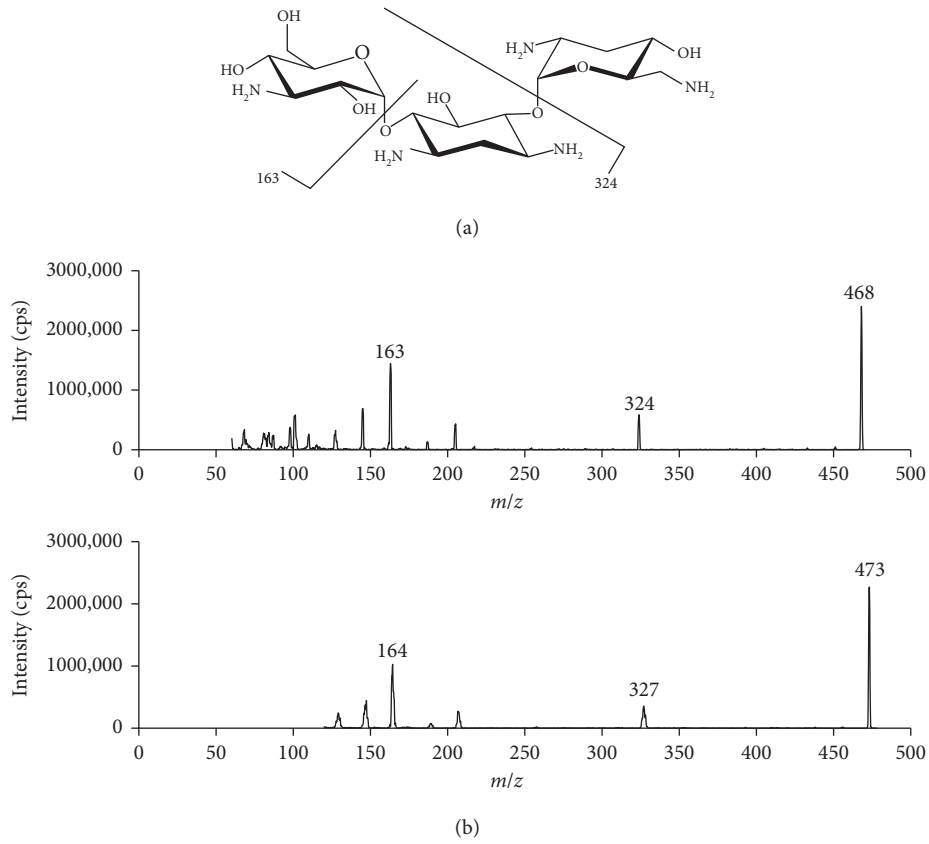

Figure 1: Product ion spectra of tobramycin (a) and deuterated tobramycin (b).

2. Experimental

2.1. Chemicals and Reagents. Tobramycin was purchased from Sigma-Aldrich (St. Louis, MO, USA). Deuterated tobramycin (TBM-d_5) was purchased from Toronto Research Chemicals (North York, Ontario, Canada). Formulated tobramycin (20 mg/2 mL, for IM or IV use) was obtained from APP Pharmaceuticals, LLC (Schaumburg, IL, USA). Common solvents (HPLC grade) and reagents (Certified ACS) were obtained from Thermo-Fisher Sci. (Fair Lawn, NJ, USA). M_9 minimal salts ×5 solution was prepared by dissolving 2.82 g Difco™ M_9 minimal salts (BD, Sparks, MD, USA) in 50 mL water. M_9 medium was prepared by adding 10 mL M_9 minimal salts ×5 solution, 5 μL 1 M $CaCl_2$, 50 μL 1 M $MgSO_4$, and 13.5 μL 20% glucose to 40 mL water.

2.2. Instrumental. The LC-MS/MS system consists of an AB Sciex API5000 Tandem Mass Spectrometer, two Shimadzu Prominence 20AD^{XR} UFLC pumps, and an SIL-20AC^{XR} autosampler managed with Analyst® 1.6.2 (AB Sciex, Redwood City, CA, USA). The gases for the MS system were supplied by an LC-MS gas generator (Source 5000™, Parker Balston Inc., Haverhill, MA, USA). LC conditions were as follows: separation was achieved on a Pursuit PFP column (2.1 × 50 mm, 3 μm) (Agilent Tech. Inc., Santa Clara, CA, USA). Mobile phase A was 20 mM NH_4FA 0.14% trifluoroacetic acid (TFA) and B was 0.1% TFA in acetonitrile (MeCN). Five-microliter sample was injected onto the column eluted at a flow rate of 0.4 mL/min in a gradient program consisting of 5% solvent B (0–0.10 min), from 5 to 20% B (0.10–1.50 min), from 20 to 80% B (1.50–1.51 min), 80% B (1.51–2.00 min), 80%–5% B (2.00–2.01 min), and 5% B (2.01–3.00 min). Retention times for TBM and the internal standard (IS) were both 0.84 min. The divert valve was set to direct the LC eluent to the mass spectrometer (MS) source at 0.6 min and to the waste line at 2.9 min. The MS conditions for TBM and the IS were optimized by separate infusion of 200 ng/mL TBM and 400 ng/mL deuterated TBM in 0.1% formic acid into the MS at a flow rate of 15 and 25 μL/min constantly while adjusting MS parameters with autotune followed by manual adjustment to achieve the maximal signal. The ions m/z 468 → 324 for TBM and m/z 473 → 327 for the IS were used for quantification in the multiple reaction monitoring (MRM) mode. The optimized compound-dependent MS parameters were 121 V (DP), 21 V (CE), and 26 V (CXP) for both TBM and the IS. DP was declustering potential, CE was collision energy, and CXP was collision cell exit potential. The instrument-dependent parameters were optimized by flow injection analysis (FIA): an aliquot of 5 μL 200 ng/mL TBM was repeatedly injected into the LC-MS/MS system while LC flow was maintained at 0.4 mL/min 50% B isocratically without column in the line. The optimized MS parameters were as follows: MS source was the TurboIon Spray ionization in positive mode (ESI^+) with turbo heater set at 500°C, curtain gas was nitrogen at 40 psi, nebulizer gas (gas 1) and auxiliary (Turbo) gas (gas 2) were zero air set at 50 psi and 60 psi, respectively, collision-deactivated

association gas was nitrogen at 12 psi, and ionspray voltage was 5500 V. Data were processed with Analyst 1.6.2. (AB Sciex, Redwood City, CA, USA).

2.3. Preparation of Calibrators, Quality Controls, and Internal Standard. As TBM used in the *in vitro* biofilm PK/PD model contains formulation ingredients, calibrators and quality controls (QCs) were prepared from formulated TBM (20 mg/2 mL) with serial dilution in M_9 medium to match the matrix in unknown samples. Calibrators consists of 50, 100, 250, 500, 1000, 2500, 5000, 10000, and 25000 ng/mL. QCs consist of 150, 1500, 20000, and 40000 ng/mL, designated as low-, medium-, high-, and extrahigh QC. The internal standard TBM-d_5 solution was prepared in water by serial dilution at a final concentration of 5000 ng/mL. The IS solution needs to stand on bench overnight before use.

2.4. Sample Preparation. M_9 samples (25 μL) were pipetted into 1 mL glass autosampler vials, to which were added 25 μL IS (5 μg/mL TBM-d_5) and 200 μL 2.5% TCA. After vortex mixed, the samples were placed in the autosampler tray. If the samples were collected from M_9 medium flowing through bacterial biofilm, the samples were centrifuged at 20000g for 3 min before adding to the sample vial. Injection volume was 5 μL.

2.5. Validation. The method was validated in terms of precision, accuracy, matrix effect, and stability, following the procedures as described previously [10]. One set of calibrators was processed for each run and injected in the beginning of the batch run. Calibration curves were constructed by linear regression of the peak area ratio of the analyte to the IS (y-axis) versus the nominal analyte concentrations (x-axis) with a weighting factor of $1/x$. The lower limit of quantification (LLOQ) was established with precision and accuracy <20%. Intraday precision and accuracy were determined by analysis of at least five replicates of each QC sample at low (150 ng/mL), medium (1500 ng/mL), and high (20000 ng/mL) concentration levels extracted with a set of calibrators in one batch. The same procedure was repeated on at least 2 different days with new samples to determine interday precision and accuracy (total: $n \geq 15$ per concentration level). Precision was reported as relative standard deviation (RSD) and accuracy as percent deviation from the nominal concentration (% dev.). Matrix effect was evaluated as follows: TBM was spiked at the concentrations of 300, 1500, and 20000 ng/mL in water and M_9 medium, respectively. Three aliquots of each sample were processed as described above (Section 2.4). The peak areas and peak area ratios of TBM in M_9 medium were compared to those in water. Values within 100 ± 15% were considered as no significant matrix effect from M_9 medium. To evaluate partial volume accuracy, 12.5 μL extrahigh QC at 40000 ng/mL was mixed with 12.5 μL M_9 medium and processed as described in Section 2.4. Stability was evaluated in the following conditions: room temperature (21–25°C) for 5 days, 3 days on the autosampler rack, 3 freeze-thaw cycles, and 6 days at −70°C. Stability of freshly prepared IS working solution was evaluated at room temperature for 24 hr and 5 days. Effects of concomitant drugs (e.g., meropenem and colistin) on quantification were evaluated by spiking them in the QC samples at a final concentration of 110 μg/mL meropenem (MP) and 20 μg/mL colistin. The measured concentrations of TBM were compared to the QC samples without these concomitant drugs.

2.6. Application. This method was used to validate a novel dynamic PK/PD model designed to study the effects of human-simulated antibiotic concentrations on *Pseudomonas aeruginosa* biofilms grown *in vitro* [11]. TBM, in conjunction with a β-lactam antibiotic such as MP, is recommended for the treatment of multidrug-resistant *Pseudomonas aeruginosa* lung infection in patients with cystic fibrosis [12]. While the formation of bacterial biofilms in the lung is a characteristic of chronic lung infection in patients with cystic fibrosis, the PD of antibiotics on biofilms is largely unknown. The concentration-time curves of single and multiple intravenous bolus doses of TBM were simulated based on human population PK parameters [13]. The target TBM peak concentration, based on a dose of 10 mg/kg in a 70 kg adult, was 32.79 mg/L with an associated $t_{1/2} = 2.75$ h. Samples were taken at $t = 0$, 1, 2, 4, 6, 8, 16, and 24 hr from the main feeding bottle and the tubing outlets from three flow cells with bacterial biofilm. All samples were shipped to our analytical lab on the same day with dry ice overnight delivery and stored at −70°C freezer until analysis. Samples were typically analyzed within a week.

3. Results and Discussion

3.1. LC-MS/MS Optimization. TBM contains five amine groups (Figure 1), making electrospray ionization in positive mode (ESI^+) the choice of the ion source. The ion m/z 468 → 324 was chosen for quantification for its signal abundancy and selectivity. Compared to product ion m/z 163, m/z 324 has less background signal. The deuterated TBM was used as the IS. However, the deuteration positions were not identified. MS scan showed that multiple forms of deuterated TBM exist, with the most abundant protonated molecule at m/z 473. Therefore, ion m/z 473 → 327 was chosen for the IS. The signal of the ion m/z 473 → 327 decreased gradually in the first few hours but remained stable after the IS solution stood on bench overnight. These observations suggested that deuteration most likely occurred on amine groups, and the stable form of IS contains a deuterium atom on each amine group (Figure 1).

Having 5 amine groups and 5 hydroxyl groups also makes TBM hardly retain on reverse-phase LC columns. Ion pair reagent TFA and TCA in the mobile phase could help to retain polar amino molecules on the reverse-phase columns; however, sensitivity may be compromised due to ion suppression. Previously, we found that TFA could change retention time of isoniazid when added into sample before injection (Supplementary Material Figure S1). However, TFA did not improve the TBM peak. Cheng et al. used TCA to modify retention time of aminoglycoside compounds [14].

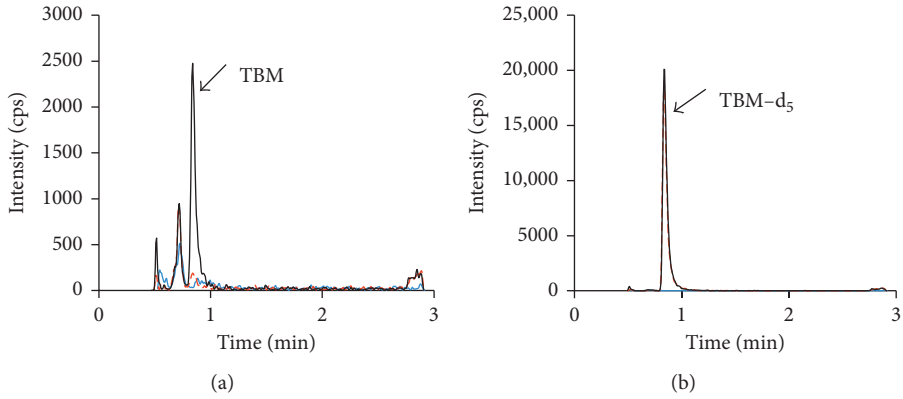

Figure 2: Chromatograms of blank M_9 medium (blue solid line), blank M_9 medium spiked with IS (red dash line), and TBM at LLOQ level (black solid line). (a) TBM channel; (b) the IS channel.

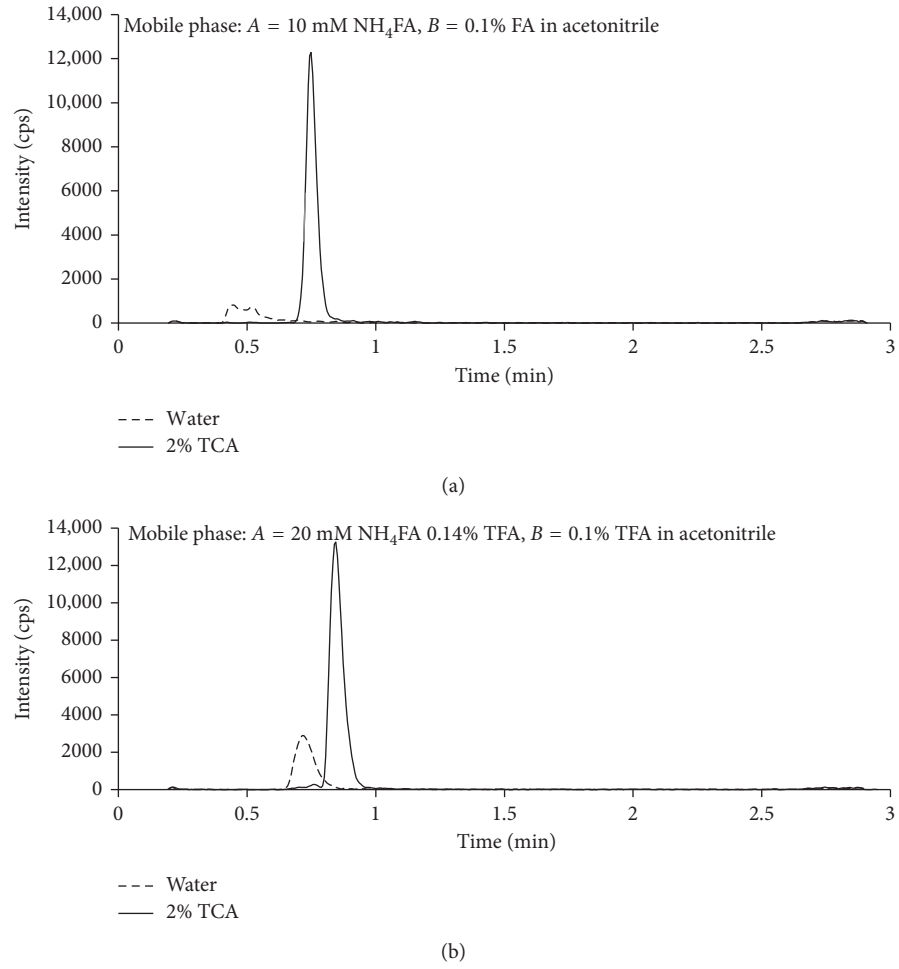

Figure 3: Impact of mobile phase solvents and sample solvents on peak shape, retention time, and signal intensity of TBM. Sample solvents: water (dash line) and 2% TCA (solid line). Mobile phase solvents: 10 mM NH_4FA (pH 4.0)-0.1% FA in MeCN (a) and 20 mM NH_4FA 0.14% TFA-0.1% TFA in MeCN (b).

We found that when the sample contained 2% TCA with a 5 μL injection volume, longer retention time of TBM was observed (Supplementary Material Figure S2). Under the final LC condition, the TBM peak was sufficiently separated from the matrix-generated peaks (Figure 2). The retention time $t_R = 0.839$ min, the estimated dead volume is $0.68\pi r^2 L = 0.118$ mL, and retention factor $k = 1.84$.

Unexpectedly, TCA also enhanced MS response of TBM. Two different sample solvents (water and 2% TCA) and two sets of mobile phase solvents were tested: (1) $A = 10$ mM

Table 1: Interday average backcalculated standard concentrations ($n = 3$).

Nominal concentration (ng/mL)	50	100	250	500	1000	2500	5000	10000	25000	R
Mean (ng/mL)	50.1	91.6	236	521	1043	2663	4973	9977	24800	0.9992
Precision (RSD, %)	3.82	6.11	3.31	2.98	3.37	2.50	8.06	3.72	2.91	0.0379
Accuracy (% dev.)	0.13	−8.37	−5.60	4.13	4.33	6.53	−0.53	−0.23	−0.80	
n	3	3	3	3	3	3	3	3	3	

Table 2: Intra- and interday precision and accuracy.

	Intraday				Interday			
Nominal (ng/mL)	50.0	150	1500	20000	50.0	150	1500	20000
Mean (ng/mL)	43.0 to 50.9	150 to 159	1533 to 1653	20450 to 20650	46.8	153	1591	20572
Precision (RSD) (%)	3.0 to 16.9	4.4 to 6.7	2.1 to 3.5	2.5 to 3.4	8.43	3.33	3.78	0.52
Accuracy (dev.) (%)	−14.0 to 1.7	0 to 5.9	2.2 to 10.2	2.3 to 3.3	−6.44	1.96	6.04	2.86
n	6	6	6	6	3	3	3	3

Table 3: Matrix effect.

Concentration (ng/ml)	TBM peak area ($\times 10^4$)		IS peak area ($\times 10^4$)		Ratio		Matrix effect		
	Water	M_9	Water	M_9	Water	M_9	TBM	IS	Ratio
Low (120)	3.60 ± 0.12	3.83 ± 0.13	8.26 ± 0.49	8.72 ± 0.53	0.436	0.439	106	106	101
Medium (1500)	18.1 ± 1.0	20.0 ± 1.4	8.80 ± 0.77	9.30 ± 0.91	2.06	2.15	110	106	104
High (17000)	378 ± 5	413 ± 18	13.7 ± 0.5	14.7 ± 0.7	27.6	28.1	109	107	102

Data represent the mean peak area (±SD) from triplicate analysis.

NH_4FA at pH 4.0; $B = 0.1\%$ FA in MeCN and (2) $A = 20$ mM NH_4FA 1.4% TFA;, $B = 0.1\%$ TFA in MeCN, using the same gradient elution method. With the commonly used mobile phase solvents (set 1), the peak shape for TBM was poor if injection solvent is water, while 2% TCA in the sample improved peak shape, signal intensity, and retention time significantly (Figure 3(a)); with mobile phase solvent set 2, the signal intensity and retention time of TBM improved further (Figure 3(b)). This improvement is critical as the interference peak from M_9 medium was then separated from the TBM peak (Figure 2). The exact mechanism of signal enhancement by TCA is unknown. Cheng et al. thought that reduced matrix effect with longer retention time contributed to the signal enhancement [14], but we observed signal enhancement in neat solution (Figure 3). The possible reason could be that TCA limited multiple charges of TBM and thus increased monocharged molecular ion ($[M+H]^+$). In addition, we observed that MS response of the IS (TBM-d_5) was also increased with the increase of TBM concentration, suggesting ion enhancement of coeluting compounds. This should not affect quantification as IS was added to all samples, and the TBM signal increased accordingly. This was confirmed with the excellent linearity of calibration curve.

3.2. Validation. Based on our initial simulation, the TBM trough concentration is expected to be >250 ng/mL. Therefore, the LLOQ in this assay was initially set at 250 ng/mL, the upper limit of quantification was set at 25000 ng/mL, and validation was performed with low (300 ng/mL), medium (1500 ng/mL), and high (20000 ng/mL) QCs. After tested the *in vitro* biofilm model, we found that the trough TBM concentration fell below 250 ng/mL, and thus, we lowered the LLOQ to 50 ng/mL and the low QC level to 150 ng/mL accordingly. Validation of intraday/interday precision and accuracy and interference of concomitant drugs were repeated with the new low QC concentration.

3.2.1. Calibration Range. At the LLOQ concentration (50 ng/mL), the signal intensity was 2100–2400 cps (peak area, 6600–7900) and signal-to-noise ratio $S/N = 30$–48 (Figure 2). This LLOQ is lower than others reported in literature. A recent study reported an LLOQ at 100 ng/mL. The detector was the same as ours, but heptafluorobutyric acid was used as ion pair reagent in the mobile phase and sample reconstitution [9]. The calibration curve was constructed with least square linear regression weighted by $1/x$. The interday backcalculated concentrations of calibrators over 3 days are listed in Table 1. The precision is within 10% and accuracy (percent deviation from the nominal value) is within ±10%, too. Representative MRM ion chromatograms of TBM from M_9 medium (double blank), M_9 medium spiked with IS (blank), and LLOQ samples are shown in Figure 2.

3.2.2. Precision and Accuracy. The intraday precision ($n = 6$) was within 7% at low, medium, and high concentrations. The interday precision, calculated with the individual mean concentration from 3 days, was within 5% at the three concentration levels. The intra- and interday accuracy was all within 15%. At the LLOQ levels, the precision and accuracy met the criteria of <20% (Table 2).

3.2.3. Matrix Effect. The matrix effect of M_9 medium on both TBM and IS signals is within 100 ± 15% (Table 3), suggesting that the matrix effect of M_9 medium was not significant. The matrix effect on the peak area ratio was

Table 4: Stability of TBM.

Conditions		% remained	RSD (%)	n
In autosampler vial, 21–25°C, 3 days				
	300 ng/mL	107	3.5	3
	20000 ng/mL	105	2.4	3
In M_9, 21–25°C, 5 days				
	300 ng/mL	104	8.1	3
	20000 ng/mL	99.2	3.6	3
3 freeze-thaw cycles				
	300 ng/mL	99.4	5.0	3
	20000 ng/mL	99.8	2.4	3
In M_9 medium, 6 days, −70°C				
	300 ng/mL	93.8	3.3	3
	20000 ng/mL	101	3.0	3
IS (5000 ng/mL) in water		102.9	0.74	3
	24 hr, 21–25°C	74.2	3.4	3
	5 days, 21–25°C	79.5	1.7	4

Table 5: Interference of potential concomitant drugs.

Concentration (ng/mL)	Control	Colistin-MP*	% dev.
150	150 ± 10	148 ± 8	−1.3
1500	1633 ± 61	1587 ± 98	−2.8
20000	20000 ± 557	19933 ± 737	−0.3

Note. Data represent the mean (SD) of triplicate analysis. *MP and colistin concentrations were 110 μg/mL and 20 μg/mL, respectively, corresponding to the highest concentrations in the *in vitro* model.

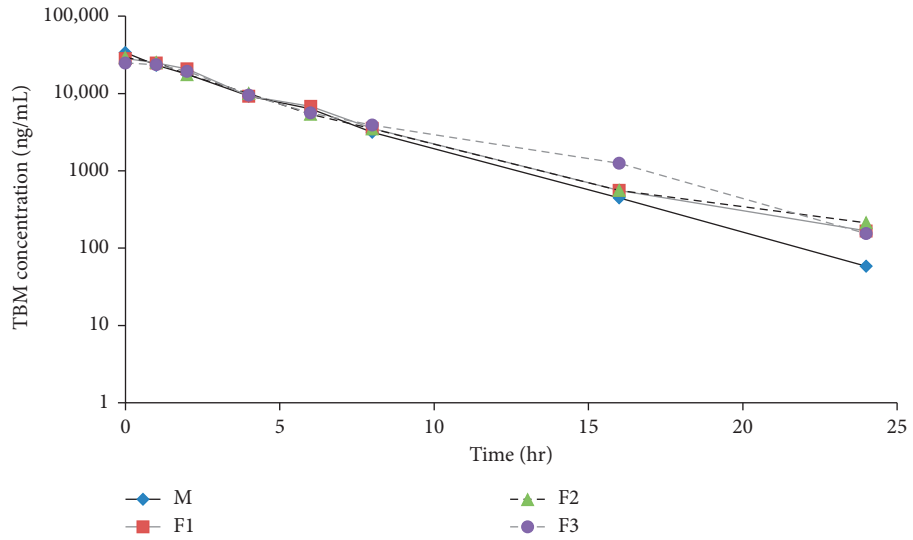

Figure 4: Concentration-time profile of tobramycin from an *in vitro* PK/PD biofilm model. Samples were taken from the feeding bottle (M) and the tubing outlets from three flow cells with bacterial biofilm (F1, F2, and F3) at designated time intervals.

even smaller, suggesting that IS compensated the matrix effect.

3.2.4. Partial Sample Volume Accuracy. As the target Cmax is 40000 ng/mL, we evaluated accuracy of the assay with an extrahigh QC (40000 ng/mL) when half sample volume was used. The precision and accuracy from six replicates of analysis were 2.2% and 2.6%, respectively. Therefore, samples above the upper limit of quantification could be analyzed with a partial volume.

3.2.5. Stability. TBM was stable in M_9 medium. No significant degradation was found under tested condition (Table 4). Further investigation is ongoing to define long-term stability in −70°C freezer.

3.2.6. Evaluation of Concomitant Drug Interference. The samples from the supported study are expected to contain MP and colistin; therefore, impact of these drugs on quantification of TBM was evaluated. In the presence of 110 μg/mL MP and 20 μg/mL colistin, the low, medium, and high QC samples could still be quantified accurately, with a small percent deviation from the samples without these drugs (Table 5).

3.3. Application. The method was applied to determine TBM concentrations used in an *in vitro* PK/PD biofilm simulator. The PK/PD analysis was reported elsewhere [15]. A representative concentration-time curve from the model is showed in Figure 4. The results demonstrate that the sensitivity of the method met the requirement of the intended study.

4. Conclusion

TCA not only improves peak shape and retention time of TBM but also increases MS signal intensity of TBM. Using a simple dilution with ion pairing reagent TCA, a sensitive LC-MS/MS method was developed and validated for determination of TBM in bacterial M_9 medium. The LLOQ was 50 ng/mL. The sensitivity of the assay met the requirement of the intended PK/PD study in an *in vitro* biofilm model system.

TCA has been used to increase retention time and sensitivity for quantification of gentamicin, kanamycin, and apramycin [14]. Here, we demonstrated application of TCA to quantification of TBM. We speculate this approach could be generalized: by addition of ion-pairing agents to samples instead of adding to mobile phase solvents, we could extend the retention time of analytes and even increase sensitivity. Acidic ion-pairing agents such as TFA and TCA could be applied to basic polar analytes such as amine-containing analytes, and basic ion-pairing agents could be added to samples of acidic polar analytes. Nevertheless, the concentration of the ion-pairing agent is critical, and selection of the ion-pairing agent is also critical.

Disclosure

This work was presented in the ACS National Meeting (http://sanfrancisco2017.acs.org/i/803418-253rd-american-chemical-society-national-meeting-expo/89). Its contents are solely the responsibility of the authors and do not necessarily represent the official views of the NIH.

Conflicts of Interest

All authors declare that they have no conflicts of interest.

Acknowledgments

This work was supported by a grant (1R01 AI097380-0121) from the National Institute of Allergy and Infectious Diseases of the National Institutes of Health and fund from the Department of Clinical Pharmacy at the University of California San Francisco.

Supplementary Materials

Figure S1: effect of TFA on retention time of isoniazid. Figure S2: optimization of TCA concentration. (*Supplementary Materials*)

References

[1] E. J. Begg and M. L. Barclay, "Aminoglycosides—50 years on," *British Journal of Clinical Pharmacology*, vol. 39, no. 6, pp. 597–603, 1995.

[2] H. C. Neu, "Tobramycin: an overview," *Journal of Infectious Diseases*, vol. 134, pp. S3–S19, 1976.

[3] C. H. Feng, S. J. Lin, H. L. Wu, and S. H. Chen, "Trace analysis of tobramycin in human plasma by derivatization and high-performance liquid chromatography with ultraviolet detection," *Journal of Chromatography B*, vol. 780, no. 2, pp. 349–354, 2002.

[4] J. A. Statler, "Determination of tobramycin using high-performance liquid chromatography with pulsed amperometric detection," *Journal of Chromatography B: Biomedical Sciences and Applications*, vol. 527, pp. 244–246, 1990.

[5] C. Ghinami, V. Giuliani, A. Menarini, F. Abballe, S. Travaini, and T. Ladisa, "Electrochemical detection of tobramycin or gentamicin according to the European Pharmacopoeia analytical method," *Journal of Chromatography A*, vol. 1139, no. 1, pp. 53–56, 2007.

[6] F. Lai and T. Sheehan, "Enhancement of detection sensitivity and cleanup selectivity for tobramycin through pre-column derivatization," *Journal of Chromatography A*, vol. 609, no. 1-2, pp. 173–179, 1992.

[7] B. G. Keevil, S. J. Lockhart, and D. P. Cooper, "Determination of tobramycin in serum using liquid chromatography-tandem mass spectrometry and comparison with a fluorescence polarisation assay," *Journal of Chromatography B*, vol. 794, no. 2, pp. 329–335, 2003.

[8] M. X. Guo, L. Wrisley, and E. Maygoo, "Measurement of tobramycin by reversed-phase high-performance liquid chromatography with mass spectrometry detection," *Analytica Chimica Acta*, vol. 571, no. 1, pp. 12–16, 2006.

[9] P. M. Bernardi, F. Barreto, and T. Dalla Costa, "Application of a LC-MS/MS method for evaluating lung penetration of tobramycin in rats by microdialysis," *Journal of Pharmaceutical and Biomedical Analysis*, vol. 134, pp. 340–345, 2016.

[10] L. Huang, P. Lizak, C. C. Dvorak, F. Aweeka, and J. Long-Boyle, "Simultaneous determination of fludarabine and clofarabine in human plasma by LC-MS/MS," *Journal of Chromatography B*, vol. 960, pp. 194–199, 2014.

[11] J. A. J. Haagensen, D. Verotta, L. Huang, A. Spormann, and K. Yang, "New in vitro model to study the effect of human simulated antibiotic concentrations on bacterial biofilms," *Antimicrobial Agents and Chemotherapy*, vol. 59, no. 7, pp. 4074–4081, 2015.

[12] P. A. Flume, P. J. Mogayzel Jr., K. A. Robinson et al., "Clinical Practice Guidelines for Pulmonary Therapies C: cystic fibrosis pulmonary guidelines: treatment of pulmonary exacerbations," *American Journal of Respiratory and Critical Care Medicine*, vol. 180, no. 9, pp. 802–808, 2009.

[13] D. J. Touw, A. J. Knox, and A. Smyth, "Population pharmacokinetics of tobramycin administered thrice daily and

once daily in children and adults with cystic fibrosis," *Journal of Cystic Fibrosis*, vol. 6, no. 5, pp. 327–333, 2007.

[14] C. Cheng, S. R. Liu, D. Q. Xiao, and S. Hansel, "The application of trichloroacetic acid as an ion pairing reagent in LC-MS-MS method development for highly polar aminoglycoside compounds," *Chromatographia*, vol. 72, no. 1-2, pp. 133–139, 2010.

[15] J. Haagensen, D. Verotta, L. Huang, J. Engel, A. M. Spormann, and K. Yang, "Spatiotemporal pharmacodynamics of meropenem- and tobramycin-treated *Pseudomonas aeruginosa* biofilms," *Journal of Antimicrobial Chemotherapy*, vol. 72, no. 12, pp. 3357–3365, 2017.

Hindawi
Journal of Analytical Methods in Chemistry
Volume 2018, Article ID 1308167, 24 pages
https://doi.org/10.1155/2018/1308167

Review Article

MS-Based Analytical Techniques: Advances in Spray-Based Methods and EI-LC-MS Applications

Federica Bianchi,[1] **Nicolò Riboni**,[1,2] **Veronica Termopoli**,[3] **Lucia Mendez**,[4] **Isabel Medina**,[4] **Leopold Ilag**,[2] **Achille Cappiello**,[3] **and Maria Careri**[1]

[1]*Department of Chemistry, Life Sciences, and Environmental Sustainability, University of Parma, Parco Area delle Scienze 17/A, 43124 Parma, Italy*
[2]*Department of Environmental Science and Analytical Chemistry, Stockholm University, 10691 Stockholm, Sweden*
[3]*Department of Pure and Applied Sciences, LC-MS Laboratory, Piazza Rinascimento 6, 61029 Urbino, Italy*
[4]*Instituto de Investigaciones Marinas, Spanish National Research Council (IIM-CSIC), Eduardo Cabello 6, 36208 Vigo, Spain*

Correspondence should be addressed to Federica Bianchi; federica.bianchi@unipr.it

Received 22 December 2017; Accepted 26 February 2018; Published 23 April 2018

Academic Editor: Gauthier Eppe

Mass spectrometry is the most powerful technique for the detection and identification of organic compounds. It can provide molecular weight information and a wealth of structural details that give a unique fingerprint for each analyte. Due to these characteristics, mass spectrometry-based analytical methods are showing an increasing interest in the scientific community, especially in food safety, environmental, and forensic investigation areas where the simultaneous detection of targeted and nontargeted compounds represents a key factor. In addition, safety risks can be identified at the early stage through online and real-time analytical methodologies. In this context, several efforts have been made to achieve analytical instrumentation able to perform real-time analysis in the native environment of samples and to generate highly informative spectra. This review article provides a survey of some instrumental innovations and their applications with particular attention to spray-based MS methods and food analysis issues. The survey will attempt to cover the state of the art from 2012 up to 2017.

1. Introduction

Mass spectrometry (MS) is one of the most powerful techniques for the detection and identification of organic and inorganic compounds. Being able to provide both molecular weight and structural information [1], it is widely used in analytical laboratories for academic research, industrial product development, and regulatory compliance as well as for proteomic or metabolomic studies, DNA characterization, drug discovery, environmental monitoring, food analysis, forensics, and homeland security.

A plethora of analytical MS-based methods based on the use of both stand-alone instruments and mass spectrometers coupled to different separation techniques such as gas and liquid chromatography (GC and LC) or capillary electrophoresis (CE) have been developed and validated in order to analyze complex matrices. Interesting review articles and book chapters dealing with advances in ionization for mass spectrometry have been lately published [2–9].

Recently, the advent of ambient MS technology paved the way for the development of a great variety of applications and innovations characterized by high throughput: the challenge of analyzing samples in their native state without sample treatment encouraged the development of new techniques among which are the spray-based ionization ones including desorption electrospray ionization (DESI) [10], paper spray ionization (PSI) [11], laser ablation electrospray ionization (LAESI) [12], and easy ambient sonic-spray ionization (EASI) [13].

Novel materials and new instrumental configurations are under study to enhance the performance of the different ion sources. Safety risks can be identified at the early stages

through nontargeted monitoring technologies. Furthermore, the variety of fragmentation strategies that can be combined in new instrumentation overall enhances work in the omics fields, particularly proteomics and metabolomics.

Although MS-based methods are getting progressively more powerful, reliable, and easily available, the main drawbacks are still related to sample complexity and preparation, mass accuracy, often requiring the use of high-resolution mass spectrometry (HRMS) to guarantee the univocal identification of the targeted compounds, and the need of high-throughput and screening analyses when a great number of samples have to be analyzed.

The aim of the proposed special issue is to cover the aspects regarding emerging features of MS-based techniques focusing on innovative LC-MS studies and ambient MS with particular attention to the spray-based ionization techniques. New materials, prototypes, and instrumental configurations able to increase the performance of the developed methods will be presented and discussed. Finally, an overview of the most recent MS-based methods in food analysis will be given. This survey will attempt to cover the state of the art from 2012 up to 2017.

2. Advances in LC-MS

Electrospray ionization (ESI) is the technique of choice to produce ions suitable for mass analysis. ESI spectra typically are characterized by single protonated or deprotonated molecular ion $(M + H)^+$, $(M - H)^-$, and/or adduct ions. The low fragmentation is a limitation in compound characterization through the use of reliable electronic libraries, making necessary the use of multistage MS (MS/MS, MS^n) or HRMS to compensate the limited structural information. LC-ESI with triple quadrupole (QqQ) MS is the most used technique for qualitative and quantitative determination of targeted nonvolatile compounds in forensic and food applications [14, 15]. In 2016, Remane et al. reviewed the literature on applications of LC-MS/MS in clinical, forensic toxicology, and doping control since 2006 [16]. It must be noted that ESI response is strictly affected by the mobile phase and sample composition as well as by the presence of coeluting interfering compounds, which may interfere with the ionization process. These phenomena are known as "matrix effects" (MEs) and can alter the response of the analytes causing either signal suppression or enhancement [17, 18]. The occurrence of ME introduces some critical analytical shortcomings in quantitative analysis by LC-MS such as reduced sensitivity, nonlinear response, and low precision. In addition, the physicochemical properties of the analytes can play an issue in the instrument response, thus introducing additional limitations. The combination of powerful MS detectors with LC has solved many problems in structural elucidation of unknown hazardous compounds [19]. In this context, HRMS is capable of providing full spectral information by adding high mass resolving power and accuracy to achieve selectivity and capability for accurate mass measurements [20–22]. HRMS is characterized by higher mass resolution, defined as the mass difference between two mass spectral peaks that can be clearly distinguished [23], and higher mass accuracy (even better than 1 ppm). In addition, high mass resolving power allows discrimination between isobaric interference and ion of interest, leading to an accurate mass measurement even with a complex background. These features increase MS selectivity for the screening of nontargeted compounds in complex matrices, providing a list of possible elemental compositions. Fu et al. have shown how important and efficient is the use of nontargeted screening with LC-HRMS to ensure quality and safety of food [24], whereas Mattarozzi and coworkers exploited the capability of HRMS for the rapid determination of melamine from melamine tableware [25]. On the downside, HRMS-based methods generate complicated data that must be processed for "total ion fragment spectra" to obtain high-quality mass spectral information. Moreover, the mass of protonated or deprotonated molecules is not sufficient to prevent unambiguous compound identification. Hence, the use of spectra-matching approaches that utilize fragmentation ions could be added to achieve additional information on the detected compounds [26, 27]. False positives and false negatives are the major obstacles when screening complex samples. False negatives can occur due to very low concentrations, matrix interferences and suppression, and weak or no ionization. Due to these disadvantages, the practical application of LC-MS and LC-HRMS is still far from the immediacy and simplicity of GC-MS. Taking into account that electron ionization (EI) allows us to obtain characteristic and highly reproducible fragmentation of the analytes, a considerable effort has been devoted by the scientific community to increase compatibility between LC and EI-based MS to develop reliable, easy-to-use, and flawless interfaces. Moreover, implementation of EI fragmentation to LC-amenable compounds could pave the way for many new fields of research.

Recent developments in miniaturized mass spectrometers have enabled these developments to be carried out to portable on-scene detection. In the next paragraphs, some of the most popular and promising techniques are described: among them are LC-MS based on EI interfaces and spray-based ionization techniques.

2.1. LC-MS Based on Electron Ionization-Mass Spectrometry Interfaces. It is known that EI is ideal for the detection of a large number of GC-amenable compounds, but with an appropriate combination of several measures, it can become suitable for many LC-amenable small molecules having MW up to approx. 600 Da. These compounds can be efficiently converted into the gas phase, fast enough to be ionized before any decomposition process.

For analysis of small-to-medium molecules, the coupling between LC and EI-MS represents a valid strategy for overcoming the main disadvantages related to ESI ionization and the use of costly and complicated techniques involving HRMS instrumentations. Furthermore, EI provides a rich fragmentation pattern with a significant amount of structural information allowing a unique automated identification with structures at the isomer level [28]. Hence, the

ability of EI for tentative identification of GC-amenable compounds is unparalleled even without HRMS.

On the downside, the coupling between LC and MS based on EI represents a significant issue in the field of analytical chemistry. The reason may be explained by the antagonist conditions of operating. The first one typically works at ambient temperature and uses very high pressure for the efficient separation of the analytes, which are sometimes dissolved in a complex mobile phase. The second one operates at a very high vacuum and high temperature. Therefore, the effort of achieving and maintaining the high vacuum required for mass spectrometry is in contrast with the intrinsic nature of HPLC, predominantly operating at high solvent flow rates. Also, the low tolerance of mass spectrometers for nonvolatile mobile phase components contrasts with an HPLC dependence on nonvolatile buffers to achieve high-resolution separations.

Since the year 2000, a few groups of researchers are working on the development of an efficient EI-based LC-MS interface.

Cappiello and his group played a significant role in the innovation and improvement of LC-EI-MS interfacing and designing a series of systems characterized by steadily increasing performance. Firstly, they presented a prototype of the LC-MS interface called Direct-EI [29–31] based on direct coupling of a low flow rate nano-HPLC with a high-vacuum EI source. The interface governs the direct introduction of a liquid-phase sample into the EI source of the mass spectrometer and the complete conversion of the liquid effluent to the gas phase prior to a conventional electron-assisted ionization. The core of the interface is represented by the nebulizer, which consists of a fused silica/PEEK capillary, to guarantee a sufficient thermal insulation. This interface was used in many different applications, not only in combination with chromatography but also in direct analysis, as a universal detector for the targeted compound. However, both nebulization and vaporization take place inside the ion source, leading to some drawbacks linked to capillary blockings. This concern is mainly due to premature evaporation of the solvent making the analysis very difficult under routine conditions. To meet the challenges of analyzing nontargeted compounds exploiting full potential of EI and the quantification of target compounds at low concentration in complex matrices, Termopoli et al. presented a new, robust, efficient interfacing mechanism coming from the ground up [32]. The new interface is called "liquid-EI" (LEI). The interface is completely independent from the rest of the instrumentation and can be adapted to any gas chromatography-mass spectrometry system, as an add-on for a rapid LC-MS conversion. Secondly, with some little tricks, it can be used with any HPLC system. Nanopumps and capillary pumps allow direct connection, and conventional HPLC needs the use of a two-way splitter to reduce the column flow rate to a level that is compatible with the interface, which is normally between 0.5 and 1 μl/min. In an LEI interface, the vaporization of the LC eluate is carried out at atmospheric pressure inside a suitable, independent microchannel right before entering the ion source, called the vaporization microchannel, representing the core of the interface. It is designed to uncouple and separate the atmospheric pressure found at the end of the HPLC system with the high-vacuum zone of the ion source. This specific place is narrow enough to prevent vacuum from entering into the spray region allowing us to have an atmospheric pressure zone where the vaporization process takes place. A removable silica-deactivated liner ensures a perfect conversion into a gas phase before entering the mass spectrometer. A narrower fused silica capillary, called the inlet, penetrates in the first portion of the liner and releases the LC eluate. An inert gas flow surrounds the gas phase through the vaporization microchannel and helps high boiling compounds to vaporize. Figure 1 shows a complete layout of the LC-MS system equipped with the LEI interface.

The rapid vaporization offered by the lined microchannel reduces the chance of thermal decomposition and capillary blockings, broadening the range of suitable applications, especially those regarding nontargeted analytes. Remarkable results were achieved in different conditions and applications.

Over the past years, Seemann and his group developed the supersonic molecular beams (SMB) LC-MS interface [34]. Their studies started from the knowledge that standard emission energy (70 eV) used in EI is not ideal for many NIST library compounds that have a weak (below 2% relative abundance) or no molecular ion. This issue is a critical point when very large and thermally labile compounds are analyzed. Furthermore, these analytes are usually less volatile and require higher EI ion source temperatures with further intra-ion source degradation, resulting in weaker molecular ion production. To achieve a reliable EI-based sample identification, a more intense production of molecular ion is needed. Thus, the best ionization method should provide the informative library searchable EI fragments combined with enhanced molecular ions, especially for the compounds that are not included in the commercially available EI libraries. Taking into account these considerations, they present a novel concept of the LC-SMB-MS system, based on the use of supersonic molecular beams, as a medium for electron ionization of vibrationally cold sample molecules in a fly-through ion source. It is able to generate library searchable EI spectra and a more intense molecular ion.

The LC-SMB-MS apparatus is schematically shown in Figure 2.

A thorough evaluation of the interface, comprising identification of unknown compounds using obtained library searchable EI mass spectra, enhanced production of molecular ions, demonstration of the absence of matrix effects, simultaneous determination of semipolar and nonpolar compounds with reasonable detection limit, and low-cost instrumentation, was provided by that research group. The group of Seemann demonstrates the feasibility of the SMB interface as a valid tool in the analysis of unknown compounds and as a low-cost LC-EI-MS system.

A third group of researchers, headed by Rigano, presented a new nano-LC-EI-MS for the determination of free fatty acids (FFAs) in mussels [34]. A selective and sensitive nano-LC-EI-MS analytical method to investigate the FFA profile in marine organisms and to monitor marine sentinels

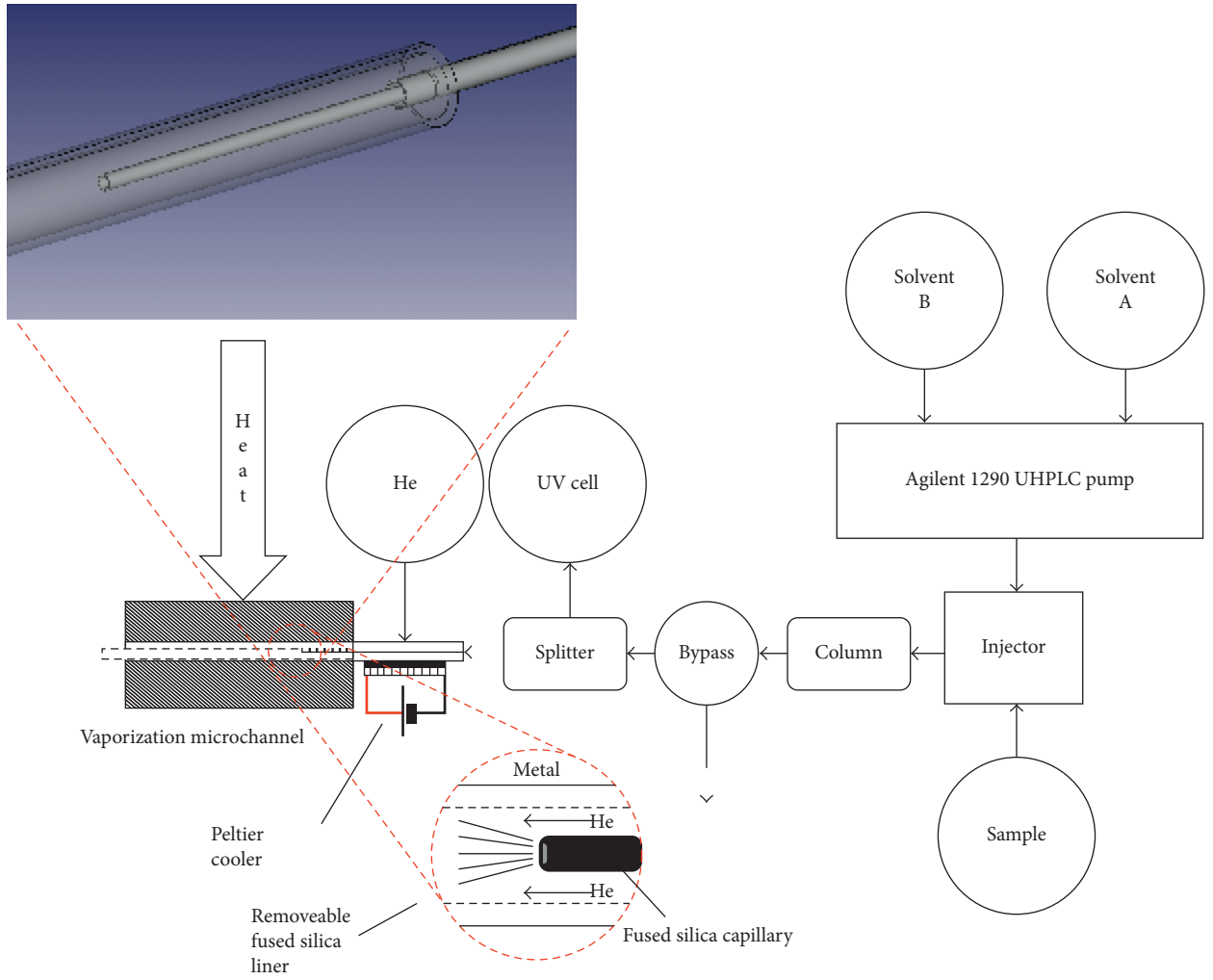

Figure 1: Global layout of the fully assembled system; the LEI interface, in gray, is between the UHPLC system and the MS detector. In the red circle, the vaporization zone is highlighted. Reprinted with permission from [33].

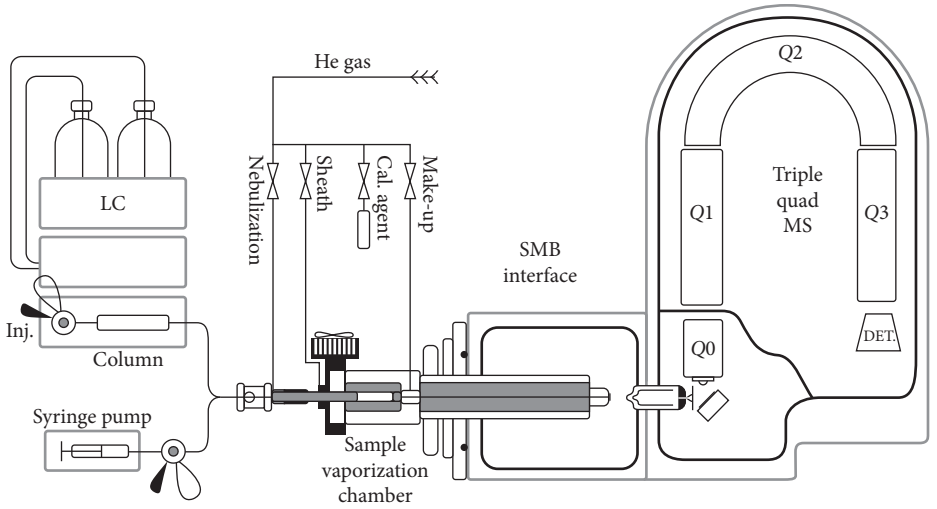

Figure 2: EI-LC-MS with the SMB system outline. The liquid is introduced either from the HPLC system after its column or from a syringe pump to the heated vaporization chamber through a pneumatic nebulizer. The helium nebulization gas enters the SMB interface through a nebulization gas line, sheath gas line, and nozzle make-up gas line. Reprinted with permission from [35].

for the assessment of environmental pollution effects was developed [35]. FFAs are minor components of the lipidome, and they are usually analyzed by GC after a derivatization step, such as methylation or trimethylsilylation, is performed to convert FA into less-polar and more-volatile moieties and improve their separation [9, 36]. However, the derivatization step, if not properly selected, can modify the FA profile due to nonhomogeneous derivatization efficiency among different compounds (saturated, unsaturated, and polyunsaturated fatty acids). In addition, oxidation or isomerization products can be generated. Relative to this issue, LC can benefit over GC techniques from direct injection of FFAs in their intact form, without any pretreatment. On the other hand, direct coupling with EI-MS can benefit from the highly informative, repeatable, and reliable MS fragmentation. Drawing conclusions of the several attempts made by each group, they are following a distinctive pathway to obtain a common goal, the development of a more useful and universal LC-EI-MS interface.

Regarding Direct-EI LC-MS, recent studies have been carried out also to increase the inertness of the electron ionization ion source by developing new materials [37, 38].

As already stated, the vaporization surface of an electron ionization MS source is a key parameter for the detection and characterization of targeted and untargeted analytes: it is known that difficulties in the vaporization process arise when compounds characterized by high molecular weight and/or polarity have to be analyzed, thus requiring both the use of inert ion sources to reduce the interactions of the analytes with the stainless steel ion source and the use of high source temperatures to promote analyte vaporization. In this field, Magrini et al. [37] proved that the use of a commercially available ceramic coating is able to improve the detection of high molecular weight and high boiling compounds like polycyclic aromatic hydrocarbons (PAHs) and hormones. More recently, Riboni et al. [38] were able to increase the inertness of the electron ionization ion source by developing different sol-gel coatings based on silica, titania, and zirconia. Again, the developed coatings were tested for the Direct-EI LC-MS determination of PAHs and steroids. The best performances in terms of both signal peak intensity and peak width were obtained by using the silica-based coating, obtaining detection limits in the low ng/ml range with a good precision (RSD <9% for PAHs and <11% for hormones). No problems associated to ion cleaning were observed after prolonged use.

3. Advances in Spray-Based Ionization Techniques

Nowadays, there is also a growing interest in the development of real-time analytical technologies capable of allowing the direct detection of trace analytes in complex samples, especially in their native environment. The development of a new class of techniques, better known as "ambient ionization techniques," has introduced a revolution in the ionization field. These techniques are able to generate ions directly from native environment of the sample at ambient pressure, without any tedious sample preparation steps or laborious time-consuming chromatographic separation.

Technically, spray-based ionization techniques are based on the use of electrospray droplets to extract the analytes from the sample and transfer them to the mass spectrometer. The most common spray-based ionization technique is DESI, in which a high-velocity pneumatically assisted ESI source generates charged microdroplets by the application of a proper potential on the ESI needle. The spray is directed towards the sample where the impact of the primary droplets with the substrate leads to the formation of a micrometer-sized thin solvent film, able to solubilize the analytes at the liquid-solid interface. Secondary droplets containing the analytes expelled by the film solvent are generated, and then, desolvation and ionization in the gas phase occur, as in the traditional ESI analysis. Finally, the ions are collected by the MS inlet.

In addition to DESI, several other techniques like nano-DESI, EASI, and LAESI have been proposed. Probe electrospray ionization (PESI) is another interesting approach based on the use of a solid conductive needle probe that replaces the traditional electrospray capillary for sample introduction. Similarly, PSI is a technique based on the loading of the sample onto a triangular piece of paper from which ions are generated by applying a high voltage in the presence of a proper solvent [11]. Spray-based methods are suitable for the analysis of different compounds, from small analytes, such as explosives [39–43], drugs [44–47], and food contaminants [48–50], to larger molecules such as lipids [51–53], peptides [54, 55], and proteins [56, 57].

3.1. Desorption Electrospray Ionization-Mass Spectrometry. DESI-MS is usually applied for surface desorption/ionization of analytes deposited on a probe material (PTFE, PMMA, glass, etc.) or directly from the sample surface. DESI-MS and DESI imaging have been successfully applied in different fields, such as forensic science [58], food control [59, 60], and clinical applications [61–63].

The derivatization of metabolites deposited in solution onto a glass plate by dropping the derivatizing reagent on the top of the dried analytes was proposed by Lubin et al. [64]. The authors successfully applied this technique to several samples, demonstrating the possibility of performing multiple and subsequent derivatization steps on the same spot.

An interesting approach was developed by Brown et al. [65] for the MS detection of fleeting reaction intermediates in electrochemical reactions utilizing a new *waterwheel* working electrode setup. The proposed technique allowed us to exploit DESI-MS operating at a low voltage. The new apparatus consisted of a round rotating platinum working electrode that was partially immersed in an aqueous electrolyte solution (Figure 3). During the rotation, a thin layer of liquid film was deposited on the electrode surface, as in a waterwheel. A three-electrode system was set by using a platinum wire counterelectrode and an Ag/AgCl reference electrode, immersed in the reservoir of electrolyte solution. The upper surface of the waterwheel was hit by a spray generated by a custom spray probe, thus allowing the

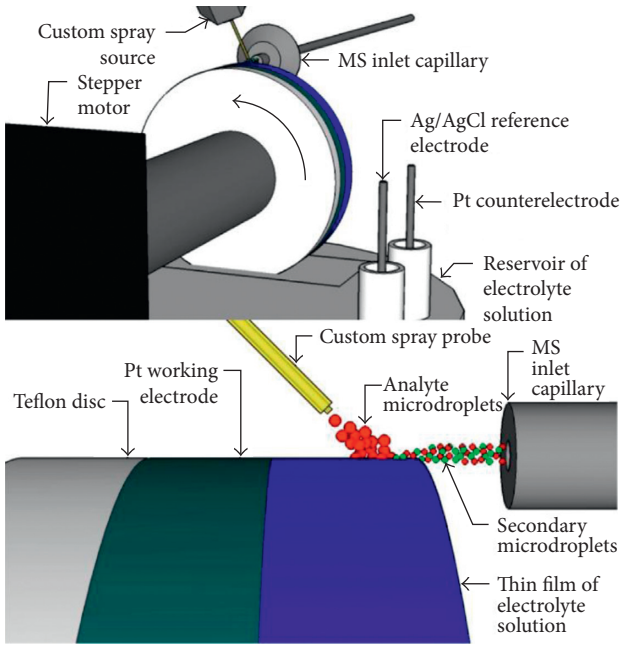

FIGURE 3: Schematic representation of the developed experimental setup. Reprinted with permission from [65].

formation of secondary droplets, analyte ionization, and their collection in the MS inlet. To avoid any electrochemical oxidation or reduction on the electrode surface, no high voltage was applied to the analyte spray, whereas a low potential (few volts) was applied to the platinum rotating electrode.

The authors tested the new apparatus towards the detection of a diimine intermediates during electrochemical oxidation of both uric acid and xanthine.

An MS-electrochemistry coupling was also proposed by Looi et al. [66], who developed a new online electrochemistry-liquid sample desorption electrospray ionization-mass spectrometry (EC-LS DESI-MS) system. In EC-LS DESI-MS, an electrosonic spray ionization source was used to generate a spray directed to the exit of the liquid sample capillary positioned perpendicularly to the spray and the MS inlet. Separately, a thin two-electrode flow-through EC cell was connected to a syringe pump and was used to perform oxidation/reduction processes. The ESSI-generated spray was able to impact the outer surface of the LS capillary, which is continuously coated by sample solution flowing at 200 μl/h, thus allowing the ionization of the analytes. This prototype was developed and tested using *N*,*N*-dimethyl-*p*-phenylenediamine (DMPA). Although oxidation of DMPA was already observed as a result of ionization of DESI-MS in positive mode, by applying a proper voltage to the online electrochemical (EC) cell, it was possible to increase the yields of the oxidation products, thus improving method sensitivity.

Although DESI is usually coupled with high-resolution mass spectrometry, its coupling with LC is possible. A novel splitting method for LC-MS applications, which allows both very fast MS detection of analytes eluted from the LC column and their online collection, was presented by Cai et al. [67, 68]. In this approach, a PEEK capillary tube with a micro-orifice is used to couple DESI with the UPLC column. By using the proposed instrumental setup, a small amount of LC eluent (few nanoliters) is ionized by DESI with negligible time delay (6~10 ms), whereas the remaining analytes exiting the tube outlet can be collected. In addition, online derivatization using reactive DESI is feasible increasing the charge of proteins and consequently enhancing the ionization yields.

An interesting novel configuration has been recently developed by Ren et al. [69]. The authors developed a method coupling slug-flow microextraction (SFME) and nanoelectrospray ionization for the MS analysis of organic compounds in blood and urine. A disposable glass capillary with a pulled tip for nano-ESI was used to perform the entire extraction and ionization process (Figure 4). Two adjacent liquid plugs were formed by injecting 5 μl of a proper organic solvent and 5 μl of body fluid (urine or blood) into the capillary. Liquid-liquid extraction of the analytes was performed by both moving the capillary and applying a push-and-pull force through air pressure. After the extraction process, a high voltage is applied to the organic solvent plug to generate the nano-ESI for MS analysis.

The proposed method was tested for the extraction and detection of different analytes, namely, methamphetamine, benzoylecgonine, verapamil, amitriptyline, epitestosterone, 6-dehydrocholesterone, 5α-androstane-3β, 17β-diol-16-one, and stigmastadienone. Major analytical features were the reduced consumption of both the organic solvent and sample. The authors demonstrated that a direct derivatization of the extracted analytes in the organic phase was feasible, thus achieving excellent sensitivity with detection limits in the 0.03–0.8 ng/ml range.

Despite its name, nanospray DESI (nano-DESI) is based on a different instrumental configuration compared to the traditional DESI: its setup presents two different silica capillaries, one for solvent delivery and the other devoted to the formation of charged liquid spray in front of the MS inlet. The two capillaries are not in direct contact, thus producing a solvent bridge on the DESI surface. The second nanospray capillary produces a self-aspirating nanospray, which is generated by applying a high voltage between the MS inlet and the primary capillary. In comparison with DESI, nano-DESI is characterized by higher efficiency in liquid transportation and sampling performances.

The capabilities of nano-DESI-MS were tested for the determination of pollutants and organic components in atmospheric fine particles by Cain et al. [70], in environmental aerosol by Tao et al. [71], and in clouds by Boone et al. [72]. In the clinical and pharmaceutical fields, both nano-DESI-MS and nano-DESI-MS imaging proved to be excellent techniques for the analysis of pharmaceuticals, biomolecules, and metabolites [73–77].

A further instrumental innovation has been proposed by Duncan and coauthors [78], who developed a pneumatically assisted nanospray desorption electrospray ionization source. The instrumental setup was based on the introduction of a secondary nebulizer replacing the self-aspirating secondary capillary in order to assist solvent

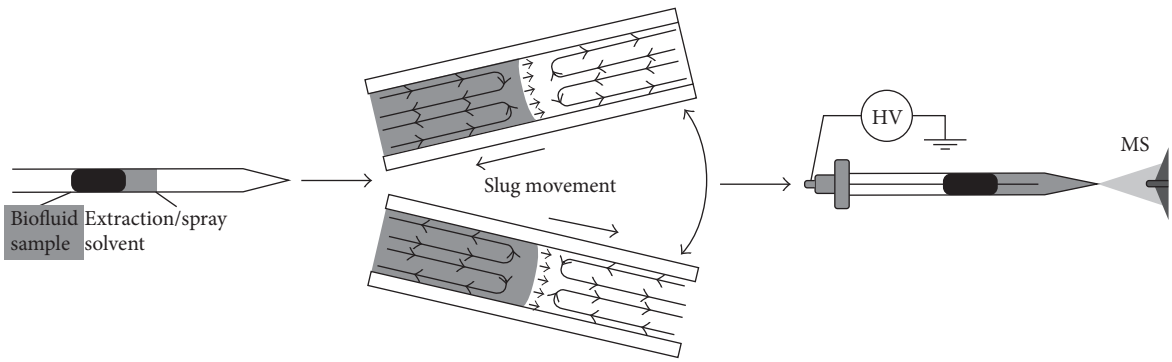

Figure 4: Schematic representation of the SFME-nano-ESI sample processing. Reprinted with permission from [69].

flow, to promote desolvation of the analyte, and to increase the distance between the nanospray and the MS inlet (Figure 5).

The developed device was tested for the analysis of rat kidney tissue sections, allowing us to obtain an improvement in sensitivity of about 1–3 orders of magnitude compared to the conventional setup. In addition, ion images characterized by high contrast, suitable for more intricate studies of metabolite distribution in biological samples, were obtained. A more complete desolvation of the analytes and reduced ionization suppression were additional features of the proposed device.

3.2. Extractive Electrospray Ionization-Mass Spectrometry and Laser Ablation Electrospray Ionization-Mass Spectrometry. Extractive electrospray ionization (EESI) has been introduced in 2006 by Chen et al. [79]. It is based on the use of two different sprayers: the ESI sprayer generates a charged solvent spray, whereas the sample sprayer has the function to nebulize the sample solution from an infusion pump. The analytes are ionized in the collision area of the two sprays, and then, they are collected by the MS inlet.

The ionization mechanism of the EESI ion source was studied by Wang et al. [80], and different MS-based methods for the analysis of organic aerosols [81], drugs [82], pesticides [83], amino acids [84], and biomarkers [85] in different matrices were developed in the recent years.

LAESI-MS is another ambient ionization technique developed in 2007 by Nemes and Vertes [12]. Since most cells used for biomedical applications are cultured adherently, the use of LAESI-MS was proposed to analyze adherent cells directly onto the culture surface, thus avoiding chemical modification deriving from their detachment [86]. In order to reduce the LAESI spot size, the authors applied a transmission geometry- (tg-) LAESI and incorporated an objective with a high numerical aperture, thus achieving spot sizes in the 10–20 μm range. This technique (Figure 6) was tested for the analysis of adherent versus suspended mammal cells, highlighting a difference in the metabolite compositions, thus proving that the cell detachment usually performed is able to produce chemical changes. On the contrary, tg-LAESI-MS allowed us to analyze directly the cells in their native state and, due to the smaller spot size, to reduce the sampled cell population by a factor of 20.

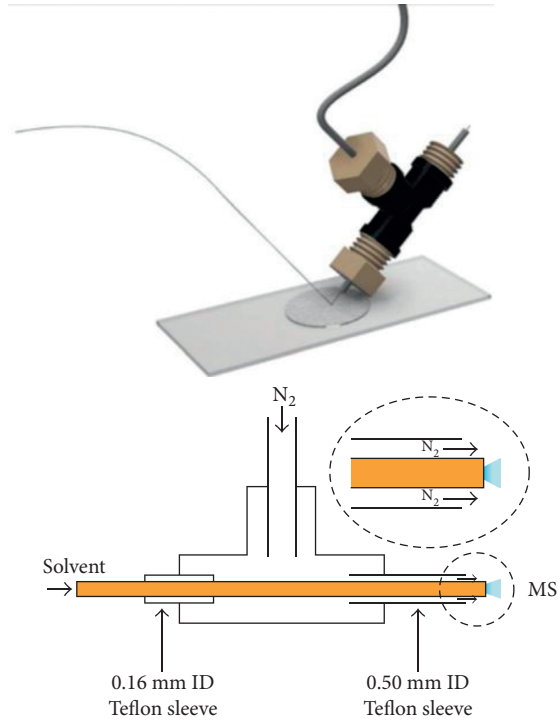

Figure 5: Picture and schematic representation of the pneumatically assisted nano-DESI ionization source. Reprinted with permission from [78].

Optical microscopy combined with LAESI-MS has been suggested by Compton et al. [87] in order to acquire both morphological and chemical information from tissue sampling. In the developed instrumental setup, laser ablation occurred inside a chamber placed under an optical microscope: the ablated particulates generated by the laser were transported through a transfer tube by using nitrogen as carrier gas and finally ionized by the ESI spray.

In order to compare the performances of the developed prototype with those of the conventional LAESI-MS, plant tissues were analyzed. In comparison with conventional LAESI, the developed technique was characterized by reduced sensitivity and dynamic range; however, these features were still sufficient for the analysis and characterization of numerous metabolites and lipids in different spatial regions of biological tissues.

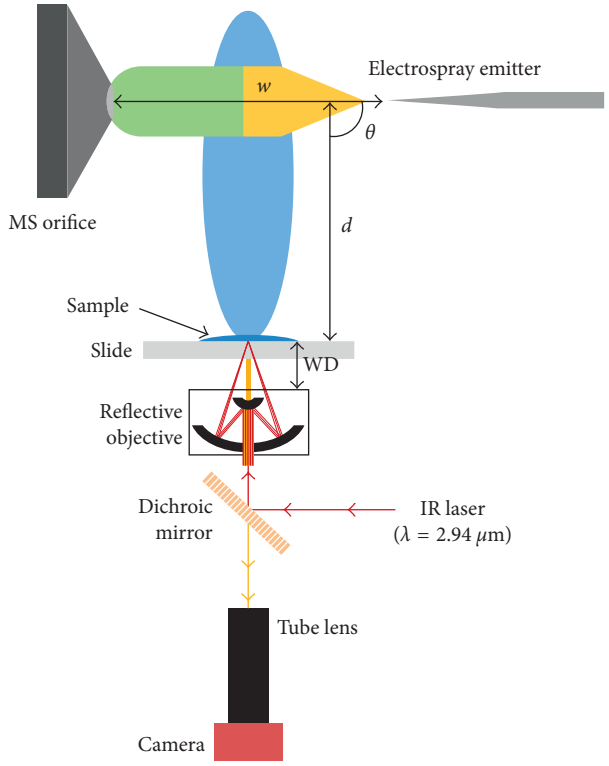

FIGURE 6: Schematic representation of tg-LAESI-MS. Reprinted with permission from [86].

3.3. Paper Spray Ionization-Mass Spectrometry. In the last ten years, approaches based on the direct ionization from solid substrates, such as paper spray, probe-based spray, leaf spray, and tissue spray, strongly increased. All these techniques are characterized by the generation of an electrospray directly from a probe. The analytes in the samples can either be ionized directly upon the substrate surface or be extracted on a probe and subsequently ionized within few minutes, thus boosting analysis speed.

Innovations in PSI-MS have been described by Duarte et al. [88] and Salentijin et al. [89] who developed 3D-printed cartridges in order to obtain a solvent reservoir, thus allowing us to prolong the spray generation from the paper tip. A supporting prototype able to automatically perform PSI-MS analysis of a great number of samples, suitable for high-throughput applications, has been designed by Shen et al. [90]. Finally, the coupling of SFME with PSI-MS for the rapid analysis of macrolide antibiotics at the trace level in biological samples such as whole blood, milk, and other body fluids has been proposed in a study carried out by Deng et al. [91]. The same approach was applied for the detection of perfluorooctanesulfonic acid and perfluorooctanoic acid from *Daphnia magna* body fluids. After the SFME extraction, the organic extract was simply spotted on the PSI paper.

Excellent results were achieved in terms of linearity range (5–500 and 0.5–50 ng/ml range for antibiotics and perfluorocompounds, resp.) and sensitivity (LOQs 0.3–1.3 and 0.03–0.30 ng/ml for antibiotics and perfluorocompounds, resp.). Recovery rates always higher than 85% were obtained.

A novel paper spray cartridge with an integrated solid-phase extraction column has been developed by Zhang and Manicke [92]. The system was designed in order to perform on the same device the extraction, preconcentration, and ionization of the analytes from complex matrices such as blood or plasma. The cartridge was divided into two parts: the bottom one containing the absorbent waste pad and the paper spray substrate and the top one presenting a hole to host the solid-phase extraction (SPE) column. The procedure for performing paper spray analysis is the following: (i) the samples are loaded onto the SPE column (sample volume from 10 μl up to hundreds of microliters); (ii) the unbounded compounds pass through the SPE column and are absorbed by the waste paper pad; (iii) after sliding the top part of the cartridge to the paper spray substrate, the analytes retained on the SPE column are eluted and analyzed by PSI-MS. The analytical performances in terms of detection and quantitation limits, recovery, and ionization suppression were evaluated for carbamazepine, atenolol, sulfamethazine, diazepam, and alprazolam. The SPE cartridge allowed both the selective enrichment of the targeted analytes from large sample volumes (up to hundreds of μl) and the removal of interfering compounds, thus enhancing signal intensities. Compared to direct PSI, the proposed method allowed us to improve quantitation limits by a factor of 14–70, obtaining limits in the 0.2–7 ng/ml range.

3.4. Wooden-Tip Electrospray Ionization-Mass Spectrometry. Wooden-tip electrospray ionization-mass spectrometry (WT-ESI-MS) is a rapid, in situ, and direct ambient technique based on the use of a wooden tip as a sampling and ionization needle. The tip is dipped into the liquid solution/matrix, and after extraction, it is directly used as an ESI probe by applying a high voltage and spray solvent. The analytes enriched on the tip are desorbed and ionized under ambient and open-air conditions.

This method has been successfully applied by Yang et al. [93] for the analysis of pesticides, toxicants, date rape drugs, and illicit additives in various food samples. The capabilities of untargeted WT-ESI-MS analysis for the identification of the sources of plant materials by using a multivariate statistic approach were exploited by Xin et al. [94], whereas Yang and Deng [95] used an internal standard WT-ESI-MS-based method to obtain the fingerprint mass spectra for rapid quality assessment and control of Shuang-Huang-Lian oral fluid, an herbal preparation registered by Chinese Pharmacopoeia. By using the internal standard and principal component analysis (PCA), it was possible to obtain the fingerprints of samples from different manufacturers. A bamboo pen nib shaped and used for sample loading and an ESI probe for the determination of 4-chloro-amphetamine was developed by Chen et al. [96], resulting in lower detection limits compared to PSI-MS and traditional WT-ESI-MS analyses.

Similarly, a WT-ESI-MS method combined with different nonpolar solvents for the detection of native proteins and protein complexes directly from raw biological samples has been proposed by Hu and Yao [97].

The applicability of field-induced wooden-tip electrospray ionization-mass spectrometry (FI-WT-ESI-MS) for high-throughput analysis of herbal medicines has been proved by Yang et al. [98]. Field-induced ESI was performed by applying a high voltage on the MS inlet, thus allowing the creation of a strong electric field between the capillary emitter and MS inlet to induce ESI from the sample solution. A high-throughput analysis device was developed by the application of sample-contactless high voltage on the MS inlet. In addition, the switch between positive and negative ion detection modes can be readily accomplished, thus providing complete MS information of the analyzed samples. This approach allowed us to boost the analysis speed: 6 s per sample was sufficient to perform the analyses.

The proposed method was applied for the rapid determination of various active ingredients in different raw herbs and herbal medicines. The obtained mass spectra were used as fingerprints for tracing the origins, establishing the authenticity and assessing the quality of herbal medicines.

Very recently, a novel and noninvasive sampling method using a watercolor pen (brush) rinsed with ethanol as a sampling tool to collect analytes from the eyelids of volunteers has been evaluated [99]. The brush was placed between the mass inlet and the ESI plume, thus allowing the desorption and ionization of the analytes. The results achieved proved the suitability of the developed technique for the semiquantitative determination of caffeine and its metabolites in eyelid samples.

3.5. Miscellaneous. Following the method developed by Pan et al. [100], based on the use of a single probe inserted into a single cell for sampling intracellular compounds by real-time MS analysis, Chen et al. [52] described a novel method for single cell analysis and lipid profiling by combining drop-on-demand inkjet cell printing and probe electrospray ionization-mass spectrometry (PESI-MS). Droplets containing single cells were generated from a cell suspension by inkjet sampling, precisely dripped onto the tungsten tip of the ESI needle, and sprayed under a high-voltage electric field. Cellular lipid fingerprints were then obtained by MS detection. The analytes from eight types of cells were detected, and PCA analysis was performed in order to differentiate the samples. The proposed platform was demonstrated to be suitable for the direct MS profiling of single-cell lipid species without derivatization or the labeling procedure.

A method for the direct characterization of metals in solid samples using electrospray laser desorption ionization-mass spectrometry (ELDI-MS) has been developed by Shiea et al. [101]. The main advantages over classic approaches were related both to the absence of sample pretreatment and to the presence of very short analysis time. Mixtures of metal-EDTA complexes were applied on a stainless steel plate and submitted to ELDI-MS analysis. The capabilities of the technique were initially tested by spotting the metal-EDTA complexes on a solid probe and performing laser ablation of the material. The ablated analytes, present as EDTA complexes, were ionized in the electrospray plume. Further experiments were carried out by deposing the sample on the probe surface while maintaining the EDTA in the ESI spray solvent (functional electrospray). Excellent results in terms of sensitivity were achieved, thus proving method reliability for the rapid analysis of metal substrates without sample preparation.

An electrostatic spray ionization (ESTASI) method for the analysis of samples deposited in or onto an insulating substrate has been proposed by Qiao and coworkers [102]. In this study, the ionization of the analytes is induced by a capacitive contactless coupling between the electrode and the sample: by applying a pulse high voltage to the electrode, an electrostatic charging of the sample occurs, leading to a bipolar spray pulse. When the applied voltage is positive, the bipolar spray pulse consists first of cations, followed by anion production. The instrumental setup can be modified in order to obtain ion emission from samples in a silica capillary, in a disposable pipette tip, and in a polymer microchannel or deposited as droplets onto an insulating poly(methyl methacrylate) plate presenting wells or hydrophilic patches. This technique proved to be suitable for the analysis of peptides and proteins.

4. Materials for Spray-Based Ionization Techniques

The development of new materials is a field of increasing interest in order to enhance the performances of analytical methods. Both high selectivity and increased ionization efficiency are demanded to detect analytes at trace levels in complex matrices and to shorten analysis time. Different studies have been published dealing with the development of novel surfaces for ambient MS. A brief overview on the most recent materials developed for spray-based ionization techniques with particular attention to DESI-MS and PSI-MS applications is described in the next paragraphs.

4.1. Materials for DESI-MS. In 2005, Takats et al. [103] demonstrated that the DESI ion source is strongly influenced by the dielectric constants of both the substrate material and the spray.

The effect of surface chemistry in the DESI ionization mechanism has been deeply investigated by Penna and coworkers [104]: the performances of different glass substrates obtained by the sol-gel technology and functionalized by using different alkylsilanes were tested and compared in terms of ionization efficiency. The substrates were characterized in terms of surface free energy and wettability. Owing to their different polarity, melamine, tetracycline, and lincomycin were used as model compounds. A significant decrease in the ionization efficiency was observed when more hydrophilic surfaces were used, thus demonstrating the pivotal role of both hydrophobicity and wettability to increase the performances of DESI-MS experiments.

More recently, a 3D printed polylactic (PLA) supports in order to detect insulin and gentamicin in chitosan gels have been proposed by Elviri and coauthors [105]. By using 3D printing, hemispherical wells were created, thus allowing us

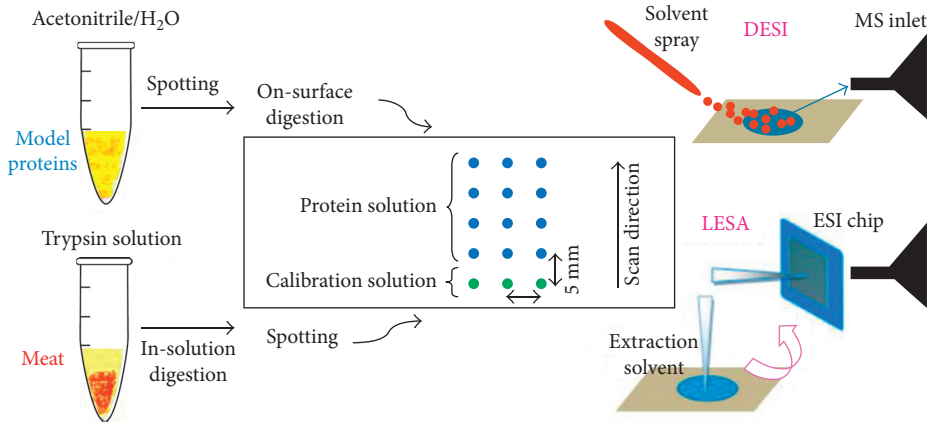

Figure 7: Schematic representation of the procedure proposed by Montowska et al. Reprinted with permission from [106].

to obtain DESI-MS responses five times higher than those achieved by using PTFE commercial slides. Improvement in terms of signal stability was also achieved, thus suggesting the capability of 3D printing technology to improve the desorption step in DESI-MS.

Novel substrates have been proposed also for proteomics and peptidomics: the capability of Permanox slides for both DESI-MS and liquid extraction surface analysis-mass spectrometry (LESA-MS) of skeletal muscle proteins obtained from a mixture of standard proteins and raw meat has been discussed in a recent study [106]. The proposed method is schematically reported in Figure 7.

In both cases, good responses were obtained with LESA-MS characterized by higher sensitivity and stability with respect to the DESI-MS approach. Finally, multivariate data analysis allowed the correct discrimination among different meat classes.

Rapid and simple analyses represent a key parameter in proteomics: an interesting study was carried out by Dulay et al. in 2015 [107]. Two hybrid organic-inorganic organosiloxane polymers functionalized by immobilized trypsin (T-OSX) for the on-surface and in situ digestion of four model proteins, that is, melittin, cytochrome c, myoglobin, and bovine serum albumin, were developed and tested under DESI-MS and nano-DESI-MS conditions. The silica polymers were obtained via sol-gel technique using methyltrimethoxysilane and dimethyl-dimethoxysilane as precursors. The OSX polymers were derivatized with trimethoxysilylbutyraldehyde and functionalized with different amounts of trypsin. In both cases, despite the low enzyme-to-substrate ratios, the achieved results proved the suitability of the developed substrates to allow on-surface protein digestion followed by direct DESI-MS analyses obtaining sequence coverages in the 65–100% range.

Taking into account that DESI-MS analyses can be performed also on liquid samples, an improvement of the apparatus commonly used for this kind of analyses has been proposed [108] by replacing the sample transfer silica capillary with a trap column filled with chromatographic stationary phase materials, such as C_4 and C_{18}. The proposed system proved to be suitable for trace analyses of both organic compounds and biomolecules such as proteins/peptides in complex matrices in the presence of high salt content. Another interesting feature was related to the covalent functionalization of the inner wall of the sample transfer capillary with enzymes, thus allowing the fast and online digestion of proteins.

Noticeable applications of DESI-MS are based on its coupling with new sampling devices and extraction and separation techniques to develop methods for high-throughput analyses.

The microfabrication of ultrathin-layer chromatography (UTLC) plates via conformal low-pressure chemical vapor deposition of silicon nitride onto patterned carbon nanotube (CNT) scaffolds, acting as surface templates, has been described by Kanyal et al. [109]. The plates were heated and oxidized to both remove the CNTs and convert Si_3N_4 into silica; finally, the plates were hydroxylated in aqueous ammonium hydroxide. The resulting UTLC phases did not show any distortion of the microfeatures and were characterized by a higher robustness in comparison to high-pressure TLC plates. Good results in terms of chromatographic performances were observed obtaining a faster separation when mixtures of lipophilic, water-soluble, and fluorescent dyes are to be analyzed. A strong reduction in terms of mobile-phase consumption and an enhanced lifetime were observed. Finally, the UPTLC plates were submitted to both DESI-MSI and direct analysis in real-time (DART)-MS analyses, showing a good compatibility with common ambient desorption and ionization techniques.

In the same year, Ewing et al. [110] described the DESI-MS detection of the low vapor pressure nerve agent simulant triethyl phosphate. The analyte was previously adsorbed onto silica gel, forming a very fine particulate that was collected by using a sticky screen sampler. The device was characterized by a stainless steel screen presenting a partially polymerized polydimethylsiloxane (PDMS) coating. The quantitative collection of the particulate sample from a contaminated surface was achieved by interfacing the sticky screen sampler with a bioaerosol collector. Finally, the sticky screen was placed onto a moveable platform mounted in front of the DESI-MS instrument, thus allowing a reproducible sample introduction system able to minimize sampling errors. DESI-MS analyses performed directly on the PDMS coating allowed us to obtain a very low detection limit suitable for trace detection.

Electrospun nylon-6 nanofiber mats for DESI-MS analysis and imprint imaging have been developed by Hemalatha et al. [111]. The nanofibers were developed by needleless electrospinning: nylon-6 was dissolved in formic acid and the solution was electrospun at room temperature. Uniform mats of varying thicknesses composed of ~200 nm diameter fibers were obtained: the properties of these materials can be tuned by varying spinning conditions and surface functionalization. As model compounds, dyes and the extract of periwinkle flower were spotted onto the nylon nanofiber mat, thus obtaining a uniform coating of the fibers. DESI-MS analysis allowed us to obtain spectra without polymer interference and reproducible DESI-MS images. The authors also demonstrated that compounds of interest could be incorporated into nanofibers during their formation by using as model compounds the crude methanol extract of periwinkle flower and tetraphenylphosphonium bromide (TPPB). The major metabolites of periwinkle were identified by DESI-MS, even though the spectrum was different compared to that obtained by spotting the sample. TPPB was detected with no nylon interference. The authors demonstrated the possibility of imprinting patterns made of printing inks, plant parts, and fungal growth on fruits on the nanofiber mats. Metabolites were identified by DESI-MS. The results highlighted that electrospun nanofiber mats could be considered as smart surfaces to capture diverse classes of compounds for rapid detection or to imprint imaging under ambient conditions.

4.2. Materials for PSI-MS. Although traditional paper spray ionization is performed on the filtering and chromatographic paper [11, 112–115], researchers have focused their attention to the development of new functionalized substrates in order to obtain substrates characterized by enhanced selectivity and sensitivity.

Very recently, Lai et al. [116] compared the ionization performances of different paper-like substrates obtained from both natural fibers and synthetic fibers, namely, gampi paper, Tengujou paper (natural), polycarbonate, polylactic acid, and poly-l-lactic acid (PLLA) (synthetic), with those of traditional chromatographic paper for the analysis of designer drugs. The surface characterization of the developed materials showed the presence of different surface morphologies able to affect PSI capabilities: gampi paper and PLLA nanofibers, characterized by a tough and extremely thin structure, were able to promote signal enhancement, thus allowing us to reach lower limits of detection. These findings could be explained by taking into account the reduced thickness of the used papers: by operating under the described conditions, a rapid evaporation of the sample molecules occurs, thus increasing the speed of the ionization process.

The analytical performances of paper with paraffin barrier (PS-PB) for the PSI-MS detection of hydroxymethylfurfural (HMF) and sugars like glucose and xylose in sugarcane liquors have been tested by Colletes et al. [117]. Microfluidic hydrophobic channels were obtained using paraffin barriers on paper substrates, thus delimiting a region for inducing the sample inlet into the mass spectrometer. The proposed stamping method allowed rapid prototyping of microfluidic paper-based analytical devices, without the need of sophisticated instrumentation. Different types of papers were investigated: an increase of the PSI-MS responses of xylose and glucose as a function of the decrease of porosity of the paper substrate was observed. PS-PB showed the best performance compared to the conventional paper and paper with two rounded corners. PS-PB was applied to detect sugars and their inhibitors in liquors from a second-generation ethanol process, thus obtaining excellent results in terms of linearity (over two orders of magnitude) and limits of detection and quantification.

Another interesting study carried out by Zhang et al. [118] proposed the use of commercially available silica-coated paper in order to increase the PSI-MS responses of therapeutic drugs in dried blood spots. The presence of silica gel particles in the cellulosic framework of the silica-coated paper produced a reduced diffusion of the blood through the substrate, thus leading to a higher percentage of blood sample available on the top side of the substrate. By operating under the optimized conditions, that is, by using dichloromethane/isopropanol (9 : 1 v/v) as a spray solvent mixture, limits of quantitation of about 0.1 ng/mL were achieved, with a sensitivity gain of 5–50-fold in comparison to chromatography papers.

CNT-coated filter paper for low-potential PSI-MS analysis of different organic molecules has been used by Narayanan and coauthors [119]: by applying a voltage of 3 V, full-range mass spectra similar to those obtained by conventional ESI at 3 kV could be recorded. The advantage of the proposed material relies on the use of very mild conditions for the ionization of the analytes, thus allowing the detection of compounds that could be easily oxidized. The performances of the proposed analytical method were assessed for a wide range of volatile and nonvolatile compounds, such as amino acids, antibiotics, and pesticides in different matrices.

Very recently, Wei et al. [120] synthesized graphene oxide (GO) nanosheet-modified N^+-nylon membrane (GOM) for the extraction of malachite green (MG), a highly toxic disinfectant, and its metabolites in liquid samples and fish meat. GO nanosheets are characterized by a very high surface area (~800 m^2/g), suitable for MG adsorption via π-π stacking and electrostatic interactions. GOM was obtained by self-deposition of GO thin films onto N^+-nylon membranes. The material was tested both as a direct spray ionization substrate and as an LDI-MS probe. The latter application resulted in no significant response, whereas the coupling between GOM and direct spray ionization allowed the quantitation of MG and its metabolites at nanomolar levels with extraction recoveries higher than 98%.

An improvement of the performances of PSI-MS in terms of sensitivity has also been achieved in a study dealing with the use of a paper substrate functionalized with urea [121]. Triangles of chromatography paper were treated with 1-[3-(trimethoxysilyl)propyl]urea to create an anion capture layer. The authors demonstrated that the urea-modified paper is an excellent substrate for PSI-MS since it is able

to reduce ionization suppression caused by anions and highly polar compounds in the negative-ion MS mode. These findings are of pivotal importance for the analysis of biological samples like urine, blood, and plant extracts.

A selective substrate for PSI-MS, based on the use of molecularly imprinted polymers (MIPs), has been proposed by Pereira et al. [122]. More precisely, a membrane spray ionization method, combining MIP extraction and PSI-MS analysis, was developed and tested for the determination of diuron and 2,4-dichlorophenoxyacetic acid from apple, banana, and grape methanolic extracts. Being used as PSI substrates, MIPs were synthesized directly on a cellulose membrane: the bulk of the MIP was made by ethylene glycol dimethacrylate, using monuron and 2,4,5-trichlorophenoxyacetic acid as templating agents. After extraction, the MIP membranes were washed to remove matrix interferences and tested as PSI-MS substrates using methanol as a spray solvent. The use of these novel materials allowed us to obtain signal intensities of the targeted analytes far higher than those obtained by nonimprinted polymers with detection limits in the μg/l range.

Bills and Manicke [123] developed a disposable paper spray cartridge containing a plasma fractionation membrane to perform on-cartridge plasma fractionation from whole blood samples. Three commercially available blood fractionation membranes, made of different materials, ranging from polymers to natural and synthetic fibers, that is, Vivid polysulfone membrane, NoviPlex plasma fractionation card, and CytoSep, were tested. Even though all the materials were capable of interacting with plasma samples with low levels of cell lysis, difficulties in terms of drug extraction were observed. In particular, Vivid polysulfone membrane and NoviPlex plasma fractionation card exhibited a high binding capability (over 30%) for all the tested drugs, whereas CytoSep showed a lower binding affinity (<17%) only for two out of five drugs. A drawback of the developed device was also related to the poor fractionation efficiency, as measured by the red blood cell content in the fractionated plasma. Quantitative analysis of plasma using PSI-MS provided results closed to those obtained by HPLC-MS without the need of offline extraction or chromatography separation.

A new zero volt-paper spray ionization (ZV-PSI) has been developed recently by Wleklinski et al. [124]: this approach is based on the generation of the electrospray by the action of the pneumatic force of the vacuum at the MS inlet. ZV-PSI analyses were performed over a large variety of samples, including tributylamine, cocaine, terabutylammonium iodide, 3,5-dinitrobenzoic acid, fludioxonil, and sodium tetraphenylborate. In comparison to classic PSI-MS, the achieved results showed a strong decrease of signal intensities for all the investigated analytes. Although the range of analytes useful for ZV-PSI-MS analysis resulted to be very similar to standard PSI-MS, differences in mass spectra were obtained. The observed behavior was related to the ionization mechanism of the proposed approach, which is strongly related to the effects of analyte surface activity. By using a Monte Carlo simulation, the mechanism regarding the formation of ions from initially uncharged droplets was also explained, thus allowing us to predict detection limits very closed to those observed experimentally and to calculate the relative surface activity of both positive and negative ions.

4.3. Materials for Wooden-Tip Electrospray Ionization-Mass Spectrometry. Surface-coated wooden-tip electrospray ionization-mass spectrometry (SCWT-ESI-MS) is a new technique based on the use of a functionalized wooden needle, acting both as extraction/enrichment phase and ESI probe. By using this strategy, the tip is coated by a proper sorbent for highly selective enrichment of targeted compounds from complex matrices, thus making it suitable for analyses at ultratrace levels. Luan suggested the use of a SCWT-ESI-MS technique to detect different analytes in complex matrices [125, 126].

The SCWT-ESI-MS technique has been applied for the detection of perfluorinated compounds (PFCs) in complex environmental and biological samples at ultratrace level [125]. Sharp wooden tips were functionalized via the silanization process by using octadecyltrimethoxysilane and *n*-octadecyldimethyl[3-(trimethoxysilyl)propyl]ammonium chloride (OTPAC), in order to obtain two different extractive phases, characterized by long alkyl chain. The two phases were tested for the extraction of PFCs spiked water. The OTPAC coating was characterized by the best enrichment capabilities: the extraction is performed not only by the reversed phase, but also by exploiting the ion exchanged adsorption mechanism. Morphological studies of the tip showed a high probe porosity, thus increasing the surface area of the material, and presence of microchannels for transport of the solvent to achieve ambient ionization MS analysis. After method optimization, the probe was tested for the detection of eight different PCFs both in pure water and in complex matrices, that is, lake water, river water, whole blood, and milk. The achieved results proved that the SCWT probe is characterized by outstanding enrichment capabilities, thus being able to enhance method sensitivity by approximately 4000–8000-folds and 100–500-folds in aqueous samples and in whole blood and milk samples, respectively. Method validation resulted in good linearity (two orders of magnitude), excellent quantitation limits (in the 0.21–1.98 ng/l range), and accuracy (recovery rates in the 89–112% range).

Similarly, a SCWT-ESI-MS-based method has been tested for the rapid and sensitive analysis of trace fluoroquinolone and macrolide antibiotics in water [126]. The wooden probe was functionalized via silanization and sulfonation reactions in order to obtain a sulfo-C_8-chain coating able to interact with the analytes with both reversed phase and ion exchange mechanisms. The SCWT-ESI-MS method was then optimized and tested for the extraction of four fluoroquinolone and two macrolide antibiotics in water at trace levels. Method sensitivity allowed us to obtain detection and quantitation limits in the 1.8–4.5 and 5.9–15.1 ng/l range, respectively. Again, linearity was verified over two orders of magnitude: good precision (RSD <14.3%) and recovery rates in the 93.6–112.6% range were other features of the developed method. Finally, the developed method was applied for the analysis of the targeted antibiotics in tap and river water samples.

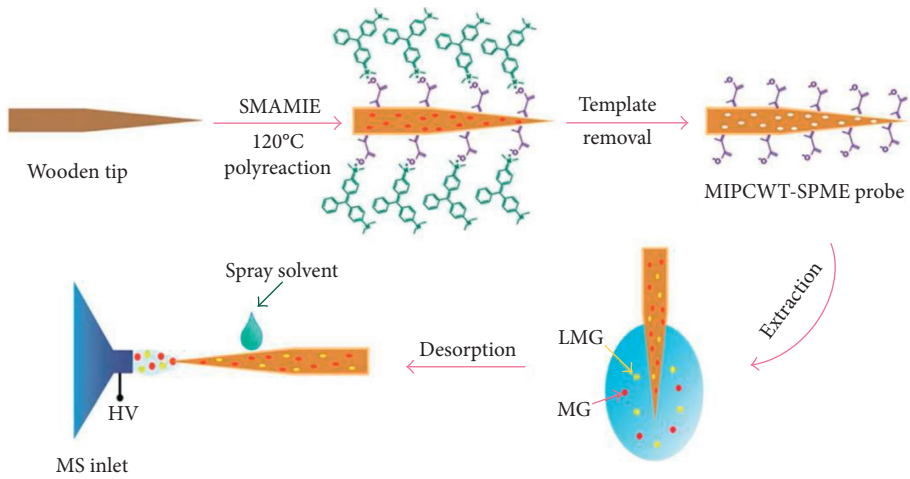

Figure 8: Schematic representation of the instrumental setup proposed by Huang. Reprinted with permission from [127].

An interesting approach based on the use of molecularly imprinted polymers as coating for SCWT-ESI-MS has been discussed in a recent study [127]. The coating was synthesized by applying a silicone-modified acrylate molecularly imprinted emulsion onto the tip surface (Figure 8). The developed material was tested for the detection at trace levels of malachite green and its metabolite leucomalachite green in aqueous samples. The MIP-SCWT probe exhibited high enrichment capabilities, allowing us to obtain detection limits at low μg/l levels. In addition, a good linearity was obtained for both the compounds (three orders of magnitude). The method proved to be suitable for high-throughput analysis and was successfully applied for the analysis of tap water, river water, and fish samples.

4.4. Miscellaneous. Similar to PSI, aluminum-foil mass spectrometry (Al-ESI-MS) was recently developed by Hu et al. [128]. This technique is based on the use of a household aluminum foil to obtain the spray ionization of the analytes. The Al foil was cut into triangles, which were folded symmetrically to obtain a mini-reservoir for the sample solution, and was connected to the high voltage supply of the mass spectrometer. The proposed technique was tested for the direct analysis of a wide variety of complex matrices, namely, energetic beverages, urine, skincare and medical creams, and herbal medicines. The inert, hydrophobic and impermeable surface of the Al foil allowed effective on-target extraction of solid samples and on-target sample clean-up, that is, removal of salts, adulterants, and detergents from proteins and peptides. Being Al an excellent heat conductor, the direct monitoring of thermal reactions, such as thermal denaturation of proteins, can be performed in an easy way by Al-ESI-MS.

In a different research study, ESTASI was applied to identify and quantify different compounds from silica gel surfaces, via direct coupling with TLC [129]. The sample spots separated by TLC were analyzed by ESTASI-MSI. The analyses were performed on both drug molecules, using normal phase TLC, and dyes using reversed phase C18 TLC plates, thus guaranteeing the analyses of compounds characterized by very different polarity. After sample separation, the hydrophobic substrate was coated with chlorotrimethylsilane to form hydrophobic surfaces, suitable for ESTASI analysis. Both TLC plates were considered ideal substrates for in situ characterization of samples by using ESTASI-MS, with efficient analyte extraction and separation. In addition, the capability of removing interfering compounds such as salts increased method performance, thus allowing the detection of the investigated analytes at trace levels.

5. MS-Based Approaches for Food Analysis

The demand for safe and high-quality foods has significantly increased in recent years. Food safety and quality have become of greater importance, and the governments of many countries have increased the amount of relevant legislation and demands for food authentication [130]. In consequence, the development of more robust, efficient, cost-effective, and powerful analytical methodologies is continuously needed in order to face these requirements. MS is one of the most suitable techniques because it is featured by excellent specificity, sensitivity, and throughput [131]. MS has been widely used in food safety and quality analysis, and recent advances in MS can provide faster and more accurate methods able to offer better qualitative and quantitative results. Additionally, coupling mass analyzers with separation techniques, such as liquid chromatography (LC-MS) and gas chromatography (GC-MS), have significantly improved food analysis for screening, identification, structural characterization, and quantitation purposes.

One of the most challenges in the application of MS in food analysis, especially in detection of contaminants, is sample preparation because foods are considered very complex matrices in which some natural components can negatively influence the analysis of the targeted compounds. Traditional methods for sample extraction include solid-liquid extraction (SLE), liquid-liquid extraction (LLE), and solid-phase extraction (SPE). More recent is the use of solid-phase microextraction (SPME), pressurized liquid extraction

(PLE), and QuEChERS (quick easy cheap effective rugged safe) [132]. The introduction of high-resolution mass spectrometers, which provide extremely high selectivity and sensitivity, or other emerging MS strategies such as ambient-ionization MS, direct food analysis, and matrix-assisted lased desorption ionization-time of flight-mass spectrometry (MALDI-TOF-MS) profiling and imaging, has strongly reduced sample preprocessing.

According to the PubMed database, since 2012 about 20000 publications dealing with developed MS-based methods for food safety and quality purposes are available. In this section, we do not intend to provide an exhaustive revision of all published studies, but an overview of the most important MS techniques proposed to evaluate food safety and quality.

5.1. MS-Based Approaches for Food-Safety Assessment. The main purpose of food analysis is to ensure food safety, thus requiring the development of accurate and reliable methodologies for the detection of microbial-related spoilage, determination of allergens, detection of environmental contaminants as well as banned external compounds, or the assessment of the occurrence of natural toxins. These methods are strongly influenced by current legislation, which establishes the requirements that an analytical method must meet for an unequivocal identification and quantification of a controlled substance in food samples, as well as the maximum residue limits (MRLs) on certain substances [133].

Being able to allow the quantification of known compounds with great selectivity and sensitivity, tandem MS detection is one of the most frequently utilized analytical approaches to determine contaminants in foods. Triple quadrupole (QqQ) mass spectrometers, running under multiple reaction monitoring (MRM) mode, are the most popular instruments for detecting contaminants in food. This detection procedure allows us to verify the compliance with European legislation on banned and controlled substances in foods [133].

Since 2010, numerous researches have used this methodology to detect pesticides in several fruits and vegetables, such as tomato [134–137], orange [138], mandarin [139], rice and red pepper [139–141], avocado [142, 143], apples and cucumbers [144, 145], mango [146], tea [147], lettuce [148], grains and cereals [149–152], soybean products [153], groundnut oil [154], and wines [155]. The same methodology was also used in the identification and quantification of veterinary drug residues in shellfish [156], meat [157, 158], eggs and milk [158], and contaminants from food contact materials [159].

Triple quadrupoles in MRM mode is also the most-extended approach to detect and quantify toxins and pathogens in food. These pathogens can contaminate foods directly or indirectly, through the productions of toxins. The control of toxin and pathogen levels is extremely important, since the consequences on health due to their contamination of food may be very serious. Following this approach, food products such as nuts [160], maize [161], shellfish [162], tomato [163], beer [164], and multicereal baby food [165] were analyzed.

Almost all these applications combine QqQ-MS with LC or GC separation methods. In some cases, LC- and GC-based techniques were also coupled with other types of MS analyzers such as ion traps (ITs) or quadrupole-linear ion traps (Q-LITs), TOF, or Q-TOF to determine food contaminants [166–168].

Multidimensional procedures allowed us to increase resolving power and separation capabilities that can be beneficial for subsequent MS-based detection, considering that the targeted compounds can reach the detector more separated in time. This is the case of comprehensive two-dimensional gas chromatography (GC × GC) that has been coupled to a TOF-MS analyzer to determine dioxin-related pollutants in complex food samples [169], to screen 68 pesticide residues in oilseed [170], or to detect and to quantify different polychlorobiphenyls (PCBs), polybrominated diphenyl ethers (PBDEs), and PAHs in fish samples [171].

More recently, HRMS analyzers, typically Q-TOF, Orbitrap-MS, and Fourier-transform ion cyclotron resonance- (FT-ICR-) MS, have been used in the field of food safety. These instruments are characterized by high resolution (100,000–1,000,000 FWHM) and high mass precision (1-2 ppm, allowing discrimination between isobaric interferences and ions of interest), thus making possible the screening of unknown compounds with a full MS scan and the construction of databases for targeted compounds. For instance, UPLC-Orbitrap-MS was used to create a database of more than 350 compounds in honey [172]. These databases included different classes of pesticides and veterinary drugs and allowed simultaneous screening of analytes and identification and quantitation of detected compounds in different honey samples. Similar UPLC-HRMS approaches have been lately used to create an accurate-mass database including the fragmentation of more than 600 different food contaminants, such as pesticides, veterinary drug residues, mycotoxins, and perfluoroalkyl substances [173]. Since the particle size of the stationary phase in UPLC is significantly lower than that observed in HPLC, UPLC yields higher speed, better resolution, increased sensitivity, and better peak capacity. Additional examples are related to the development of LC-Orbitrap-MS-based methods for pesticide screening in vegetables and fruits [174], as well as for the analysis of 18 selected mycotoxins in baby food [175].

Ambient MS-based techniques have also been widely applied for food safety purposes: different ionization techniques have been used like LAESI-MS to detect neurotoxin domoic acid in shellfish [176], DESI-MS for the rapid detection of shellfish poisoning toxins in mussels [39], and PSI-MS for the determination of pesticides in fruits and vegetables [114].

5.2. MS-Based Approaches for Food Quality Assessment. Besides food safety, food quality is one of the main concerns of the modern food industry. Food quality encompasses multiple factors, since food authentication and adulteration of food characteristics include food ingredients, such as lipids, proteins, oligosaccharides, vitamins, and carbohydrates, and additives, such as preservatives, antioxidants, and chemicals used for flavor, color, and odor. As a consequence, the

evaluation of food quality usually represents a very complex task that needs to consider multiple aspects to achieve the appropriate food quality. Food composition, aroma, flavor, or nutritional properties are among the most important features that need to be evaluated in food quality assessments.

Several MS-based approaches have been used to determine food quality. The most recent publications have mainly used nontargeted MS-based approaches, which very often included the coupling LC-MS and/or GC-MS.

Among LC-MS analytical methods, LC-HRMS techniques have been used for quality evaluation of raw turmeric form different regions [177], for the discrimination of grapes according to plant sterol content [178], for the analysis of the metabolome of the Graciano *Vitis vinifera* wine variety [179], and for the investigation of the quality and authenticity of saffron [180] and strawberries . Moreover, methods based on the UPLC combined with HRMS were developed to assess the authentication and the evaluation of possible adulterations in saffron [181] and fruits juices [182, 183]. The last two methods rely on the feasibility of the application of the UPLC-QToF platform to perform both nontargeted and targeted methods to select potential biomarkers, which should make it possible to develop a targeted method (less sophisticated instrumentation and simpler data analysis) for routine analysis. Similarly, the combination of nontargeted and targeted methods was reported for the qualitative analysis of curcuminoids in turmeric [184]. In this case, nontargeted analysis was performed by using LC-QTOF-MS/MS and the targeted approach by LC-QTRAP-MS/MS.

In the LC-MS-based approaches devoted to food quality assessment, it is noteworthy to highlight the use of hydrophilic interaction chromatography (HILIC), especially in metabolomics approaches. HILIC columns allow profiling highly polar and hydrophilic compounds providing complementary metabolic information to reversed-phase LC. In spite of several caveats associated to HILIC, such as variability in retention times, low peak efficiency, and long re-equilibration times after gradient elution, this methodology has been successfully used to analyze contamination and degradation of infant formulas [185], to separate and detect marine toxins [186], or to identify biomarkers of meat quality [187].

GC-MS-based approaches have also been widely used to evaluate food quality. In these approaches, GC was coupled to a huge diversity of mass analyzers: from simple MS instruments, like quadrupole (Q) [188–192], IT [193], to high-resolution instruments [194–198], as well as hybrid analyzers [199–201]. Studies of the effect of volatile compounds for the classification of saffron based on the concentration of biomarkers [188], classification of olive oils on the basis of their quality parameters [200], the establishment of differences between wine grape cultivars [194], or the detection of milk or meat adulteration [78, 190] are only some of examples relying on the use of GC-MS platforms in food quality analysis.

Besides the much more common LC-MS and GC-MS platforms to assess food quality, comprehensive two-dimensional GC [202] and CE methods [186] coupled to TOF analyzers have also been applied. GC × GC allowed the creation of a panel of biomarkers of rice flavor quality through establishing associations between volatile metabolites and perception of rice aroma [202]. These results are valuable for breeding programs since they can be used to choose pleasant rice aromas. In the latter, the feasibility of using a polymer-coated-capillary for the separation of anionic metabolites in both orange juice and wine has been demonstrated [186]. It offers a complementary coverage of the metabolome of these samples to those provided by other analytical techniques.

In addition to spray-based ionization techniques [203–206], mass spectrometry imaging (MSI) is another useful technique for food safety and quality control through monitoring the spatial distribution of bioactive components and contaminants in food samples. Until recently, MSI was largely performed with MALDI. MALDI-TOF-MSI was successfully applied to investigate the distribution of toxic glycoalkaloids in potato tubers [207], to identify the site of capsaicin in *Capsicum* fruits [208], and to observe both the tissue site of 10 anthocyanin species in blueberries [209] and the posttranslational modified sites in the alpha-melanocyte-stimulatin hormone for carp and goldfish pituitary tissue, as well as their ratio change under different environmental conditions [210]. Although MALDI-MSI can detect compounds in a tissue section without extraction, purification, separation, or labeling, the slow speed of the analysis and the need for matrix deposition in MALDI-MS are critical disadvantages in food imaging applications because they involve analyte diffusion able to affect the original molecular distribution. The development of various ambient ionization techniques revived interest in MSI because of the direct surface sampling in front of a mass spectrometer with submillimeter resolution and no sample preparation. These techniques permit rapid, direct measurement of compounds present on the condensed sample phase and have become potential analytical tools for direct profile-imaging analysis in an atmospheric pressure environment, thus being particularly useful for food-quality control purposes.

Although the application of these techniques in food analysis is not yet fully established, some examples can be found in literature. As an example, ELDI-MS was applied to obtain the molecular profiling and spatial distribution of particular active components in two edible fungi species [211] as well as alpha-solanine and alpha-chaconine in potato [212].

DESI-MSI was used to reveal the spatial distribution of chlorogenic acids and sucrose across the bean endosperm [213], as well as the spatial and temporal distribution of rohitukine and related compounds during various stages of seed development [214]. LAESI allowed macroscopic and microscopic imaging of pesticides, mycotoxins, and plant metabolites in different matrices [215].

6. Conclusions

MS-based techniques represent a highly valuable tool for environmental, bioanalytical, food safety, and food-quality control purposes and their application in these fields strongly increased in the past years. Despite the numerous advantages of MS-based methods, one of the most challenging aspects is still related to the analysis of complex matrices for the detection of nontarget or unknown compounds. The creation of detailed libraries of compounds, including MS-based information such as accurate mass,

isotopic patterns, and collision-induced fragmentation, is strongly demanded.

Innovations in ambient MS allowed the development of analytical methods characterized by high-throughput and minimal sample preparation, thus allowing the analysis of samples in their native ambient. However, an important feature to be discussed when ambient MS methods are used is related to the concentration of the detected compounds on the sample surface that might not represent the actual concentration in the whole sample, thus not matching the requirements of current legislation or official methods of analysis.

Nomenclature

CE: Capillary electrophoresis
CNT: Carbon nanotube
DART: Direct analysis in real time
DESI: Desorption electrospray ionization
DMPA: *N*,*N*-dimethyl-*p*-phenylenediamine
EASI: Easy ambient sonic-spray ionization
EC: Electrochemical
EESI: Extractive electrospray ionization
EI: Electron ionization
ELDI: Electrospray laser desorption ionization
ESI: Electrospray ionization
ESTASI: Electrostatic spray ionization
FA: Fatty acid
FFA: Free fatty acid
FI: Field-induced
FT-ICR: Fourier-transform ion cyclotron resonance
GC: Gas chromatography
GC × GC: Two-dimensional gas chromatography
GO: Graphene oxide
GOM: Graphene oxide membrane
HMF: Hydroxymethylfurfural
HILIC: Hydrophilic interaction liquid chromatography
HPLC: High-performance liquid chromatography
HRMS: High-resolution mass spectrometry
LIT: Linear ion trap
IT: Ion trap
LAESI: Laser ablation electrospray ionization
LC: Liquid chromatography
LEI: Liquid-electron ionization
LESA: Liquid extraction surface analysis
LLE: Liquid-liquid extraction
LS: Liquid sample
LOQ: Limit of quantitation
MALDI: Matrix-assisted laser desorption/ionization
ME: Matrix effect
MG: Malachite green
MIP: Molecularly imprinted polymer
MRL: Maximum residue limit
MRM: Multiple reaction monitoring
MS: Mass spectrometry
MSI: Mass spectrometry imaging
MS/MS: Tandem mass spectrometry
OTPAC: Octadecyldimethyl[3-(trimethoxysilyl)propyl] ammonium chloride
PAHs: Polycyclic aromatic hydrocarbons
PB: Paraffin barrier
PBDE: Polybrominated diphenyl ether
PCB: Polychlorobiphenyl
PDMS: Polydimethylsiloxane
PESI: Probe electrospray ionization
PFC: Perfluorinated compound
PMMA: Poly(methyl methacrylate)
PLA: Polylactate
PLE: Pressurized liquid extraction
PLLA: Poly-l-lactic acid
PSI: Paper spray ionization
PTFE: Polytetrafluoroethylene
Q: Quadrupole
QqQ: Triple quadrupole
QuEChERS: Quick easy cheap effective rugged safe
RSD: Relative standard deviation
SCWT: Surface-coated wooden tip
SFME: Slug-flow microextraction
SLE: Solid-liquid extraction
SMB: Supersonic molecular beam
SPE: Solid-phase extraction
SPME: Solid-phase microextraction
TLC: Thin-layer chromatography
TOF: Time of flight
TPPB: Tetraphenylphosphonium bromide
UPLC: Ultraperformance liquid chromatography
UTLC: Ultrathin-layer chromatography
WT: Wooden tip
ZV-PSI: Zero volt-paper spray ionization.

Conflicts of Interest

The authors declare that they have no conflicts of interest.

References

[1] T. Kind and O. Fiehn, "Advances in structure elucidation of small molecules using mass spectrometry," *Bioanalytical Reviews*, vol. 2, no. 1–4, pp. 23–60, 2010.

[2] R. Chen, J. Deng, L. Fang et al., "Recent applications of ambient ionization mass spectrometry in environmental analysis," *Trends in Environmental Analytical Chemistry*, vol. 15, pp. 1–11, 2017.

[3] M. Smoluch, P. Mielczarek, and J. Silberring, "Plasma-based ambient ionization mass spectrometry in bioanalytical sciences," *Mass Spectrometry Reviews*, vol. 35, no. 1, pp. 22–34, 2016.

[4] X. Ma and Z. Ouyang, "Ambient ionization and miniature mass spectrometry system for chemical and biological analysis," *TrAC Trends in Analytical Chemistry*, vol. 85, pp. 10–19, 2016.

[5] C. W. Klampfl and M. Himmelsbach, "Direct ionization methods in mass spectrometry: an overview," *Analytica Chimica Acta*, vol. 890, pp. 44–59, 2015.

[6] C. Y. Shi and C. H. Deng, "Recent advances in inorganic materials for LDI-MS analysis of small molecules," *Analyst*, vol. 141, no. 10, pp. 2816–2826, 2016.

[7] B. B. Schneider, E. G. Nazarov, F. Londry, P. Vouros, and T. R. Covey, "Differential mobility spectrometry/mass spectrometry history, theory, design optimization, simulations, and applications," *Mass Spectrometry Reviews*, vol. 35, no. 6, pp. 687–737, 2015.

[8] T. J. Kauppila, J. A. Syage, and T. Benter, "Recent developments in atmospheric pressure photoionization-mass spectrometry," *Mass Spectrometry Reviews*, vol. 36, no. 3, pp. 423–449, 2017.

[9] P. M. Peacock, W. J. Zhang, and S. Trimpin, "Advances in ionization for mass spectrometry," *Analytical Chemistry*, vol. 89, no. 1, pp. 372–388, 2017.

[10] Z. Takàts, J. M. Wiseman, B. Gologan, and R. G. Cooks, "Mass spectrometry sampling under ambient conditions with desorption electrospray ionization," *Science*, vol. 306, no. 5695, pp. 471–473, 2004.

[11] H. Wang, J. Liu, R. G. Cooks, and Z. Ouyang, "Paper spray for direct analysis of complex mixtures using mass spectrometry," *Angewandte Chemie International Edition*, vol. 49, no. 5, pp. 877–880, 2010.

[12] P. Nemes and A. Vertes, "Laser ablation electrospray ionization for atmospheric pressure, in vivo, and imaging mass spectrometry," *Analytical Chemistry*, vol. 79, no. 21, pp. 8098–8106, 2007.

[13] L. Li and K. A. Schug, "On- and off-line coupling of separation techniques to ambient ionization mass spectrometry," *LCGC North America*, vol. 9, no. 4, pp. 8–14, 2011.

[14] A. Herrmann, J. Rosen, D. Jansson, and K. E. Hellenas, "Evaluation of a generic multi-analyte method for detection of >100 representative compounds correlated to emergency events in 19 food types by ultrahigh-pressure liquid chromatography-tandem mass spectrometry," *Journal of Chromatography A*, vol. 1235, pp. 115–124, 2012.

[15] F. T. Peters, "Recent advances of liquid chromatography-(tandem) mass spectrometry in clinical and forensic toxicology," *Clinical Biochemistry*, vol. 44, no. 1, pp. 54–65 2011.

[16] D. Remane, D. K. Wissenbach, and F. T. Peters, "Recent advances of liquid chromatography–(tandem) mass spectrometry in clinical and forensic toxicology—an update," *Clinical Biochemistry*, vol. 49, no. 13-14, pp. 1051–1071, 2016.

[17] F. T. Peters and D. Remane, "Aspects of matrix effects in applications of liquid chromatography-mass spectrometry to forensic and clinical toxicology–a review," *Analytical and Bioanalytical Chemistry*, vol. 403, no. 8, pp. 2155–2172, 2012.

[18] F. Gosetti, E. Mazzucco, D. Zampieri, and M. C. Gennaro, "Signal suppression/enhancement in high-performance liquid chromatography tandem mass spectrometry," *Journal of Chromatography A*, vol. 1217, no. 25, pp. 3929–3937, 2010.

[19] A. K. Malik, C. Blasco, and Y. Pico, "Liquid chromatography-mass spectrometry in food safety," *Journal of Chromatography A*, vol. 1217, no. 25, pp. 4018–4040, 2010.

[20] A. Kaufmann, "The current role of high-resolution mass spectrometry in food analysis," *Analytical and Bioanalytical Chemistry*, vol. 403, no. 5, pp. 1233–1249, 2013.

[21] F. Hernandez, J. V. Sancho, M. Ibanez, E. Abad, T. Portoles, and L. Mattioli, "Current use of high-resolution mass spectrometry in the environmental sciences," *Analytical and Bioanalytical Chemistry*, vol. 403, no. 5, pp. 1251–1264, 2012.

[22] M. M. Gomez-Ramos, C. Ferrer, O. Malato, A. Aguera, and A. R. Fernandez-Alba, "Liquid chromatography-high-resolution mass spectrometry for pesticide residue analysis in fruit and vegetables: screening and quantitative studies," *Journal of Chromatography A*, vol. 1287, pp. 24–37, 2013.

[23] A. G. Marshall and C. L. Hendrickson, "High-resolution mass spectrometers," *Annual Review of Analytical Chemistry*, vol. 1, no. 1, pp. 579–599, 2008.

[24] Y. Fu, C. Zhao, X. Lu, and G. Xu, "Nontargeted screening of chemical contaminants and illegal additives in food based on liquid chromatography-high resolution mass spectrometry," *TrAC Trends in Analytical Chemistry*, vol. 96, pp. 89–98, 2017.

[25] M. Mattarozzi, M. Milioli, C. Cavalieri, F. Bianchi, and M. Careri, "Rapid desorption electrospray ionization-high resolution mass spectrometry method for the analysis of melamine migration from melamine tableware," *Talanta*, vol. 101, pp. 453–459, 2012.

[26] B. O. Crews, A. J. Pesce, R. West, H. Nguyen, and R. L. Fitzgerald, "Evaluation of high-resolution mass spectrometry for urine toxicology screening in a pain management setting," *Journal of Analytical Toxicology*, vol. 36, no. 9, pp. 601–607, 2012.

[27] F. Guale, S. Shahreza, J. P. Waltersheid, H. H. Chen, C. Arndt, and A. T. Kelly, "Validation of LC-TOF-MS screening for drugs, metabolites, and collateral compounds in forensic toxicology specimens," *Journal of Analytical Toxicology*, vol. 37, no. 1, pp. 17–24, 2013.

[28] F. W. McLafferty, *Interpretation of Mass Spectra*, University Science Books, Mill Valley, CA, USA, 1980.

[29] A. Cappiello, G. Famiglini, P. Palma, E. Pierini, V. Termopoli, and H. Trufelli, "Direct-EI in LC-MS: towards a universal detector for small-molecule applications," *Mass Spectrometry Reviews*, vol. 30, no. 6, pp. 1242–1255, 2011.

[30] P. Palma, G. Famiglini, H. Trufelli, E. Pierini, V. Termopoli, and A. Cappiello, "Electron ionization in LC-MS: recent developments and applications of the direct-EI LC-MS interface," *Analytical and Bioanalytical Chemistry*, vol. 399, no. 8, pp. 2683–2693, 2011.

[31] A. Cappiello, G. Famiglini, P. Palma, V. Termopoli, F. Capriotti, and N. Cellar, "Identification potential of direct-EI LC–MS interfacing in small-molecule applications," *Journal of Separation Science*, vol. 5, pp. 13–17, 2013.

[32] V. Termopoli, G. Famiglini, P. Palma, M. Piergiovanni, and A. Cappiello, "Atmospheric pressure vaporization mechanism for coupling a liquid phase with electron ionization mass spectrometry," *Analytical Chemistry*, vol. 89, no. 3, pp. 2049–2056, 2017.

[33] F. Rigano, A. Albergamo, D. Sciarrone, M. Beccaria, G. Purcaro, and L. Mondello, "Nano liquid chromatography directly coupled to electron ionization mass spectrometry for free fatty acid elucidation in mussel," *Analytical Chemistry*, vol. 88, no. 7, pp. 4021–4028, 2016.

[34] B. Seemann, T. Alon, S. Tsizin, A. B. Fialkov, and A. Amirav, "Electron ionization LC-MS with supersonic molecular beams-the new concept, benefits and applications," *Journal of Mass Spectrometry*, vol. 50, no. 11, pp. 1252–1263, 2015.

[35] G. A. Harris, A. S. Galhena, and F. M. Fernandez, "Ambient sampling/ionization mass spectrometry: applications and current trends," *Analytical Chemistry*, vol. 83, no. 12, pp. 4508–4538, 2011.

[36] M. Domin and R. Cody, *Ambient Ionization Mass Spectrometry*, Royal Society of Chemistry, Cambridge, UK, 2015.

[37] L. Magrini, G. Famiglini, P. Palma, V. Termopoli, and A. Cappiello, "Boosting the detection potential of liquid chromatography-electron ionization mass spectrometry using a ceramic coated ion source," *Journal of the American Society for Mass Spectrometry*, vol. 27, no. 1, pp. 153–160, 2016.

[38] N. Riboni, L. Magrini, F. Bianchi, M. Careri, and A. Cappiello, "Sol-gel coated ion sources for liquid chromatography-direct electron ionization mass spectrometry," *Analytica Chimica Acta*, vol. 978, pp. 35–41, 2017.

[39] F. Bianchi, A. Gregori, G. Braun, C. Crescenzi, and M. Careri, "Micro-solid-phase extraction coupled to desorption electrospray ionization-high-resolution mass spectrometry for the analysis of explosives in soil," *Analytical and Bioanalytical Chemistry*, vol. 407, no. 3, pp. 931–938, 2014.

[40] N. L. Sanders, S. Kothari, G. Huang, G. Salazar, and R. G. Cooks, "Detection of explosives as negative ions directly from surfaces using a miniature mass spectrometer," *Analytical Chemistry*, vol. 82, no. 12, pp. 5313–5316, 2010.

[41] I. Cotte-Rodríguez, Z. Takats, N. Talaty, H. Chen, and R. G. Cooks, "Desorption electrospray ionization of explosives on surfaces: sensitivity and selectivity enhancement by reactive desorption electrospray ionization," *Analytical Chemistry*, vol. 77, no. 21, pp. 6755–6764, 2005.

[42] N. Talaty, C. C. Mulligan, D. R. Justes, A. U. Jackson, R. J. Noll, and R. G. Cooks, "Fabric analysis by ambient mass spectrometry for explosives and drugs," *Analyst*, vol. 133, no. 11, pp. 1532–1540, 2008.

[43] I. Cotte-Rodriguez, H. Hernandez-Soto, H. Chen, and R. G. Cooks, "In situ trace detection of peroxide explosives by desorption electrospray ionization and desorption atmospheric pressure chemical ionization," *Analytical Chemistry*, vol. 80, no. 5, pp. 1512–1519, 2008.

[44] J. M. Wiseman, D. R. Ifa, Y. Zhu et al., "Desorption electrospray ionization mass spectrometry: imaging drugs and metabolites in tissues," *Proceedings of the National Academy of Sciences*, vol. 105, no. 47, pp. 18120–18125, 2008.

[45] T. J. Kauppila, N. Talaty, T. Kuuranne, T. Kotiaho, R. Kostiainen, and R. G. Cooks, "Rapid analysis of metabolites and drugs of abuse from urine samples by desorption electrospray ionization-mass spectrometry," *Analyst*, vol. 132, no. 9, pp. 868–875, 2007.

[46] T. J. Kauppila, J. M. Wiseman, R. A. Ketola, T. Kotiaho, R. G. Cooks, and R. Kostiainen, "Desorption electrospray ionization mass spectrometry for the analysis of pharmaceuticals and metabolites," *Rapid Communications in Mass Spectrometry*, vol. 20, no. 3, pp. 387–392, 2006.

[47] Z. Lin, S. Zhang, M. Zhao, C. Yang, D. Chen, and X. Zhang, "Rapid screening of clenbuterol in urine samples by desorption electrospray ionization tandem mass spectrometry," *Rapid Communications in Mass Spectrometry*, vol. 22, no. 12, pp. 1882–1888, 2008.

[48] H. Chen, J. Zheng, X. Zhang, M. Luo, Z. Wang, and X. Qiao, "Surface desorption atmospheric pressure chemical ionization mass spectrometry for direct ambient sample analysis without toxic chemical contamination," *Journal of Mass Spectrometry*, vol. 42, no. 8, pp. 1045–1056, 2007.

[49] R. J. Fussell, D. Chan, and M. Sharman, "An assessment of atmospheric-pressure solids-analysis probes for the detection of chemicals in food," *TrAC Trends in Analytical Chemistry*, vol. 29, no. 11, pp. 1326–1335, 2010.

[50] C. Black, O. P. Chevallier, and C. T. Elliott, "The current and potential applications of ambient mass spectrometry in detecting food fraud," *TrAC Trends in Analytical Chemistry*, vol. 82, pp. 268–278, 2016.

[51] E. Hiyama, A. Ali, S. Amer et al., "Direct lipido-metabolomics of single floating cells for analysis of circulating tumor cells by live single-cell mass spectrometry," *Analytical Sciences*, vol. 31, no. 12, pp. 1215–1517, 2015.

[52] F. Chen, L. Lin, J. Zhang, Z. He, K. Uchiyama, and J. M. Lin, "Single-cell analysis using drop-on-demand inkjet printing and probe electrospray ionization mass spectrometry," *Analytical Chemistry*, vol. 88, no. 8, pp. 4354–4360, 2016.

[53] X. Gong, Y. Zhao, S. Cai et al., "Single cell analysis with probe ESI-mass spectrometry: detection of metabolites at cellular and subcellular levels," *Analytical Chemistry*, vol. 86, no. 8, pp. 3809–3816, 2014.

[54] Z. Takats, J. M. Wiseman, D. R. Ifa, and R. G. Cooks, "Desorption electrospray ionization (DESI) analysis of tryptic digests/peptides," *Cold Spring Harbor Protocols*, vol. 2008, no. 5, p. pdb.prot4993, 2008.

[55] S. P. Pasilis, V. Kertesz, G. J. Van Berkel, M. Schulz, and S. Schorcht, "Using HPTLC/DESI-MS for peptide identification in 1D separations of tryptic protein digests," *Analytical and Bioanalytical Chemistry*, vol. 391, no. 1, pp. 317–324, 2008.

[56] G. Parsiegla, B. Shrestha, F. Carriere, and A. Vertes, "Direct analysis of phycobilisomal antenna proteins and metabolites in small cyanobacterial populations by laser ablation electrospray ionization mass spectrometry," *Analytical Chemistry*, vol. 84, no. 1, pp. 34–38, 2012.

[57] Z. P. Yao, "Characterization of proteins by ambient mass spectrometry," *Mass Spectrometry Reviews*, vol. 31, no. 4, pp. 437–447, 2012.

[58] M. Morelato, A. Beavis, P. Kirkbride, and C. Roux, "Forensic applications of desorption electrospray ionisation mass spectrometry (DESI-MS)," *Forensic Science International*, vol. 226, no. 1–3, pp. 10–21, 2013.

[59] C. Ibáñez, V. García-Cañas, A. Valdés, and C. Simó, "Novel MS-based approaches and applications in food metabolomics," *TrAC Trends in Analytical Chemistry*, vol. 52, pp. 100–111, 2013.

[60] M. Castro-Puyana and M. Herrero, "Metabolomics approaches based on mass spectrometry for food safety, quality and traceability," *TrAC Trends in Analytical Chemistry*, vol. 52, pp. 74–87, 2013.

[61] P. Nemes and A. Vertes, "Ambient mass spectrometry for in vivo local analysis and in situ molecular tissue imaging," *TrAC Trends in Analytical Chemistry*, vol. 34, pp. 22–34, 2012.

[62] E. R. St John, M. Rossi, P. Pruski, A. Darzi, and Z. Takats, "Intraoperative tissue identification by mass spectrometric technologies," *TrAC Trends in Analytical Chemistry*, vol. 85, pp. 2–9, 2016.

[63] Y. Yang, Y. Huang, J. Wu, N. Liu, J. Deng, and T. Luan, "Single-cell analysis by ambient mass spectrometry," *TrAC Trends in Analytical Chemistry*, vol. 90, pp. 14–26, 2017.

[64] A. A. Lubin, D. Cabooter, P. Augustijns, and F. Cuyckens, "One drop chemical derivatization – DESI-MS analysis for metabolite structure identification," *Journal of Mass Spectrometry*, vol. 50, no. 7, pp. 871–878, 2015.

[65] T. A. Brown, H. Chen, and R. N. Zare, "Identification of fleeting electrochemical reaction intermediates using desorption electrospray ionization mass spectrometry," *Journal of the American Chemical Society*, vol. 137, no. 23, pp. 7274–7277, 2015.

[66] W. D. Looi, B. Brown, L. Chamand, and A. Brajter-Toth, "Merits of online electrochemistry liquid sample desorption electrospray ionization mass spectrometry (EC/LS DESI MS)," *Analytical and Bioanalytical Chemistry*, vol. 408, no. 9, pp. 2227–2238, 2016.

[67] Y. Cai, D. Adams, and H. Chen, "A new splitting method for both analytical and preparative LC/MS," *Journal of the*

American Society for Mass Spectrometry, vol. 25, no. 2, pp. 286–292, 2014.

[68] Y. Cai, Y. Liu, R. Helmy, and H. Chen, "Coupling of ultrafast LC with mass spectrometry by DESI," *Journal of The American Society for Mass Spectrometry*, vol. 25, no. 10, pp. 1820–1823, 2014.

[69] Y. Ren, M. N. McLuckey, J. Liu, and Z. Ouyang, "Direct mass spectrometry analysis of biofluid samples using slug-flow microextraction nano-electrospray ionization," *Angewandte Chemie International Edition*, vol. 53, no. 51, pp. 14124–14127, 2014.

[70] J. Cain, A. Laskin, M. R. Kholghy, M. J. Thomson, and H. Wang, "Molecular characterization of organic content of soot along the centerline of a coflow diffusion flame," *Physical Chemistry Chemical Physics*, vol. 16, no. 47, pp. 25862–25875, 2014.

[71] S. Tao, X. Lu, N. Levac et al., "Molecular characterization of organosulfates in organic aerosols from Shanghai and Los Angeles urban areas by nanospray-desorption electrospray ionization high-resolution mass spectrometry," *Environmental Science & Technology*, vol. 48, no. 18, pp. 10993–11001, 2014.

[72] E. J. Boone, A. Laskin, J. Laskin et al., "Aqueous processing of atmospheric organic particles in cloud water collected via aircraft sampling," *Environmental Science & Technology*, vol. 49, no. 14, pp. 8523–8530, 2015.

[73] C. Cardoso-Palacios and I. Lanekoff, "Direct analysis of pharmaceutical drugs using nano-DESI MS," *Journal of Analytical Methods in Chemistry*, vol. 2016, Article ID 3591908, 6 pages, 2016.

[74] J. Watrous, P. Roach, B. Heath, T. Alexandrov, J. Laskin, and P. C. Dorrestein, "Metabolic profiling directly from the Petri dish using nanospray desorption electrospray ionization imaging mass spectrometry," *Analytical Chemistry*, vol. 85, no. 21, pp. 10385–10391, 2013.

[75] H. M. Bergman and I. Lanekoff, "Profiling and quantifying endogenous molecules in single cells using nano-DESI MS," *Analyst*, vol. 142, no. 19, pp. 3639–3647, 2017.

[76] H. M. Bergman, E. Lundin, M. Andersson, and I. Lanekoff, "Quantitative mass spectrometry imaging of small-molecule neurotransmitters in rat brain tissue sections using nanospray desorption electrospray ionization," *Analyst*, vol. 141, no. 12, pp. 3686–3695, 2016.

[77] C. C. Hsu, P. T. Chou, and R. N. Zare, "Imaging of proteins in tissue samples using nanospray desorption electrospray ionization mass spectrometry," *Analytical Chemistry*, vol. 87, no. 22, pp. 11171–11175, 2015.

[78] D. Duncan, H. M. Bergman, and I. Lanekoff, "A pneumatically assisted nanospray desorption electrospray ionization source for increased solvent versatility and enhanced metabolite detection from tissue," *Analyst*, vol. 142, no. 18, pp. 3424–3431, 2017.

[79] H. W. Chen, A. Venter, and R. G. Cooks, "Extractive electrospray ionization for direct analysis of undiluted urine, milk and other complex mixtures without sample preparation," *Chemical Communications*, vol. 42, no. 19, pp. 2042–2044, 2006.

[80] R. Wang, A. J. Gröhn, L. Zhu et al., "On the mechanism of extractive electrospray ionization (EESI) in the dual-spray configuration," *Analytical and Bioanalytical Chemistry*, vol. 402, no. 8, pp. 2633–2643, 2012.

[81] P. J. Gallimore and M. Kalberer, "Characterizing an extractive electrospray ionization (EESI) source for the online mass spectrometry analysis of organic aerosols," *Environmental Science & Technology*, vol. 47, no. 13, pp. 7324–7331, 2013.

[82] G. K. Koyanagi, V. Blagojevic, and D. K. Bohme, "Applications of extractive electrospray ionization (EESI) in analytical chemistry," *International Journal of Mass Spectrometry*, vol. 379, pp. 146–150, 2015.

[83] M. Deng, T. Yu, H. Luo, T. Zhu, X. Huang, and L. Luo, "Direct detection of multiple pesticides in honey by neutral desorption-extractive electrospray ionization mass spectrometry," *International Journal of Mass Spectrometry*, vol. 422, pp. 111–118, 2017.

[84] N. Xu, Z. Q. Zhu, S. P. Yang et al., "Direct detection of amino acids using extractive electrospray ionization tandem mass spectrometry," *Chinese Journal of Analytical Chemistry*, vol. 41, no. 4, p. 523, 2013.

[85] X. Li, X. Fang, Z. Yu et al., "Direct quantification of creatinine in human urine by using isotope dilution extractive electrospray ionization tandem mass spectrometry," *Analytica Chimica Acta*, vol. 748, pp. 53–57, 2012.

[86] R. S. Jacobson, R. L. Thurston, B. Shrestha, and A. Vertes, "In situ analysis of small populations of adherent mammalian cells using laser ablation electrospray ionization mass spectrometry in transmission geometry," *Analytica Chimica Acta*, vol. 87, no. 24, pp. 12130–12136, 2015.

[87] L. R. Compton, B. Reschke, J. Friend, M. Powell, and A. Vertes, "Remote laser ablation electrospray ionization mass spectrometry for non-proximate analysis of biological tissues," *Rapid Communications in Mass Spectrometry*, vol. 29, no. 1, pp. 67–73, 2015.

[88] L. C. Duarte, T. C. de Carvalho, E. O. Lobo-Júnior, P. V. Abdelnur, B. G. Vaza, and W. K. T. Coltro, "3D printing of microfluidic devices for paper-assisted direct spray ionization mass spectrometry," *Analytical Methods*, vol. 8, no. 3, pp. 496–503, 2016.

[89] G. I. J. Salentijn, H. P. Permentier, and E. Verpoorte, "3D-printed paper spray ionization cartridge with fast wetting and continuous solvent supply features," *Analytical Chemistry*, vol. 86, no. 23, pp. 11657–11665, 2014.

[90] L. Shen, J. Zhang, Q. Yang, N. E. Manicke, and Z. Ouyang, "High throughput paper spray mass spectrometry analysis," *Clinica Chimica Acta*, vol. 420, pp. 28–33, 2013.

[91] J. Deng, W. Wang, Y. Yang et al., "Slug-flow microextraction coupled with paper spray mass spectrometry for rapid analysis of complex samples," *Analytica Chimica Acta*, vol. 940, pp. 143–149, 2016.

[92] C. Zhang and N. E. Manicke, "Development of a paper spray mass spectrometry cartridge with integrated solid phase extraction for bioanalysis," *Analytical Chemistry*, vol. 87, no. 12, pp. 6212–6219, 2015.

[93] B. Yang, F. Wang, W. Deng et al., "Wooden-tip electrospray ionization mass spectrometry for trace analysis of toxic and hazardous compounds in food samples," *Analytical Methods*, vol. 7, no. 14, pp. 5886–5890, 2015.

[94] G. Z. Xin, B. Hu, Z. Q. Shi et al., "Rapid identification of plant materials by wooden-tip electrospray ionization mass spectrometry and a strategy to differentiate the bulbs of *Fritillaria*," *Analytica Chimica Acta*, vol. 820, pp. 84–91, 2014.

[95] Y. Yang and J. Deng, "Internal standard mass spectrum fingerprint: a novel strategy for rapid assessing the quality of Shuang-Huang-Lian oral liquid using wooden-tip electrospray ionization mass spectrometry," *Analytica Chimica Acta*, vol. 837, pp. 83–92, 2014.

[96] H. K. Chen, C. H. Lin, J. T. Liu, and C. H. Lin, "Electrospray ionization using a bamboo pen nib," *International Journal of Mass Spectrometry*, vol. 356, pp. 37–40, 2013.

[97] B. Hu and Z. P. Yao, "Detection of native proteins using solid-substrate electrospray ionization mass spectrometry with nonpolar solvents," *Analytica Chimica Acta*, vol. 1004, pp. 51–57, 2017.

[98] Y. Yang, J. Deng, and Z. P. Yao, "Field-induced wooden-tip electrospray ionization mass spectrometry for high-throughput analysis of herbal medicines," *Analytica Chimica Acta*, vol. 887, pp. 127–137, 2015.

[99] Y. W. Liou, K. Y. Chang, and C. H. Lin, "Sampling and profiling caffeine and its metabolites from an eyelid using a watercolor pen based on electrospray ionization/mass spectrometry," *International Journal of Mass Spectrometry*, vol. 422, pp. 51–55, 2017.

[100] N. Pan, W. Rao, N. R. Kothapalli, R. Liu, A. W. G. Burgett, and Z. Yang, "The single-probe: a miniaturized multifunctional device for single cell mass spectrometry analysis," *Analytical Chemistry*, vol. 86, no. 19, pp. 9376–9380, 2014.

[101] C. Shiea, Y. L. Huang, S. C. Cheng, Y. L. Chen, and J. Shiea, "Determination of elemental composition of metals using ambient organic mass spectrometry," *Analytica Chimica Acta*, vol. 968, pp. 50–57, 2017.

[102] L. Qiao, R. Sartor, N. Gasilova et al., "Electrostatic-spray ionization mass spectrometry," *Analytical Chemistry*, vol. 84, no. 17, pp. 7422–7430, 2012.

[103] Z. Takats, J. M. Wiseman, and R. G. Cooks, "Ambient mass spectrometry using desorption electrospray ionization (DESI): instrumentation, mechanisms and applications in forensics, chemistry, and biology," *Journal of Mass Spectrometry*, vol. 40, no. 10, pp. 1261–1275, 2005.

[104] A. Penna, M. Careri, N. D. Spencer, and A. Rossi, "Effects of tailored surface chemistry on desorption electrospray ionization mass spectrometry: a surface-analytical study by XPS and AFM," *Journal of the American Society for Mass Spectrometry*, vol. 26, no. 8, pp. 1311–1319, 2015.

[105] L. Elviri, R. Foresti, A. Bianchera, M. Silvestri, and R. Bettini, "3D-printed polylactic acid supports for enhanced ionization efficiency in desorption electrospray mass spectrometry analysis of liquid and gel samples," *Talanta*, vol. 155, pp. 321–328, 2016.

[106] M. Montowska, W. Rao, M. R. Alexander, G. A. Tucker, and D. A. Barrett, "Tryptic digestion coupled with ambient desorption electrospray ionization and liquid extraction surface analysis mass spectrometry enabling identification of skeletal muscle proteins in mixtures and distinguishing between beef, pork, horse, chicken, and turkey meat," *Analytical Chemistry*, vol. 86, no. 9, pp. 4479–4487, 2014.

[107] M. T. Dulay, L. S. Eberlin, and R. N. Zare, "Protein analysis by ambient ionization mass spectrometry using trypsin-immobilized organosiloxane polymer surfaces," *Analytical Chemistry*, vol. 87, no. 24, pp. 12324–12330, 2015.

[108] S. Cheng, J. Wang, Y. Cai, J. A. Loo, and H. Chen, "Enhancing performance of liquid sample desorption electrospray ionization mass spectrometry using trap and capillary columns," *International Journal of Mass Spectrometry*, vol. 392, pp. 73–79, 2015.

[109] S. S. Kanyal, T. T. Häbe, C. V. Cushman et al., "Microfabrication, separations, and detection by mass spectrometry on ultrathin-layer chromatography plates prepared via the low-pressure chemical vapor deposition of silicon nitride onto carbon nanotube templates," *Journal of Chromatography A*, vol. 1404, pp. 115–123, 2015.

[110] K. J. Ewing, D. Gibson, J. Sanghera, and F. Miklos, "Desorption electrospray ionization–mass spectrometric analysis of low vapor pressure chemical particulates collected from a surface," *Analytica Chimica Acta*, vol. 853, pp. 368–374, 2015.

[111] R. G. Hemalatha, M. A. Ganayee, and T. Pradeep, "Electrospun nanofiber mats as "smart surfaces" for desorption electrospray ionization mass spectrometry (DESI MS)-based analysis and imprint imaging," *Analytical Chemistry*, vol. 88, no. 11, pp. 5710–5717, 2016.

[112] C. H. Lin, W. C. Liao, H. K. Chen, and T. Y. Kuo, "Paper spray-MS for bioanalysis," *Bioanalysis*, vol. 6, no. 2, pp. 1–10, 2014.

[113] Q. Yang, H. Wang, J. D. Maas et al., "Paper spray ionization devices for direct, biomedical analysis using mass spectrometry," *International Journal of Mass Spectrometry*, vol. 312, pp. 201–207, 2012.

[114] H. Evard, A. Kruve, R. Lõhmus, and I. Leito, "Paper spray ionization mass spectrometry: study of a method for fast-screening analysis of pesticides in fruits and vegetables," *Journal of Food Composition and Analysis*, vol. 41, pp. 221–225, 2015.

[115] Z. P. Zhang, X. N. Liu, and Y. J. Zheng, "Ambient ionization-paper spray ionization and its application," *Chinese Journal of Analytical Chemistry*, vol. 42, no. 1, pp. 145–152, 2014.

[116] P. H. Lai, P. C. Chen, Y. W. Liao, J. T. Liu, C. C. Chen, and C. H. Lin, "Comparison of gampi paper and nanofibers to chromatography paper used in paper spray-mass spectrometry," *International Journal of Mass Spectrometry*, vol. 375, pp. 14–17, 2015.

[117] T. C. Colletes, P. T. Garcia, R. B. Campanha et al., "A new insert sample approach to paper spray mass spectrometry: a paper substrate with paraffin barriers," *Analyst*, vol. 141, no. 5, pp. 1707–1713, 2016.

[118] Z. Zhang, W. Xu, N. E. Manicke, R. G. Cooks, and Z. Ouyang, "Silica coated paper substrate for paper-spray analysis of therapeutic drugs in dried blood spots," *Analytical Chemistry*, vol. 84, no. 2, pp. 931–938, 2012.

[119] R. Narayanan, D. Sarkar, R. G. Cooks, and T. Pradeep, "Molecular ionization from carbon nanotube paper," *Angewandte Chemie International Edition*, vol. 53, no. 23, pp. 5936–5940, 2014.

[120] S. C. Wei, S. Fan, C. W. Lien et al., "Graphene oxide membrane as an efficient extraction and ionization substrate for spray-mass spectrometric analysis of malachite green and its metabolite in fish samples," *Analytica Chimica Acta*, vol. 1003, pp. 42–48, 2018.

[121] J. Liu, Y. He, S. Chen, M. Ma, S. Yao, and B. Chen, "New urea-modified paper substrate for enhanced analytical performance of negative ion mode paper spray mass spectrometry," *Talanta*, vol. 166, pp. 306–314, 2017.

[122] I. Pereira, M. F. Rodrigues, A. R. Chaves, and B. G. Vaz, "Molecularly imprinted polymer (MIP) membrane assisted direct spray ionization mass spectrometry for agrochemicals screening in foodstuffs," *Talanta*, vol. 178, pp. 507–514, 2018.

[123] B. J. Bills and N. E. Manicke, "Development of a prototype blood fractionation cartridge for plasma analysis by paper spray mass spectrometry," *Clinical Mass Spectrometry*, vol. 2, pp. 18–24, 2016.

[124] M. Wleklinski, Y. Li, S. Bag et al., "Zero volt paper spray ionization and its mechanism," *Analytical Chemistry*, vol. 87, no. 13, pp. 6786–6793, 2015.

[125] J. Deng, Y. Yang, L. Fang, L. Lin, H. Zhou, and T. Luan, "Coupling solid-phase microextraction with ambient mass spectrometry using surface coated wooden-tip probe for

rapid analysis of ultra trace perfluorinated compounds in complex samples," *Analytical Chemistry*, vol. 86, no. 22, pp. 11159–11166, 2014.

[126] J. Deng, T. Yu, Y. Yao et al., "Surface-coated wooden-tip electrospray ionization mass spectrometry for determination of trace fluoroquinolone and macrolide antibiotics in water," *Analytica Chimica Acta*, vol. 954, pp. 52–59, 2017.

[127] Y. Huang, Y. Ma, H. Hu et al., "Rapid and sensitive detection of trace malachite green and its metabolite in aquatic products using molecularly imprinted polymer-coated wooden-tip electrospray ionization mass spectrometry," *RSC Advances*, vol. 7, no. 82, pp. 52091–52100, 2017.

[128] B. Hu, P. K. So, and Z. P. Yao, "Electrospray ionization with aluminum foil: a versatile mass spectrometric technique," *Analytica Chimica Acta*, vol. 817, pp. 1–8, 2014.

[129] X. Zhong, L. Qiao, B. Liu, and H. H. Girault, "Ambient in situ analysis and imaging of both hydrophilic and hydrophobic thin layer chromatography plates by electrostatic spray ionization mass spectrometry," *RSC Advances*, vol. 5, no. 92, pp. 75395–75402, 2015.

[130] V. Garcia-Canas, M. Herrero, E. Ibanez, and A. Cifuentes, "Food analysis: present, future, and foodomics," *Analytical Chemistry*, vol. 84, no. 23, pp. 10150–10159, 2012.

[131] M. Herrero, C. Simo, V. Garcia-Canas, E. Ibanez, and A. Cifuentes, "Foodomics: MS-based strategies in modern food science and nutrition," *Mass Spectrometry Reviews*, vol. 31, no. 1, pp. 49–69, 2012.

[132] F. Cacciola, P. Donato, M. Beccaria, P. Dugo, and L. Mondello, "Advances in LC-MS for food analysis," *LC GC Europe*, vol. 25, no. 5, pp. 15–24, 2012.

[133] *European Union Commission Decision 2002/657/EC*, 2002.

[134] G. C. R. M. Andrade, S. H. Monteiro, J. G. Francisco, L. A. Figueiredo, R. G. Botelho, and V. L. Tornisielo, "Liquid chromatography–electrospray ionization tandem mass spectrometry and dynamic multiple reaction monitoring method for determining multiple pesticide residues in tomato," *Food Chemistry*, vol. 175, pp. 57–65, 2015.

[135] O. Golge and B. Kabak, "Evaluation of QuEChERS sample preparation and liquid chromatography–triple-quadrupole mass spectrometry method for the determination of 109 pesticide residues in tomatoes," *Food Chemistry*, vol. 176, pp. 319–332, 2015.

[136] F. Diniz Madureira, F. A. da Silva Oliveira, W. R. de Souza, A. P. Pontelo, M. L. Gonçalves de Oliveira, and G. Silva, "A multi-residue method for the determination of 90 pesticides in matrices with a high water content by LC-MS/MS without clean-up," *Food Additives & Contaminants: Part A*, vol. 29, no. 4, pp. 665–678, 2012.

[137] A. Garrido-Frenich, M. M. Martín Fernández, L. Díaz Moreno, J. L. Martínez-Vidal, and N. López-Gutiérrez, "Multiresidue pesticide analysis of tuber and root commodities by QuEChERS extraction and UPLC coupled to tandem MS," *Journal of AOAC International*, vol. 95, no. 5, pp. 1319–1330, 2012.

[138] O. Golge and B. Kabak, "Determination of 115 pesticide residues in oranges by high-performance liquid chromatography–triple-quadrupole mass spectrometry in combination with QuEChERS method," *Journal of Food Composition and Analysis*, vol. 41, pp. 86–97, 2015.

[139] J. Cho, J. Lee, C. U. Lim, and J. Ahn, "Quantification of pesticides in food crops using QuEChERS approaches and GCeMS/MS," *Food Additives & Contaminants: Part A*, vol. 33, no. 12, pp. 1803–1816, 2016.

[140] S. S. Shida, S. Nemoto, and R. Matsuda, "Simultaneous determination of acidic pesticides in vegetables and fruits by liquid chromatography–tandem mass spectrometry," *Journal of Environmental Science and Health, Part B*, vol. 50, no. 3, pp. 151–162, 2015.

[141] C. Rasche, B. Fournes, U. Dirks, and K. Speer, "Multi-residue pesticide analysis (gas chromatography–tandem mass spectrometry detection)–improvement of the quick, easy, cheap, effective, rugged, and safe method for dried fruits and fat-rich cereals–benefit and limit of a standardized apple purée calibration (screening)," *Journal of Chromatography A*, vol. 1403, pp. 21–31, 2015.

[142] L. Han, J. Matarrita, Y. Sapozhnikova, and S. J. Lehotay, "Evaluation of a recent product to remove lipids and other matrix co-extractives in the analysis of pesticide residues and environmental contaminants in foods," *Journal of Chromatography A*, vol. 1449, pp. 17–29, 2016.

[143] B. D. Morris and R. B. Schriner, "Development of an automated column solid-phase extraction cleanup of QuEChERS extracts, using a zirconia-based sorbent, for pesticide residue analyses by LC-MS/MS," *Journal of Agricultural and Food Chemistry*, vol. 63, no. 21, pp. 5107–5119, 2015.

[144] G. Ramadan, M. Al Jabir, N. Alabdulmalik, and A. Mohammed, "Validation of a method for the determination of 120 pesticide residues in apples and cucumbers by LC-MS/MS," *Drug Testing and Analysis*, vol. 8, no. 5-6, pp. 498–510, 2016.

[145] M. A. Zhao, Y. N. Feng, Y. Z. Zhu, and J. H. Kim, "Multi-residue method for determination of 238 pesticides in Chinese cabbage and cucumber by liquid chromatography-tandem mass spectrometry: comparison of different purification procedures," *Journal of Agricultural and Food Chemistry*, vol. 62, no. 47, pp. 11449–11456, 2014.

[146] N. Fleury-Filho, C. A. Nascimento, E. O. Faria, A. R. Crunivel, and J. M. Oliveira, "Within laboratory validation of a multi-residue method for the analysis of 98 pesticides in mango by LC tandem MS," *Food Additives & Contaminants: Part A*, vol. 29, no. 4, pp. 641–656, 2012.

[147] T. Cajka, C. Sandy, V. Bachavolva et al., "Streamlining sample preparation and GC tandem MS analysis of multiple pesticide residues in tea," *Analytica Chimica Acta*, vol. 743, pp. 51–60, 2012.

[148] V. Havolt, S. Goscinny, and M. Deridder, "A simple multi-residue method for the determination of pesticides in fruits and vegetables using a methanolic extraction and ultra-high-performance liquid chromatography-tandem mass spectrometry: optimization and extension of scope," *Journal of Chromatography A*, vol. 1384, pp. 53–66, 2015.

[149] S. Walorczyk and D. Drozdzynski, "Improvement and extension to new analytes of a multi-residue method for the determination of pesticides in cereals and dry animal feed using gas chromatography-tandem quadrupole mass spectrometry revisited," *Journal of Chromatography A*, vol. 1251, pp. 219–231, 2012.

[150] O. Lacina, M. Zachariasova, J. Urbavolva, M. Vaclavikova, T. Cajka, and J. Hajslova, "Critical assessment of extraction methods for the simultaneous determination of pesticide residues and mycotoxins in fruits, cereals, spices and oil seeds employing UPLC tandem MS," *Journal of Chromatography A*, vol. 1262, pp. 8–18, 2012.

[151] J. Wang, W. Chow, and W. Cheung, "Application of a tandem mass spectrometer and core-shell particle column for the determination of 151 pesticides in grains," *Journal of Agricultural and Food Chemistry*, vol. 59, no. 16, pp. 8589–8608, 2011.

[152] Z. He, L. Wang, Y. Peng, M. Luo, W. Wang, and X. Liu, "Multiresidue analysis of over 200 pesticides in cereals using a QuEChERS and gas chromatography-tandem mass spectrometry-based method," *Food Chemistry*, vol. 169, pp. 372–380, 2015.

[153] A. Paleníkova, G. Martínez-Domínguez, F. J. Arrebola, R. Romero-Gonzalez, S. Hrouzkova, and A. Garrido Frenich, "Multifamily determination of pesticide residues in soya-based nutraceutical products by GC/MS-MS," *Food Chemistry*, vol. 173, pp. 796–807, 2015.

[154] S. Chawla, H. K. Patel, K. M. Vaghela et al., "Development and validation of multi residue analytical method in cotton and groundnut oil for 87 pesticides using low temperature and dispersive cleanup on gas chromatography and liquid chromatography-tandem mass spectrometry," *Analytical and Bioanalytical Chemistry*, vol. 408, no. 3, pp. 983–997, 2016.

[155] D. L. Christodoulou, P. Kanari, P. Hadjiloizou, and P. Constantivolu, "Pesticide residues analysis in wine by liquid chromatography–tandem mass spectrometry and using ethyl acetate extraction method: validation and pilot survey in real samples," *Journal of Wine Research*, vol. 26, no. 2, pp. 81–98, 2015.

[156] G. R. Chang, H. S. Chen, and F. Y. Lin, "Analysis of banned veterinary drugs and herbicide residues in shellfish by liquid chromatography-tandem mass spectrometry (LC/MS/MS) and gas chromatography-tandem mass spectrometry (GC/MS/MS)," *Marine Pollution Bulletin*, vol. 113, no. 1-2, pp. 579–584, 2016.

[157] M. E. Dasenaki, C. S. Michali, and N. S. Thomaidis, "Analysis of 76 veterinary pharmaceuticals from 13 classes including aminoglycosides in bovine muscle by hydrophilic interaction liquid chromatography–tandem mass spectrometry," *Journal of Chromatography A*, vol. 1452, pp. 67–80, 2016.

[158] D. Chen, J. Yu, Y. Tao et al., "Qualitative screening of veterinary anti-microbial agents in tissues, milk, and eggs of food-producing animals using liquid chromatography coupled with tandem mass spectrometry," *Journal of Chromatography B*, vol. 1017-1018, pp. 82–88, 2016.

[159] M. Aznar, A. Rodriguez-Lafuente, P. Alfaro, and C. Nerin, "UPLC-Q-TOF-MS analysis of non-volatile migrants from new active packaging materials," *Analytical and Bioanalytical Chemistry*, vol. 404, no. 6-7, pp. 1945–1957, 2012.

[160] B. Skribic, J. Zivancev, and M. Godula, "Multimycotoxin analysis of crude extracts of nuts with ultra-high performance liquid chromatography/tandem mass spectrometry," *Journal of Food Composition and Analysis*, vol. 34, no. 2, pp. 171–177, 2014.

[161] M. Ludovici, C. Ialongo, M. Reverberi, M. Beccaccioli, M. Scarpari, and V. Scala, "Quantitative profiling of oxylipins through comprehensive LC-MS/MS analysis of *Fusarium verticillioides* and maize kernels," *Food Additives & Contaminants: Part A*, vol. 31, no. 12, pp. 2026–2033, 2014.

[162] M. García-Altares, A. Casavolva, V. Bane, J. Diogene, A. Furey, and P. de la Iglesia, "Confirmation of pinnatoxins and spirolides in shellfish and passive samplers from Catalonia (Spain) by liquid chromatography coupled with triple quadrupole and high-resolution hybrid tandem mass spectrometry," *Marine Drugs*, vol. 12, no. 6, pp. 3706–3732, 2014.

[163] Y. Rodriguez-Carrasco, J. Manes, H. Berrada, and C. Juan, "Development and validation of a LC-ESI-MS/MS method for the determination of alternaria toxins alternariol, alternariol methyl-ether and tentoxin in tomato and tomato based products," *Toxins*, vol. 8, no. 11, p. 328, 2016.

[164] Y. Rodriguez-Carrasco, M. Fattore, S. Albrizio, H. Berrada, and J. Manes, "Occurrence of *Fusarium mycotoxins* and their dietary intake through beer consumption by the European population," *Food Chemistry*, vol. 178, pp. 149–155, 2015.

[165] C. Juan, J. Mañes, A. Raiola, and A. Ritieni, "Evaluation of beauvericin and enniatins in Italian cereal products and multicereal food by liquid chromatography coupled to triple quadrupole mass spectrometry," *Food Chemistry*, vol. 140, no. 4, pp. 755–762, 2013.

[166] K. Zhang, J. W. Wong, P. Yang et al., "Protocol for an electrospray ionization tandem mass spectral product ion library: development and application for identification of 240 pesticides in foods," *Analytical Chemistry*, vol. 84, no. 13, pp. 5677–5684, 2012.

[167] M. I. Cervera, T. Portoles, E. Pitarch, J. Beltran, and F. Hernandez, "Application of gas chromatography time-of-flight mass spectrometry for target and non-target analysis of pesticide residues in fruits and vegetables," *Journal of Chromatography A*, vol. 1244, pp. 168–177, 2012.

[168] F. Lambertini, V. Di Lallo, D. Catellani, M. Mattarozzi, M. Careri, and M. Suman, "Reliable liquid chromatography-mass spectrometry method for investigation of primary aromatic amines migration from food packaging and during industrial curing of multilayer plastic laminates," *Journal of Mass Spectrometry*, vol. 49, no. 9, pp. 870–877, 2014.

[169] C. Planche, J. Ratel, F. Mercier, P. Blinet, L. Debrauwer, and E. Engel, "Assessment of comprehensive two-dimensional gas chromatography-time-of-flight mass spectrometry based methods for investigating 206 dioxin-like micropollutants in animal-derived food matrices," *Journal of Chromatography A*, vol. 1392, pp. 74–81, 2015.

[170] X. Wang, P. Li, W. Zhang et al., "Screening for pesticide residues in oil seeds using solid-phase dispersion extraction and comprehensive two-dimensional gas chromatography time-of-flight mass spectrometry," *Journal of Separation Science*, vol. 35, no. 13, pp. 1634–1643, 2012.

[171] K. Kalachova, J. Pulkrabova, T. Cajka, L. Drabova, and J. Hajslova, "Implementation of comprehensive two-dimensional GC-time-of-flight-MS for the simultaneous determination of halogenated contaminants and polycyclic aromatic hydrocarbons in fish," *Analytical and Bioanalytical Chemistry*, vol. 403, no. 10, pp. 2813–2824, 2012.

[172] M. L. Gomez-Perez, P. Plaza-Bolavols, R. Romero-Gonzalez, J. L. Martinez-Vidal, and A. Garrido-Frenich, "Comprehensive qualitative and quantitative determination of pesticides and veterinary drugs in honey using liquid chromatography-Orbitrap high resolution mass spectrometry," *Journal of Chromatography A*, vol. 1248, pp. 130–138, 2012.

[173] P. Perez-Ortega, F. J. Lara-Ortega, J. F. García-Reyes, B. Gilbert-Lopez, M. Trojavolwicz, and A. Molina-Díaz, "A feasibility study of UHPLC-HRMS accurate-mass screening methods for multiclass testing of organic contaminants in food," *Talanta*, vol. 160, pp. 704–712, 2016.

[174] H. G. J. Mol, P. Zomer, and M. de Koning, "Qualitative aspects and validation of a screening method for pesticides in vegetables and fruits based on liquid chromatography coupled to full scan high resolution (Orbitrap) mass spectrometry," *Analytical and Bioanalytical Chemistry*, vol. 403, no. 10, pp. 2891–2908, 2012.

[175] J. Rubert, K. J. James, J. Manes, and C. Soler, "Applicability of hybrid linear ion trap-high resolution mass spectrometry and quadrupole-linear ion trap-mass spectrometry for

mycotoxin analysis in baby food," *Journal of Chromatography A*, vol. 1223, pp. 84–92, 2012.

[176] D. G. Beach, C. M. Walsh, and P. McCarron, "High-throughput quantitative analysis of domoic acid directly from mussel tissue using laser ablation electrospray ionization—tandem mass spectrometry," *Toxicon*, vol. 92, pp. 75–80, 2014.

[177] M. Guijarro-Díez, L. Volzal, M. L. Marina, and A. L. Crego, "Metabolomic fingerprinting of saffron by LC/MS: novel authenticity markers," *Analytical and Bioanalytical Chemistry*, vol. 407, no. 23, pp. 7197–7213, 2015.

[178] L. Millán, M. C. Sampedro, A. Sanchez et al., "Liquid chromatography–quadrupole time of flight tandem mass spectrometry–based targeted metabolomic study for varietal discrimination of grapes according to plant sterols content," *Journal of Chromatography A*, vol. 1454, pp. 67–77, 2016.

[179] M. Arbulu, M. C. Sampedro, A. Gomez-Caballero, M. A. Goicolea, and R. J. Barrio, "Untargeted metabolomic analysis using liquid chromatography quadrupole time-of-flight mass spectrometry for non-volatile profiling of wines," *Analytica Chimica Acta*, vol. 858, pp. 32–41, 2015.

[180] J. Rubert, O. Lacina, M. Zachariasova, and J. Hajslova, "Saffron authentication based on liquid chromatography high resolution tandem mass spectrometry and multivariate data analysis," *Food Chemistry*, vol. 204, pp. 201–209, 2016.

[181] A. Kårlund, U. Moor, G. McDougall, M. Lehtonen, R. O. Karjalainen, and K. Hanhineva, "Metabolic profiling discriminates between strawberry (*Fragaria* × *ananassa* Duch.) cultivars grown in Finland or Estonia," *Food Research International*, vol. 89, pp. 647–653, 2016.

[182] Z. Jandric, D. Roberts, M. N. Rathor, A. Abrahim, M. Islam, and A. Cannavan, "Assessment of fruit juice authenticity using UPLC-QToF MS: a metabolomics approach," *Food Chemistry*, vol. 148, pp. 7–17, 2014.

[183] Z. Jandric, M. Islam, D. K. Singh, and A. Cannavan, "Authentication of Indian citrus fruit/fruit juices by untargeted and targeted metabolomics," *Food Control*, vol. 72, pp. 181–188, 2017.

[184] S. Jin, C. Song, S. Jia et al., "An integrated strategy for establishment of curcuminoid profile in turmeric using two LC–MS/MS platforms," *Journal of Pharmaceutical and Biomedical Analysis*, vol. 132, pp. 93–102, 2017.

[185] K. Inoue, C. Tanada, T. Sakamoto et al., "Metabolomics approach of infant formula for the evaluation of contamination and degradation using hydrophilic interaction liquid chromatography coupled with mass spectrometry," *Food Chemistry*, vol. 181, pp. 318–324, 2015.

[186] M. Mattarozzi, M. Milioli, F. Bianchi et al., "Optimization of a rapid QuEChERS sample treatment method for HILIC-MS2 analysis of paralytic shellfish poisoning (PSP) toxins in mussels," *Food Control*, vol. 60, pp. 138–145, 2016.

[187] A. K. Subbaraj, Y. H. Brad-Kim, K. Fraser, and M. M. Farouk, "A hydrophilic interaction liquid chromatography–mass spectrometry (HILIC-MS) based metabolomics study on colour stability of ovine meat," *Meat Science*, vol. 117, pp. 163–172, 2016.

[188] G. Aliakbarzadeh, H. Sereshti, and H. Parastar, "Pattern recognition analysis of chromatographic fingerprints of *Crocus sativus* L. secondary metabolites towards source identification and quality control," *Analytical and Bioanalytical Chemistry*, vol. 408, no. 12, pp. 3295–3307, 2016.

[189] F. R. Pinu, S. de Carvalho-Silva, A. P. Trovatti Uetanabaro, and S. G. Villas-Boas, "Vinegar metabolomics: an explorative study of commercial balsamic vinegars using gas chromatography-mass spectrometry," *Metabolites*, vol. 6, no. 3, p. 22, 2016.

[190] P. Scano, A. Murgia, F. M. Pirisi, and P. Caboni, "A gas chromatography-mass spectrometry-based metabolomic approach for the characterization of goat milk compared with cow milk," *Journal of Dairy Science*, vol. 97, no. 10, pp. 6057–6066, 2014.

[191] L. L. Monti, C. A. Bustamante, S. Osorio et al., "Metabolic profiling of a range of peach fruit varieties reveals high metabolic diversity and commonalities and differences during ripening," *Food Chemistry*, vol. 190, pp. 879–888, 2016.

[192] M. N. A. Khalil, M. I. Fekry, and M. A. Farag, "Metabolome based volatiles profiling in 13 date palm fruit varieties from Egypt via SPME GC-MS and chemometrics," *Food Chemistry*, vol. 217, pp. 171–181, 2017.

[193] I. Akhatou, R. Gonz alez-Domínguez, and A. Fern andez-Recamales, "Investigation of the effect of genotype and agronomic conditions on metabolomic profiles of selected strawberry cultivars with different sensitivity to environmental stress," *Plant Physiology and Biochemistry*, vol. 101, pp. 14–22, 2016.

[194] A. Cuadros-Ivolstroza, S. Ruíz-Lara, E. Gonz alez, A. Eckardt, L. Willmitzer, and H. Pena-Cortes, "GC-MS metabolic profiling of Cabernet Sauvignon and Merlot cultivars during grapevine berry development and network analysis reveals a stage- and cultivar-dependent connectivity of primary metabolites," *Metabolomics*, vol. 12, no. 2, p. 39, 2016.

[195] B. Khakimov, R. J. Mongi, K. M. Sørensen, B. K. Ndabikunze, B. E. Chove, and S. B. Engelsen, "A comprehensive and comparative GC-MS metabolomics study of non-volatiles in Tanzanian grown mango, pineapple, jackfruit, baobab and tamarind fruits," *Food Chemistry*, vol. 213, pp. 691–699, 2016.

[196] J. Welzenbach, C. Neuhoff, C. Looft, K. Schellander, E. Tholen, and C. Große-Brinkhaus, "Different statistical approaches to investigate porcine muscle metabolome profiles to highlight new biomarkers for pork quality assessment," *PLoS One*, vol. 11, no. 2 article e0149758, 2016.

[197] G. Min-Lee, D. Ho-Suh, E. Sung-Jung, and C. Hwan-Lee, "Metabolomics provides quality characterization of commercial gochujang (fermented pepper paste)," *Molecules*, vol. 21, no. 7, p. 921, 2016.

[198] D. E. Lee, G. R. Shin, S. Lee et al., "Metabolomics reveal that amino acids are the main contributors to antioxidant activity in wheat and rice gochujangs (Korean fermented red pepper paste)," *Food Research International*, vol. 87, pp. 10–17, 2016.

[199] E. J. Gu, D. W. Kim, G. J. Jang et al., "Mass-based metabolomic analysis of soybean sprouts during germination," *Food Chemistry*, vol. 217, pp. 311–319, 2017.

[200] C. Sales, M. I. Cervera, R. Gil, T. Portoles, E. Pitarch, and J. Beltran, "Quality classification of Spanish olive oils by untargeted gas chromatography coupled to hybrid quadrupole-time of flight mass spectrometry with atmospheric pressure chemical ionization and metabolomics-based statistical approach," *Food Chemistry*, vol. 216, pp. 365–373, 2017.

[201] D. K. Trivedi, K. A. Hollywood, N. J. W. Rattray et al., "Meat, the metabolites: an integrated metabolite profiling and lipidomics approach for the detection of the adulteration of beef with pork," *Analyst*, vol. 141, no. 7, pp. 2155–2164, 2016.

[202] V. D. Daygon, S. Prakash, M. Calingacion et al., "Understanding the jasmine phenotype of rice through metabolite profiling and sensory evaluation," *Metabolomics*, vol. 12, no. 4, p. 63, 2016.

[203] L. Di Donna, D. Taverna, S. Indelicato, A. Napoli, G. Sindona, and F. Mazzotti, "Rapid assay of resveratrol in red wine by paper spray tandem mass spectrometry and isotope dilution," *Food Chemistry*, vol. 229, pp. 354–357, 2017.

[204] H. V. Pereira, V. S. Amador, M. M. Sena, R. Augusti, and E. Piccin, "Paper spray mass spectrometry and PLS-DA improved by variable selection for the forensic discrimination of beers," *Analytica Chimica Acta*, vol. 940, pp. 104–112, 2016.

[205] J. A. Reis Teodoro, H. V. Pereira, M. M. Sena, E. Piccin, J. J. Zacca, and R. Augusti, "Paper spray mass spectrometry and chemometric tools for a fast and reliable identification of counterfeit blended Scottish whiskies," *Food Chemistry*, vol. 237, pp. 1058–1064, 2017.

[206] A. K. Meher and Y. C. Chen, "Analysis of volatile compounds by open-air ionization mass spectrometry," *Analytica Chimica Acta*, vol. 966, pp. 41–46, 2017.

[207] M. Ha, J. H. Kwak, Y. Kim, and O. P. Zee, "Direct analysis for the distribution of toxic glycoalkaloids in potato tuber tissue using matrix-assisted laser desorption/ionization mass spectrometric imaging," *Food Chemistry*, vol. 133, no. 4, pp. 1155–1162, 2012.

[208] S. Taira, S. Shimma, I. Osaka et al., "Mass spectrometry imaging of the capsaicin localization in the *Capsicum* fruits," *International Journal of Biotechnology for Wellness Industries*, vol. 1, pp. 61–66, 2012.

[209] Y. Yoshimura, H. Evolmoto, T. Moriyama, Y. Kawamura, M. Setou, and N. Zaima, "Visualization of anthocyanin species in rabbiteye blueberry *Vaccinium ashei* by matrix-assisted laser desorption/ionization imaging mass spectrometry," *Analytical and Bioanalytical Chemistry*, vol. 403, no. 7, pp. 885–1895, 2012.

[210] A. Yasuda, Y. Tatsu, and Y. Shigeri, "Characterization of triacetyl-α-melanocyte-stimulating hormone in carp and goldfish," *General and Comparative Endocrinology*, vol. 175, no. 2, pp. 270–276, 2012.

[211] M.-Z. Huang, S.-C. Cheng, S.-S. Jhang et al., "Ambient molecular imaging of dry fungus surface by electrospray laser desorption ionization mass spectrometry," *International Journal of Mass Spectrometry*, vol. 325–327, pp. 172–182, 2012.

[212] S. S. Jhang, M.-Z. Huang, and J. Shiea, "Ambient molecular imaging of toxins within a sprouted potato slice by ELDI/MS," in *Proceedings of the 60th ASMS Conference on Mass Spectrometry and Allied Topics*, Vancouver, BC, Canada, May 2012.

[213] R. Garrett, C. M. Rezende, and D. R. Ifa, "Revealing the spatial distribution of chlorogenic acids and sucrose across coffee bean endosperm by desorption electrospray ionization-mass spectrometry imaging," *LWT-Food Science and Technology*, vol. 65, pp. 711–717, 2016.

[214] P. M. Kumara, A. Srimany, G. Ravikanth, R. U. Shaanker, and T. Pradeep, "Ambient ionization mass spectrometry imaging of rohitukine, a chromone anti-cancer alkaloid, during seed development in *Dysoxylum binectariferum* Hook.f (Meliaceae)," *Phytochemistry*, vol. 116, pp. 104–110, 2015.

[215] M. W. Nielen and T. A. van Beek, "Macroscopic and microscopic spatially-resolved analysis of food contaminants and constituents using laser-ablation electrospray ionization mass spectrometry imaging," *Analytical and Bioanalytical Chemistry*, vol. 406, no. 27, pp. 6805–6815, 2014.

Hindawi
Journal of Analytical Methods in Chemistry
Volume 2018, Article ID 1292954, 20 pages
https://doi.org/10.1155/2018/1292954

Research Article

High-Precision In Situ $^{87}Sr/^{86}Sr$ Analyses through Microsampling on Solid Samples: Applications to Earth and Life Sciences

Sara Di Salvo,[1] Eleonora Braschi,[2] Martina Casalini,[1] Sara Marchionni,[1] Teresa Adani,[1] Maurizio Ulivi,[1] Andrea Orlando,[2] Simone Tommasini,[1] Riccardo Avanzinelli,[1,2] Paul P. A. Mazza,[1] Sandro Conticelli,[1,2] and Lorella Francalanci[1,2]

[1]*Dipartimento di Scienze della Terra, Università degli Studi di Firenze, via Giorgio La Pira 4, 50121 Firenze, Italy*
[2]*C.N.R., Istituto Geoscienze e Georisorse, U.O. di Firenze, via Giorgio La Pira 4, 50121 Firenze, Italy*

Correspondence should be addressed to Eleonora Braschi; eleonora.braschi@igg.cnr.it

Received 15 December 2017; Accepted 18 February 2018; Published 22 April 2018

Academic Editor: Veronica Termopoli

An analytical protocol for high-precision, in situ microscale isotopic investigations is presented here, which combines the use of a high-performing mechanical microsampling device and high-precision TIMS measurements on micro-Sr samples, allowing for excellent results both in accuracy and precision. The present paper is a detailed methodological description of the whole analytical procedure from sampling to elemental purification and Sr-isotope measurements. The method offers the potential to attain isotope data at the microscale on a wide range of solid materials with the use of minimally invasive sampling. In addition, we present three significant case studies for geological and life sciences, as examples of the various applications of microscale $^{87}Sr/^{86}Sr$ isotope ratios, concerning (i) the pre-eruptive mechanisms triggering recent eruptions at Nisyros volcano (Greece), (ii) the dynamics involved with the initial magma ascent during Eyjafjallajökull volcano's (Iceland) 2010 eruption, which are usually related to the precursory signals of the eruption, and (iii) the environmental context of a MIS 3 cave bear, *Ursus spelaeus*. The studied cases show the robustness of the methods, which can be also be applied in other areas, such as cultural heritage, archaeology, petrology, and forensic sciences.

1. Introduction

In situ radiogenic isotope determinations with microscale resolution, especially of Sr, can represent a powerful tool in different fields of geological and life sciences. In particular, this technique is nowadays one of the most important methods for the investigation and interpretation of magmatic processes, as well as of environmentally-induced responses of terrestrial mammals; it has the potential to greatly enhance our understanding of not only volcanic systems and the related magma genesis and evolution, but also of the physiological mechanisms behind specific organic adaptations.

In situ $^{87}Sr/^{86}Sr$ provides significant data on the (i) source heterogeneities of magmas, (ii) crystallization histories within shallow level magmatic reservoirs, and (iii) magma residence times prior to eruptions (e.g., [1–10]). Since crystals record changes occurring in the environment in which they grow (e.g., [7, 11–15]), isotopic investigations at grain and subgrain scales on rock-forming minerals provide information on mineral-whole rock equilibria that constrain the magmatic processes occurring during magma evolution (e.g., mixing, mingling, crystals recycling, crustal contamination, or metasomatism). In addition, variation of Sr-isotope composition from core to rim within the same crystal can shed light on the complex pre-eruptive history of active volcanoes. Therefore, combining micro-(small-scale) isotope data with textural and petrographic data provides significant information on crystals residence time, magma production rates, and recharge dynamics (e.g., [5–8, 16–18]).

Sr-isotopic investigation has recently gained popularity in other fields, such as archaeology, anthropology, biology, cultural heritage, environmental and food studies, forensics, life and medical sciences, and palaeontology. (e.g., [19–38]). $^{87}Sr/^{86}Sr$ on tooth enamel and bone tissues gained particular attention over the last years in life studies, archaeology, palaeontology, and forensic sciences (e.g., [39–48]). In situ analyses of $^{87}Sr/^{86}Sr$ using laser ablation and multicollector-inductively coupled plasma mass spectrometry (LA-MC-ICPMS) for tooth enamel, bones, and rocks were developed in the early new millennium but have met variable success (e.g., [49–53]). At the same time, microscale sampling through drilling and micro-Sr isotope analyses by thermal ionisation mass spectrometry (TIMS) was also developed on geological materials (e.g., [6, 18, 54]). As compared with mechanical microdrilling plus TIMS procedures, LA-MC-ICPMS has the advantage of significantly reducing the time of analyses, but at the expense of precision of the measured isotope ratio; this is generally due to smaller Sr signals and the need to correct for isobaric interferences (e.g., [16, 53]).

We present a detailed protocol for in situ sampling through microdrilling, Sr purification, and thermal ionisation mass spectrometer (TIMS) high-precision determinations of small amounts of Sr (<10 ng) in both biological and geological materials at the same error levels. In situ $^{87}Sr/^{86}Sr$ analysis is presented in three case studies which deal with the following: (i) plagioclase crystals from Nisyros volcano (Greece), (ii) glassy matrix of single glassy clasts from the 2010 eruption of the Eyjafjallajökull volcano (Iceland), and (iii) bones and teeth from fossil remains of the *Ursus spelaeus*. In these three examples, the in situ Sr-isotope approach permits to constrain petrological and volcanological processes and to effectively outline the life habits and habitat exploitation of extinct living species. The three presented cases aim to show the high potential of the methodology, validating its wide-scale applicability in many other areas, such as cultural heritage, archaeology, and forensic sciences.

2. Materials and Methods

Technological improvements on mass spectrometer and microsampling devices allow researchers to collect and analyse small amounts of sample (few micrograms of sample, containing nanograms of Sr) with no loss of precision in the isotopic determination. In situ analyses have many important advantages over more typical ones on bulk samples. In geological applications, it allows to preserve the textural information and thus to combine it with the isotopic and geochemical composition of specific portions of the samples. In archaeology and palaeontology, this method has the advantage of minimising the damage and/or destruction of samples, thereby leaving significant amounts available for further applications.

The procedure consists in three main stages: (i) in situ sampling through microdrilling, (ii) sample digestion and purification of the element of interest, in our case Sr, and (iii) measurement of the isotope ratios (i.e., $^{87}Sr/^{86}Sr$) through thermal ionisation mass spectrometry (TIMS). Our Radiogenic Isotope Laboratory at the Department of Earth Sciences of the Florence University is equipped with a modern MicroMill™ grinder device, an ultraclean laboratory ("Class 1000") for microsamples digestion and elemental separation and a thermal ionisation mass spectrometer (ThermoFinningan™ Triton-Ti®) for isotopic measurements.

Compared to classic, bulk sample analyses (generally measured on 100–150 ng of Sr [55]), small-sample analysis (typically 5 to 10 ng of Sr) has the drawback of being more exposed to contamination from Sr alien to the sample. In situ micro-Sr measurements therefore require continued testing of laboratory blanks during the whole analytical procedure.

2.1. In Situ Sampling

2.1.1. The Microdrilling Device. Microsampling on minerals, glasses, and tooth enamel reported in this paper was performed using a microdrilling device capable of high resolution milling (New Wave-Merchantek MicroMill™, https://www.esi.com/products/laser-processing/milling/micromill/). The MicroMill (Figure 1(a)) combines a binocular microscope (with 6.7x–40x magnifying power) with remotely controlled submicron stage resolution and positional accuracy and a real-time video observation (at 3x digital magnification). It includes a low-eccentricity high-torque milling chuck, with variable speed (1,200–35,000 rpm), wherein a tungsten carbide or diamond-tipped bit is fixed, and an automated high-precision sliding stage on which the sample is loaded (Figure 1). The open stage architecture can accommodate thin sections or mounts and also larger solid samples such as bones, shells, ceramics, and plastics. The plug where the bit is hosted moves with adjustable speed for both spin and vertical movement, along the Z direction. The stage moves along the X-Y direction with a precision of 1 μm and maximum shift of 5 cm, allowing a high spatial resolution to the micron scale. This yields high spatial resolution, to the micron scale, and allows small-size sampling (i.e., a few μg of powder). The digital camera, placed next to the milling chunk (Figure 1(c)), shows a live image of the stage and of the bit position (Figure 2(a)). Using the microscope position mode (scope position), the optical image of the sample can be monitored on the PC screen prior to and after the sampling (Figure 2(b)).

The device allows in situ microsampling on several types of solid materials such as rocks, minerals, glasses, plastics, bone tissues, ceramics, metals, and alloys. The designed software package also allows performing different milling patterns such as holes arranged randomly, lines, or rasters (Figure 2(b)). Fine adjustment of milling velocity helps the microsampling of solid materials with different hardness.

Microsampling on geological (e.g., rock, minerals, and glasses) and archaeological materials (glasses, ceramics, teeth, and bones) is performed using either thick polished sections (some 100 μm thick) or sample mounts (e.g., small chunks, chips, fragments of bones, and teeth). In our case studies, we used thick, polished sections for mineral and volcanic glasses and mounts for the teeth; both were fixed on the stage using either a double-sided adhesive tape or hot glue, to avoid sample displacement during milling. Thick, polished sections are preferable for geological samples because they permit to

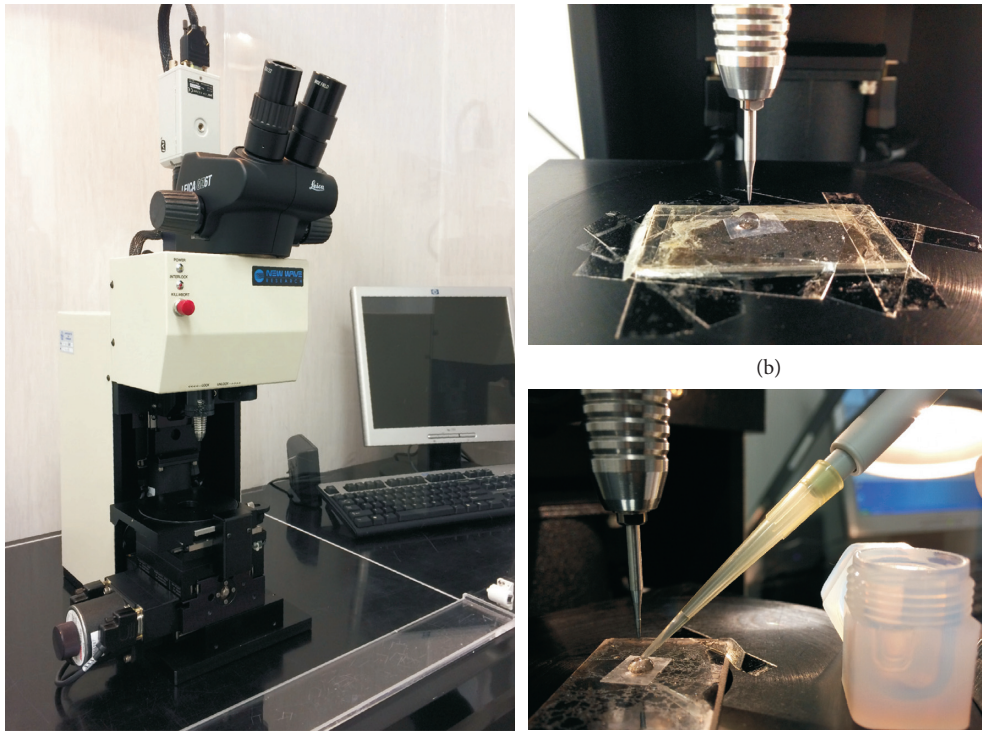

(a) (b) (c)

Figure 1: (a) The New Wave-Merchantek Micromill device operating at the Department of Earth Sciences–University of Firenze; (b) image of a petrographic polish thick section fixed on the sample stage under the tungsten carbide drilling bit that is locked into the milling chuck. A Milli-Q droplet constrained by the Parafilm is placed on the section in order to collect the powder during the drill; and (c) sample slurry recovery from the drilled surface into the digestion beaker.

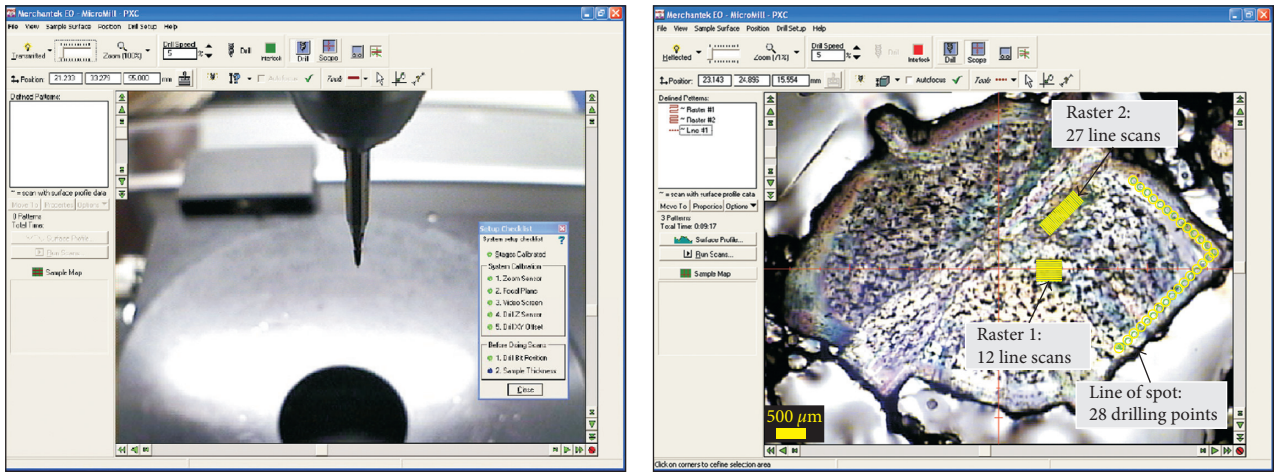

(a) (b)

Figure 2: (a) Live image of the sample stage and drill bit shown by the digital camera placed next to the milling chuck; (b) microscope view image showing a zoned plagioclase crystal with drilling pattern. Two rasters (in yellow) are set up to drill the plagioclase core, whereas a line of spot is set up for the rim microdrilling.

characterise the petrographic features of the samples and thus to perform the microsampling according to their textural properties.

2.1.2. Milling Procedure and Sample Collection. A droplet of Milli-Q® water is placed with a micrometric pipette on the selected area prior to milling; this is performed by sticking a small punched square of warmed-up Parafilm™ on the sample surface (Figure 1(c)). The water droplet retains the powder produced by the milling, which can then be easily collected by pipetting; it has also the effect of cooling the microdrill bit while milling. Before each drilling session, the drill bit is ultrasonically cleaned with pure ethanol and then rinsed with Milli-Q water.

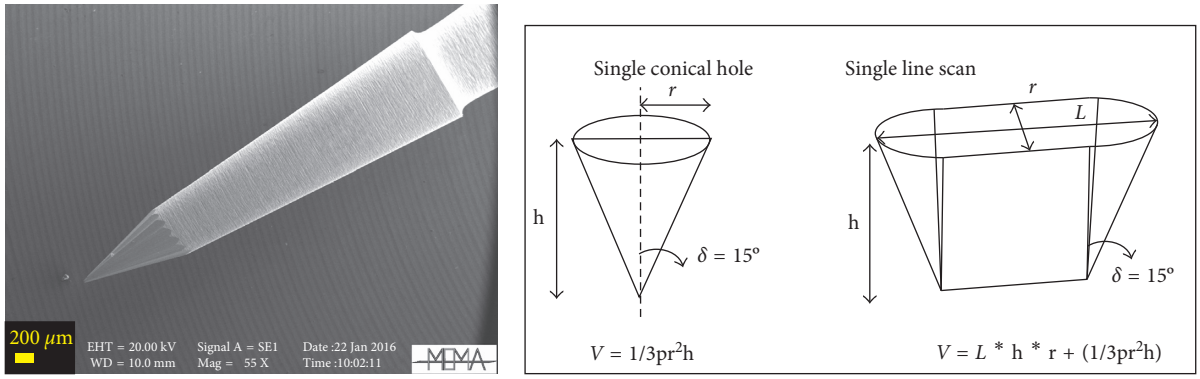

(a) (b)

Figure 3: (a) SEM imaging of a tungsten carbide drill bit used for milling: the tip angle is 30° and geometrical shape of (b) a single conical hole and single line scan.

The instrument software provides different drilling patterns and depths: single or multiple independent holes, spot lines, grids, line scans, or rasters (Figure 2(b)). Milling spot lines (or grids) are more accurate, but more time-consuming; they were used for the geological material (crystals and volcanic ashes) which requires more precise spatial resolution between the different zones of the same crystal or between the thin films of glass. Milling failure, such as crystal breaking, was prevented by setting a slow scan speed and splitting the milling into two or more steps. Line scans, which are performed faster but less accurately, were used for drilling the teeth. The number of points, lines, or rasters to be milled (which accounts for the amount of Sr to be collected) need to obtain a sufficient quantity of Sr for the TIMS measurements and can be calculated based on (i) the Sr content of the sample (independently determined by LA-ICPMS), (ii) the geometry of the drill bit, and (iii) the drilling pattern and the depth. Tips of different size and shape can be used for the drilling; therefore, the volume of material actually removed from different depths of a single hole or at different depths and lengths of a single line needs to be carefully calculated. The tungsten carbide mill bits supplied with the microdrill device (Komet–Brassler), have conical shape with an angle of 30° (Figure 3). The volume removed during each drilling is equivalent to that of the conical tip and dependent on the geometry of the drilling pattern, as well as on the specific depth (Figure 3). The minimum amount of sample that needs to be drilled depends also on the total procedural blank, which should be at least two orders of magnitude lower than the total amount of Sr collected from the sample.

After milling was completed, the sample slurry was collected with a micropipette in a PFA beaker and then transferred in the clean lab for sample digestion and elemental purification. The blanks of the milling procedure were determined by keeping the drill bit tip into a Milli-Q water droplet on the sample surface (accurately cleaned before use) for as long as the average sampling time; the droplet was then processed as an ordinary sample. The amount of Sr in the blank was then determined through isotope dilution, by adding a single-spike solution (enriched in ^{84}Sr).

2.2. Sample Dissolution and Sr Purification. The purification of the element of interest, in our case Sr, is crucial to obtain high-precision isotopic measurements for at least two reasons. First, it avoids isobaric interferences on the masses that will be analysed by mass spectrometry; in the specific case of Sr isotope measurements, even a small amount of ^{87}Rb will add to ^{87}Sr, yielding an overestimate of the ^{87}Sr/^{86}Sr ratio. Secondly, the presence of other elements of the matrix will compete with Sr during the thermal ionisation process, reducing the Sr signal and thus yielding less accurate measurements. The possibility of collecting and processing the sample for the purification of the element of interest is one of the major advantages of the method presented here over other methodologies, which do not achieve the same degree of accuracy and precision. The LA-MC-ICPMS methods allow faster data acquisition and higher sample throughput than mechanical microdrilling plus TIMS procedures, thanks to the possibility of introducing the samples directly into the mass spectrometer without chemical separation. On the other hand, LA-MC-ICPMS measurements require careful monitoring and corrections to minimize isobaric interferences in order to achieve suitable analytical accuracy and precision (e.g., [49, 53, 54, 56]).

Powder digestion and Sr purification were carried out in our ultraclean laboratory ("Class 1000") aiming at the following: (i) optimising the separation of Sr and Rb to avoid interference of ^{87}Rb with ^{87}Sr, (ii) purifying the Sr collection form all the matrix analytes, (iii) maximising the yield of the columns during the chromatographic purification, and (iv) preserving low procedural blanks. Sample digestion was performed by sequential HF-HNO_3-HCl as described in [55]. Chromatographic Sr purification was performed using Eichrom® Sr-Spec™ resins (100–150 μm) in quartz microcolumns (0.14 ml volume; Figure 4). Matrix elements were flushed out through elution with 14 column volumes of 3 N HNO_3. Sr was then collected in Milli-Q (13 column volumes). The collected Sr fractions were further treated with concentrated HNO_3 and H_2O_2 (fluxing at 150°C on a hotplate) to remove any organic residue. After this final step, samples were diluted in HNO_3 (10 vol.%) and were finally ready for loading on filaments for mass measurements. The

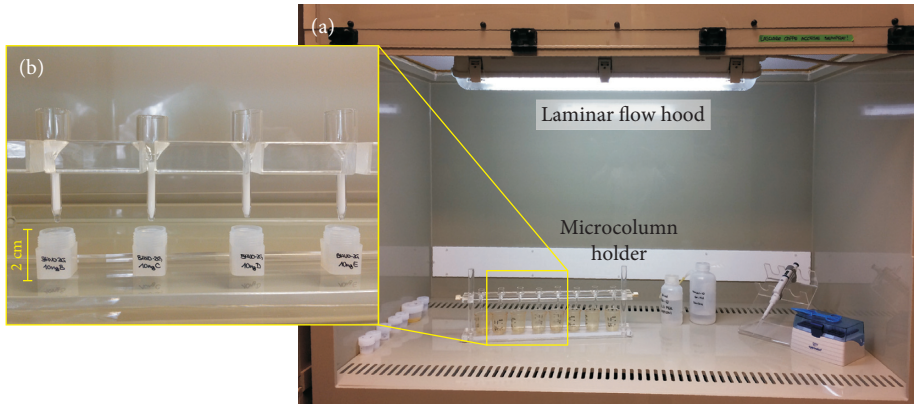

Figure 4: (a) Image of the laminar flow hood used for chemical processing and Sr separation of microdrilled samples; (b) image of quartz microcloumns filled with approximately 140 μl of specific chromatographic resin (Eichrom Sr-Spec, 100–150 μm) with high Sr-recovery efficiency, for Sr element extraction.

Table 1: Blank contamination level.

	Laboratory blanks			Isotope ratios on blanks		
Standard procedure on large size samples	Sr pg	1 SD	*n*	$^{87}Sr/^{86}Sr$	1 SD	*n*
	127	60	32	0.707497	0.000060	5
Procedure on small size samples						
Total procedure (drilling, digestion, and elemental selection)	38	19	16			
Chemical digestion and separation	17	6	12			

1 SD, standard deviation (external precision); *n*, numbers of blank measurements; the average Sr-isotope value obtained from 5 unspiked blanks is reported to fully characterize the potential contamination component.

whole analytical procedure was performed with acids of ultra-pure quality.

In order to thoroughly assess the contamination levels, we measured two types of blanks, one considering only the amount of Sr deriving from the chemical digestion and Sr separation, the other accounting for the whole procedure, including the drilling process, as described in the previous section. The results were 17 ± 6 (1 SD, $n = 12$) and 38 ± 19 pg (1 SD, $n = 16$), respectively, over a 14-month period (Table 1), thus allowing sampling as low as 4 ng of Sr for isotope analysis.

2.3. $^{87}Sr/^{86}Sr$ Measurements on TIMS. Sr isotope ratios were determined using a multicollector, thermal ionization mass spectrometer (TIMS: ThermoFinningan Triton-Ti™) (Figure 5), equipped with nine moveable collectors, which allow to simultaneously detect all the natural masses of Sr (^{84}Sr, ^{86}Sr, ^{87}Sr, and ^{88}Sr). The mass of ^{85}Rb was also measured to monitor possible ^{87}Rb interference, but it was always lower than the detection limit of the instrument, confirming the quality of the separation procedure described above. A detailed description of instrumental characteristics and performances are given in [55], along with standardised routine, measuring conditions, and setting for normal-sized samples (100–150 ng of Sr). Instrumental mass bias (e.g., [57–59]) was corrected to the natural value of $^{86}Sr/^{88}Sr = 0.1194$ using an exponential law (e.g., [55, 59]).

The most critical aspects of measuring small-size samples are related to (i) the procedure of sample loading onto the filaments and (ii) the measurement mode (i.e., static versus multidynamic, e.g., [55, 59]). Both are very important to maximise the Sr signal during the measurements, to balance the analysis time and the analytical errors that are a function of sample size.

The measurement protocol was tested by replicate analyses of an international certified standard (NIST-SRM987), properly diluted to attain sample sizes (5 to 10 ng Sr) comparable to those of the microsamples. Then, we tested the whole procedure, from in situ sampling (<10 ng of Sr) to isotope measurement, on the international glass reference sample BHVO-2G. BHVO-2G reference sample is a synthetic basaltic glass (provided by USGS) obtained by melting the BHVO-2 powder collected from a Hawaiian lava flow. The glassy slices are supplied in epoxy resin mounts (https://crustal.usgs.gov/geochemical_reference_standards/microanalytical_RM.html).

2.3.1. Sample Loading onto Filament. The Sr fraction collected from the columns was dissolved into 1 μl HNO_3 10 vol.% and loaded on single Re filaments under a horizontal laminar flow hood. Due to the small amount of Sr available, it is important to confine the sample on the smallest possible area on the filament, so that the whole loaded sample can be ionised at the same time from a single spot. To attain this, a thin layer of Parafilm™ was melted at both sides of the filament surface, to prevent any spreading of the solution, leaving a small gap (1 mm) for the droplet at the center on the filament (Figure 5(b)). The loading was performed by sandwiching the sample between two 0.5 μl

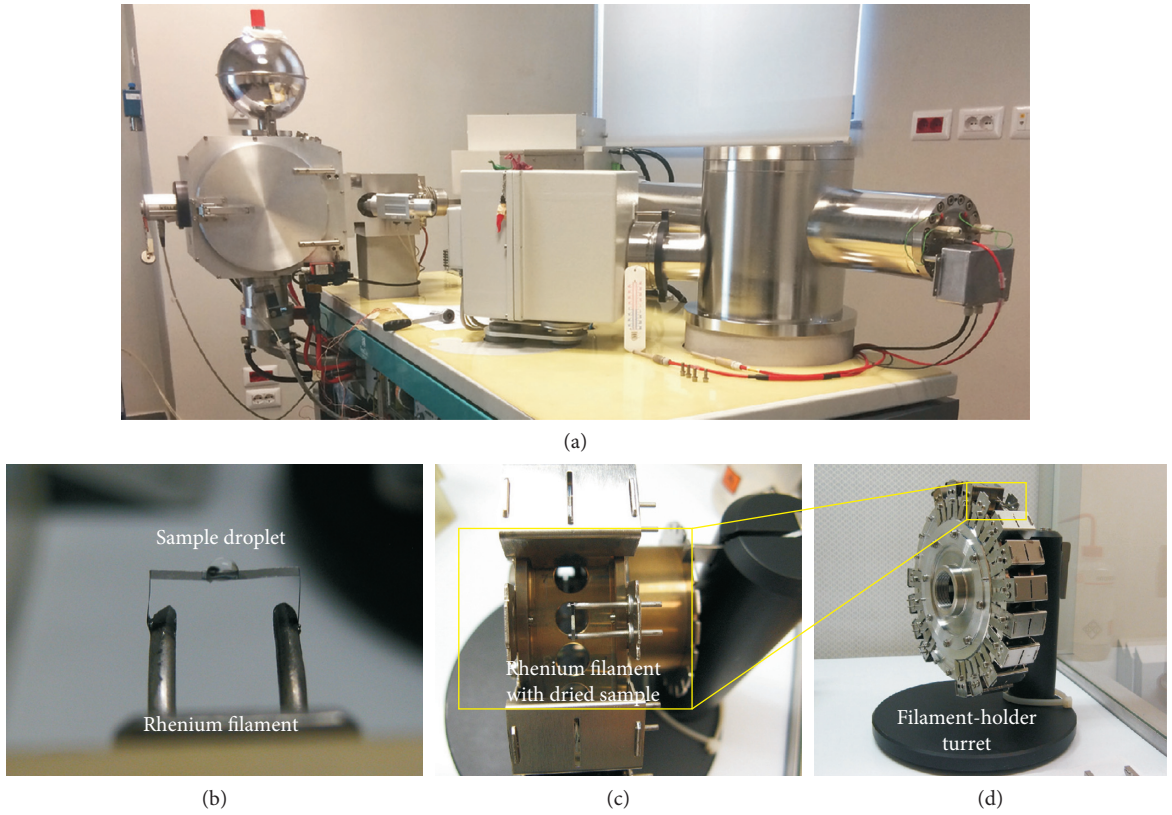

FIGURE 5: (a) The ThermoFinningan Triton-Ti multicollector, thermal ionization mass spectrometer (TIMS) at the University of Firenze; (b) single-rhenium filament with a sample droplet on top; (c) detail of a single filament, holding a dried sample loaded on a sample holder turret that can host 21 filament positions; (d) the turret is ready for the installation into the thermal ionization mass spectrometer.

drops of $TaCl_5$ activator solution [55] and 0.5 μl of H_3PO_4 solution (6 vol.%), respectively. $TaCl_5$ activator was added for enhancing Sr ionisation efficiency and H_3PO_4 for stabilising Sr isotope fractionation during measurement. All the solutions (i.e., activator, sample, and H_3PO_3) were slowly dried by passing a current on the filament, which was increased at the end of the procedure until the filament starts glowing. The loaded filaments were then placed on the filament-holder turret and then inserted into the mass spectrometer (Figures 5(c) and 5(d)).

2.3.2. Measurement Procedure Reproducibility and Accuracy. The measurement routine was established to obtain the best internal and external precisions, and the accuracy, on $^{87}Sr/^{86}Sr$, was achieved by experimentally comparing runs performed in *static* versus *dynamic* conditions at a variable number of cycles and integration times. A detailed description of the *static* and *dynamic* methods is provided in [55, 59]. In brief, the static mode consists of simultaneous measurements of all isotopes in a single "jump," so that the magnetic field remains static and the masses always hit the same detectors (Table 2). *Static* measurements have the advantage of considerably reducing the acquisition time in comparison with the *dynamic* mode, which becomes important when little amount of Sr is available, as dealing with small samples. The main limitation of this method is related to the uncertainty on the Faraday cup efficiency and on the drift of the electronics (i.e., the amplifiers). The Triton-Ti is equipped with a virtual amplifier, which enables a variable connection between amplifiers and Faraday cups and allows a complete switching between amplifiers and cups during a single measurement. However, the virtual amplifier is not able to correct for the different Faraday cup efficiency and its variation with time.

In contrast, the *dynamic* (or *multidynamic*) mode is a peak-jumping procedure where a number of different cup configurations are employed for determining a single isotopic ratio (Table 2). This means that each isotope beam is measured sequentially in different Faraday cups, so that two $^{87}Sr/^{86}Sr_{double}$ values (Table 2) can be calculated without cup efficiency biases and drifts of the electronics (Table 2). The two $^{87}Sr/^{86}Sr_{double}$ values are then geometrically averaged to obtain a single $^{87}Sr/^{86}Sr_{triple}$ value.

The best configuration for *static* mode measurements was found by measuring 300 cycles with an integration time of 8 s, which corresponds to a total measuring time of about 35 minutes for each sample. For *dynamic* mode measurements, we performed 120 cycles (each including 3 magnetic jumps), with 8 s of integration time and an idle time of 3 s between the different jumps, for a total of 70 minutes for each sample.

In both *static* and *dynamic* methods, the filament was slowly warmed up, for a total of about 45 minutes, to stabilise the ion emission until the suitable intensity is achieved. During the heating, the beam was accurately optimised by peak-centering and focusing. The optimal beam intensity for

Table 2: Cup configuration schemes of static (a) and dynamic (b) mode measurements.

Cup	L4	L3	L2	L1	C (Far)	H1	H2	H3	H4
(a) Static collection mode									
		^{84}Sr	^{85}Rb	^{86}Sr	^{87}Sr	^{88}Sr			
(b) Dynamic collection mode									
Jump 1			^{85}Rb	^{85}Rb	^{86}Sr	^{87}Sr	^{88}Sr		
Jump 2 (main)		^{84}Sr	^{86}Sr	^{86}Sr	^{87}Sr	^{88}Sr			
Jump 3				^{87}Sr	^{88}Sr				
Sr double									

Combining the measurements from two different magnetic field position (jump 1-2 and jump 2-3 above), it is possible to evaluate two independent $^{87}Sr/^{86}Sr_{double}$ defined as follows: $[^{87}Sr/^{86}Sr]_{1\text{-}2} = \sqrt{[^{87}Sr_{H1}/^{86}Sr_C]_1 \cdot [^{87}Sr_C/^{88}Sr_{H1}]_2 \cdot [^{88}Sr/^{86}Sr]_N}$ and $[^{87}Sr/^{86}Sr]_{2\text{-}3} = \sqrt{[^{87}Sr_C/^{86}Sr_{L1}]_2 \cdot [^{87}Sr_{L1}/^{88}Sr_C]_3 \cdot [^{88}Sr/^{86}Sr]_N}$. The numbers outside the parentheses are relative to the three different magnetic field positions, the subscript of each isotope refers to the cup on which it is measured, and $[^{88}Sr/^{86}Sr]_N$ is the natural ratio (i.e., 8.375209)

the measurement varied from *static* to *dynamic* mode, with higher intensity allowed by the shorter *static* (3–3.5 V on ^{88}Sr) mode with respect to *dynamic* (1.5–2 V on ^{88}Sr) mode, which instead requires maintaining a stable beam, owing to the longer duration of the measurement.

The results are shown in Figure 6 and Table 3. *Static* and *dynamic* mode measurements on NIST-SRM987 reference samples (10 ng of Sr measured) yielded $^{87}Sr/^{86}Sr$ average values of 0.710247 ± 0.000026 (2 SD, $n = 30$) and 0.710251 ± 0.000018 (2 SD, $n = 51$), respectively, with internal precisions of 13 ppm (2 SE) and 16 ppm (2 SE), respectively. Both values are within the recommended reference value for NIST-SRM987 ($^{87}Sr/^{86}Sr = 0.710248 \pm 0.000011$; Figures 6 (a) and 6(b) and Table 3 [59]). *Static* measurement reduced the experimental time but showed a worse external reproducibility than that obtained in *dynamic* mode (Figures 6(a) and 6(b)), yet maintaining similar internal precision. Therefore, the *dynamic* mode was chosen for the experimental work both on the international glass standard BHVO-2G and on the unknown samples. Further measurements of SRM987 in the *dynamic* mode were performed after the initial testing, along with the studied samples, yielding consistent results ($^{87}Sr/^{86}Sr = 0.710252 \pm 0.000018$, 2 SD, $n = 47$; Figure 6(c)).

Results on the BHVO-2G are reported in Table 3. The results were also compared to standard measurements (150 ng of Sr) on the BHVO-2 powder reference sample. BHVO-2G versus BHVO-2 results found for micro- and normal-size samples, respectively, are well within the internal analytical error (Table 3) and in agreement with the reference values reported in [60, 61] for bulk powder (i.e., standard BHVO-2). The significantly larger standard deviation of the micro-drilled BHVO-2G measurements, with respect to both micro-Sr SRM987 and BHVO-2 powder data, is likely partly related to small isotopic heterogeneities of the glass standard. The few available micro-Sr data on the same sample provide similar averages and reproducibility of our data [54, 62] (Table 3).

Comparing our results with LA-MC-ICPMS data is more difficult; in fact, the latter vary largely depending on the material used for the analyses. External reproducibility obtained with LA-MC-ICPMS on material with high Sr contents and low Rb/Sr (e.g., apatite [49, 53], marine shells, and synthetic plagioclase [16]) is comparable or slightly worse than that attained with our method; yet, small but significant differences in accuracy have been reported [53]. On the other hand, the internal and external reproducibility worsen significantly (e.g., by a factor 5 to 10 in [16]) in materials with low Sr and high Rb/Sr.

In summary, the method presented here generally provides more accurate and precise results than LA-MC-ICPMS, independently on the nature of the analysed material, despite being more time-consuming. It is therefore suitable for a wider range of applications.

3. Applications

In this section, we report three case studies, two of which were previously published [8, 10], as examples of possible applications of the presented methodology in different fields of science. Indeed, in the last decade, the in situ isotope microsampling approach has been used and applied in many pilot studies in a wide range of research fields, including, among others, palaeoenvironmental and palaeoecologic reconstructions (i.e., [53, 63]) and climate changes (i.e., [64]).

In the three presented case studies, the samples were thoroughly characterised both texturally (optical microscope and SEM) and chemically (electron micro probe analyses) before drilling. The strontium element concentrations (in ppm) in all the samples was then determined through LA-ICPMS.

3.1. Micro-Sr Isotope in Minerals. Rock-forming minerals in igneous rocks display variable chemical composition depending on several processes and parameters such as (i) the physicochemical conditions of the magmas, (ii) open system processes (e.g., magma mixing and mingling), and (iii) recycling of cumulated crystals triggered by new arrivals of magma within crustal reservoirs. Radiogenic isotope ratios in minerals, or portions of them, can be used as a petrogenetic "DNA" to record the history of the magma reservoir (*crystal isotope stratigraphy*, e.g., [7]) and their evolution within the crust (e.g., [1, 5, 7, 8, 65–67]). Combining in situ Sr-isotope fingerprints with other approaches, such as textural evidences and crystal size distribution, offers the opportunity to understand the processes and timescales through which magmas are stored, differentiated, and delivered prior to eruption (e.g., [5–7, 13, 14, 16, 18, 54, 68, 69]).

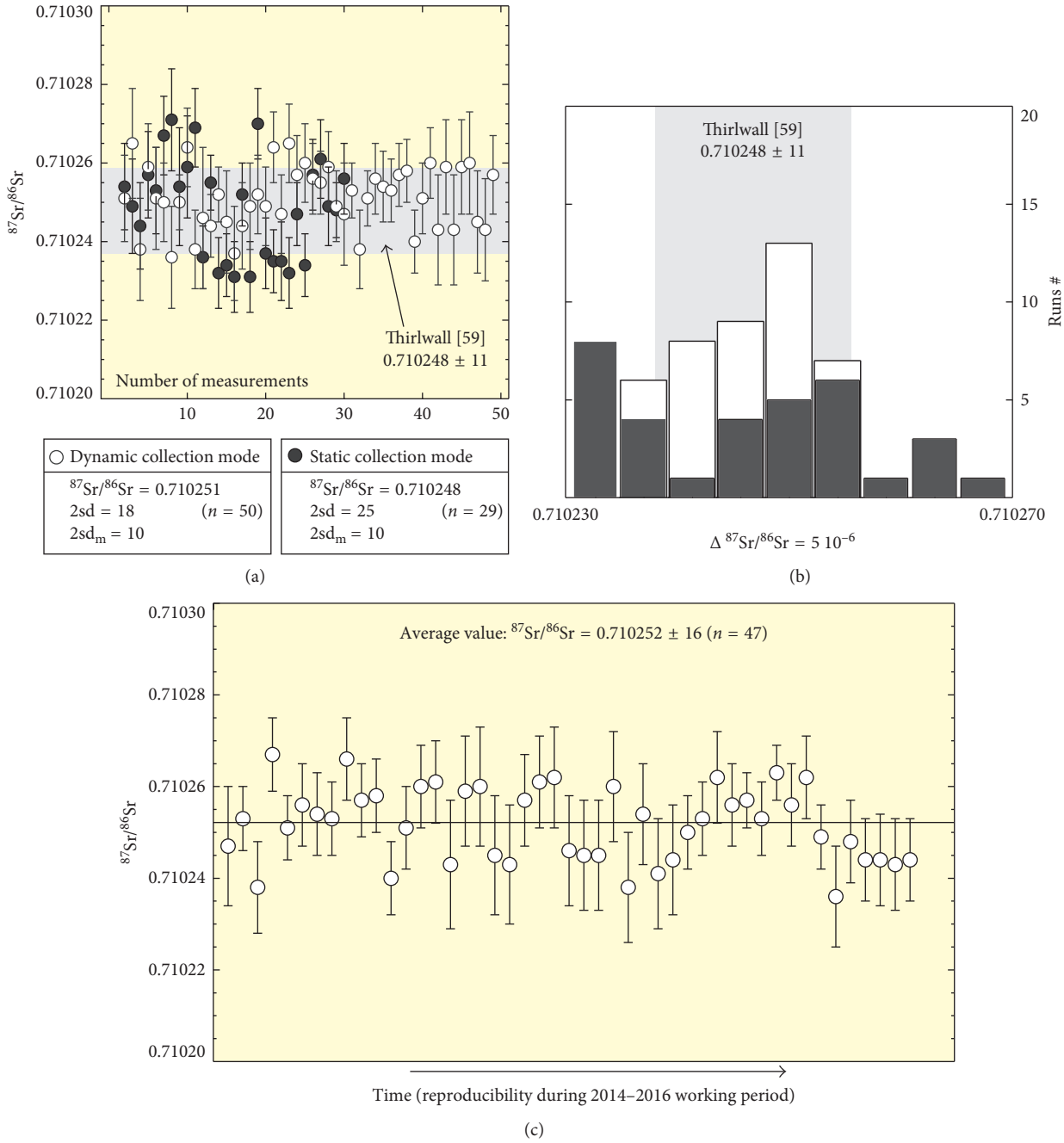

Figure 6: (a) Reproducibility and accuracy for repeated measurements of $^{87}Sr/^{86}Sr$ on 12 ng load size of NSIT-SRM987 standard material for static versus dynamic collection mode over a period of 10 months. Each single measurement is plotted with the relative error bars. The grey-shaded field shows the [59] recommended value range. (b) Distribution of the $^{87}Sr/^{86}Sr$ values measured all over the period of analysis with the static and dynamic collection mode: the static collection mode (black filled columns) shows a worst external reproducibility than that obtained in the dynamic mode (open columns); indeed the dynamic mode gives measurements that reasonably fit a Gaussian distribution pattern with the more representative $^{87}Sr/^{86}Sr$ values centered within the [59] recommended interval (grey shade fields); (c) reproducibility and accuracy trend of $^{87}Sr/^{86}Sr$ 12 ng load size of NSIT-SRM987 measured in the dynamic collection mode throughout the setup period (from 2014 to 2016).

The case study presented here is related to the active Nisyros volcano, the easternmost volcanic island of the South Aegean Active Volcanic Arc (Figure 7) [5, 70–76]. Nisyros volcanic products are typically porphyritic rocks, with clear petrographic evidence of recurrent mixing and mingling of different magmas during the whole volcano's history, which is likely interpreted as the triggering mechanism for its eruptions (e.g., [74, 77, 78]). Sr-isotope determinations at the subcrystal scale, along with detailed petrographic microscopic textural evidence, provided significant data for better defining the interaction of different magmas, concerning pre-eruptive mechanisms. The

Table 3: Accuracy and reproducibility on reference standard material (NIST-SRM987 and BHVO-2).

Standard	Sr content	$^{87}Sr/^{86}Sr$	2 SD	n	Reference
Within run measurement on international standard NIST-SRM987					
Large size loading (ng)					
SRM987	150	0.710253	0.000016	59	Long-term reproducibility (from 2013)
SRM987	150	0.710248	0.000011	427	Thirlwall [59]
Small size loading					
SRM987	10	0.710252	0.000016	47	This study
SRM987	12	0.710259	0.000018	92	Charlier et al. [54]
Drilling procedure on BHVO-2 glass					
BHVO-2 glass	<10	0.703490	0.000092	9	This study
BHVO-2 glass	10	0.703492	0.000094	3	Charlier et al. [54]
		$^{87}Sr/^{86}Sr$	2 SE		
BHVO-2 powder	150	0.703469	0.000004	1	This study
		$^{87}Sr/^{86}Sr$	2 SD		
BHVO-2 powder	—	0.703479	0.000020	12	Weis et al. [60]

2 SD, two standard deviation (external precision); 2 SE, two standard error of the mean; n, numbers of measurements; literature data are reported in italics below our mean values for references.

study focused, in particular, on postcaldera, rhyodacitic dome magmas of the final Nisyros activity emplaced after the caldera-forming rhyolitic explosive eruption of upper pumice. These rhyodacitic lavas contain magmatic enclaves (Figures 7(a) and 7(c)), with basaltic andesite to andesite compositions interpreted, based on their textural features, as quenched portions of mafic magmas included in the cooler, more evolved rhyodacitic host melt (Figures 7(b) and 7(c)) (e.g., [8, 78]).

In situ Sr-isotope ratios were determined on plagioclase phenocrysts (Figures 7(c)–7(e)), from both domes and enclaves, which preserve evidence of the complex history of interaction between the mafic (i.e., enclaves) and felsic (i.e., rhyodacitic domes) magmas in their growing zones [8]. The $^{87}Sr/^{86}Sr$ values determined on micromilled samples from the different growth zones of the plagioclase phenocrysts show clear Sr-isotope disequilibria between (i) cores and rims of single crystals (Figures 7(c)–7(e)) and (ii) the crystals and the host magmas (Figure 7(e)). This suggests that some of the phenocrysts that had formed in the rhyolitic magmas were later enclosed (as xenocrysts) within the more mafic one (i.e., as enclaves). Whereas the rim of the phenocrysts is isotopically intermediate between the rhyolitic and mafic magmas (Figure 7(f)), their cores show higher $^{87}Sr/^{86}Sr$ values, quite close to that of the previously erupted upper pumice magma. This clearly indicates that the phenocrysts originated in a different, older system. In this light, the large plagioclase phenocrysts found inside the dome lavas and enclaves can be interpreted as recycled from previously cumulated crystals (called "antecrysts" by Davidson et al. [7]).

These results have also demonstrated that the dome lavas are multicomponent magmas formed by progressive mingling/mixing processes between (i) a rhyolitic, and more Sr-radiogenic melt derived from the original upper pumice magmas, and (ii) the enclave-forming mafic, and less Sr-radiogenic, melts refilling the felsic magma chamber.

The constraints involved in interpreting in situ isotope data have further implications for the timing and style of eruption. The inferred delay between the mafic input (i.e., enclaves) and the relative dome eruption allows time for reheating and consequent drop in magma viscosity, thus favouring dome extrusion rather than explosive activity [8, 78].

3.2. Micro-Sr Isotope in Natural Glasses. Glasses are found in nature generated by rapid quenching of molten material. They represent a volumetrically small component of crustal rocks and can have different genesis (i.e., volcanic, lightning strikes, meteorite impact, and anthropogenic). In this light, the radiogenic isotopic compositions (i.e., Sr, Nd, and Pb) can provide fundamental information to discriminate among the processes involved in their formation. Glasses constitute the main component of ash and pyroclastic deposits, and their composition and Sr-isotope signature can provide important information in defining the triggering mechanisms of explosive eruptions (e.g., [10, 69, 79–84]). Glasses may also be found in ceramics, as well as in other artefacts. Sr-isotope data are therefore also important to define the possible source of raw materials for pottery, which is particularly relevant for cultural heritage, or to track trade routes in archaeology (e.g., [85–88]). Microscopic scale Sr-isotopic measurements on glasses would help in minimising the amount of sample that needs to be milled, which is of crucial importance both dealing with small-sized volcanic ashes and ejecta and with human artefact of archaeological interest.

The present study is a case study of submicroscopic scale Sr-isotopic determination on ashes of the 2010 Eyjafjallajökull (Iceland) volcano's explosive eruption, which caused enormous disruption to air travel across the northern hemisphere (Figure 8(a)) (e.g., [89–94]). This eruption represents a unique opportunity to test the potential of microscale Sr-isotope determinations on ash glasses from tephra deposits that were well preserved within the ice/snow pack [10]. The population of tephra is composed by four different types of ash fragments: (i) fluidal, (ii) coarsely vesicular, (iii) spongy fine vesicular, and (iv) blocky (Figure 8(b); [93]), generated by different fragmentation processes during the eruption. A detailed microanalytical geochemical and in situ Sr-isotope study performed on glassy groundmass of single ash clast showed unusually high $^{87}Sr/^{86}Sr$ values (up

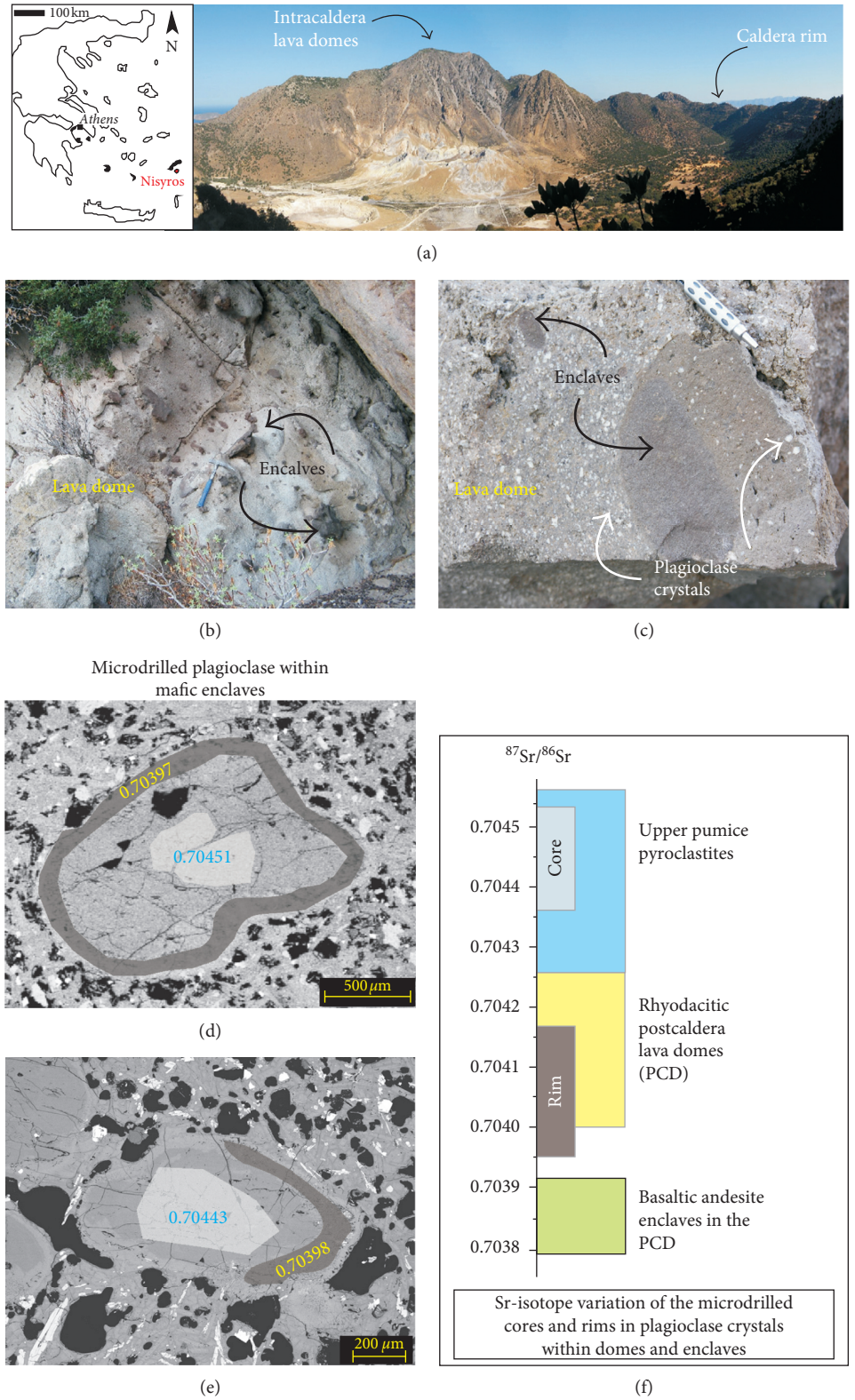

Figure 7: Results of micro-Sr isotope studies on plagioclase crystals from the last magmatic activity of Nisyros volcano (Greece). (a) Landscape view of the Nisyros caldera and its lava domes outpoured during the final magmatic activity of the volcano; (b) image of a lava dome outcrop rich in magmatic enclaves. Notably, the enclaves occurs as well-defined body with rounded and smooth surfaces; (c) specific image of a lava dome and enclave, both rich in large plagioclase crystals; (d and e) back-scattered electron microscope images of two representative plagioclase crystals selected for micro-Sr investigation with microdrill. The shaded areas represent the crystal zones drilled for Sr-isotope analyses, both on cores and rims; (f) $^{87}Sr/^{86}Sr$ variation of the drilled cores and rims compared to the range of $^{87}Sr/^{86}Sr$ of host whole rock (domes and enclaves) and upper pumice whole rock.

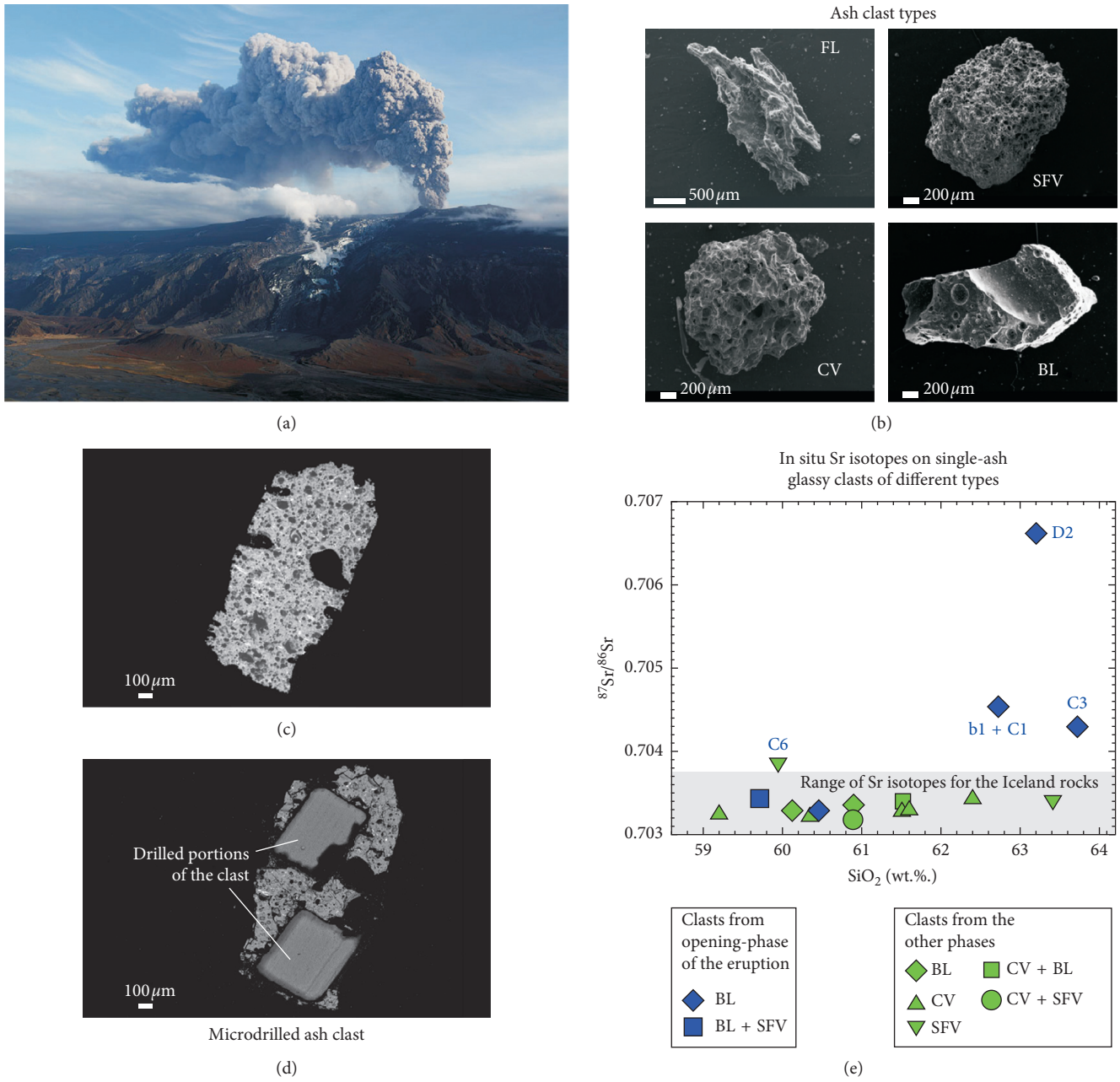

FIGURE 8: Results of micro-Sr isotopes in volcanic ash glasses of the 2010 explosive eruption of Eyjafjallajökull volcano (Iceland). (a) Spectacular image of the ash cloud erupted by the volcano during the early stage of the 2010 activity (https://hiticeland.com/places_and_photos_from_iceland/eyjafjallajokull causing); (b) back-scattered electron microscope images of different clast types sampled in the basal level of the fallout deposit related to the open phase of the 2010 eruption. FL = fluidal; SFV = spongy finely vesicular; CV = coarse vesicular; and BL = blocky. Scale bars are in micron; comparison between back-scattered electron microscope images of clasts before (c) and after (d) in situ microdrilling. Scale bars are in micron; (e) $^{87}Sr/^{86}Sr$ versus SiO_2 (wt.%) diagram of matrix glasses sampled from single, glassy ash clasts. In situ microsampling for Sr-isotope determinations on glass and plagioclase have been obtained by microdrilling technique. Error bars are inside the symbols.

to 0.70668) for Icelandic volcanism (0.7026–0.7037 [94]) (Figure 8(c)); these high isotopic values were also associated to atypical elemental compositions compared to most of the juvenile ash fragments of the eruption. The anomalous, high Sr-radiogenic clasts belong to the blocky type (Figure 8 (b)) and are concentrated in the first, thin ash level emplaced during the initial phase of eruptive activity. These clasts originated from the magma quenched from the contact with the ice cap filling the summit caldera of the volcano [10]. These anomalous findings in the Icelandic magmatic environment can be explained supposing that during its rise and before intruding into the ice cover, the erupting magma selectively assimilated hydrothermal minerals (i.e., zeolites, silica phases, and anhydrite) with seawater-

related high-Sr isotopic ratios, hosted in altered volcanic/epiclastic rocks. This selective assimilation took place at the tip edge of the first rising magma body, resulting in a high degree of contamination restricted to the rather small amount of melt directly in contact with the hydrothermal veins. Indeed, evidence for this process is recorded only by the very first erupted juveniles (i.e., the blocky clasts). The results obtained through submicroscopic-scale micromilling and relative Sr-isotope determination revealed the dynamics of the processes involved in the initial stages of magma ascent to the surface; this provides significant insights into the interpretation of the precursory signals of the eruption (mostly consisting of ground deformation or increased seismicity) [10]. These transient processes, which interested only a small, well-confined part of the magma, cannot be detected using traditional, Sr-isotope determination on whole-rock samples but can be revealed only analysing single-glassy clasts separately.

3.3. Micro-Sr Isotope in Teeth and Bones. Due to their similar chemical properties, Sr can substitute for Ca in the bioapatite [$Ca_5(PO_4,CO_3)_3(OH,F)$] of mammalian bones and teeth, reaching contents of few hundreds of ppm that allows the isotope analysis by microdrilling. The Sr isotope composition of human and animal hard tissues is a function of their dietary habits (e.g., [22]) and depends on the isotopic composition of the food and water ingested during life, which in turn are related to the geological substrate [95–97].

Sr isotopes have been successfully used, along with other stable and radiogenic isotope systematics (i.e., $\delta^{13}C$ and $\delta^{18}O$ and Pb isotopes), not only to track the source regions of migrants and migration pathways, as well as the hunting and trading areas of human populations, but also to study and define the dietary habits of humans and animals (e.g., [23, 44, 95–106]).

A pioneering study [107] demonstrated that migrant individuals who moved between different geologic regions might be traced by comparing $^{87}Sr/^{86}Sr$ in adult tooth enamel, formed between four and twelve years of age, and in the bones, which remodel throughout life and therefore representative of adulthood [30]. Unlike bones and dentine, dental enamel formed during childhood [108] remains unaltered throughout the years. Different $^{87}Sr/^{86}Sr$ in the teeth and bones of an individual may thus reflect the fact that it moved around the landscape passing through different isotopic environments during its youth and maturity [109, 110]. Teeth enamel is generally preferred to dentine and bones in the analysis of Sr concentrations and isotope ratios because it is virtually unaffected by postmortem diagenesis (e.g., [111–113]).

The micro-scale Sr-isotope measurements of samples obtained using the submicroscopic-scale micromill technique is perfectly able to discriminate between enamel and dentine in single-tooth samples. In addition, this technique increases the accuracy of sampling and also reduces the amount of specimen to be destroyed for high-precision Sr-isotope analysis.

Ursus spelaeus was an endemic, widespread European Late Pleistocene species. In contrast to many other taxa, it has fairly rich fossil records, especially thanks to its recurrent use of caves or shelters for winter hibernation [114–116]. Caves were frequently used by bears for many generations, and numerous individuals eventually died in them, so that significant quantities of their remains accumulated over considerable periods of time.

Many studies used stable isotopes to determine the dietary habits of living and extinct bears (e.g., [117–121]), but until now only a small number of papers have considered employing Sr isotopes to possibly elucidate the factors influencing habitat use and gain insights into the foraging behaviour of cave bears [122]. We report here the first $^{87}Sr/^{86}Sr$ data obtained through in situ microsampling on teeth and bones of *Ursus spelaeus* found in Grotta all'Onda cave. The study was aimed at defining the lifestyle and feeding behaviour of one of the most prominent European Late Pleistocene mammals [123–125].

Grotta all'Onda cave is located 708 m above sea level (a.s.l.) in the Apuan Alps nearby the village of Camaiore (Tuscany, Italy) (Figure 9), in a sub-Mediterranean habitat [126]. The cave opens at the base of the Tuscan Nappe, at the contact between the "Calcare a Rhaetavicula Contorta Formation" (i.e., Upper Triassic dolomitic-limestone of the Tuscan Nappe) and the "Argilliti Varicolori Formation" (i.e., Lower Cretaceous shales) (Figure 9). The Rhaetavicula Contorta Formation is a polygenic breccia, mainly including metamorphic clasts, known as "Brecce di Grotta all'Onda" (Figure 9) (http://www502.regione.toscana.it/geoscopio/geologia.html). The fossil remains of *Ursus spelaeus* were recovered during a 1999 excavation. Radiocarbon dating of bone yielded ages ranging from 38.22 to 38.28 ky (BP) [127]. Six different specimens were selected for Sr isotope analysis; these include three lower molars (SCT4, SCT5, and SCT6) from layers 7J4, 7J3, and 7J5, respectively and three metapodial bones, SCT 1 (third metacarpal), SCT 2 (fourth metatarsal), and SCT3 (fourth metatarsal), from layers 7J4, 7J5, and 7J3, respectively (Figures 9(c) and 10(a)–10(b)–10(c)–10(d)). Two whole soil (i.e., cave earth) samples, SCT7 and SCT8, were also collected from the representative layers 7J4 and 7J5 (Figure 9(c)).

All the three teeth had well-preserved dentin and very thin enamel layer (Figure 10). In contrast, the three bones were rather differently preserved and had different porosity. In particular, SCT3 was the most heavily mineralised and best preserved, whereas SCT1 was densely vacuolated and preserved higher amounts of organic components.

Major element analyses of these specimens revealed that the enamel bioapatite was more mineralised than that of dentin and bones. Moreover, the dentin bioapatite was found enriched in Sr and in other trace elements [128].

For the purpose of this study, dentin and enamel of the teeth and cortical sections of the bones from Grotta all'Onda were micromilled and analysed for micro-Sr isotope determination. The two soil samples were also processed for Sr-isotope determination using the traditional, large sample method [37, 55]. The $^{87}Sr/^{86}Sr$ data are reported in Table 4. Tooth enamel shows higher $^{87}Sr/^{86}Sr$ and lower Sr/Ca than

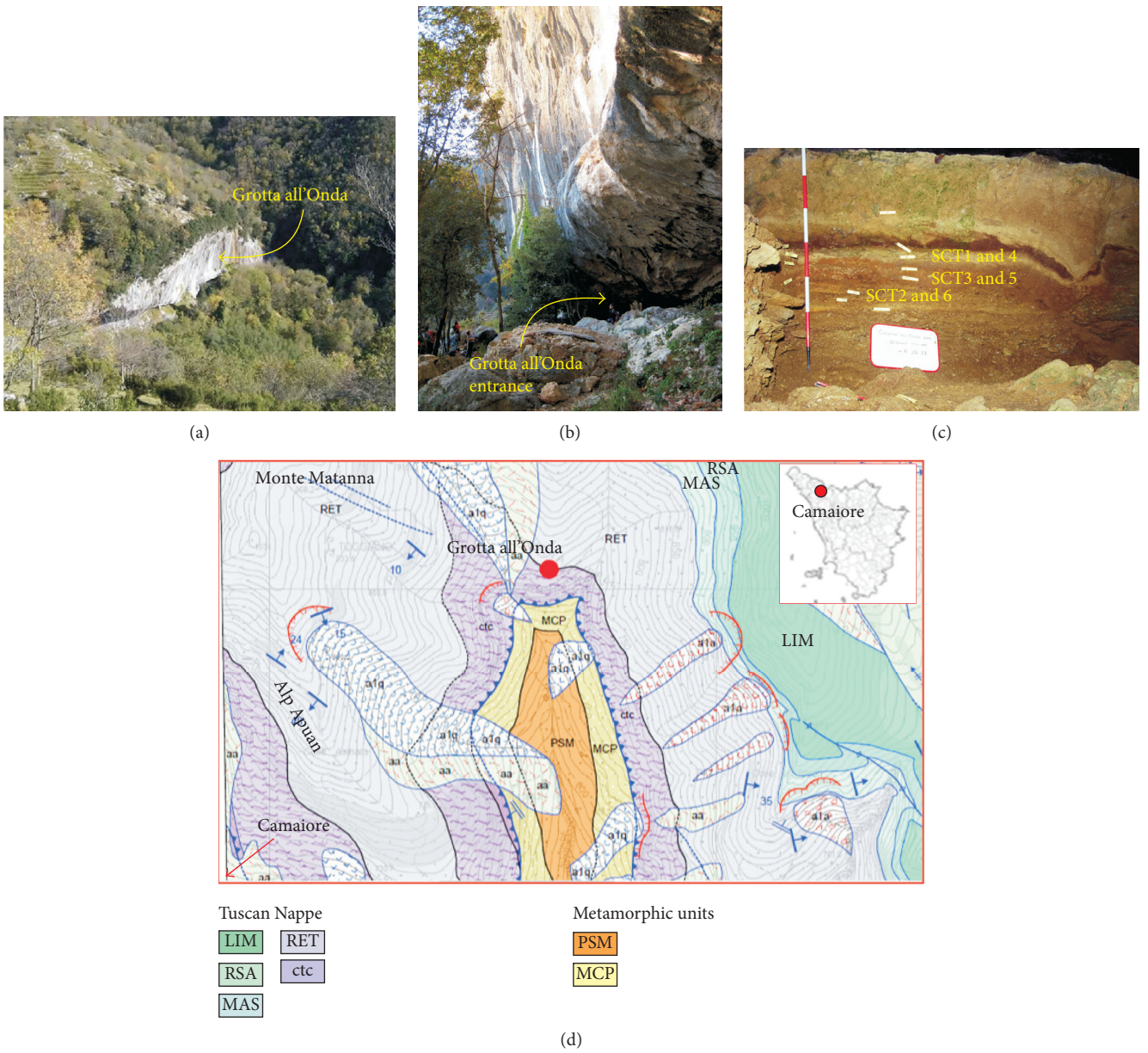

Figure 9: The *Ursus spelaeus* finding environment. (a) Image of the Grotta all'Onda cave from the above, showing the well-defined cut of the Mt. Matanna flank where the cave is located; (b) image of the entrance of the Grotta all'Onda cave; (c) image of the soil stratigraphy from which the *Ursus spelaeus* fossil remains have been sampled during the 1999 field campaign; (d) geological sketch map of the area around the Grotta all'Onda cave (http://www502.regione.toscana.it/geoscopio/geologia.html#). Formation of the Tuscan Nappe unit: LIM: "*Calcare Secifero di Limano*" formation; RSA: "*Rosso Ammonitico*" formation; MAS: "Calcare Massiccio" formation; RET: "*Raethavicola Contorta*" formation, Late Triassic dolomitic-limestones; ctc: cataclastic formation made by a polygenic breccias of mainly metamorphic limestone clasts. Tuscan metamorphic units: PSM: "Pseudomacigno" formation; MCP: "Cipollini" formation.

microsamples of dentin and bones do (Figures 10(e) and 10(f)). This strongly suggests that $^{87}Sr/^{86}Sr$ of tooth enamel is unaffected by diagenetic alteration, in contrast to the other organic-rich samples (i.e., bones and dentin). The $^{87}Sr/^{86}Sr$ composition of the dentin samples is close to that of the local soil samples (Figure 10(e)); even closer to the latter is that of the bone samples, with the only exception of SCT3 due to its high degree of mineralisation.

These results, despite the relatively recent age of the fossil specimens (ca. 40 ka [127]), indicate that bone tissues have been more exposed to *postmortem* diagenetic exchange processes compared to more heavily mineralized enamel. This speaks for a possible isotope reequilibration between dentin and bones (but not enamel) and soil, due to Sr exchange with percolating fluids. The soil samples have $^{87}Sr/^{86}Sr$ values comparable to those of the "Calcare a Rhaetavicula Contorta" formation, which forms the cave's bedrock [129], through which fluids filter into the cave (Figure 10(e)).

In summary, our study shows that the Grotta all'Onda bones and dentin are unsuitable to determine the

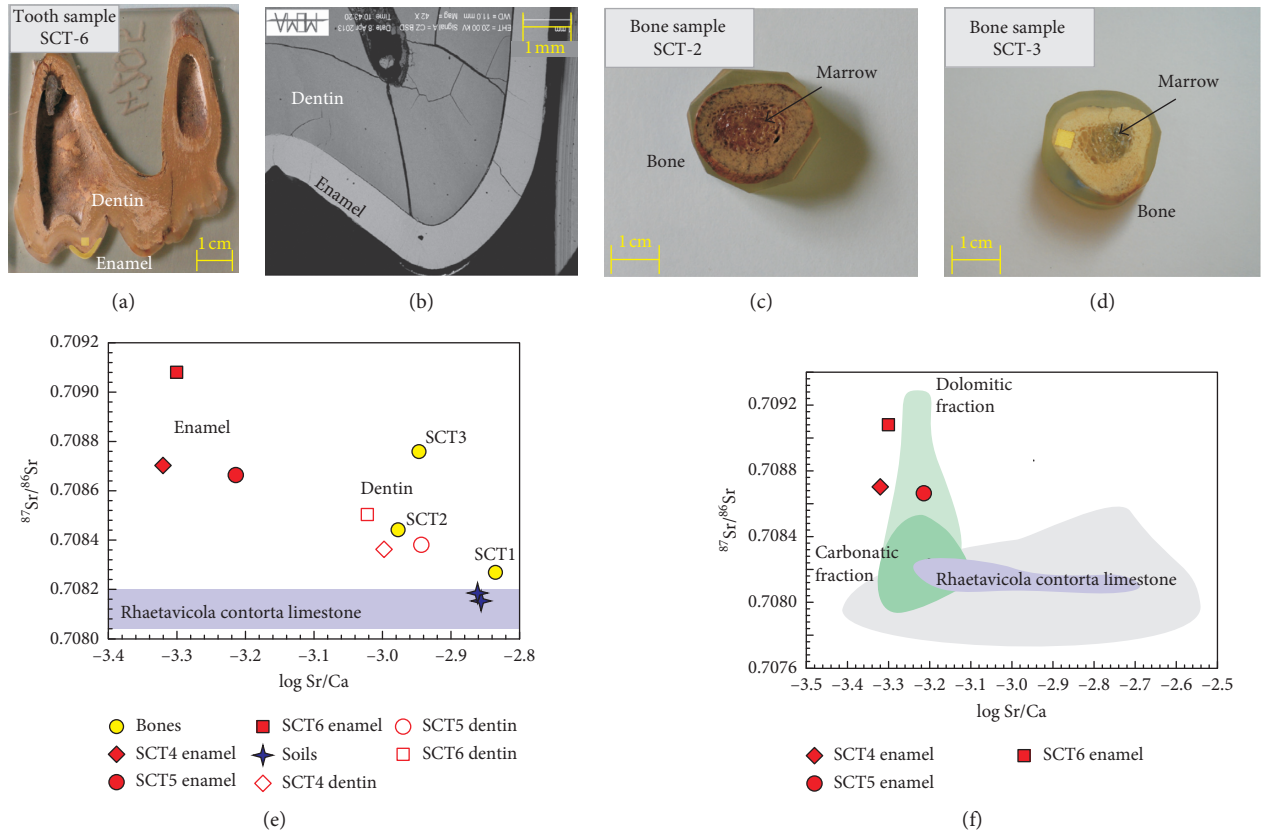

FIGURE 10: Results of micro-Sr isotopes in teeth and bones of the *Ursus spelaeus*. (a) Representative image of one tooth sample, sectioned for microdrilling. The thin layer of enamel is well evident with respect to the lighter inner dentin. In yellow are reported the two drilling sites on dentin and enamel; (b) particular back-scattered electron microscopy image of the edge of the tooth showing dentin (dark grey) and enamel (light grey) portion; (c and d) images of two of the analysed bones properly prepared in epoxy resin mounts for microdrilling sampling. In yellow is reported the drilling site; (e) $^{87}Sr/^{86}Sr$ versus Sr/Ca (in log scale) diagram showing the results obtained from the analyses of enamel and dentin in the three teeth, compared with bones of the *Ursus spelaeus* specimen. The $^{87}Sr/^{86}Sr$ of soils in which the fossils have been sampled are also reported together with the Sr-isotope field of the *Raetavicola Contorta* limestone for comparison. (See text for detail) (f) $^{87}Sr/^{86}Sr$ versus Sr/Ca (in log scale) diagram comparing the Sr-isotope values of dentin from the three teeth samples with the Sr-isotope range fields of the different geologic formations forming the bedrock outcropping in the area of the Grotta all'Onda cave.

TABLE 4: (a) $^{87}Sr/^{86}Sr$ results obtained on microsamples of tooth dentine and enamel and bones of the *Ursus spelaeus* specimen. (b) $^{87}Sr/^{86}Sr$ soils sampled in the Grotta all'Onda cave from which the fossil remains were collected.

Sample	Type	Sr content (ppm)	$^{87}Sr/^{86}Sr$	2 SE	Log (Sr/Ca) Average
(a) Teeth and bones					
STC1	Bone	510	0.708268	0.000006	−2.84
STC2	Bone	352	0.708441	0.000006	−2.98
STC3	Bone	359	0.708758	0.000006	−2.95
STC4-1	Enamel	187	0.708703	0.000005	−3.32
STC4-2	Dentin	360	0.708362	0.000006	−3.00
STC5-1	Enamel	211	0.708663	0.000005	−3.21
STC5-2	Dentin	384	0.708380	0.000006	−2.94
STC6-1	Enamel	179	0.709081	0.000005	−3.30
STC6-2	Dentin	339	0.708504	0.000006	−3.02
(b) Soils					
STC7	Soil	204	0.708184	0.000006	−2.86
STC8	Soil	228	0.708155	0.000006	−2.86

2 SE: two standard error of the mean.

characteristics of the habitat where the cave bear lived, due to their interaction with percolating water and their consequent contamination by the soils in which they had been preserved. In contrast, the $^{87}Sr/^{86}Sr$ ratios of the tooth enamel results unaltered and realistically reflects the original values achieved during the cave bear's life. The isotopic composition of the

enamel samples is consistent with that of the "Calcare Massiccio Formation" and in particular with the dolomite fraction [129] (Figure 10(f)). The mismatch between the $^{87}Sr/^{86}Sr$ values of the enamel samples and those of the cave soils (Figure 10(e)) (i.e., local substrata of the cave) indicate that the cave bear died away from its customary habitat. Bears cannot indeed find food in caves, where they find refuge as shelter for winter hibernation or for night resting. The enamel isotopic values obtained during our study indicate that *Ursus spelaeus* from Grotta all'Onda roamed in search for food within a confined area not far from the cave, where the "Calcare Massiccio" is largely exposed and did not move too far from the area during its whole life.

4. Summary and Conclusions

The present study show the potential of $^{87}Sr/^{86}Sr$ determination by TIMS on micro-scale samples, based on micromilling solid specimens, not only for geological applications, but also for other fields, such as archaeology, forensics, medical, and life sciences, where it has hardly, if ever, been used. Reported here is a detailed description of all the analytical protocols, including results on replicate analyses of international standards (SRM 987 and BHVO-2G), which yield good accuracy and precision. In addition, three case studies are presented, performed in our laboratory, where in situ microdrilled Sr isotopes have been used in different fields of application.

The first case study on micro-Sr isotope determination at subgrain microscopic scale regards the petrogenetic processes relevant to the understanding of the plumbing system dynamics under active volcanoes. This example revealed the role played by the interaction of different magmas, which are normally characterised by distinct $^{87}Sr/^{86}Sr$ signatures, comingled in the plumbing system of the Nisyros volcano, which was capable of triggering the eruption.

The second case regards volcanic glasses with extremely low total Sr content (i.e., tholeiitic). The micromilling determination of $^{87}Sr/^{86}Sr$ ratio was performed on ashes, with different shapes and nature, erupted by different phases, during the 2010 eruption of Eyjafjallajökull volcano (Iceland). The $^{87}Sr/^{86}Sr$ data provide information on the eruptive mechanism involved during the eruption, as well as on the interaction between the magma and the hydrothermally-derived minerals attained before the thawing of the ice cap; it also provides significant insights into the interpretation of the precursory signals of the eruption.

The third case displays the use of $^{87}Sr/^{86}Sr$ microdrilled in enamel, dentin, and bones, to show that only enamel has more chances to preserve the original Sr-isotope signatures than bone and dentin. The analysis also revealed the close relationship existing between the radiogenic-Sr of the organic materials and that of the geologic Cretaceous substratum of the Apuan Alps, which provides valuable insights into the palaeoenvironment of the local cave bears. In this case, the Sr isotopes proved particularly useful for determining the foraging habits of extinct mammals, which substantiates the well-known statement "YOU ARE WHAT YOU EAT" (cit. Anthelme Brillat-Savarin).

Conflicts of Interest

The authors declare that there are no conflicts of interest regarding the publication of this paper.

Authors' Contributions

Lorella Francalanci provided the input to the set-up and the development of the in situ micro-Sr isotope procedure at the Radiogenic Isotope Laboratory of Firenze, providing also continuous scientific stirring and encouraging to the other research fellows, coauthors of the present paper.

Acknowledgments

The research on volcanic rocks was financially supported by PRIN 2010-2011 and 2015 with Grants 2010TT22SC_001 and 20158A9CBM, respectively. Regione Toscana government supported the salary of Sara Di Salvo through a "Pegaso" fellowship. The studies on the *Ursus spelaeus* had no financial support, and the analytical work expenses were covered by the "Radiogenic Lab" of the University of Florence. The authors are grateful for the suggestions of an anonymous reviewer, which improved the paper.

References

[1] F. J. Tepley and J. P. Davidson, "Mineral-scale Sr-isotope constraints on magma evolution and chamber dynamics in the Rum layered intrusion, Scotland," *Contributions to Mineralogy and Petrology*, vol. 145, no. 5, pp. 628–641, 2003.

[2] G. Perini III, F. J. Tepley, J. P. Davidson, and S. Conticelli, "The origin of K-feldspar megacrysts hosted in alkaline potassic rocks from central Italy: a track for low-pressure processes in mafic magmas," *Lithos*, vol. 66, no. 3-4, pp. 223–240, 2003.

[3] D. Morgan, S. Blake, N. Rogers et al., "Time scales of crystal residence and magma chamber volume from modelling of diffusion profiles in phenocrysts: vesuvius 1944," *Earth and Planetary Science Letters*, vol. 222, no. 3-4, pp. 933–946, 2004.

[4] W. Siebel, E. Reitter, T. Wenzel, and U. Blaha, "Sr isotope systematics of K-feldspars in plutonic rocks revealed by the Rb-Sr microdrilling technique," *Chemical Geology*, vol. 222, no. 3-4, pp. 183–199, 2005.

[5] L. Francalanci, G. R. Davies, W. Lustenhouwer, S. Tommasini, P. R. Mason, and S. Conticelli, "Intra-grain Sr isotope evidence for crystal recycling and multiple magma reservoirs in the recent activity of Stromboli volcano, southern Italy," *Journal of Petrology*, vol. 46, no. 10, pp. 1997–2021, 2005.

[6] L. Francalanci, R. Avanzinelli, I. Nardini, M. Tiepolo, J. P. Davidson, and R. Vannucci, "Crystal recycling in the steady-state system of the active Stromboli volcano: a 2.5-ka story inferred from in situ Sr-isotope and trace element data," *Contributions to Mineralogy and Petrology*, vol. 163, no. 1, pp. 109–131, 2012.

[7] J. P. Davidson, D. J. Morgan, B. L. A. Charlier, R. Harlou, and J. M. Hora, "Microsampling and isotopic analysis of igneous rocks: implications for the study of magmatic systems," *Annual Review of Earth and Planetary Sciences*, vol. 35, no. 1, pp. 273–311, 2007.

[8] E. Braschi, L. Francalanci, S. Tommasini, and G. E. Vougioukalakis, "Unraveling the hidden origin and migration of plagioclase phenocrysts by in situ Sr isotopes: the case of final dome activity at Nisyros volcano, Greece," *Contributions to Mineralogy and Petrology*, vol. 167, no. 3, p. 988, 2014.

[9] S. Conticelli, E. Boari, L. Burlamacchi et al., "Geochemistry and Sr-Nd-Pb isotopes of Monte Amiata Volcano, Central Italy: evidence for magma mixing between high-K calc-alkaline and leucititic mantle-derived magmas," *Italian Journal of Geosciences*, vol. 134, no. 2, pp. 266–290, 2015.

[10] M. Pistolesi, R. Cioni, L. Francalanci et al., "The onset of an eruption: selective assimilation of hydrothermal minerals during pre-eruptive magma ascent of the 2010 summit eruption of Eyjafjallajökull volcano, Iceland," *Journal of Volcanology and Geothermal Research*, vol. 327, pp. 449–458, 2016.

[11] J. N. Christensen, A. N. Halliday, D. C. Lee, and C. M. Hall, "In situ Sr isotopic analysis by laser ablation," *Earth and Planetary Science Letters*, vol. 136, no. 1-2, pp. 79–85, 1995.

[12] J. P. Davidson and F. J. Tepley, "Recharge in volcanic systems: evidence from isotope profiles of phenocrysts," *Science*, vol. 275, no. 5301, pp. 826–829, 1997.

[13] J. P. Davidson, L. Font, B. L. Charlier, and F. J. Tepley, "Mineral-scale Sr isotope variation in plutonic rocks–a tool for unravelling the evolution of magma systems," *Earth and Environmental Science Transactions of the Royal Society of Edinburgh*, vol. 97, no. 4, pp. 357–367, 2006.

[14] B. L. A. Charlier, O. Bachmann, J. P. Davidson, M. A. Dungan, and D. J. Morgan, "The upper crustal evolution of a large silicic magma body: evidence from crystal-scale Rb–Sr isotopic heterogeneities in the Fish Canyon magmatic system, Colorado," *Journal of Petrology*, vol. 48, no. 10, pp. 1875–1894, 2007.

[15] B. L. Charlier, C. J. Wilson, and J. P. Davidson, "Rapid open-system assembly of a large silicic magma body: time-resolved evidence from cored plagioclase crystals in the Oruanui eruption deposits, New Zealand," *Contributions to Mineralogy and Petrology*, vol. 156, no. 6, pp. 799–813, 2008.

[16] J. P. Davidson, F. J. Tepley, Z. Palacz, and S. Meffan-Main, "Magma recharge, contamination, and residence times revealed by in situ laser ablation isotopic analysis of feldspar in volcanic rocks," *Earth and Planetary Science Letters*, vol. 184, no. 2, pp. 427–442, 2001.

[17] F. J. Tepley, J. P. Davidson, R. I. Tilling, and J. G. Arth, "Magma mixing, recharge and eruption histories recorded in plagioclase phenocrysts from El Chichon Volcano, Mexico," *Journal of Petrology*, vol. 41, no. 9, pp. 1397–1411, 2000.

[18] D. J. Morgan, D. A. Jerram, D. G. Chertkoff et al., "Combining CSD and isotopic microanalysis: magma supply and mixing processes at Stromboli Volcano, Aeolian Islands, Italy," *Earth and Planetary Science Letters*, vol. 260, no. 3-4, pp. 419–431, 2007.

[19] P. Horn, P. Schaaf, B. Holbach, S. Hölzl, and H. Eschnauer, "$^{87}Sr/^{86}Sr$ from rock and soil into vine and wine," *Zeitschrift für Lebensmitteluntersuchung und-Forschung A*, vol. 196, no. 5, pp. 407–409, 1993.

[20] J. L. Banner and J. Kaufman, "The isotopic record of ocean chemistry and diagenesis preserved in non-luminescent brachiopods from Mississippian carbonate rocks, Illinois and Missouri," *Geological Society of America Bulletin*, vol. 106, no. 8, pp. 1074–1082, 1994.

[21] G. Åberg, G. Fosse, and H. Stray, "Man, nutrition and mobility: a comparison of teeth and bone from the Medieval era and the present from Pb and Sr isotopes," *Science of the Total Environment*, vol. 224, no. 1, pp. 109–119, 1998.

[22] R. C. Capo, B. W. Stewart, and O. A. Chadwick, "Strontium isotopes as tracers of ecosystem processes: theory and methods," *Geoderma*, vol. 82, no. 1–3, pp. 197–225, 1998.

[23] B. L. Beard and C. M. Johnson, "Strontium isotope composition of skeletal material can determine the birth place and geographic mobility of humans and animals," *Journal of Forensic Science*, vol. 45, no. 5, pp. 1049–1061, 2000.

[24] S. Tommasini, G. R. Davies, and T. Elliott, "Lead isotope composition of tree rings as bio-geochemical tracers of heavy metal pollution: a reconnaissance study from Firenze, Italy," *Applied Geochemistry*, vol. 15, no. 7, pp. 891–900, 2000.

[25] M. Vanhaeren, F. d'Errico, I. Billy, and F. Grousset, "Tracing the source of Upper Palaeolithic shell beads by strontium isotope dating," *Journal of Archaeological Science*, vol. 31, no. 10, pp. 1481–1488, 2004.

[26] C. M. R. Almeida and M. T. S. Vasconcelos, "Lead contamination in Portuguese red wines from the Douro region: from the vineyard to the final product," *Journal of Agricultural and Food Chemistry*, vol. 51, no. 10, pp. 3012–3023, 2003.

[27] J. A. Evans and S. Tatham, "Defining "local signature" in terms of Sr isotope composition using a tenth-to twelfth-century Anglo-Saxon population living on a Jurassic clay-carbonate terrain, Rutland, UK," *Geological Society, London, Special Publications*, vol. 232, no. 1, pp. 237–248, 2004.

[28] S. Hölzl, P. Horn, A. Rossmann, and S. Rummel, "Isotope-abundance ratios of light (bio) and heavy (geo) elements in biogenic tissues: methods and applications," *Analytical and Bioanalytical Chemistry*, vol. 378, no. 2, pp. 270–272, 2004.

[29] S. Kelly, K. Heaton, and J. Hoogewerff, "Tracing the geographical origin of food: the application of multi-element and multi-isotope analysis," *Trends in Food Science & Technology*, vol. 16, no. 12, pp. 555–567, 2005.

[30] R. A. Bentley and C. Knipper, "Geographical patterns in biologically available strontium, carbon and oxygen isotope signatures in prehistoric SW Germany," *Archaeometry*, vol. 47, no. 3, pp. 629–644, 2005.

[31] P. Degryse, J. Schneider, U. Haack et al., "Evidence for glass "recycling" using Pb and Sr isotopic ratios and Sr-mixing lines: the case of early Byzantine Sagalassos," *Journal of Archaeological Science*, vol. 33, no. 4, pp. 494–501, 2006.

[32] S. Rummel, S. Hoelzl, P. Horn, A. Rossmann, and C. Schlicht, "The combination of stable isotope abundance ratios of H, C, N and S with $^{87}Sr/^{86}Sr$ for geographical origin assignment of orange juices," *Food Chemistry*, vol. 118, no. 4, pp. 890–900, 2010.

[33] S. Vorkelius, G. D. Lorenz, S. Rummel et al., "Strontium isotopic signatures of natural mineral waters, the reference to a simple geological map and its potential for authentication of food," *Food Chemistry*, vol. 118, no. 4, pp. 933–940, 2010.

[34] B. P. Kennedy, A. Klaue, J. D. Blum, C. L. Folt, and K. H. Nislow, "Reconstructing the lives of fish using Sr isotopes in otoliths," *Canadian Journal of Fisheries and Aquatic Sciences*, vol. 59, no. 6, pp. 925–929, 2011.

[35] C. Durante, C. Baschieri, L. Bertacchini et al., "Geographical traceability based on $^{87}Sr/^{86}Sr$ indicator: a first approach for PDO Lambrusco wines from Modena," *Food Chemistry*, vol. 141, no. 3, pp. 2779–2787, 2013.

[36] S. Marchionni, E. Braschi, S. Tommasini et al., "High-precision $^{87}Sr/^{86}Sr$ analyses in wines and their use as a geological fingerprint for tracing geographic provenance," *Journal of*

Agricultural and Food Chemistry, vol. 61, no. 28, pp. 6822–6831, 2013.

[37] S. Marchionni, A. Buccianti, A. Bollati et al., "Conservation of $^{87}Sr/^{86}Sr$ isotopic ratios during the winemaking processes of "Red" wines to validate their use as geographic tracer," *Food Chemistry*, vol. 190, pp. 777–785, 2016.

[38] V. Vinciguerra, R. Stevenson, K. Pedneault, A. Poirier, J.-F. Hélie, and D. Widory, "Strontium isotope characterization of wines from Quebec, Canada," *Food Chemistry*, vol. 210, pp. 121–128, 2016.

[39] P. L. Koch, J. Heisinger, C. Moss, R. W. Carlson, M. L. Fogel, and A. K. Behrensmeyer, "Isotopic tracking of change in diet and habitat use in African elephants," *Science*, vol. 267, no. 5202, p. 1340, 1995.

[40] A. Sillen, G. Hall, and R. Armstrong, "Strontium calcium ratios (Sr/Ca) and strontium isotopic ratios ($^{87}Sr/^{86}Sr$) of *Australopithecus robustus* and *Homo* sp. From Swartkrans," *Journal of Human Evolution*, vol. 28, no. 3, pp. 277–285, 1995.

[41] G. Grupe, "Preservation of collagen in bone from dry, Sandy soil," *Journal of Archaeological Science*, vol. 22, no. 2, pp. 193–199, 1995.

[42] G. Grupe, T. D. Price, and F. Söllner, "Mobility of Bell Beaker people revealed by strontium isotope ratios of tooth and bone: a study of southern Bavarian skeletal remains. A reply to the comment by Peter Horn and Dieter Müller-Sohnius," *Applied Geochemistry*, vol. 14, no. 2, pp. 271–275, 1999.

[43] P. Willey, A. Galloway, and L. Snyder, "Bone mineral density and survival of elements and element portions in the bones of the Crow Creek massacre victims," *American Journal of Physical Anthropology*, vol. 104, no. 4, pp. 513–528, 1997.

[44] K. A. Hoppe, P. L. Koch, R. W. Carlson, and S. D. Webb, "Tracking mammoths and mastodons: reconstruction of migratory behavior using strontium isotope ratios," *Geology*, vol. 27, no. 5, pp. 439–442, 1999.

[45] T. D. Price, J. H. Burton, and R. A. Bentley, "The characterization of biologically available strontium isotope ratios for the study of prehistoric migration," *Archaeometry*, vol. 44, no. 1, pp. 117–135, 2002.

[46] R. A. Bentley, T. D. Price, and E. Stephan, "Determining the "local" $^{87}Sr/^{86}Sr$ range for archaeological skeletons: a case study from Neolithic Europe," *Journal of Archaeological Science*, vol. 31, no. 4, pp. 365–375, 2004.

[47] J. A. Evans, J. Montgomery, G. Wildman, and N. Boulton, "Spatial variations in biosphere $^{87}Sr/^{86}Sr$ in Britain," *Journal of the Geological Society*, vol. 167, no. 1, pp. 1–4, 2010.

[48] J. H. Burton and T. D. Price, "Seeking the local $^{87}Sr/^{86}Sr$ ratio to determine geographic origins of humans," in *ACS Symposium Series*, pp. 309–320, ACS Publication, Washington, DC, USA, 2013.

[49] F. Lugli, A. Cipriani, C. Peretto, M. Mazzucchelli, and D. Brunelli, "In situ high spatial resolution $^{87}Sr/^{86}Sr$ ratio determination of two Middle Pleistocene (ca 580 ka) *Stephanorhinus hundsheimensis* teeth by LA–MC–ICP–MS," *International Journal of Mass Spectrometry*, vol. 412, pp. 38–48, 2017.

[50] T. Prohaska, C. Latkoczy, G. Schultheis, M. Teschler-Nicola, and G. Stingeder, "Investigation of Sr isotope ratios in prehistoric human bones and teeth using laser ablation ICP-MS and ICP-MS after Rb/Sr separation," *Journal of Analytical Atomic Spectrometry*, vol. 17, no. 8, pp. 887–891, 2002.

[51] S. R. Copeland, M. Sponheimer, P. J. le Roux et al., "Strontium isotope ratios ($^{87}Sr/^{86}Sr$) of tooth enamel: a comparison of solution and laser ablation multicollector inductively coupled plasma mass spectrometry methods," *Rapid Communications in Mass Spectrometry*, vol. 22, no. 20, pp. 3187–3194, 2008.

[52] A. Simonetti, M. R. Buzon, and R. A. Creaser, "In situ elemental and Sr isotope investigation of human tooth enamel by Laser Ablation-(MC)-ICP-MS: success and pitfalls," *Archaeometry*, vol. 50, no. 2, pp. 371–385, 2008.

[53] J. Lewis, C. D. Coath, and A. W. G. Pike, "An improved protocol for $^{87}Sr/^{86}Sr$ by laser ablation multi-collector inductively coupled plasma mass spectrometry using oxide reduction and a customised plasma interface," *Chemical Geology*, vol. 390, pp. 173–181, 2014.

[54] B. L. A. Charlier, C. Gimbre, D. Morgan et al., "Methods of microsampling and high-precision analysis of strontium and rubidium isotopes at single crystal scale for petrological and geochronological applications," *Chemical Geology*, vol. 232, no. 3-4, pp. 144–133, 2006.

[55] R. Avanzinelli, E. Boari, S. Conticelli et al., "High precision Sr, Nd, and Pb isotopic analyses using the new generation Thermal Ionisation Mass Spectrometer ThermoFinningan Triton-Ti®," *Periodico di Mineralogia*, vol. 74, no. 3, pp. 147–166, 2005.

[56] D. L. Hoffmann, C. Spötl, and A. Mangini, "Micromill and in situ laser ablation sampling techniques for high spatial resolution MC-ICPMS U-Th dating of carbonates," *Chemical Geology*, vol. 259, no. 3-4, pp. 253–261, 2009.

[57] A. Eberhart, R. Delwiche, and Z. Geiss, "Isotopic effects in single filament thermal ion sources," *Zeitschrift für Naturforschung A*, vol. 19, no. 6, pp. 736–740, 1964.

[58] W. A. Russel, D. A. Papanastassiou, and T. A. Tombrello, "Ca isotope fractionation on the Earth and other solar system materials," *Geochimica et Cosmochimica Acta*, vol. 42, no. 8, pp. 1075–1090, 1978.

[59] M. F. Thirlwall, "Long-term reproducibility of multicollector Sr and Nd isotope ratio analysis," *Chemical Geology*, vol. 94, no. 2, pp. 85–104, 1991.

[60] D. Weis, B. Kieffer, C. Maerschalk et al., "High-precision isotopic characterization of USGS reference materials by TIMS and MC-ICP-MS," *Geochemistry, Geophysics, Geosystems*, vol. 7, no. 8, 2006.

[61] J. B. Mahoney, D. Weiss, B. Keiffer et al., "Ongoing isotopic characterization of USGS standards: MC-ICPMS and TIMS data from the Pacific Centre for isotopic and geochemical research, University of British Columbia," in *Proceedings of Geological Society of America, Seattle Annual Meeting, Paper 117-118*, Seattle, WA, USA, October 2003.

[62] M. Elburg, P. Vroon, B. van der Wagt, and A. Tchalikian, "Sr and Pb isotopic composition of five USGS glasses (BHVO-2G, BIR-1G, BCR-2G, TB-1G, NKT-1G)," *Chemical Geology*, vol. 223, no. 4, pp. 196–207, 2005.

[63] C. Spötl and D. Mattey, "Stable isotope microsampling of speleothems for palaeoenvironmental studies: a comparison of microdrill, micromill and laser ablation techniques," *Chemical Geology*, vol. 235, no. 1-2, pp. 48–58, 2006.

[64] C. Saenger, R. I. Gabitov, J. Farmer, J. M. Watkins, and R. Stone, "Linear correlations in bamboo coral $\delta^{13}C$ and $\delta^{18}O$ sampled by SIMS and micromill: evaluating paleoceanographic potential and biomineralization mechanisms using δ^{11} B and Δ_{47} composition," *Chemical Geology*, vol. 454, pp. 1–14, 2017.

[65] K. M. Knesel, J. P. Davidson, and W. A. Duffield, "Evolution of silicic magma through assimilation and subsequent recharge: evidence from Sr isotopes in sanidine phenocrysts, Taylor Creek Rhyolite, NM," *Journal of Petrology*, vol. 40, no. 5, pp. 773–786, 1999.

[66] G. S. Wallace and G. W. Bergantz, "Reconciling heterogeneity in crystal zoning data: an application of shared characteristic diagrams at Chaos Crags, Lassen Volcanic Center, California," *Contributions to Mineralogy and Petrology*, vol. 149, no. 1, pp. 98–112, 2005.

[67] O. Bachmann and G. W. Bergantz, "Gas percolation in upper-crustal silicic crystal mushes as a mechanism for upward heat advection and rejuvenation of near-solidus magma bodies," *Journal of Volcanology and Geothermal Research*, vol. 149, no. 1-2, pp. 85–102, 2006.

[68] L. Font, J. P. Davidson, D. G. Pearson, G. M. Nowell, D. A. Jerram, and C. J. Ottley, "Sr and Pb isotope micro-analysis of plagioclase crystals from Skye lavas: an insight into open-system processes in a flood basalt province," *Journal of Petrology*, vol. 49, no. 8, pp. 1449–1471, 2008.

[69] V. M. Martin, J. Davidson, D. Morgan, and D. A. Jerram, "Using the Sr isotope compositions of feldspars and glass to distinguish magma system components and dynamics," *Geology*, vol. 38, no. 6, pp. 539–542, 2010.

[70] G. M. Di Paola, "Volcanology and petrology of Nisyros island (Dodecanese Greece)," *Bulletin Volcanologique*, vol. 38, no. 3, pp. 944–987, 1974.

[71] G. P. Wyers and M. Barton, "Polybaric evolution of calc-alkaline magmas from Nisyros, southeastern Hellenic Arc, Greece," *Journal of Petrology*, vol. 30, no. 1, pp. 1–37, 1989.

[72] K. S. Seymour and D. Vlassopoulos, "Magma mixing at Nisyros volcano, as inferred from incompatible trace-element systematics," *Journal of Volcanology and Geothermal Research*, vol. 50, no. 3, pp. 273–299, 1992.

[73] G. Vougioukalakis, "Volcanic stratigraphy and evolution of Nisyros island," *Bulletin of the Geological Society of Greece*, vol. 28, no. 2, pp. 239–258, 1993.

[74] L. Francalanci, J. C. Varekamp, E. G. Vougioukalakis, M. J. Defant, F. Innocenti, and P. Manetti, "Crystal retention, fractionation and crustal assimilation in a convecting magma chamber, Nisyros Voclano, Greece," *Bulletin of Volcanology*, vol. 56, no. 8, pp. 601–620, 1995.

[75] L. Francalanci, J. C. Varekamp, E. G. Vougioukalakis, F. Innocenti, and P. Manetti, "Is there a compositional gap at Nisyros volcano? A comment on: magma generation at the easternmost section of the Hellenic arc: Hf, Nd, Pb and Sr isotope geochemistry of Nisyros and Yali volcanoes (Greece)," *Lithos*, vol. 95, no. 3-4, pp. 458–461, 2007.

[76] C. Longchamp, A. Skopelitis, C. Bonadonna, and O. Bachmann, "Characterization of tephra deposits with limited exposure: the example of the two largest explosive eruptions at Nisyros volcano (Greece)," *Bulletin of Volcanology*, vol. 73, no. 9, pp. 1337–1352, 2011.

[77] E. M. Limburg and J. C. Varekamp, "Young pumice deposits on Nisyros, Greece," *Bulletin of Volcanology*, vol. 54, no. 1, pp. 68–77, 1991.

[78] E. Braschi, L. Francalanci, and G. E. Vougioukalakis, "Inverse differentiation pathway by multiple mafic magma refilling in the last magmatic activity of Nisyros Volcano, Greece," *Bulletin of Volcanology*, vol. 74, no. 5, pp. 1083–1100, 2012.

[79] M. Rautenschlein, G. A. Jenner, J. Hertogen et al., "Isotopic and trace element composition of volcanic glasses from the Akaki Canyon, Cyprus: implications for the origin of the Troodos ophiolite," *Earth and Planetary Science Letters*, vol. 75, no. 4, pp. 369–383, 1985.

[80] N. Blum and J. H. Crocket, "Repetitive cyclical volcanism in the Late Archean Larder Lake Group near Kirkland Lake, Ontario: implications of geochemistry on magma genesis," *Precambrian Research*, vol. 54, no. 2-4, pp. 173–194, 1992.

[81] M. F. Roden, T. Trull, S. R. Hart, and F. A. Frey, "New He, Nd, Pb, and Sr isotopic constraints on the constitution of the Hawaiian plume: results from Koolau Volcano, Oahu, Hawaii, USA," *Geochimica et Cosmochimica Acta*, vol. 58, no. 5, pp. 1431–1440, 1994.

[82] P. R. Castillo, E. Klein, J. Bender et al., "Petrology and Sr, Nd, and Pb isotope geochemistry of mid-ocean ridge basalt glasses from the 11 45′ N to 15 00′ N segment of the East Pacific Rise," *Geochemistry, Geophysics, Geosystems*, vol. 1, no. 11, 2000.

[83] L. Melluso, V. Morra, P. Brotzu et al., "Geochronology and petrogenesis of the Cretaceous Antampombato–Ambatovy complex and associated dyke swarm, Madagascar," *Journal of Petrology*, vol. 46, no. 10, pp. 1963–1996, 2005.

[84] G. Conde, P. D. Ihinger, and E. E. Frahm, "Water speciation in Anatolian Obsidian: quenched magmatic water vs low temperature hydration," *Geochimica et Cosmochimica Acta*, vol. 73, p. A239, 2009.

[85] P. Degryse, A. Boyce, N. E. Satullo et al., "Isotopic discriminants between late Bronze Age glasses from Egypt and the Near East," *Archaeometry*, vol. 52, no. 3, pp. 380–388, 2010.

[86] J. Henderson, J. Evans, and K. Nikita, "Isotopic evidence for the primary production, provenance and trade of Late Bronze Age glass in the Mediterranean," *Mediterranean Archaeology and Archaeometry*, vol. 10, no. 1, pp. 1–24, 2010.

[87] M. Ganio, K. Latruwe, D. Brems, P. Muchez, F. Vanhaecke, and P. Degryse, "The Sr–Nd isolation procedure for subsequent isotopic analysis using multi-collector ICP-mass spectrometry in the context of provenance studies on archaeological glass," *Journal of Analytical Atomic Spectrometry*, vol. 27, no. 8, pp. 1335–1341, 2012.

[88] E. Gliozzo, E. Braschi, F. Giannetti, A. Langone, and M. Turchiano, "New geochemical and isotopic insights into the Late Antique Apulian glass and the HIMT1 and HIMT2 glass productions—the glass vessels from San Giusto (Foggia, Italy) and the diagrams for provenance studies," *Archaeological and Anthropological Sciences*, pp. 1–30, 2017.

[89] F. Sigmundsson, S. Hreinsdóttir, A. Hooper et al., "Intrusion triggering of the 2010 Eyjafjallajokull explosive eruption," *Nature*, vol. 468, no. 7322, pp. 426–430, 2010.

[90] E. Kaminski, S. Tait, F. Ferrucci, M. Martet, B. Hirn, and P. Husson, "Estimation of ash injection in the atmosphere by basaltic volcanic plumes: the case of the Eyjafjallajökull 2010 eruption," *Journal of Geophysical Research: Solid Earth*, vol. 116, no. 9, 2011.

[91] M. T. Gudmundsson, T. Thordarson, A. Höskuldsson et al., "Ash generation and distribution from the April-May 2010 eruption of Eyjafjallajökull, Iceland," *Scientific Reports*, vol. 2, no. 1, p. 572, 2012.

[92] P. W. Webley, T. Steensen, M. Stuefer, G. Grell, S. Freita, and M. Pavolonis, "Analyzing the Eyjafjallajökull 2010 eruption using satellite remote sensing, lidar and WRF-Chem dispersion and tracking model," *Journal of Geophysical Research: Atmospheres*, vol. 117, no. 20, 2012.

[93] R. Cioni, M. Pistolesi, A. Bertagnini, C. Bonadonna, A. Hoskuldsson, and B. Scateni, "Insights into the dynamics and evolution of the 2010 Eyjafjallajökull summit eruption (Iceland) provided by volcanic ash textures," *Earth and Planetary Science Letters*, vol. 394, pp. 111–123, 2014.

[94] O. Sigmarsson, J. Maclennan, and M. Carpentier, "Geochemistry of igneous rocks in Iceland: a review," *Jökull*, vol. 58, pp. 139–160, 2008.

[95] T. D. Price, S. Nakamura, S. Suzuki, J. H. Burton, and V. Tiesler, "New isotope data on Maya mobility and enclaves at Classic Copan, Honduras," *Journal of Anthropological Archaeology*, vol. 36, pp. 32–47, 2014.

[96] P. A. Slater, K. M. Hedman, and T. E. Emerson, "Immigrants at the Mississippian polity of Cahokia: strontium isotope evidence for population movement," *Journal of Archaeological Science*, vol. 44, pp. 117–127, 2014.

[97] A. J. Waterman, D. W. Peate, A. M. Silva, and J. T. Thomas, "In search of homelands: using strontium isotopes to identify biological markers of mobility in late prehistoric Portugal," *Journal of Archaeological Science*, vol. 42, pp. 119–127, 2014.

[98] A. L. Rheingold, S. Hues, and M. N. Cohen, "Strontium and zinc content in bone as an indication of diet," *Journal of Chemical Education*, vol. 60, no. 3, pp. 233-234, 1983.

[99] C. Gilbert, J. Sealy, and A. Sillen, "An investigation of barium, calcium and strontium as palaeodietary indicators in the Southwestern Cape, South Africa," *Journal of Archaeological Science*, vol. 21, no. 2, pp. 173–184, 1994.

[100] T. D. Price, C. M. Johnson, J. A. Ezzo, J. Ericson, and J. H. Burton, "Residential mobility in the prehistoric southwest United States: a preliminary study using strontium isotope analysis," *Journal of Archaeological Science*, vol. 21, no. 3, pp. 315–330, 1994.

[101] T. D. Price, L. Manzanilla, and W. D. Middleton, "Immigration and the ancient city of Teotihuacan in Mexico: a study using strontium isotope ratios in human bone and teeth," *Journal of Archaeological Science*, vol. 27, no. 10, pp. 903–913, 2000.

[102] J. H. Burton, T. D. Price, L. Cahue, and L. E. Wright, "The use of barium and strontium abundances in human skeletal tissues to determine their geographic origin," *International Journal of Osteoarchaeology*, vol. 13, no. 1-2, pp. 88–95, 2003.

[103] D. Mueller and E. Heinzle, "Stable isotope-assisted metabolomics to detect metabolic flux changes in mammalian cell cultures," *Current Opinion in Biotechnology*, vol. 24, no. 1, pp. 54–59, 2013.

[104] T. Tütken and T. Vennemann, "Stable isotope ecology of Miocene large mammals from Sandelzhausen, southern Germany," *Paläontologische Zeitschrift*, vol. 83, no. 1, pp. 207–226, 2009.

[105] L. A. Gregoricka, "Residential mobility and social identity in the periphery: strontium isotope analysis of archaeological tooth enamel from southeastern Arabia," *Journal of Archaeological Science*, vol. 40, no. 1, pp. 452–464, 2013.

[106] E. McManus, J. Montgomery, J. Evans, A. Lamb, R. Brettell, and J. Jelsma, "To the land or to the sea: diet and mobility in Early Medieval Frisia," *Journal of Island and Coastal Archaeology*, vol. 8, no. 2, pp. 255–277, 2013.

[107] J. E. Ericson, "Strontium isotope characterization in the study of prehistoric human ecology," *Journal of Human Evolution*, vol. 14, no. 5, pp. 503–514, 1985.

[108] S. Hillson, *Dental Anthropology*, Cambridge University Press, Cambridge, UK, 1996.

[109] J. E. Ericson, "Some problems and potentials of strontium isotope analysis for human and animal ecology," in *Stable Isotopes in Ecological Research*, pp. 252–259, Springer, New York, NY, USA, 1989.

[110] J. C. Sealy, N. J. van der Merwe, A. Sillen, F. J. Kruger, and H. W. Krueger, "87Sr86Sr as a dietary indicator in modern and archaeological bone," *Journal of Archaeological Science*, vol. 18, no. 3, pp. 399–416, 1991.

[111] B. K. Nelson, M. J. Deniro, M. Schoeninger, D. J. De Paolo, and P. E. Hare, "Effects of diagenesis on strontium, carbon, nitrogen and oxygen concentration and isotopic composition of bone," *Geochimica et Cosmochimica Acta*, vol. 50, no. 9, pp. 1941–1949, 1986.

[112] P. Budda, B. L. J. Montgomery, P. Rainbird, R. G. Thomas, and S. M. Young, "Pb and Sr isotope composition of human dental enamel: an indicator of Pacific Islander population dynamics," in *Le Pacifique de 5000 à 2000 avant le présent: suppléments à l'histoire d'une colonisation = The Pacific from 5000 to 2000 BP: Colonisation and Transformations*, G. Jean-Christophe and I. Lilley, Eds., Institut de recherche pour le développement, Marseille, France, 1999.

[113] M. Sponheimer and J. A. Lee-Thorp, "Enamel diagenesis at South African Australopith sites: implications for paleoecological reconstruction with trace elements," *Geochimica et Cosmochimica Acta*, vol. 70, no. 7, pp. 1644–1654, 2006.

[114] C. Hänni, V. Laudet, D. Stehelin, and P. Taberlet, "Tracking the origins of the cave bear (*Ursus spelaeus*) by mitochondrial DNA sequencing," *Proceedings of the National Academy of Sciences*, vol. 91, no. 25, pp. 12336–12340, 1994.

[115] P. Argenti and P. P. Mazza, "Mortality analysis of the Late Pleistocene bears from Grotta Lattaia, central Italy," *Journal of Archaeological Science*, vol. 33, no. 11, pp. 1552–1558, 2006.

[116] I. Martini, M. Coltorti, P. P. Mazza, M. Rustioni, and F. Sandrelli, "The latest *Ursus spelaeus* in Italy, a new contribution to the extinction chronology of the cave bear," *Quaternary Research*, vol. 81, no. 1, pp. 117–124, 2014.

[117] H. Bocherens, M. Fizet, and A. Mariotti, "Diet, physiology and ecology of fossil mammals as inferred from stable carbon and nitrogen isotope biogeochemistry: implications for Pleistocene bears," *Palaeogeography, Palaeoclimatology, Palaeoecology*, vol. 107, no. 3-4, pp. 213–225, 1994.

[118] H. Bocherens, D. Billiou, M. Patou-Mathis, D. Bonjean, M. Otte, and A. Mariotti, "Paleobiological implications of the isotopic signatures (^{13}C, ^{15}N) of fossil mammal collagen in Scladina Cave (Sclayn, Belgium)," *Quaternary Research*, vol. 48, no. 3, pp. 370–380, 1997.

[119] H. Bocherens, M. Stiller, K. A. Hobson et al., "Niche partitioning between two sympatric genetically distinct cave bears (*Ursus spelaeus* and *Ursus ingressus*) and brown bear (*Ursus arctos*) from Austria: isotopic evidence from fossil bones," *Quaternary International*, vol. 245, no. 2, pp. 238–248, 2011.

[120] D. Fernández-Mosquera, M. Vila-Taboada, and A. Grandal-d'Anglade, "Stable isotopes data ($\delta^{13}C$, $\delta^{15}N$) from the cave bear (*Ursus spelaeus*): a new approach to its palaeoenvironment and dormancy," *Proceedings of the Royal Society of London B: Biological Sciences*, vol. 268, no. 1472, pp. 1159–1164, 2001.

[121] M. P. Richards, M. Pacher, M. Stiller et al., "Isotopic evidence for omnivory among European cave bears: late Pleistocene *Ursus spelaeus* from the Peştera cu Oase, Romania," *Proceedings of the National Academy of Sciences*, vol. 105, no. 2, pp. 600–604, 2008.

[122] Z. Nerudová, M. Nývltová Fišáková, and J. Míková, "Palaeoenvironmental analyses of animal remains from the Kůlna Cave (Moravian Karst, Czech Republic)," *Quartär*, vol. 61, 2014.

[123] O. Loreille, L. Orlando, M. Patou-Mathis, M. Philippe, P. Taberlet, and C. Hänni, "Ancient DNA analysis reveals divergence of the cave bear, *Ursus* spelaeus, and brown bear, Ursus arctos, lineages," *Current Biology*, vol. 11, no. 3, pp. 200–203, 2001.

[124] L. Orlando, D. Bonjean, H. Bocherens et al., "Ancient DNA and the population genetics of cave bears (*Ursus spelaeus*) through space and time," *Molecular Biology and Evolution*, vol. 19, no. 11, pp. 1920–1933, 2002.

[125] M. Pacher and A. J. Stuart, "Extinction chronology and palaeobiology of the cave bear (*Ursus spelaeus*)," *Boreas*, vol. 38, no. 2, pp. 189–206, 2009.

[126] A. Berton, M. Bonato, A. Borsato et al., "Nuove datazioni radiometriche con il metodo U/Th sulle formazioni stalagmitiche di Grotta all'Onda," *Rivista di Scienze Preistoriche*, vol. 53, pp. 241–256, 2003.

[127] G. Molara, "Resti faunistici provenienti dai livelli del Pleistocene superior di Grotta all'Onda (Camaiore, Lucca)," in *Atti del 6° Convegno Nazionale di Archeozoologia*, pp. 57–62, Centro visitatori del Parco dell'Orecchiella, Lucca, Italy, 2009.

[128] T. Adani, *Applicazioni delle sistematiche geochimiche ed isotopiche a reperti fossili Quaternari*, M.S. thesis, Earth Sciences Department, Università degli Studi di Firenze, 2013.

[129] G. Cortecci and L. Lupi, "Carbon, oxygen and strontium isotope geochemistry of carbonates rocks from the Tuscan Nappe, Italy," *Mineral Petrol Acta*, vol. 37, pp. 63–80, 1994.

Hindawi
Journal of Analytical Methods in Chemistry
Volume 2018, Article ID 8274131, 8 pages
https://doi.org/10.1155/2018/8274131

Research Article

Development and Validation of an LC-MS/MS Method and Comparison with a GC-MS Method to Measure Phenytoin in Human Brain Dialysate, Blood, and Saliva

Raphael Hösli,[1,2] **Stefan König**,[3] **and Stefan F. Mühlebach**[1]

[1]*Clinical Pharmacy and Epidemiology, Hospital Pharmacy, University of Basel, Spitalstrasse 26, CH-4031 Basel, Switzerland*
[2]*Spitalzentrum Biel, Apotheke, Vogelsang 84, CH-2501 Biel-Bienne, Switzerland*
[3]*Division of Forensic Medicine, University of Bern, Bühlstrasse 20, CH-3012 Bern, Switzerland*

Correspondence should be addressed to Stefan F. Mühlebach; stefan.muehlebach@unibas.ch

Received 12 December 2017; Revised 7 February 2018; Accepted 25 February 2018; Published 1 April 2018

Academic Editor: Federica Bianchi

Phenytoin (PHT) is one of the most often used critical dose drugs, where insufficient or excessive dosing can have severe consequences such as seizures or toxicity. Thus, the monitoring and precise measuring of PHT concentrations in patients is crucial. This study develops and validates an LC-MS/MS method for the measurement of phenytoin concentrations in different body compartments (i.e., human brain dialysate, blood, and saliva) and compares it with a formerly developed GC-MS method that measures PHT in the same biological matrices. The two methods are evaluated and compared based on their analytical performance, appropriateness to analyze human biological samples, including corresponding extraction and cleanup procedures, and their validation according to ISO 17025/FDA Guidance for Industry. The LC-MS/MS method showed a higher performance compared with the GC-MS method. The LC-MS/MS was more sensitive, needed a smaller sample volume (25 μL) and less chemicals, was less time consuming (cleaning up, sample preparation, and analysis), and resulted in a better LOD (<1 ng/mL)/LOQ (10 ng/mL). The calibration curve of the LC-MS/MS method (10–2000 ng/mL) showed linearity over a larger range with correlation coefficients $r^2 > 0.995$ for all tested matrices (blood, saliva, and dialysate). For larger sample numbers as in pharmacokinetic/pharmacodynamic studies and for bedside as well as routine analyses, the LC-MS/MS method offers significant advantages over the GC-MS method.

1. Introduction

Sensitive and specific quantification methods are of critical importance when monitoring individualized drug therapy in patients or investigating drug concentration in forensic toxicology [1]. Critical dose drugs but also newly developed and designed complex drugs require analytical methods to check for effective drug delivery to target tissues and to minimize toxicity in sensitive organs or cells. When such drugs have to be used in patients with varying pharmacokinetics (PK) (e.g., ICU patients), an appropriate therapeutic drug monitoring (TDM), which allows, for example, to correlate the drug concentration in easy accessible plasma samples with those in the tissue of action, becomes even more relevant for a safe and efficient drug treatment [2].

Phenytoin (PHT) belongs to the most widely prescribed drugs to prevent and control most types of seizure disorders and to treat epilepsy [3]. It is one of the most often used critical dose drugs where insufficient or excessive dosing can have severe consequences such as seizures or toxicity. Thus, the monitoring and precise measuring of PHT concentrations in patients is crucial [4, 5]. As an example, in forensic toxicology, epilepsy patients under PHT treatment who have been involved in an accident have to be analyzed in order to verify whether the PHT concentration was adequate or possibly the reason for the accident [6]. However, there are several characteristics of PHT including a relatively low therapeutic index, difficult pharmacokinetics (PK) and pharmacodynamics (PD), saturable oxidative biotransformation, and the nonlinear clearance, which complicate a therapeutic

drug monitoring (TDM) aimed at preventing intoxication of patients or treatment failures [7].

Thus, researchers and practitioners are interested in specific, sensitive, robust, and cost-effective methods to identify PHT concentrations in patients. Thereby, several compartments to measure the PHT concentration could be addressed such as blood, saliva, and CNS fluid (microdialysate). The correlation of PHT in different body compartments is not yet completely understood and has only recently been addressed by researchers who have compared the measurement of PHT in these different compartments with a GC-MS method [8]. While the GC-MS has long been the standard method in forensic testing, LC-MS/MS methods have become more common, as they generally offer some advantages over GC-MS [9]. Recently, researchers have developed an LC-MS/MS method to measure PHT in one specific body compartment (i.e., blood plasma or serum) [10]. Missing, however, is a thorough comparison of the performance of these two analytical methods in the detection and analysis of PHT in different body compartments (i.e., blood, saliva, and samples from brain tissue microdialysis).

The aim of the present study was to develop and validate an LC-MS/MS method for the measurement of PHT concentrations in different body compartments such as blood and saliva, as well as samples from brain tissue microdialysis often used in neurology and neurosurgery, where antiepileptic therapy is often mandatory [11, 12], and to compare its efficiency with a formerly developed GC-MS method [8]. The fact that this established GC-MS method measured PHT in the same biological matrices (i.e., blood, saliva, and human brain dialysate) enables a reliable comparison with regard to the performance of GC-MS versus LC-MS/MS in measuring PHT in different body compartments. The two methods are evaluated and compared based on their analytical performance, appropriateness to analyze human biological samples, including corresponding extraction and cleanup procedures, and their validation according to ISO 17025/FDA Guidance for Industry [13]. Finally, the suitability of the two analytical methods for PK/PD studies, bedside measurement, and forensic use is discussed. In addition, the LC-MS/MS method developed in the current study is compared with an established LC-MS/MS method which measured PHT in blood plasma samples [10].

2. Materials and Method

2.1. Chemicals and Samples Used for the Development of the LC-MS/MS Method and Its Validation. PHT reference substance was purchased from Desitin Pharma GmbH (Liestal, Switzerland) and from the European Pharmacopoeia (PHT Ph. Eur. Standard, EDQM, Strasbourg, France). The IS for LC-MS/MS was PHT-D_{10} (PHT D-10, $C_{15}H_2D_{10}N_2O_2$, MW = 262.33) in methanol (MeOH) (100 μg/mL) from Cerilliant (Round Rock, TX).

Calcium chloride, perchloric acid, citric acid monohydrate, potassium chloride, magnesium chloride hexahydrate, sodium chloride, sodium hydroxide, and the solvents (methanol, acetic acid 100%, and acetone) were of analytical grade and purchased from Merck (Darmstadt, Germany). Artificial cerebrospinal fluid (aCSF; dialysate solution) was prepared according to M Dialysis AB (Stockholm, Sweden) [14]. Blood CPDA-1 (anticoagulant citrate phosphate dextrose adenine solution; to simplify only named blood in the following) was obtained from the Blood Donor Center (Bern, Switzerland). Saliva was obtained from one of the investigators. 20–60 μL PHT-containing samples from patients collected from a 2 μL/min flow rate brain microdialysis and 2 mL of CPDA containing PHT patient blood samples were provided by the Department of Neurosurgery (Kantonsspital Aarau AG, Switzerland and Centre Hospitalier Universitaire Vaudois, Switzerland). All biological samples (blood and dialysates) were frozen and stored at −24°C. Before sample analysis, the samples were thawed at room temperature for 30 minutes and homogenized by shaking with a vortex for one minute.

2.2. Internal Standards, Calibrator Standard System Suitability Testing, and Sample Preparation. The internal standard (IS) stock solution was prepared by adding 100 μL of the PHT-D_{10} (100 μg/mL) to 9900 μL of MeOH. 5 mL of this solution was added to 95 mL of 1 M perchloric acid aqueous solution to get the final concentration of 50.0 ng/mL, which is used as IS working solution. The PHT reference stock solution (1.00 mg/mL) was used to obtain eight calibration (Cal) solutions with concentrations of 2000, 1000, 500, 250, 100, 50, 20, and 10 ng/mL PHT. 20 μL of these Cal solutions were added to 980 μL of the biomatrices to get the Cal working solutions. For quality control (QC), solutions with 1600, 400, 30, and 10 ng/mL PHT were prepared out of PHT reference stock solution (1.00 mg/mL).

The IS working solution of 75 μL was added either to an aliquot of 25 μL Cal working solution, QC solutions, or 25 μL sample from patients containing PHT. The sample preparation for the LC-MS/MS consisted of pipetting 75 μL of IS working solution to 25 μL sample into a deep well plate (0.6 mL, Chemie Brunschwig AG, Basel, Switzerland) covered by a sealing mat (Silicone, Chemie Brunschwig AG, Basel, Switzerland). The well plates were rigorously shaken for 5 minutes and then centrifuged (4.500 U/min; Mikro 22R, Hettich Instruments, Andreas Hettich AG, Bäch, Switzerland) for 30 minutes at about 8°C (Figure 1). The processed samples were ready for the LC-MS/MS analysis.

2.3. LC-MS/MS Settings. The prepared samples were placed into the autosampler (Dionex WPS-3000TSL Olten, Switzerland) which was set at 8°C. With a100 μL syringe from the autosampler, 10 μL of the prepared samples was injected into a 130 μL loop. The solvent rack (Dionex SRD-3600, Olten, Switzerland) carried the mobile phase A (H_2O + HCOOH (100 + 0.1, v + v)) and phase B (MeCN + HCOOH (100 + 0.1, v + v)). These mobile phases were delivered by three pumps (binary pump 1 (flow 0.350 mL/min) and isocratic pump 2 (flow 0.200 to 1.000 mL/min) (Dionex pump HPG-3200A, Olten, Switzerland), and binary pump 3 (Dionex pump ISO-3100A, Olten, Switzerland)) connected to a triple stage quadrupole mass spectrometer with linear ion-trap capability (3200 QTrap, Analyst Software Version 1.5.1, Applied

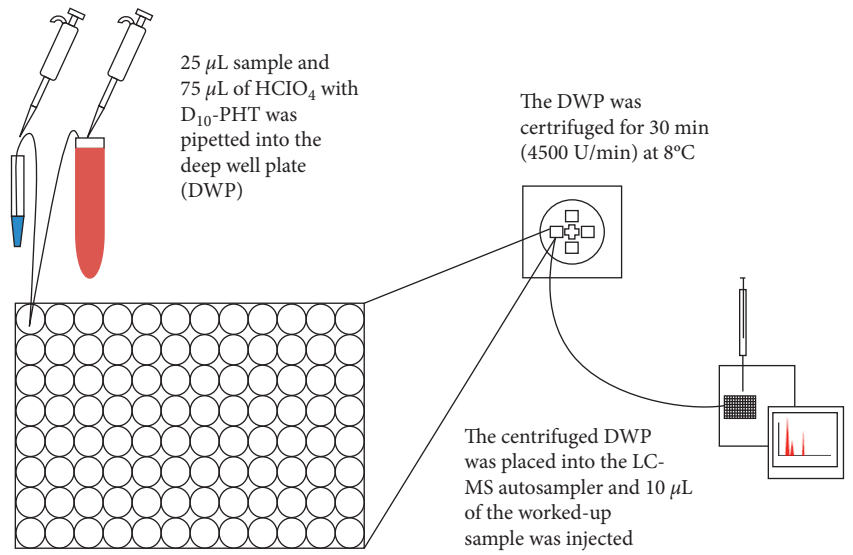

Figure 1: Sample preparation for the LC-MS/MS analyses for blood, saliva, and aCSF samples.

Table 1: Settings of the HPLC program.

Time (minutes)	Pump 1 (main column (MC))			Pumps 2 and 3 (trapping column (TC))			
	%*B*	Flow (μL/min)	Comments	%*B*	Flow (μL/min)	Flow pump 5 (H_2O + 0.1% HCOOH) (μL/min)	Switching valve
0	35	500	Start MS and pumps	50	300	800	TC → waste, MC → MS (loading)
0.5	35		Start gradient	50	300	800	TC → MC → MS (eluting)
0.6	↓						
1	97.5			50	20	20	
2	97.5						TC → waste, MC → MS
2.5	35			50	300	800	Reequilibration

Biosystems/MDS Sciex, Toronto, Canada) (Table 1). For the mass spectrometric detection, SRM scan mode (selective reaction monitoring) was used. SRM transitions and mass spectrometric conditions were as follows: transition: 253.1 → 182.2 (PHT) and 253.1 → 192.2 (PHT-D_{10}); orifice (V): 36; collision energy (eV): 41 (PHT) and 51 (PHT-D_{10}); and dwell time (msec): 100. Electrospray ionization was performed in positive ion mode for the analyte and the IS. The following instrument parameters for ionization were used: ion source voltage: 5000 volt, curtain gas: 25, gas 1: 40 and gas 2: 60; and the CAD gas was set to 5 (arbitrary units for the gas settings). As trapping column, a Phenomenex Gemini Polar column (2.0 × 10 mm, 5 μm; Brechbühler AG, Schlieren, Switzerland) temperated to room temperature was used. The main column Phenomenex Synergy Polar RP column (2.0 × 50 mm; Brechbühler AG, Schlieren, Switzerland) was placed into the column oven (Cluzeau Info Labo CrocoCil) set on 50°C with a column thermostat (Dionex TCC-3100, Olten, Switzerland) including switching valve (Figure 2). This system was operated by Analyst Software (Version 1.5.1, AB Sciex, Toronto, Canada).

2.4. Validation of the LC-MS/MS Method according to ISO 17025/FDA Guidance for Industry. The validation was carried out according to ISO 17025/FDA Guidance for Industry including selectivity, sensitivity, accuracy, recovery of PHT, reproducibility and suitability of the calibration curves, stability of PHT, and matrix effects. The selectivity and sensitivity (absence of PHT) were verified by analyzing blank samples without PHT (extraction and matrix effects). For the accuracy, QCs and Cal samples were analyzed. The recovery of PHT was analyzed by measuring QCs at different levels. The reproducibility and suitability of the calibration curves was measured by a complete series of Cal 1 to Cal 8 (LC-MS/MS) analyses. The limit of detection (LOD) and the limit of quantification (LOQ) were analyzed using Cal 1 (LC-MS/MS 10 ng/mL PHT). The LOD was checked as a signal-to-noise (*S*/*N*) ratio of more than 4 : 1. The LOQ was considered as 5 times the response to a blank sample. The stability tests consisted of the freeze-thaw stability of PHT, which was determined after 3 freeze-thaw cycles. The short-term stability was analyzed by keeping the samples thawed at ambient temperature for at least 6 hours, frozen for at least 12 hours at −25°C ± 5°C, and again thawed, worked-up, and analyzed. Postpreparative stability was evaluated to determine whether an analytical run can be reinjected in the case of instrument failure and, furthermore, whether the preparation of a large number of samples could be done at once. Therefore, one of the validation runs was analyzed a second time after 7 days. The described criteria for Cal curves, QC, accuracy, and precision had to be met.

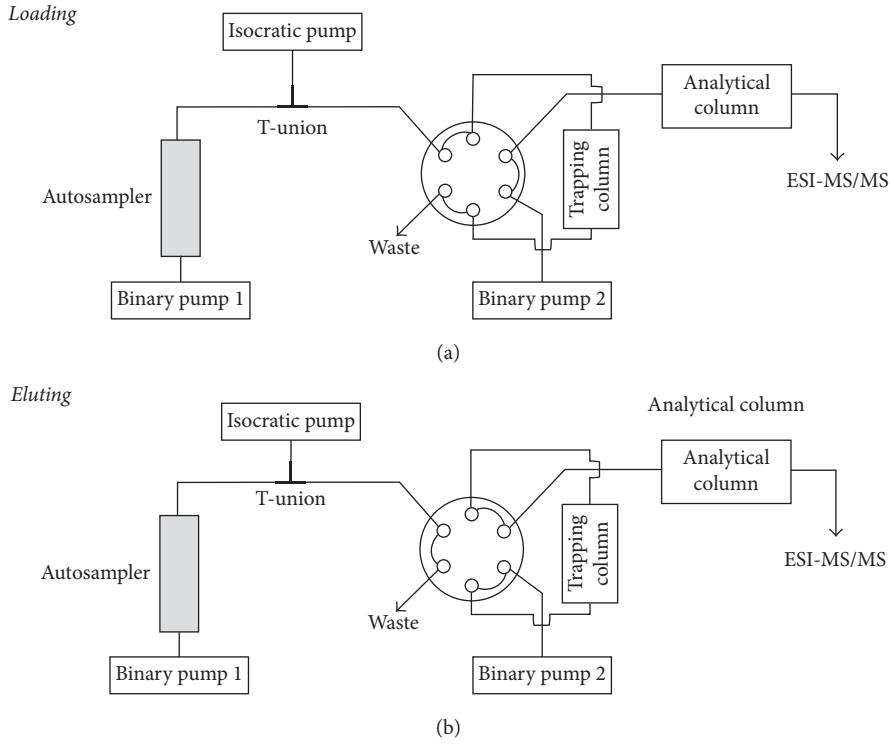

Figure 2: LC-MS/MS settings.

Matrix effects were analyzed by comparing the calibration curves generated with the three matrices aCSF, blood, and saliva. PHT microdialysis and blood samples from patients were analyzed to demonstrate the suitability of the method for biological samples from patients.

2.5. Comparison of the LC-MS/MS and the GC-MS Method. The LC-MS/MS method was evaluated and compared with the GC-MS method published by Hösli et al. [8] with regard to its analytical performance, appropriateness to analyze human biological samples, including corresponding extraction and cleanup procedures, and its validation according to ISO 17025/FDA Guidance for Industry.

The statistical data were calculated with Microsoft Excel and IBM SPSS Statistics 22. To compare the different matrices, a one-way ANOVA was calculated. The corresponding values were checked for significance by *t*-tests.

3. Results

3.1. Validation of the LC-MS/MS Method. The retention time (RT) for PHT and for PHT-D_{10} (IS) was about 2.8 min (Figure 3). The selectivity and sensitivity were checked; all blank samples were negative. The recovery of PHT after precipitation with $HClO_4$ was 89.5% for QC1 (10 ng/mL) and 97.1% for QC3 (1600 ng/mL) compared to the amount found in unprepared samples (=100%). The LOD calculated as *S*/*N* ratio of 4 : 1 for this method in aCSF, saliva, and blood was set at <1 ng/mL. The LOQ calculated as 5 times the response/blank was 10 ng/mL PHT. For the accuracy, the Cal 1 to Cal 8 were assessed. The calibrator values showed min–max deviations of 1–8% for Cal 2 (20 ng/mL) to Cal 8 (2000 ng/mL) with 3% for Cal 1 (10 ng/mL). The calibration curves for all three matrices were linear. The regression coefficients (r^2) of the three different matrices were $r^2_{\text{blood}} = 0.996$ ($n = 3$), $r^2_{\text{dialysate}} = 0.997$ ($n = 6$), and $r^2_{\text{saliva}} = 0.995$ ($n = 3$). Reinjection after 7 days showed no difference in accuracy. The sample volume needed was 25 μL. The sample preparation time was about 2 min per sample (6 hours for 182 samples). The run time for one LC-MS/MS analyses was 7 min.

3.2. Comparison of the LC-MS/MS with the GC-MS Method. After validation of the LC-MS/MS method, it was compared with the referred GC-MS method [8]. Table 2 shows the comparative results of the two methods for their analytical performance, appropriateness to analyze human biological samples, including corresponding extraction and cleanup procedures, and its validation according to ISO 17025/FDA Guidance for Industry (Table 2).

The selectivity and the sensitivity were met by both methods, and the recovery showed no differences (Table 2). But the accuracy differed between the two methods. The GC-MS method showed a higher variation at Cal 1 (20%) than the LC-MS/MS method (Cal 1 = 3%). As expected, the biggest difference in terms of analytical performance between the two methods was observed by the LOQ (GC-MS = 50 ng/mL; LC-MS/MS = 10 ng/mL) and LOD (GC-MS = 15 ng/mL; LC-MS/MS = <1 ng/mL) (Table 2).

Both methods showed linear regression coefficients (r^2) higher than 0.995 in all three different matrices for the PHT calibration curve. The calibration range of the LC-MS/MS

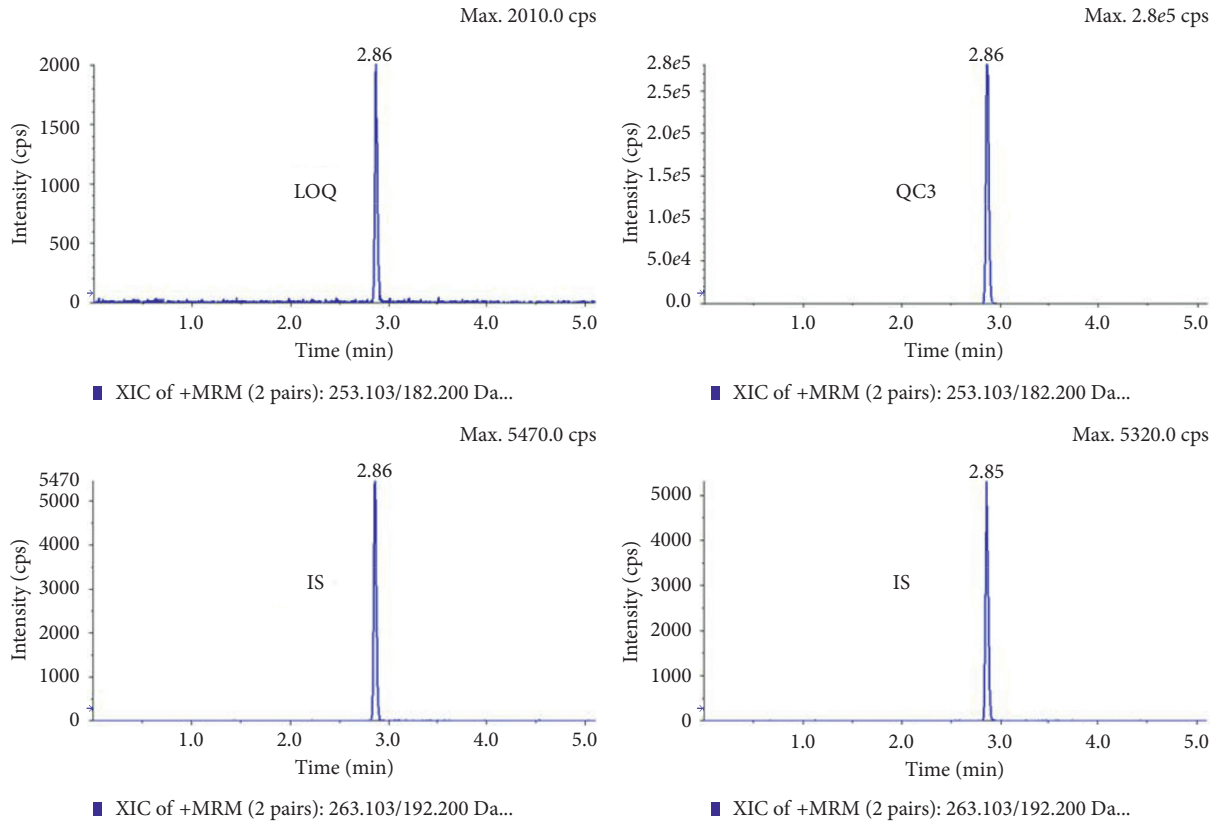

Figure 3: Chromatogram of phenytoin (illustrated for LOQ (10 ng/mL) and QC3 (400 ng/mL)) with PHT-D_{10} as IS (50 ng/mL).

Table 2: Comparison of the GC-MS [8] versus LC-MS/MS method.

Criterion	GC-MS	LC-MS/MS
Retention time	PHT 15.12 min, IS MPPH 16.15 min	PHT and PHT-D_{10} 2.8 min
Selectivity/sensitivity (absence of PHT)	Good peak differentiation and quantification of PHT. All blank samples were negative (no presence of PHT)	All blank samples were negative (no presence of PHT)
Recovery	94.1% for QC2 (100 ng/mL) 94.3% for QC5 (1000 ng/mL)	89.5% for QC1 (10 ng/mL) 97.1% for QC3 (1600 ng/mL)
LOD (calculated as S/N ratio of 4 : 1)	15 ng/mL	<1 ng/mL
LOQ (calculated as 5 times the response/blank)	50 ng/mL	10 ng/mL
Accuracy	The calibrator values showed min–max percent deviations of 1–20% for Cal 1 (50 ng/mL) to Cal 6 (1200 ng/mL)	The calibrator values showed min–max percent deviations of 1–8% for Cal 1 (10 ng/mL) to Cal 8 (2000 ng/mL)
Regression coefficient, r^2	$r^2_{blood} = 0.998$ $(n = 2)$ $r^2_{dialysate} = 0.999$ $(n = 8)$ $r^2_{saliva} = 0.999$ $(n = 2)$	$r^2_{blood} = 0.996$ $(n = 3)$ $r^2_{dialysate} = 0.997$ $(n = 6)$ $r^2_{saliva} = 0.995$ $(n = 3)$
Calibration range	50–1200 ng/mL	10–2000 ng/mL
Run time per analysis	30 min	7 min
Injection volume of the sample	2.0 μL	10 μL
Sample preparation time	5 h for 25 samples	6 h for 182 samples
Stability of the processed samples	Dried extracts were stable for ≥4 weeks (min/max deviation 4%). No effect by reinjection and storage (33 h) on the autosampler	Reinjection after 7 days showed no difference in accuracy
Sample volume needed	50 μL	25 μL

(from 10 ng/mL to 2000 ng/mL) is twice as large as of the GC-MS (50 ng/mL to 1200 ng/mL). The stability of the samples after extraction and cleaning up was demonstrated for both methods. The sample preparation procedure is demonstrated in Figure 1 for LC-MS/MS and Figure 4 for GC-MS.

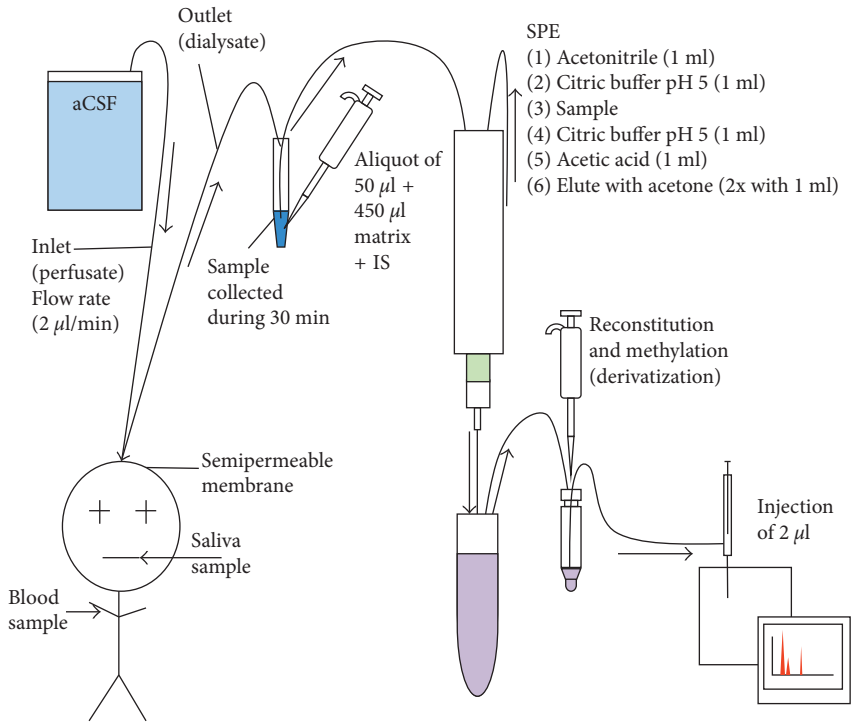

Figure 4: Sample preparation for the GC-MS analyses [8].

3.3. Comparison of the LC-MS/MS Method with a Formerly Established LC-MS/MS Method. Recently, a LC-MS/MS method has been developed which measures PHT in blood plasma or serum [10]. For the measurement of PHT in blood, the newly validated LC-MS/MS method can hence also be compared with this recently published study. The two methods show some similarities such as an identical IS (100 μg/mL PHT-d10), similar sample volumes needed (25 μL versus 20 μL [10]), and a comparable retention time (2.8 min versus approximately 2.1 min [10]). Both methods showed linear regression coefficients (r^2) higher than 0.99 in the blood matrix. The accuracy was similar as both studies showed deviations of <10%. With regard to the calibration range and the calibration solution, the two LC-MS/MS methods differ. While the LC-MS/MS method developed in this study showed a calibration range from 10 ng/mL to 2000 ng/mL, the calibration curve of the published LC-MS/MS method [10] ranged from 100 ng/mL to 4000 ng/mL. The calibration solution in the current study was the respective biological matrix (e.g., blood). In the published study [10], phosphate-buffered saline was used as the calibration solution.

4. Discussion

In this study, a LC-MS/MS method to measure PHT in different biological samples was successfully validated and compared with a similarly validated GC-MS method [8]. Overall, the LC-MS/MS method showed to be a more specific analytical method with a higher general performance (Table 2). The LC-MS/MS method needed less sample volume, less chemicals, and less analytical time and therefore resulted in less costs for the sample preparation.

Concerning the LOD, there was a huge difference between the two methods. The LOD of the LC-MS/MS method was 15 times better than the one of the GC-MS methods: the LOD of the LC-MS/MS method was <1 ng/mL compared to 15 ng/mL for the GC-MS method (increments by a factor of ten). Similarly, the difference in LOQ was 5 times lower in LC-MS/MS (10 ng/ml) compared to GC-MS (50 ng/mL). The LOQ for the LC-MS/MS could be set even lower than 10 ng/ml PHT (Cal 1). The FDA guidelines which claim a minimal reproducibility at the LOQ level of 20% were well below (deviation to target PHT amount: <8% in aCSF ($n = 6$), <4% in blood ($n = 3$), <9% in saliva ($n = 3$); accuracy: aCSF 103%, blood 101%, and saliva 106%). The LOQ of the GC-MS method and hence the lowest concentration level (Cal 1 at 50 ng/ml) of the calibration curve showed a deviation value of 19%. The LC-MS/MS method, in contrast, showed a value of only 3% deviation at the lowest Cal (10 ng/mL). This difference is of high importance, as samples with even lower concentrations could be reliably analyzed.

The calibration range (from 10 ng/mL to 2000 ng/mL) of the LC-MS/MS method was twice as large as of the GC-MS method (50 ng/mL to 1200 ng/mL). This indicates that the LC-MS/MS method is more powerful and effective over a larger range of concentration, since the linearity is given over a larger area (10 ng/mL–2000 ng/mL) compared to the GC-MS method (50 ng/mL–1200 ng/mL).

As IS, two different substances were used. MPPH as a structurally related compound was used for the GC-MS method. As IS for LC-MS/MS, deuterated PHT (PHT-D_{10}) was used, which is the same molecule as PHT and differs only by the molecular mass (+1). All the physicochemical processes upon cleanup and analysis are identical or highly

similar for PHT and PHT-D_{10}. MMPH, however, could be chemically affected in a different way than PHT, which could lead to a systematic bias in a given situation [15].

Regarding the sample preparation procedure, the LC-MS/MS (Figure 1) showed an important advantage compared to the GC-MS method as it only needs 3 steps of sample preparation compared to 11 steps necessary for the GC-MS method including a solid-phase extraction (SPE) and derivatization with a more critical chemical trimethylsulfonium (TMSH) (Figure 4). This resulted in significant shortening of the overall analysis: Preparation of the samples before injection for GC-MS is about ten times more time consuming than for the LC-MS/MS. For the GC-MS method, researchers needed 5 hours to prepare 25 samples (5 samples/h), whereas for the LC-MS/MS method 182 samples were prepared in 6 hours (30.3 samples/h), which corresponds to 6 times the amount of prepared samples per hour compared to the GC-MS method.

From the exposure side, the volumes are much larger and the exposure to the chemicals are more prolonged with the GC-MS method compared to the sample cleanup for the LC-MS/MS method. Especially, the derivatization agent TMSH is critical to handle because of toxicity. The risk of serious and even irreversible effects through inhalation, skin contact, or eye exposure is well known. TMSH is also considered to be teratogenic. Therefore, the potential health risk for the laboratory staff handling the samples can be reduced by the LC-MS/MS method and the elimination of a safety critical agent.

The amount of biological samples needed for the GC-MS method (50 μL) was twice as much as for the LC-MS/MS (25 μL). The sample volume is a critical point for PK/PD studies, where, for example, by continuing dialysis from brain in neurosurgical patients only small volumes of samples per time point/period are available. For 50 μL dialysate about 25 minutes collecting time is necessary at the usual flow rate of ~2 μL per minute [12, 16]. Therefore, not a requested specific time point, but a rather large time segment is represented which can influence the requested results. The reduced sample volume needed (25 μL) for the LC-MS/MS analyses reduces the dialyses time needed per sample to about 15 minutes. The smaller the dialysis time, the more precise correlations of the respective tissue concentration with plasma/blood samples can be made.

Furthermore, LC-MS/MS also has the shorter run time. The time needed for 100 GC-MS analyses would be approximately 50 hours. The LC-MS/MS method, in contrast, needs only 11 hours and 40 minutes for 100 analyses. This is a time saving of more than 38 hours. While this may not be highly relevant for forensic purposes, for bedside and routine analyses (real-time) and PK/PD studies with larger numbers of samples, this factor is relevant. Also, when the time between taking a sample and the result needed is short, as it is in TDM to adjust subsequent dosing for PHT treatment, this time saving is crucial.

The costs for one way materials per sample was about 50% lower for the LC-MS/MS compared to the GC-MS method. Especially because no SPE device was needed. Also, the reduced work load for the laboratory technician must be considered as an imported cost factor.

Finally, the appropriateness of the method also depends on the biological matrix. Both methods can generally be used to measure PHT in blood and saliva, as the sample volume is less limiting. As mentioned before, however, for dialysates, the most difficult aspect is to get enough sample volume. Therefore, the LC-MS/MS method needing only half of the sample volume compared to the GC-MS method is more suited for microdialysate measurements. With respect to the LOD/LOQ, the LC-MS/MS method is also better suited for PK/PD studies, as it allows to include patients with low PHT dosages.

In addition, the newly established LC-MS/MS method was compared with a recently published LC-MS/MS method [10]. While this study measured PHT only in one body compartment (i.e., blood plasma or serum), the current LC-MS/MS method was developed and validated for the measurement of PHT in different body compartments (i.e., blood, saliva, and samples from brain tissue microdialysis often used in neurology and neurosurgery). The calibration range of the published LC-MS/MS method [10] (from 100 ng/mL to 4000 ng/mL) is appropriate for the measurement of PHT in blood plasma. As the PHT concentrations in brain tissue dialysates are much smaller than in blood plasma, the LC-MS/MS method of the current study was more appropriate for such samples, showing a lower calibration range from 10 ng/mL to 2000 ng/mL. Finally, as the aim of this study was to measure PHT in different biological matrices, a general substitute solution for blood plasma such as phosphate-buffered saline [10] could not be used. Instead, the fluid of the respective body compartment was used as calibration solution (e.g., artificial cerebrospinal fluid (aCSF) for the measurement of PHT in the brain tissue dialysates). This also eliminates a potential analytical bias due to matrix effects.

5. Conclusion

In this study, a LC-MS/MS method to measure PHT in different biological samples (i.e., human brain dialysate, blood, and saliva) was developed and validated under circumstances that ensured a high comparability with an established GC-MS method [8]. Overall, the study concludes that LC-MS/MS is not only better performing in human PHT concentration measuring or comparable drug PK/PD studies but is the only one to be used for bedside analysis. The time-consuming sample preparation and the long run time of the GC-MS method delay the result, which is critical in TDM. The higher sensitivity, the smaller needed sample volume, the better LOD/LOQ, the less time-consuming cleaningup and sample preparation procedure, and the shorter run time make the LC-MS/MS method the preferred analytical procedure.

Conflicts of Interest

The authors declare that they have no conflicts of interest.

References

[1] S. Deeb, D. A. McKeown, H. J. Torrance, F. M. Wylie, B. K. Logan, and K. S. Scott, "Simultaneous analysis of 22 antiepileptic drugs in postmortem blood, serum and plasma

using LC–MS-MS with a focus on their role in forensic cases," *Journal of Analytical Toxicology*, vol. 38, no. 8, pp. 485–494, 2014.

[2] S. L. von Winckelmann, I. Spriet, and L. Willems, "Therapeutic drug monitoring of phenytoin in critically ill patients," *Pharmacotherapy*, vol. 28, no. 11, pp. 1391–1400, 2008.

[3] E. H. Grover, Y. Nazzal, and L. J. Hirsch, "Treatment of convulsive status epilepticus," *Current Treatment Options in Neurology*, vol. 18, no. 3, 2016.

[4] M. F. Wu and W. H. Lim, "Phenytoin: a guide to therapeutic drug monitoring," *Proceedings of Singapore Healthcare*, vol. 22, no. 3, pp. 198–202, 2013.

[5] A. Tobler, R. Hösli, S. Mühlebach, and A. Huber, "Free phenytoin assessment in patients: measured versus calculated blood serum levels," *International Journal of Clinical Pharmacy*, vol. 38, no. 2, pp. 303–309, 2016.

[6] L. Nilsson, B. Y. Farahmand, P. G. Persson, I. Thiblin, and T. Tomson, "Risk factors for sudden unexpected death in epilepsy: a case-control study," *The Lancet*, vol. 353, no. 9156, pp. 888–893, 1999.

[7] E. Martin, T. N. Tozer, L. B. Sheiner, and S. Riegelman, "The clinical pharmacokinetics of phenytoin," *Journal of Pharmacokinetics and Biopharmaceutics*, vol. 5, no. 6, pp. 579–596, 1977.

[8] R. Hösli, A. Tobler, S. König, and S. Mühlebach, "A quantitative phenytoin GC-MS method and its validation for samples from human ex situ brain microdialysis, blood and saliva using solid-phase extraction," *Journal of Analytical Toxicology*, vol. 37, no. 2, pp. 102–109, 2013.

[9] E. R. Perez, J. A. Knapp, C. K. Horn, S. L. Stillman, J. E. Evans, and D. P. Arfsten, "Comparison of LC–MS-MS and GC–MS analysis of benzodiazepine compounds included in the drug demand reduction urinalysis program," *Journal of Analytical Toxicology*, vol. 40, no. 3, pp. 201–207, 2016.

[10] J. Peat, C. Frazee, and U. Garg, "Quantification of free phenytoin by liquid chromatography tandem mass spectrometry (LC/MS/MS)," *Methods in Molecular Biology*, vol. 1383, pp. 241–246, 2016.

[11] E. P. Thelin, L. H. Keri, P. J. Carpenter, and A. H. Hutchinson, "Microdialysis monitoring in clinical traumatic brain injury and its role in neuroprotective drug development," *AAPS Journal*, vol. 19, no. 2, 2017.

[12] Y. Yamamoto, M. Danhof, and C. M. Elizabeth de Lange, "Microdialysis: the key to physiologically based model prediction of human CNS target site concentrations," *AAPS Journal*, vol. 19, no. 4, 2017.

[13] FDA, *Guidance for Industry, Bioanalytical Method Validation*, U.S Department of Health and Human Services, Food and Drug Administration, Center for Drug Evaluation and Research (CDER), Center for Veterinary Medicine (CVM), Rockville, MD, 2001.

[14] Perfusion Fluid, 2017, http://www.mdialysis.com/iscus/iscus-international/products/catheter-accessories/perfusion-fluid.

[15] J. Wieling, "LC-MS-MS experiences with internal standards," *Chromatographia Supplement*, vol. 55, pp. 107–113, 2002.

[16] H. K. Kimelberg, "Water homeostasis in the brain: basic concepts," *Neuroscience*, vol. 129, no. 4, pp. 851–860, 2004.

Hindawi
Journal of Analytical Methods in Chemistry
Volume 2018, Article ID 8341630, 9 pages
https://doi.org/10.1155/2018/8341630

Research Article

Analysis of Polycyclic Aromatic Hydrocarbons in Ambient Aerosols by Using One-Dimensional and Comprehensive Two-Dimensional Gas Chromatography Combined with Mass Spectrometric Method: A Comparative Study

Yun Gyong Ahn,[1] **So Hyeon Jeon**,[1] **Hyung Bae Lim**,[2] **Na Rae Choi**,[3] **Geum-Sook Hwang**,[1] **Yong Pyo Kim**,[4] **and Ji Yi Lee**[3]

[1]*Western Seoul Center, Korea Basic Science Institute, Seoul 03759, Republic of Korea*
[2]*Air Quality Research Division, National Institute of Environmental Research, Incheon 22689, Republic of Korea*
[3]*Department of Environmental Science and Engineering, Ewha Womans University, Seoul 03759, Republic of Korea*
[4]*Department of Chemical Engineering and Material Science, Ewha Womans University, Seoul 03760, Republic of Korea*

Correspondence should be addressed to Ji Yi Lee; yijiyi@ewha.ac.kr

Received 14 December 2017; Revised 6 February 2018; Accepted 19 February 2018; Published 1 April 2018

Academic Editor: Federica Bianchi

Advanced separation technology paired with mass spectrometry is an ideal method for the analysis of atmospheric samples having complex chemical compositions. Due to the huge variety of both natural and anthropogenic sources of organic compounds, simultaneous quantification and identification of organic compounds in aerosol samples represents a demanding analytical challenge. In this regard, comprehensive two-dimensional gas chromatography with time-of-flight mass spectrometry (GC×GC-TOFMS) has become an effective analytical method. However, verification and validation approaches to quantify these analytes have not been critically evaluated. We compared the performance of gas chromatography with quadrupole mass spectrometry (GC-qMS) and GC×GC-TOFMS for quantitative analysis of eighteen target polycyclic aromatic hydrocarbons (PAHs). The quantitative obtained results such as limits of detection (LODs), limits of quantification (LOQs), and recoveries of target PAHs were approximately equivalent based on both analytical methods. Furthermore, a larger number of analytes were consistently identified from the aerosol samples by GC×GC-TOFMS compared to GC-qMS. Our findings suggest that GC×GC-TOFMS would be widely applicable to the atmospheric and related sciences with simultaneous target and nontarget analysis in a single run.

1. Introduction

Human health research associated with polycyclic aromatic hydrocarbons (PAHs) has raised concerns because certain PAHs are classified as probable human carcinogens [1–4] and have shown tumorigenic activity and endocrine disrupting activity in mammals [5]. The US EPA has included 16 of them in the list of priority pollutants and has established a maximum contaminant level of 0.2 μg/L for benzo[a]pyrene in drinking water [6]. In the European Union (EU), eight PAHs have been identified as priority hazardous substances in the field of water policy [7]. The EPA priority 16 PAHs and two additional PAHs are now being monitored by European agencies, and they have sought to quantify the individual concentrations of benzo[e] pyrene and perylene in environmental samples [6]. PAHs are found in ambient air in the gas phase and as sorbents to aerosols [8]. Thus, air monitoring of PAHs to quantify inhalation exposure and to identify other organic compounds is important for insight into photochemical reactions. The quantification and identification of organic compounds in air samples is an important feature of atmospheric chemistry and represents some demanding analytical challenges [9].

For these reasons, a key issue in current analytical methods is the ability to measure a large number of compounds with quantitative analysis for target analytes. Comprehensive two-dimensional gas chromatography (GC×GC) coupled with mass spectrometry (MS) can screen for nontarget compounds with fast identification of the compounds in an entire sample [10]. Therefore, previous studies applied GC×GC-MS for the identification of numerous compounds present in air samples [11–13]. However, there are limitations on the validation of simultaneous quantification and identification of analytes in air samples. Correspondingly, a validation of simultaneous identification and quantification of PAHs and other compounds in air samples by GC×GC–MS is required. A TOF mass spectrometer was used to acquire sufficient data from a comprehensive two-dimensional chromatographic technique that generated multiple narrow peaks from the short secondary column [14, 15]. Generally, GC coupled with quadrupole MS (GC-qMS) in the selected ion monitoring (SIM) mode has been used for quantitative analysis of PAHs in air samples because of its selective detection for specific target compounds [16, 17]. However, a GC×GC-TOFMS validated method suitable for the quantification of target PAHs in an aerosol sample compared with GC-qMS in the SIM mode has not yet been reported. The aim of this study was to evaluate the effectiveness of GC×GC-TOFMS in the quantitative analysis of target PAHs as well as the fast identification of multiple compounds for aerosol samples. The validity of the quantitative results obtained by both GC×GC-TOFMS and GC-qMS in the SIM mode was demonstrated by several method performance parameters such as linearity, accuracy, and repeatability.

2. Experimental

2.1. Air Sampling. The total suspended particle (TSP) samples were collected at Asan Engineering Building, Ewha Womans University, Seoul, South Korea (37.56°N, 126.94°E, 20 m above ground level), with a PUF sampler (Tisch, TE-1000) on a quartz fiber filter (Quartz fiber filter, QFF, Ø10.16 cm, Whatman, UK). The sampling site is located in the mixed resident area, commercial area, forest area, and nearby roadside. A total of 67 filter samples were obtained during summer (August 12–30, 2013) and winter (January 27–February 16, 2014) and day (9 a.m.~6 p.m.) and night (8 p.m.~6 a.m.). Prior to sampling, the quartz fiber filters were baked for 8 h in an electric oven at 550°C to remove possible organic contaminants. The sampled filters were wrapped in aluminum foils and stored in a freezer at −20°C until analysis.

2.2. Chemicals. All organic solvents were of GC grade and purchased from Burdick and Jackson (Phillipsburg, NJ, USA). Standard solutions of target PAHs (Table 1 for their full chemical names and information) except Per and BeP for quantitative analysis were purchased as a mixture at a concentration of 2000 μg/mL in dichloromethane from Supelco (Bellefonte, PA, USA). Per and BeP standards (>99%) were purchased from Aldrich (St. Louis, MI, USA), and a standard mixture of eighteen PAHs was prepared at a concentration of 1000 μg/mL. Deuterium-labeled internal standards of seven PAHs were purchased from Aldrich (St. Louis, MI, USA) and Chiron (Trondheim, Norway) and used for the spiking test as listed in Table 1. Working standard solutions (0.01~10 μg/mL) were prepared and then stored at −20°C prior to use.

2.3. Preparation of Samples. Air sampling filters were extracted with a mixture of dichloromethane and methanol (3 : 1, v/v) two times using an accelerated solvent extractor (ASE) (Dionex ASE-200) at 40°C and 1700 psi for 5 min. Prior to the extraction, seven deuterated internal standards (Nap-d8, Ace-d10, Phen-d10, Fla-d10, Chr-d12, Per-d12, and BghiPer-d12) were spiked in the filters to compensate for matrix effects during the extraction procedure. Extracts were blown down to 1 mL using a nitrogen evaporator (TurboVap II, Caliper Life Sciences). GC×GC-TOFMS analysis was carried out using an Agilent GC (Wilmington, Delaware, USA)-Quad-jet thermal modulation Pegasus 4D TOFMS (LECO, St. Joseph, MI, USA). The sample was injected in the splitless mode at 300°C. The GC×GC columns were as follows: DB-5MS (30 m × 0.25 mm ID, film thickness of 0.25 μm) and 1.17 m DB-17MS (0.18 mm OD, 0.18 μm film). The operating conditions of GC-MS and GC×GC-TOFMS are summarized in Table 2.

3. Results and Discussion

3.1. GC-qMS and GC×GC-TOFMS for Characterization of Aerosol Samples. In most studies, separation and quantification of PAHs in aerosol samples have been analyzed using a conventional GC-qMS [18]. Flame ionization detection (FID) has also been widely used for quantification as it features a higher response to PAHs which contain only carbon and hydrogen, while oxygenates and other species that contain heteroatoms tend to have a lower response factor [19]. However, this nonspecific detector may not distinguish inferences, which include a large fraction of aliphatic and aromatic compounds in aerosol samples from alkylated PAH homologues. The coupling of GC with MS is increasingly becoming the analytical tool of choice in this regard because of its superior selectivity and sensitivity. Among the most common analyzers including TOF [20], ion trap, and qMS [21, 22], qMS is the most widely adopted technique for routine analysis of PAHs [23]. GC-qMS data acquisition takes advantages of both a full mass scan range (scan mode) and specific ion masses for target analytes (SIM mode). The sensitivity in the SIM mode is higher than that in the scan mode of GC-qMS due to the increased dwell time on each monitored ion for trace analysis in some matrices such as in atmospheric aerosols [24, 25]. GC-TOFMS has a much faster spectral acquisition rate than GC-qMS does, which is up to 500 full mass scans per second [26]. Consequently, this system is able to widen the application of GC×GC techniques providing very narrow chromatographic peaks, typically 50~600 ms at the baseline with

Table 1: Information of target PAHs in the study.

Compound	Abbreviation	CAS number	Molecular formula	MW	Quantitative ion	Qualifier ion	Retention time		
							GC-qMS (min)	GC×GC-TOFMS	
								t_{r1} (min)	t_{r2} (s)
Naphthalene-d_8[a]	Nap-d_8	1146-65-2	$C_{10}D_8$	136.2	136	137	12.25	13.40	1.34
Naphthalene	Nap	91-20-3	$C_{10}H_8$	128.2	128	129	12.34	13.47	1.35
Acenaphthylene	Acy	208-96-8	$C_{12}H_8$	152.2	152	153	19.08	19.56	1.55
Acenaphthene-d_{10}[a]	Ace-d_{10}	15067-26-2	$C_{12}D_{10}$	164.2	162	164	19.47	20.12	1.52
Acenaphthene	Ace	83-32-9	$C_{12}H_{10}$	154.2	153	154	19.61	20.28	1.52
Fluorene	F	86-73-7	$C_{13}H_{10}$	166.2	166	165	21.61	22.28	1.53
Phenanthrene-d_{10}[a]	Phen-d_{10}	1518-22-2	$C_{14}D_{10}$	188.2	188	189	25.91	25.96	1.68
Phenanthrene	Phen	85-01-8	$C_{14}H_{10}$	178.2	178	179	26.01	26.04	1.71
Anthracene	Ant	120-12-7	$C_{14}H_{10}$	178.2	178	179	26.14	26.20	1.68
Fluoranthene-d_{10}[a]	Fla-d_{10}	93951-69-0	$C_{16}D_{10}$	212.2	212	213	30.99	30.68	1.84
Fluoranthene	Fla	206-44-0	$C_{16}H_{10}$	202.2	202	203	31.08	30.68	1.87
Pyrene	Pyr	129-00-0	$C_{16}H_{10}$	202.2	202	203	32.25	31.56	1.98
Benz[a]anthracene	BaA	56-55-3	$C_{18}H_{12}$	228.2	228	226	37.20	36.28	2.21
Chrysene-d_{12}[a]	Chr-d_{12}	1719-03-5	$C_{18}D_{12}$	240.3	240	236	37.42	36.28	2.27
Chrysene	Chr	218-01-9	$C_{18}H_{12}$	228.3	228	226	37.54	36.44	2.26
Benzo[b]fluoranthene	BbF	205-99-2	$C_{20}H_{12}$	252.3	252	253	41.55	40.12	2.76
Benzo[k]fluoranthene	BkF	207-08-9	$C_{20}H_{12}$	252.3	252	253	41.65	40.28	2.74
Benzo[e]pyrene	BeP	192-97-2	$C_{20}H_{12}$	252.3	252	253	42.90	41.08	3.16
Benzo[a]pyrene	BaP	50-32-8	$C_{20}H_{12}$	252.3	252	253	43.09	41.24	3.23
Perylene-d_{12}[a]	Per-d_{12}	1520-96-3	$C_{20}D_{12}$	264.3	264	260	43.46	41.40	3.36
Perylene	Per	198-55-0	$C_{20}H_{12}$	252.3	252	253	43.57	41.48	3.47
Indeno[1,2,3-cd] pyrene	IP	193-39-5	$C_{22}H_{12}$	276.3	276	277	48.09	45.48	0.71
Dibenz[a,h]anthracene	DBahAnt	53-70-3	$C_{22}H_{14}$	278.3	278	279	48.12	45.64	0.82
Benzo[ghi] perylene-d_{12}[a]	BghiPer-d_{12}	93951-66-7	$C_{22}D_{12}$	288.3	288	284	49.92	46.52	1.54
Benzo[ghi]perylene	BghiPer	191-24-2	$C_{22}H_{12}$	276.3	276	277	50.13	46.68	1.78

[a]Internal standard.

Table 2: GC-qMS and GC×GC-TOFMS operating conditions.

Parameters	GC-qMS	GC×GC-TOFMS
Injector settings		
Injection volume	1 μL	1 μL
Inlet mode	Splitless	Splitless
Carrier gas	He (99.999%)	He (99.999%)
Carrier gas flow	1.0 mL·min^{-1}	1.3 mL·min^{-1}
Inlet temperature	280°C	300°C
GC oven temperature		
Initial temperature	1 min at 60°C	1 min at 60°C
First rate	6°C/min to 310°C	6°C/min to 300°C
Isothermal pause	15 min at 310°C	15 min at 300°C
2nd oven temperature offset	—	5°C, relative to the 2nd oven temperature
Modulator		
Modulator temperature offset	—	15°C, relative to the 2nd oven temperature
Modulator period	—	4.00 s
Hot pulse time	—	1.00 s
Cool time between stages	—	1.40 s
MS		
Mass range	40~550	40~550
Electron energy	70 eV	70 eV
Ion source temperature	230°C	230°C

sufficient density of data points per chromatographic peak [27]. Environmental samples are generally complex, often with more than hundreds of compounds containing structural isomers and homologues spread over a wide range of concentration and volatility. Accordingly, multidimensional separation is an advanced technique offering the possibility of greatly enhanced selectivity using different separation mechanisms for the analysis of complex environmental samples [28–30]. In this study, a set of columns DB-5×DB-17 ms was applied to increase the resolution and peak capacity. The fast scanning Pegasus 4D TOFMS system was combined to allow efficient processing of data acquisition, handling, peak detection, and deconvolution. In the one-dimensional column, a 30 m-long DB-5 ms (5% diphenyl/95% dimethyl polysiloxane) stationary phase was used to separate analytes based on volatility and combined with a 1.17 m-long DB-17 ms column (50% diphenyl/50% dimethyl polysiloxane) allowing relative polarity-based separation. Figure 1 shows GC×GC-TOFMS chromatograms of aerosol samples collected at day and night during winter in Seoul, South Korea. To compare the identification ability of GC×GC-TOFMS with GC-qMS, analysis with GC-qMS in the scan mode was performed. A comparison of the one-dimensional chromatograms of the same samples obtained by GC-qMS is shown in Figure 2. 2D chromatograms enable the visual classification of chemically related compounds into groups. It was rare to see that the early-eluting

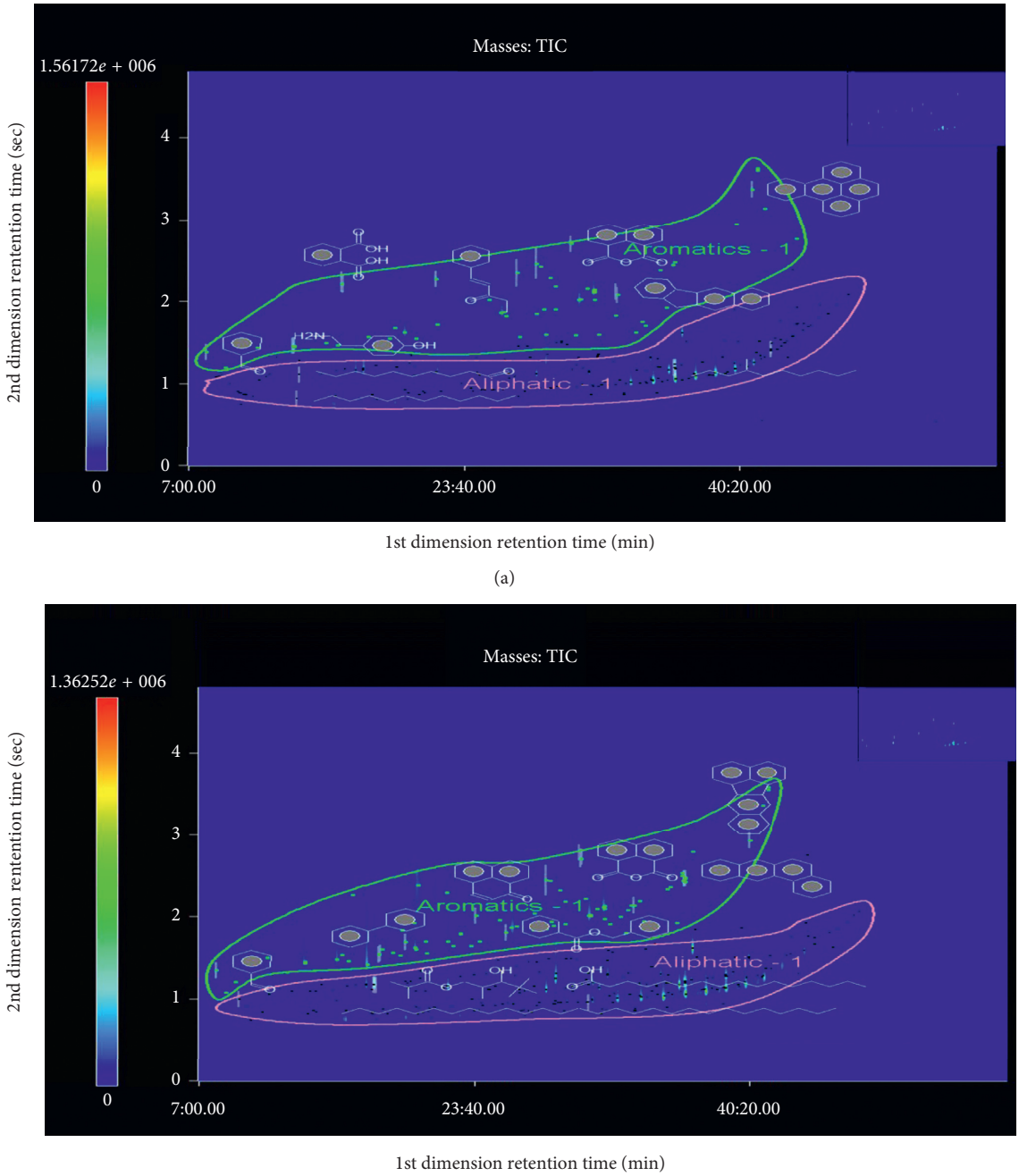

Figure 1: GC×GC-TOFMS plots of aerosol samples collected during day (a) and night (b) of winter in Seoul, Korea. A total of 251 and 297 peaks were identified in aerosol samples collected during day (a) and night (b), respectively. Aromatic and aliphatic classes were drawn to divide two regions for ease of viewing.

analytes have an extreme volatility in the chromatogram, as shown in Figure 2. Because of the large losses of these analytes during sample extraction and concentration, particle-associated semivolatile analytes were mainly detected and classified according to their aromatic and aliphatic hydrocarbon groups.

Meanwhile, analytes from the GC-qMS chromatogram were separated based on their vapor pressures or boiling points. The GC×GC technique is rather well suited for group separations, and classifying compounds into chemical-related groups could be useful for source identification of atmospheric aerosols by means of the large amount of chemical data handling. The combined use with TOFMS provides rapid and reliable identification of analytes using their deconvoluted pure mass spectra. The major limitation of qMS is its limited scan rate; therefore, quantification and identification is seriously compromised because of the mass spectral skew due to the variations in ion abundances at different regions of a chromatographic peak [31, 32]. The numbers of identified chromatographic peaks analyzed by

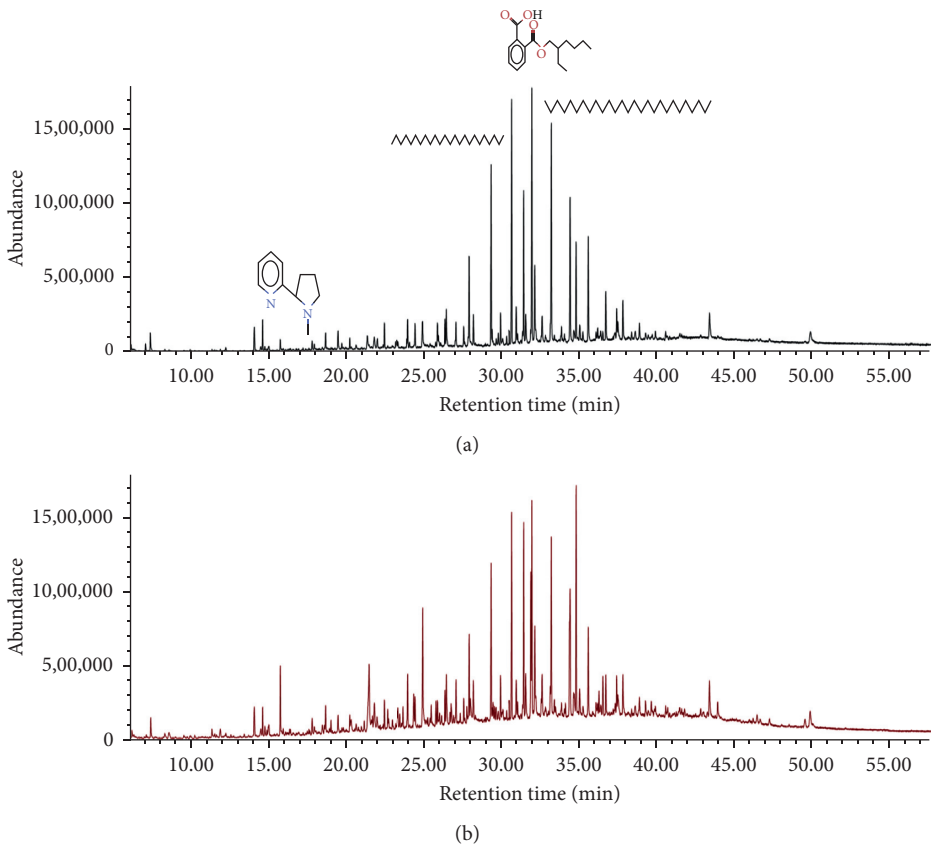

Figure 2: Total ion chromatograms of aerosol samples collected in day (a) and night (b) of winter in Seoul, Korea, obtained by GC-qMS. A total of 35 and 64 peaks were identified in aerosol samples collected during day (a) and night (b), respectively. The analytes were separated based on their boiling points.

GC-qMS using the same signal threshold setting from the aerosol samples collected at day and night were 35 and 64, respectively. In the case of results obtained by GC×GC-TOFMS, 251 and 297 peaks from the day- and night-time aerosol samples were, respectively, assigned by individual spectral deconvolution. As a result, phthalic anhydride and 1,2-naphthalic anhydride as the markers of secondary formation for gas-phase PAH reactions were identified in the aerosol sample, as shown in Figure 3. Since the products formed through photochemical reactions are often more toxic than their parent PAHs in atmosphere [17], significant efforts have been expended to identify the photochemical products with PAHs in the fields of atmospheric or environmental sciences. In the case of results obtained using GC-qMS, phthalic anhydride and 1,2-naphthalic anhydride were not detected in the same sample. Limitations of one-dimensional separation have been reported for these photochemical products and complex mixtures of the aerosol sample because of their diverse polarities in a single run [33, 34]. Contrastively, two anhydrides associated with secondary organic aerosol formation were clearly separated and detected by GC×GC-TOFMS. Therefore, it showed advantages for nontarget screening to identify molecular markers or chemical patterns more representative of the aerosol state observed in ambient air.

3.2. Validation of GC-qMS and GC×GC-TOFMS for Quantification of PAHs. GC-qMS and GC×GC-TOFMS were tested individually in order to evaluate their analytical performances. The calibration linearity (regression coefficient, R^2) and relative response factor (RRF) are presented in Table 3. The RRF is the ratio between a signal produced by an individual native analyte and the corresponding isotopically labeled analogue of the analyte (as an internal standard). For calculating RRF, 2 ng of each target PAH and each corresponding deuterated internal standard was spiked, and the relative sensitivity in both the methods was compared. Despite the high-speed scanning performance of GC×GC-TOFMS, the RRFs obtained by this method were approximately equivalent to those obtained by GC-qMS. RRF expresses the sensitivity of a detector for a given substance relative to a standard substance [35, 36]. Thus, it indicated that the sensitivity of GC×GC-TOFMS relative to target PAHs is comparable in quantitative analysis. Calibration curves were generated using the peak area for the 18 PAHs at seven concentrations ranging from 0.01 to 10 μg/mL. The linearity was assessed by calculating the regression equation and the correlation coefficient by the least squares method, as shown in Table 3. The R^2 values were greater than 0.999 for GC-qMS and 0.99 for GC×GC-TOFMS. Although data processing for quantification by GC×GC-TOFMS was derived from the combined peak areas

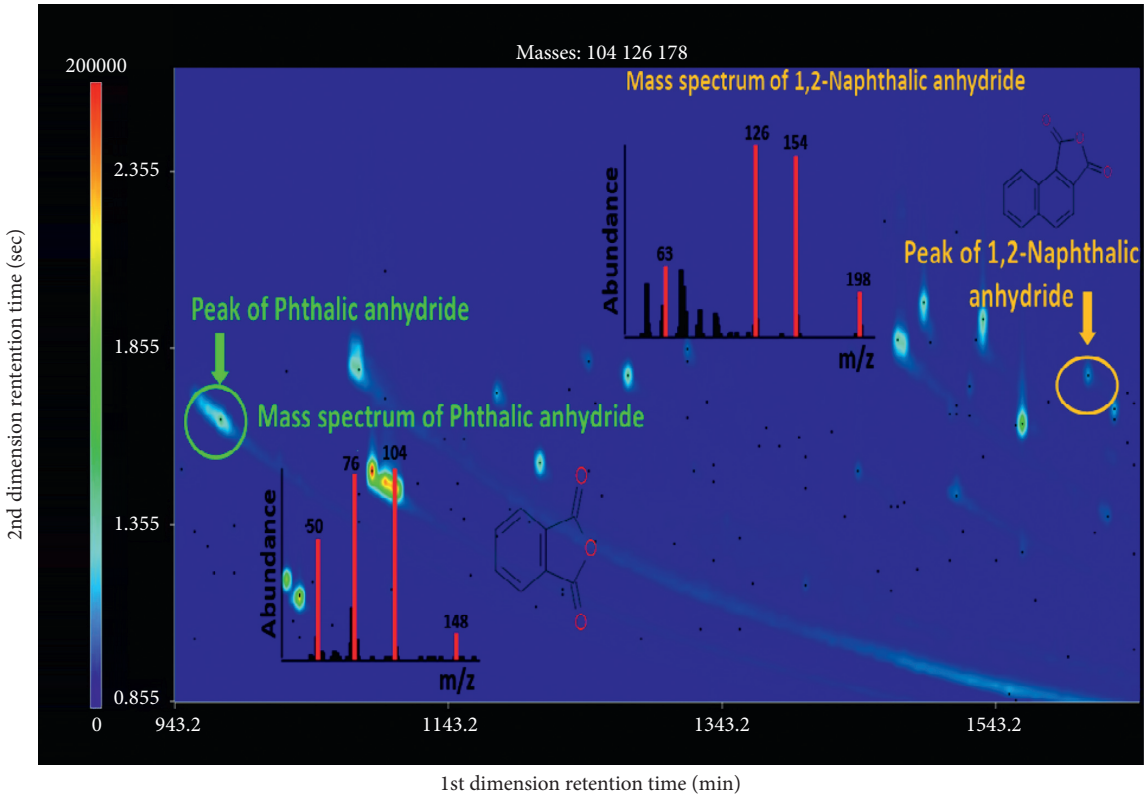

Figure 3: GC×GC chromatograms and mass spectrums of phthalic anhydride (marked as green) and 1,2-naphthalic anhydride (marked as yellow) in the aerosol sample. GC×GC chromatograms of phthalic anhydride and 1,2-naphthalic anhydride were certified by molecular ions of m/z 148 and 198, respectively.

Table 3: Relative response factors (RRFs) and calibrations of 18 PAHs obtained by the compared methods.

Compound	GC-qMS				GC×GC-TOFMS			
	RRF[a]	Slope	Intercept	R^2	RRF	Slope	Intercept	R^2
Nap	1.04	0.515	−0.003	0.9999	1.69	0.560	0.049	0.9971
Acy	1.57	0.808	−0.004	1.0000	1.95	1.026	−0.012	0.9999
Ace	1.03	0.439	0.009	0.9999	1.16	0.553	−0.006	0.9994
F	1.29	0.667	−0.006	1.0000	1.11	0.609	−0.021	0.9997
Phe	1.17	0.572	−0.004	0.9998	1.47	0.763	−0.039	0.9979
Ant	0.98	0.547	−0.017	0.9992	0.93	0.431	−0.010	0.9982
Fla	1.30	0.678	−0.001	1.0000	1.43	0.802	−0.021	0.9995
Pyr	1.31	0.686	−0.004	0.9999	1.62	0.910	−0.055	0.9972
BaA	0.98	0.575	−0.019	0.9997	1.42	0.574	−0.004	0.9998
Chr	1.06	0.563	−0.003	1.0000	1.26	0.651	−0.005	0.9998
BbF	0.99	0.535	−0.008	0.9999	1.69	0.848	−0.028	0.9993
BkF	1.11	0.576	−0.011	0.9998	0.88	0.327	−0.012	0.9977
BeP	0.91	0.455	−0.007	0.9996	0.90	0.530	−0.014	0.9997
BaP	0.88	0.505	−0.014	0.9997	0.83	0.477	−0.030	0.9985
Per	0.89	0.475	−0.008	0.9998	1.11	0.521	-0.023	0.9979
IP	1.37	0.717	−0.023	0.9995	1.25	0.660	-0.062	0.9922
DBahAnt	1.24	0.629	−0.019	0.9996	1.16	0.490	-0.074	0.9898
BghiPer	1.24	0.594	−0.010	1.000	1.53	0.710	-0.036	0.9991

[a]RRF expresses the sensitivity of a detector for a given analyte relative to its corresponding deuterated internal standards; RRF = $(A_x C_{is})/(A_{is} C_x)$, where A_x is the peak area of a quantifying ion for a given analyte being measured; A_{is} is the peak area of a quantifying ion for its corresponding internal standard; C_x is the concentration of a given analyte; and C_{is} is the concentration of its corresponding internal standard.

for the slices of modulated peaks in contrast to production of the single measured peak by GC-qMS, the results meet the criteria for acceptable linearity within this calibration range.

Naturally, the development of quantitative GC×GC studies based on the quantitative results associated with sophisticated implementation for modulated peaks has been delayed

Table 4: Limits of detection and quantification and recoveries of 18 PAHs obtained by the compared methods.

Compound	LOD[a] (ng)		LOQ[b] (ng)		Recovery ± RSD (%)	
	GC-qMS	GC×GC-TOFMS	GC-qMS	GC×GC-TOFMS	GC-qMS	GC×GC-TOFMS
Nap	0.07	0.40	0.21	1.19	94.4 ± 4.2	135 ± 45
Acy	0.17	0.07	0.51	0.22	119 ± 12	116 ± 15
Ace	0.05	0.17	0.16	0.52	105 ± 5.3	105 ± 7.8
F	0.04	0.15	0.13	0.44	158 ± 28	130 ± 29
Phe	0.10	0.34	0.31	1.03	94.5 ± 5.3	86.3 ± 16
Ant	0.19	0.31	0.58	0.92	90.4 ± 4.6	95.1 ± 20
Fla	0.05	0.14	0.16	0.41	90.3 ± 3.9	105 ± 13
Pyr	0.08	0.36	0.25	1.09	97.4 ± 5.3	97.2 ± 13
BaA	0.12	0.09	0.37	0.27	93.4 ± 4.9	86.9 ± 8.2
Chr	0.04	0.08	0.13	0.24	95.8 ± 5.8	101 ± 16
BbF	0.05	0.18	0.15	0.53	96.1 ± 5.7	92.3 ± 10
BkF	0.09	0.35	0.28	1.05	94.2 ± 6.5	105 ± 12
BeP	0.13	0.13	0.40	0.38	92.6 ± 5.8	92.7 ± 5.7
BaP	0.12	0.24	0.37	0.72	93.6 ± 5.3	104 ± 9.0
Per	0.11	0.34	0.32	1.02	93.0 ± 5.5	92.5 ± 8.6
IP	0.15	0.65	0.16	1.94	95.0 ± 5.4	93.9 ± 8.5
DBahAnt	0.13	1.05	0.40	3.14	94.9 ± 5.5	95.8 ± 5.7
BghiPer	0.09	0.22	0.27	0.66	94.6 ± 6.0	87.0 ± 8.5

[a]LOD, smallest amount of analyte that is statistically different from the blank; [b]LOQ, smallest amount of analyte that can be measured with reasonable accuracy.

compared with qualitative reports. Recently, the approach to quantifying multiple analytes at once with comprehensive two-dimensional GC has been extensively studied in accordance with the improvement of data processing for the integration of modulated peaks [37, 38]. In this study, the modulated peaks of each PAH was automatically combined and integrated by the ChromaTOF software based on a similarity of spectra within an allowable time difference between the second dimension peaks in the neighboring slices of the chromatogram. Recovery test was performed by spiking known amounts of the 18 PAH compounds in a prebaked clean filter at a final concentration of 2 μg/mL and analyses of each through all the experiment procedures were compared using the two different methods. Six duplicate tests were performed, and the results of the recovery are shown in Table 4. The average recoveries were in the range of 90.3 to 158% with relative standard deviations (RSDs) ranging from 3.9 to 28% for GC-qMS, while the recoveries were from 86.3 to 135% for GC×GC-TOFMS, with RSDs ranging from 5.7 to 45%. Most of the targeted PAH compounds were afforded acceptable recoveries, excluding F and Nap by using the two analytical methods due to the high volatility of these compounds. Compared with the reproducibility as expressed in %RSDs, the values obtained by GC-qMS were slightly lower than those obtained by GC×GC-TOFMS; however, the %RSD values of the targeted PAHs excluding F and Nap were acceptable (<20% RSD). These observations may vary for the versatile GC×GC technique, since the reproducibility of the modulation phase is dependent on the type of modulator, the stability of the stationary phases, and the chemistry of the analyte, regarding interaction with the stationary phase as presented in several prior studies [39, 40]. The LOD and LOQ were determined based on the standard deviation (SD) of the intersection of the analytical curve (s) and the slope of the curve (S) as $\mathrm{LOD} = 3.3 \times (s/S)$ and $\mathrm{LOQ} = 10 \times (s/S)$. The LOD and LOQ for each PAH compound obtained from both the methods are shown in Table 4. The LOD and LOQ values of the 18 PAH compounds obtained by GC-qMS were similar to the results of previous studies [10, 41, 42]. Thus, the suitability of GC×GC-TOFMS for quantification of PAHs was proven by comparing the results with those obtained using GC-qMS.

4. Conclusion

A fast scanning GC×GC-TOFMS was compared to a GC-qMS for the determination of PAHs in aerosol samples. For separation, identification, and characterization, GC×GC-TOFMS was advantageous over GC-qMS owing to the increased peak capacity, and its results showed enhanced detectability and structured chromatograms for nontarget analysis. The qualitative mass separation by TOFMS combined with an automated peak-finding capability provided the resolution of complex mixed mass spectra, resulting from overlapping chromatographic peaks and spectral deconvolution of individual mass spectra for unknown analytes. Furthermore, the obtained quantitative results such as LODs, LOQs, and recoveries of the 18 target PAHs were approximately equivalent for both the analytical methods. Thus, GC×GC-TOFMS had advantages for the simultaneous quantification and qualification of PAHs and other organic compounds in a single run. Because of its high degree of separation and capability of spectral deconvolution of overlapping peaks in highly complex samples, comprehensive GC×GC-TOFMS may become a useful platform in many other fields of research.

Conflicts of Interest

The authors declare that they have no conflicts of interest.

Acknowledgments

This research was supported by the Bio-Synergy Research Project (no. NRF-2017M3A9C4065961) of the Ministry of Science, ICT, and Future Planning through the National Research Foundation and the Korea Basic Science Institute Grant (no. C37705). This research was also supported by the Basic Science Research Program through the National Research Foundation of Korea (NRF) funded by the Ministry of Education (no. NRF-2016R1A2B4015143)

References

[1] IARC, "Polynuclear aromatic compounds, Part 1. Chemical, environmental and experimental data," *IARC Monographs on the Evaluation of the Carcinogenic Risk of Chemicals to Humans*, vol. 32, pp. 1–453, 1983.

[2] World Health Organization, "Environmental health criteria," in *International Programme on Chemical Safety (IPCS)*, vol. 171, WHO, Geneva, Switzerland, 1998.

[3] V. Vestreng, "Emission data reported to UNECE/EMEP: quality assurance and trend analysis and presentation of WebDab: MSC-W status report 2002," Research report, University of Oslo, Oslo, Norway, 2002.

[4] L.-B. Liu, L. Yan, J.-M. Lin, T. Ning, K. Hayakawa, and T. Maeda, "Development of analytical methods for polycyclic aromatic hydrocarbons (PAHs) in airborne particulates: a review," *Journal of Environmental Sciences*, vol. 19, no. 1, pp. 1–11, 2007.

[5] E. Cavalieri, R. Roth, E. Rogan, C. Grandjean, and J. Althoff, "Mechanisms of tumor initiation by polycyclic aromatic hydrocarbons," *Carcinogenesis*, vol. 3, pp. 273–287, 1978.

[6] Z. Zelinkova and T. Wenzl, "The occurrence of 16 EPA PAHs in food—a review," *Polycyclic Aromatic Compounds*, vol. 35, no. 2–4, pp. 248–284, 2015.

[7] T. Wenzl, R. Simon, E. Anklam, and J. Kleiner, "Analytical methods for polycyclic aromatic hydrocarbons (PAHs) in food and the environment needed for new food legislation in the European Union," *Trends in Analytical Chemistry*, vol. 25, pp. 716–725, 2006.

[8] H. I. Abdel-Shafy and M. S. Mansour, "A review on polycyclic aromatic hydrocarbons: source, environmental impact, effect on human health and remediation," *Egyptian Journal of Petroleum*, vol. 25, no. 1, pp. 107–123, 2016.

[9] U. Pöschl, "Atmospheric aerosols: composition, transformation, climate and health effects," *Angewandte Chemie International Edition*, vol. 44, no. 46, pp. 7520–7540, 2005.

[10] M. A. Bari, G. Baumbach, B. Kuch, and G. Scheffknecht, "Particle-phase concentrations of polycyclic aromatic hydrocarbons in ambient air of rural residential areas in southern Germany," *Air Quality, Atmospheric Health*, vol. 3, no. 2, pp. 103–116, 2010.

[11] D. A. Lane, A. Leithead, M. Baroi, J. Y. Lee, and L. A. Graham, "The detection of polycyclic aromatic compounds in air samples by GC×GC-TOFMS," *Polycyclic Aromatic Compounds*, vol. 28, no. 4-5, pp. 545–561, 2008.

[12] D. A. Lane and J. Y. Lee, "Detection of known photochemical decomposition products of PAH in particulate matter from pollution episodes in Seoul, Korea," *Polycyclic Aromatic Compounds*, vol. 30, no. 5, pp. 309–320, 2010.

[13] J. Y. Lee, D. A. Lane, J. B. Heo, S.-M. Yi, and Y. P. Kim, "Quantification and seasonal pattern of atmospheric reaction products of gas phase PAHs in PM2.5," *Atmospheric Environment*, vol. 55, pp. 17–25, 2012.

[14] R. J. Vreuls, J. Dallüge, and U. A. T. Brinkman, "Gas chromatography–time-of-flight mass spectrometry for sensitive determination of organic microcontaminants," *Journal of Microcolumn Separations*, vol. 11, no. 9, pp. 663–675, 1999.

[15] C. Weickhardt, F. Moritz, and J. Grotemeyer, "Time-of-flight mass spectrometry: state-of the-art in chemical analysis and molecular science," *Mass Spectrometry Reviews*, vol. 15, no. 3, pp. 139–162, 1996.

[16] M. X. Xie, F. Xie, Z. W. Deng, and G. S. Zhuang, "Determination of polynuclear aromatic hydrocarbons in aerosol by solid-phase extraction and gas chromatography–mass spectrum," *Talanta*, vol. 60, no. 6, pp. 1245–1257, 2003.

[17] R. Atkinson and J. Arey, "Atmospheric chemistry of gas-phase polycyclic aromatic hydrocarbons: formation of atmospheric mutagens," *Environmental Health Perspectives*, vol. 102, no. 4, pp. 117–126, 1994.

[18] J. D. Pleil, T. L. Vossler, W. A. McClenny, and K. D. Oliver, "Optimizing sensitivity of SIM mode of GC/MS analysis for EPA's TO-14 air toxics method," *Journal of the Air & Waste Management Association*, vol. 41, no. 3, pp. 287–293, 1991.

[19] D. L. Poster, M. M. Schantz, L. C. Sander, and S. A. Wise, "Analysis of polycyclic aromatic hydrocarbons (PAHs) in environmental samples: a critical review of gas chromatographic (GC) methods," *Analytical and Bioanalytical Chemistry*, vol. 386, no. 4, pp. 859–881, 2006.

[20] W. Welthagen, J. Schnelle-Kreis, and R. Zimmermann, "Search criteria and rules for comprehensive two-dimensional gas chromatography–time-of-flight mass spectrometry analysis of airborne particulate matter," *Journal of Chromatography A*, vol. 1019, no. 1-2, pp. 33–249, 2003.

[21] A. Filipkowska, L. Lubecki, and G. Kowalewska, "Polycyclic aromatic hydrocarbon analysis in different matrices of the marine environment," *Analytica Chimica Acta*, vol. 547, no. 2, pp. 243–254, 2005.

[22] K. Ravindra, A. F. L. Godoi, L. Bencs, and R. Van Grieken, "Low-pressure gas chromatography–ion trap mass spectrometry for the fast determination of polycyclic aromatic hydrocarbons in air samples," *Journal of Chromatography A*, vol. 1114, no. 2, pp. 278–281, 2006.

[23] M. Bergknut, K. Frech, P. L. Andersson, P. Haglund, and M. Tysklind, "Characterization and classification of complex PAH samples using GC–qMS and GC–TOFMS," *Chemosphere*, vol. 65, no. 11, pp. 2208–2215, 2006.

[24] T. Tran, *Characterization of Crude Oils and Atmospheric Organic Compounds by Using Comprehensive Two-Dimensional Gas Chromatography Technique (GC×GC)*, Ph.D. thesis, Applied Sciences, RMIT University, Melbourne VIC, Australia, 2009.

[25] Environmental Protection Agency (EPA), *Compendium Method TO-13A, Determination of Polycyclic Aromatic Hydrocarbons (PAHs) in Ambient Air Using Gas Chromatography/Mass Spectrometry (GC/MS)*, EPA, Cincinnati, OH, USA, 1999.

[26] S. H. Jeon, J. H. Shin, Y. P. Kim, and Y. G. Ahn, "Determination of volatile alkylpyrazines in microbial samples using gas chromatography-mass spectrometry coupled with head space-solid phase microextraction," *Journal of Analytical Science and Technology*, vol. 7, no. 1, p. 16, 2016.

[27] A. R. Fernández-Alba, *TOF-MS within Food and Environmental Analysis*, vol. 58, Elsevier, Amsterdam, Netherlands, 2012.

[28] J. H. Winnike, X. Wei, K. J. Knagge, S. D. Colman, S. G. Gregory, and X. Zhang, "Comparison of GC-MS and

GC×GC-MS in the analysis of human serum samples for biomarker discovery," *Journal of Proteome Research*, vol. 14, no. 4, pp. 1810–1817, 2015.

[29] L. I. Osemwengie and G. W. Sovocool, "Evaluation of comprehensive 2D gas chromatography-time-of-flight mass spectrometry for 209 chlorinated biphenyl congeners in two chromatographic runs," *Chromatography Research International*, vol. 2011, Article ID 675920, 14 pages, 2011.

[30] J. Zrostĺíková, J. Hajšlová, and T. Čajka, "Evaluation of two-dimensional gas chromatography–time-of-flight mass spectrometry for the determination of multiple pesticide residues in fruit," *Journal of Chromatography A*, vol. 1019, no. 1-2, pp. 173–186, 2003.

[31] P. Antle, C. D. Zeigler, Y. Gankin, and J. A. Robbat, "New spectral deconvolution algorithms for the analysis of polycyclic aromatic hydrocarbons and sulfur heterocycles by comprehensive two-dimensional gas chromatography-quadrupole mass spectrometery," *Analytical Chemistry*, vol. 85, no. 21, pp. 10369–10376, 2013.

[32] S. Samanipour, P. Dimitriou-Christidis, J. Gros, A. Grange, and J. Samuel Arey, "Analyte quantification with comprehensive two-dimensional gas chromatography: assessment of methods for baseline correction, peak delineation, and matrix effect elimination for real samples," *Journal of Chromatography A*, vol. 1375, pp. 123–139, 2015.

[33] P. Mills and W. Guise Jr., "A multidimensional gas chromatographic method for analysis of n-butane oxidation reaction products," *Journal of Chromatographic Science*, vol. 34, no. 10, pp. 431–459, 1996.

[34] R. M. Flores and P. V. Doskey, "Using multidimensional gas chromatography to group secondary organic aerosol species by functionality," *Atmospheric Environment*, vol. 96, pp. 310–321, 2014.

[35] S. Pongpiachan, P. Hirunyatrakul, I. Kittikoon, and C. Khumsup, "Parameters influencing on sensitivities of polycyclic aromatic hydrocarbons measured by Shimadzu GCMS-QP2010 ultra," in *Advanced Gas Chromatography–Progress in Agricultural, Biomedical and Industrial Applications*, M. Ali Mohd, Ed., InTech, Rijeka, Croatia, 2012.

[36] European Pharmacopoeia 7.0, Section 2.2.46, *Chromatographic Separation Techniques*, 2010.

[37] P. Marriott and C. Mühlen, "The modulation ratio in comprehensive two-dimensional gas chromatography: a review of fundamental and practical considerations," *Scientia Chromatographica*, vol. 8, no. 1, pp. 7–23, 2016.

[38] J. Krupcik, P. Majek, R. Gorovenko, J. Blasko, R. Kubinec, and P. Sandra, "Considerations on the determination of the limit of detection and the limit of quantification in one-dimensional and comprehensive two-dimensional gas chromatography," *Journal of Chromatography A*, vol. 1396, no. 117, pp. 117–130, 2015.

[39] P. M. Antle, C. D. Zeigler, N. M. Wilton, and A. Robbat Jr., "A more accurate analysis of alkylated PAH and PASH and its implications in environmental forensics," *International Journal of Environmental Analytical Chemistry*, vol. 94, no. 4, pp. 332–347, 2014.

[40] T. Cajka, "Gas chromatography–time-of-flight mass spectrometry in food and environmental analysis," in *Comprehensive Analytical Chemistry*, I. Ferrer, Ed., pp. 271–302, Elsevier, Amsterdam, Netherlands, 2013.

[41] B. Lazarov, R. Swinnen, M. Spruyt et al., "Optimisation steps of an innovative air sampling method for semi volatile organic compounds," *Atmospheric Environment*, vol. 79, pp. 780–786, 2013.

[42] H. C. Menezes and Z. de Lourdes Cardeal, "Determination of polycyclic aromatic hydrocarbons from ambient air particulate matter using a cold fiber solid phase microextraction gas chromatography–mass spectrometry method," *Journal of Chromatography A*, vol. 1218, no. 21, pp. 3300–3305, 2011.